NUMERICAL ANALYSIS OF A FUNCTIONALLY GRADED BEAM WITH A UNIFIED HIGHER ORDER BEAM THEORY AND B-SPLINE COLLOCATION METHOD

Thesis submitted by

AMALENDU BISWAS

DOCTOR OF PHILOSOPHY
(Engineering)

DEPARTMENT OF MECHANICAL ENGINEERING
FACULTY COUNCIL OF ENGINEERING & TECHNOLOGY
JADAVPUR UNIVERSITY
KOLKATA, INDIA

2024

Dedicated to

my mother, my father, my wife, my son, both of my PhD guide Sir

&

my friend Dr. Deepak Mahapatra

INDEX NO: 41/16/E

1. Title of the Thesis:

NUMERICAL ANALYSIS OF A FUNCTIONALLY GRADED BEAM WITH A UNIFIED HIGHER ORDER BEAM THEORY AND B-SPLINE COLLOCATION METHOD

2. Name, Designation and Institution of the Supervisor:

DR. SAMAR CHANDRA MONDAL

Professor,
Department of Mechanical Engineering,
Jadavpur University,
Kolkata – 700032, India.

DR. SUSENJIT SARKAR

Professor,
Department of Mechanical Engineering,
Jadavpur University,
Kolkata – 700032, India.

3. List of Publications:

Published

1. Biswas, A., Mahapatra, D., Mondal, S. C., & Sarkar, S. (2024). Higher Order Approximations for Bending of FG Beams Using B-Spline Collocation Technique. *Mechanics of Advanced Composite Structures*, *11*(1), 159-176. DOI: 10.22075/macs.2023.29936.1480 (SCOPUS Indexed)
2. Biswas, A., Mandal, S. C., Sarkar, S., Mahapatra, D., & Bhowmick, S. (2024, January). Unified higher order beam theory for behavioral study of FG beams. In *AIP Conference Proceedings* (Vol. 2960, No. 1). AIP Publishing. doi.org/10.1063/5.0183238 (SCOPUS Indexed)

4. List of Patents: *Nil*

5. List of Presentations in National/International Conferences/ Workshops:

1. Fourth International Conference on Recent Advances in Mechanical Infrastructure (ICRAM 2022) at Institute of Infrastructure Technology Research and Management (IITRAM), Ahmedabad.

Declarations

I hereby declare that except where specific reference is made to the work of others, the contents of this thesis are original and have not been submitted in whole or in part for consideration for any other degree or qualification in this, or any other university. This thesis is my own work and contains nothing which is the outcome of work done in collaboration with others, except as specified in the text and Acknowledgements.

Amalendu Biswas 19.03.2024 03.06.2025

Amalendu Biswas, March, 2024

"Statement of Originality"

I, **AMALENDU BISWAS** registered on **OCTOBER 28, 2016** do hereby declare that this thesis entitled **"NUMERICAL ANALYSIS OF A FUNCTIONALLY GRADED BEAM WITH A UNIFIED HIGHER ORDER BEAM THEORY AND B-SPLINE COLLOCATION METHOD"** contains literature survey and original research work done by the undersigned candidate as part of Doctoral studies.

All information in this thesis have been obtained and presented in accordance with existing academic rules and ethical conduct. I declare that, as required by these rules and conduct, I have fully cited and referred all materials and results that are not original to this work.

I also declare that I have checked this thesis as per the "Policy on Anti Plagiarism, Jadavpur University, 2024", and the level of similarity as checked by iThenticate software is 3%.

Amalendu Biswas ~~19.03.2024~~ 03.06.2025

Signature of AMALENDU BISWAS:

Date: ~~19.03.2024~~ 03.06.2025

Certified by Supervisors:

~~19.03.2024~~ 03.06.2025

DR. SAMAR CHANDRA MONDAL

Professor,
Department of Mechanical Engineering,
Jadavpur University,
Kolkata – 700032, India.

Professor
Dept. of Mechanical Engineering
Jadavpur University, Kolkata-32

~~19/03/2024~~ 03/06/2025

DR. SUSENJIT SARKAR

Professor,
Department of Mechanical Engineering,
Jadavpur University,
Kolkata – 700032, India.

Professor
Dept. of Mechanical Engineering
Jadavpur University, Kolkata-32

CERTIFICATE FROM THE SUPERVISORS

This is to certify that the thesis entitled **"NUMERICAL ANALYSIS OF A FUNCTIONALLY GRADED BEAM WITH A UNIFIED HIGHER ORDER BEAM THEORY AND B-SPLINE COLLOCATION METHOD"** submitted by **Shri Amalendu Biswas**, who got his name registered on **October 28, 2016** for the award of Ph. D. (Engineering) degree of Jadavpur University is absolutely based upon his own work under the supervision of **Dr. Samar Chandra Mondal** & **Dr. Susenjit Sarkar** and that neither his thesis nor any part of the thesis has been submitted for any degree / diploma or any other academic award anywhere before.

19.03.2024 03.06.2025

DR. SAMAR CHANDRA MONDAL

Professor,
Department of Mechanical Engineering,
Jadavpur University,
Kolkata – 700032, India.

Professor
Dept. of Mechanical Engineering
Jadavpur University, Kolkata-32

19/03/2024 03/06/2025

DR. SUSENJIT SARKAR

Professor,
Department of Mechanical Engineering,
Jadavpur University,
Kolkata – 700032, India.

Professor
Dept. of Mechanical Engineering
Jadavpur University, Kolkata-32

ACKNOWLEDGEMENT

"I have always believed, and I still believe, that whatever good or bad fortune may come our way we can always give it meaning and transform it into something of value."

— Hermann Hesse, Siddhartha

I strongly feel that, it is our beliefs which make path to our destiny. Different people come into our lives, some of whom influence our deeds in such a way that we assimilate their conduct in our personality and thus we move to what is destined for us. The pursuing of PhD is also like a life of short span filled with different ups and downs, challenges and inspirations which ultimately lead to our goal and when we look back, we find the negatives too had a reason in making the realization of the goal. Apart from attaining a degree it thus makes us humble and grateful and this is the ultimate aim of life.

The pursuing of PhD for me has also been a journey of hopes and moments of despair that are to be cherished as moments to remember throughout my life. And I would take this opportunity to heartily acknowledge all those who have been there to support and motivate.

First and foremost, I would like to extend my sincere thanks and gratitude to my PhD supervisors Dr. Samar Chandra Mondal and Dr. Susenjit Sarkar for their unwavering support and guidance in this course of my PhD research work. Whenever any challenging and demoralising situation raised in this journey of PhD research, every time they pulled me out of those situations with their knowledge, expertise, encouragement and very caring guidance. Without their support, it must not have been possible for me to achieve this priceless goal. No word would be sufficient enough to express my lifelong gratitude towards my supervisors

Without mentioning the contribution of my friend and philosopher, Dr. Deepak Mahapatra, in my PhD research work, this acknowledgement would remain incomplete. At every step in my PhD research work he helped me a lot in all respect.

Without his support and guidance my PhD research would not have been completed at all. It is not possible to express my heartfelt thanks to him in words.

I also appreciate and acknowledge support and encouragement which I have received from Dr. Amit Karmakar, Head of the Department, Mechanical Engineering and Dr. Dulal Krishna Mondal during this journey of perusing PhD degree from Jadavpur University. I would like to thank the staffs of the Mechanical Department and Faculty Council of Engineering & Technology for their assistance and support throughout my studies.

In this occasion I would like take an opportunity to convey my sincere thanks to Mr. Pradeep Agrawal, CEO, KBT and Dr. Sukanta Sarkar, HOD, Mechanical for their support and encouragement in pursuing my PhD degree. Also, I would like to express my heartfelt thanks to my colleagues, especially Dr. Sumanta Banerjee, Dr. Amal Kumar Roy, Prof. Manik Barman, Prof. Pritam Ghosh, Prof. Bamkim Pattanayak, Dr. Arup Jyoti Bhawal, Prof. Sudipta Roy and Dr. Ranojit Banerjee for their encouragements and motivations at stressful times in the tenure of my PhD.

I am very much grateful to my wife for her indomitable support and patience she extended to me unconditionally whenever I needed. Without her cooperation it could have been very much difficult for me to complete this journey.

It is very difficult to mention each and every one who has helped me to complete my research work successfully. I do recall with gratitude the assistance rendered by one and all.

Lastly and most importantly, I would like to offer my cordial homage to my parents. I like to pay my tribute to them for their blessings, encouragement and motivation throughout my academic career. In this regard I would like to mention here that, without my mother's help I probably could not even start my PhD degree.

17-03-2014
03.08.2015

AMALENDU BISWAS

Table of Contents

Abstract

Beams are essential components of all types of structures. Beams can be used to idealize or represent various structural elements, like, cutting tools, robotic arms, wind mill blades, helicopter rotor blades, heart valves, and many more. The notion of functionally graded materials (FGM) emerged in an attempt to design a new type of particulate composite material as an alternate to the standard fibrous composites due to their frequently occurring delamination failure. So, it is anticipated that using beams with functionally graded materials will increase their dependability and safety. As functionally graded materials are all customized materials so it is necessary to investigate the behaviour of functionally graded beams thoroughly with all types of variations in gradation parameters for the process of design and development. This study examines the deformation and stress behaviours of a functionally graded (FG) material beam under mechanical as well as thermo-mechanical loading circumstances.

To analyse behaviour of an FG beam thoroughly a new type of unified higher order beam theory has been derived in context of Third order Shear Deformation Theory (TSDT). To take into account of the influence of non-linearity on the beam behaviour, von-Karman principle has also been integrated into the formulation. Adaptation of principle of stationary total potential through von-Karman's principle has enabled to incorporate higher order terms (up to 6^{th} order) to examine behaviour of beams more minutely for various cases of material gradations under different mechanical and thermo-mechanical loads. The material's properties, such as its modulus of elasticity, stiffness, coefficient of thermal expansion, and thermal conductivity, have been assumed to vary over the thickness of the beam but Poisson's ration has been taken constant.

Standard problems from few previous works [33, 128] have been solved using the mathematical model developed in the present work under mechanical load as well as thermo-mechanical load to determine transverse deflection, axial stress and shear stress. It has been observed that the results of transverse deflection and axial stress have been validated with the results of the work from the base papers [33, 128] under mechanical and thermal load both. But it has also been observed that result of shear stress differs considerably with the results determined by the authors in [33] and [128]. It has been concluded that due to incorporation of 6^{th} order derivative in the mathematical model this difference in shear stress has been appeared because in the mathematical model derived by the authors of [33] and [128], up to 4^{th} order derivative appeared.

In the present work it has also been experienced that analysis of FG beams with dimensional discontinuities is not possible with analytical method. For this reason, FEA codes have been developed to analyse FG beams with circular and elliptical holes under static loadings.

List of abbreviation

FG	Functionally Graded
FGM	Functionally Graded Material
NURBS	Non-Uniform Rational Bezier Spline
IGA	Iso-Geometric Analysis
FEA	Finite Element Analysis
SIF	Stress Intensity Factor
FSDT	First Order Shear Deformation Theory
SSDT	Second Order Shear Deformation Theory
TSDT	Third Order Shear Deformation Theory
Al	Aluminum
SiC	Silicon Carbide
SPS	Spark Plasma Sintering
AFG	Axially Functionally Graded
TD	Temperature Dependent
TID	Temperature Independent
APDL	Ansys Parametric Design Language
CBT	Classical Beam Theory
EBBT	Euler Bernoulli Beam Theory
TBT	Timoshenko Beam Theory
HSDT	Higher
P-FGM	Power law-Functionally Graded Material
S-FGM	Sigmoid law-Functionally Graded Material
E-FGM	Exponential law-Functionally Graded Material
LTD	Linear Temperature Distribution
NLTD	Non-Linear Temperature Distribution

List of Figures

List of Tables

Chapter 1: **Background and Motivation**

1.1 Introduction

The material sciences and technology are undergoing a revolution in the modern period. Researchers are working hard to create novel, intelligent materials to meet the need for increased reliability and efficiency of machines and structures. The invention of Functionally Graded Materials (FGMs) was motivated by the observation of naturally occurring materials, such as bamboo, human bones, teeth, etc., which exhibit superior qualities in their behavior due to the progressive fluctuation in their properties. The development of very high-grade particulate composite materials with proper material gradation laws and parameters has completely changed engineering and materials science research. Such advanced composites with smooth and continuous property variation along a specified path and in a desired pattern are called functionally graded (FG) materials. Such materials exhibit a progressive change in structure and composition (volume of constituents) over volume, leading to a smooth shift in the material's properties that differ from the parent materials. Lay Traditional composites fail because of the rapid concentration of interface stress caused by their layered composition; in contrast, FGMs exhibit no interface phenomenon since their characteristics change gradually or continuously. Changing the material elements' makeup (by volume) is the most popular way to produce FGMs (figure 1.1). The percentage by volume at that position governs the subsequent properties of the parent material, which are obtained by varying the composition (volume) of elements of such materials in a predetermined manner.

Though the idea of FGM was first documented in the middle of the 1980s, the overall notion of gradually changing the characteristics of composites and polymers were germinated ways back in the early 1970s [4]. The incubation of FGM began during the

Japanese hypersonic space plane project, where the primary goal was to create a material with specific properties to lessen the thermal stresses at the refractory layer interface. These thermal stresses were the main cause of spacecraft failure during the spacecraft's entry into the earth's atmosphere, where there was a thermal gradient of roughly 1000K in a thickness of 1cm. Therefore, FGM for this kind of application is composed of metal on one side and refractory ceramic on the other. This will work well to provide high temperature toughness and strength with low residual stresses and stress concentration since the smooth property variation there almost eliminates any interface. Graded qualities for an appropriate combination of contrast materials (other FGMs) are thought to have multiple application areas with increased dependability and safety, in addition to the use of FGM as a thermal barrier. As a result, it is possible to apply FGMs in a number of fields, including biomedical, electronics, optical, nuclear, aerospace, energy conservation, and many more [4].

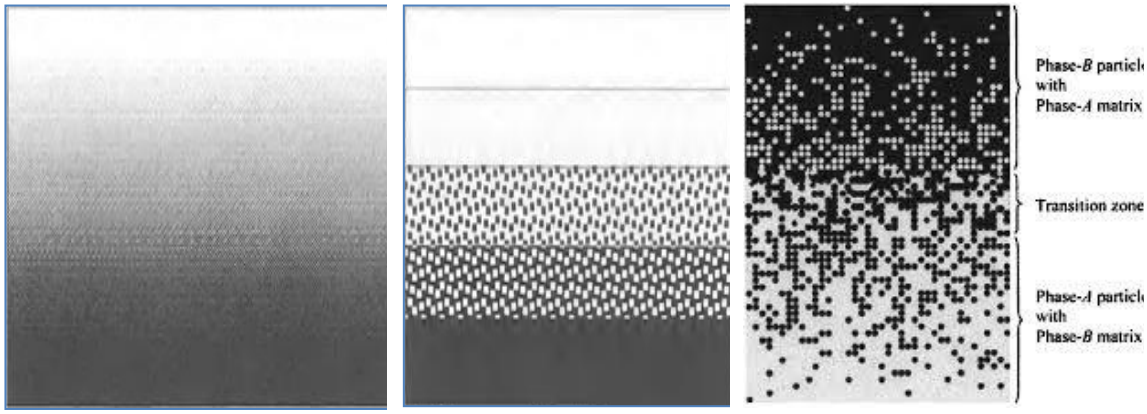

(a) (b) (c)

Figure 1.1 a) Continuous, b) stepwise graded structures [4],
c) An FGM with the volume fractions of constituent phases graded in one (vertical) direction [131]

In a functionally graded material, the ingredient composition is varied in such a manner and in a direction such that, desired sequence of attributes and properties can be obtained. Various types of graded composite materials have been schematically represented in figure 1.1. There are two methods related to the production of FGM: one involves the use of fiber reinforcement in an ordered variation and other one is variation of particles. Particulate composite FGMs are manufactured utilizing a variety of processes, including

thermal spray, powder metallurgy, high-speed centrifugal casting, and others, to regulate the volume fraction of the particle constituents [8]. Though there is still much to learn about the processing of FGMs, given the speed at which technology is developing, it is anticipated that FGM processing will become commercially viable very soon.

Many studies have focused on simulating the behavior functionally graded material under various loading. When designing applications, a precise and realistic estimate of the material behavior is quite helpful. The specific shape, size, and orientation of the FGMs vary with position, and their volume fraction affects their volume-dependent properties in addition to the individual component properties. This is because the FGMs have a tailored variation of microstructure that was introduced especially during their formation. Furthermore, in a thermal environment where each unique property is also temperature-dependent, the situation becomes even more complex. Many methods, such as the rule of mixtures and the Mori-Tanaka scheme in the micromechanics model, are currently widely utilized to estimate the behavior of FGMs. Nonetheless, another area of research pertinent to FGMs has been to produce a fair approximation of material property based on micro-structural investigations and the existing experimental data.

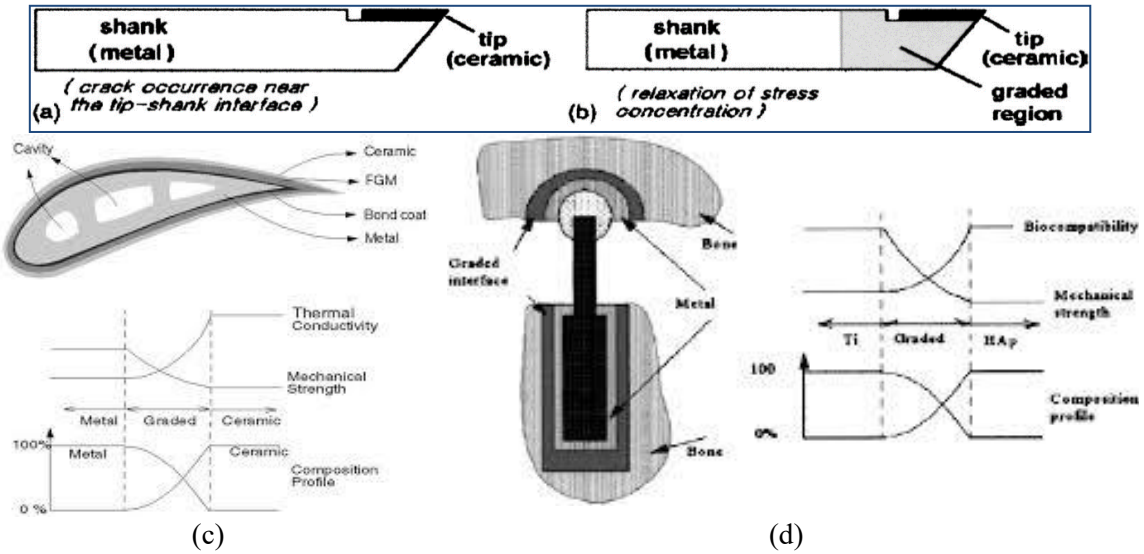

Figure 1.2 a) & b) FGM application for relaxation of stress concentration in lathe bits [12], c) FGM application for a turbine blade design [12], d) FGM interface within a hip replacement prosthesis [12]

As was previously said, FGMs are believed to be the preferable option in many critical applications because of their superior properties. They have the potential to completely transform and composite technologies in design processes if their manufacturing costs can be lowered. As FGM is a customized material and can be manufactured with controlled parameters like composition of particles, gradations laws, direction of variation etc to have desired property distributions corresponding to any specific requirements, their potential applications in a variety of engineering fields make them highly versatile (figure 1.2). Therefore, research on the theoretical and experimental aspects of using FGMs in engineering design is highly important and essential for the development of new technologies.

Almost all of the applications that were previously covered include beams or structures that resemble beams. Beams can be used to idealize a variety of structural components, including cutting tools, robotic arms, space erectable booms, turbine blades, helicopter rotor blades, heart valves, and many more. Structural components known as beams provide resistance against bending under applied loads. Beams are typically made of long, prismatic bars with normal loads applied to the bars' axes. A beam's load carrying capacities are determined by first analyzing the equilibrium needs for the beam as a whole, and then analyzing a portion of the beam for equilibrium conditions. The statics principles are necessary for the analysis of the forces. In order to determine the distribution of stress, strain, and displacement within a beam that is subjected to a specified system of forces, several requirements pertaining to specific physical laws, material qualities, and geometry must be taken into account. Numerous beam models have been used in the past to address engineering issues [14] and offer the kind of reliable, accurate forecasts that are necessary for design.

For the successful designing of various beam like and plate like structures in critical applications composite materials remains first choice for the engineers in 20th century. These are good for many uses and have a high stiffness to strength ratio. Investigation on behavior of laminated composite beam and plate under static and dynamic loadings have emerged as a major field of study in recent years. However, composites have an innate issue with de-bonding and de-lamination, and interfacial failure endures when exposed to thermo-mechanical environments. FGMs' properties gradually vary, therefore using them to these kinds of applications will undoubtedly increase their performance in terms of safety and longevity.

Due to technological advancement in method of computing high accuracy in design and analysis of machine and machine components with large and complicated design parameters are achievable. It is now possible to obtain an approximate solution of complicated governing equations for a variety of static and dynamic non-linearities, for which the direct solutions are extremely difficult to find. This is made possible by advances in computer speed and accuracy. Several reports that identify approximations by meshing (dividing the domain into smaller entities) have been published. These methods include finite difference and finite element techniques. However, mesh-less techniques like the spectral method and boundary element method are also attracting the attention of academics in more recent publications.

As it is comparatively easy to solve governing equations numerically using Collocation methods, they are often used by researchers to solve various complex problems approximately. A differential equation is satisfied, to a certain degree of tolerance, at a limited number of locations known as collocation points in a collocation method. The foundation of a collocation approach is assessing a differential equation's accuracy at a limited number of collocation locations. This technique's primary benefits are its low

computational cost and ease of use. However, this technique's application is limited to a relatively confined area due to its low level of precision.

Among all the collocation methods, B-spline collocation method is best because, use of B-spline as approximation polynomials enhances the accuracy of the collocation technique and thus it becomes appropriate for the numerical solutions of intricate governing equations. It has been noted that the application of the B-spline basis function collocation technique to engineering issue solving is growing. B-splines are very well suited for curve fitting applications because of their superior local control and smoothness at the interface characteristics. The objective is to link the low computing cost of collocation with the improved accuracy and smoothness of B-spline basis functions. It has been demonstrated that this method can be just as effective as other well-known methods like finite element analysis and finite difference methods. Comparing the B-spline Collocation Method to the Finite Element and Finite Difference Methods reveals a few key advantages. The B-spline Collocation Method has an advantage over the Finite Difference Method in that it offers a piecewise-continuous, closed form solution. Working with intricate forms and profiles can benefit from the use of finite element formulation; nevertheless, B-spline collocation methods have an advantage over finite element methods in that the former procedure is easier to understand and apply to differential equation problems.

Since the 1980s, B-spline collocation has been used to solve heat transfer and fluid flow issues. Several reports on convection-radiation and fluid-heat-mass transfer studies have been published. In contrast, structural analysis has seen less use of B-spline collocation and a much smaller number of reported studies. Because of its flexibility and smoothness, researchers have recently become interested in the use of Non-uniform Rationalized B-splines (NURBS) in isogeometric analysis (IGA) [128, 143] and isogeometric collocation. Therefore, it is believed that the B-spline collocation technique

can be highly useful in getting approximate solutions to the non-uniform FG beam behavior in a temperature environment.

Till now discussion has been taken place on solution of FGM beam and beam like structures made of functionally graded materials with various gradation laws under different types of loading static or dynamic, mechanical or thermal or thermo-mechanical through analytical formulation process and numerical solution methods. But, in case of complicated structure topology, it becomes very much difficult to formulate an FG beam problem analytically and solve by collocation method. The best alternative method for this case is solving problems of complicated geometry with any FEA software by using its programming module. Many authors have adopted this method [139-142] to solve problems like determination of stress intensity factor (SIF) of any FG beams and plates with various dimensional discontinuity under linear and non-linear loading.

1.2 Need for the research

Because of delamination and stress discontinuity, traditional laminated composites are inherently vulnerable to failing under thermo-mechanical conditions. Functionally graded materials, which have additional safety and dependability for the gradual variation in attributes, will be chosen for such circumstances. It is believed that FGMs will become the most popular material for many applications if processing manufacturing of FGM becomes more affordable with technical advancements. Therefore, it is imperative that a thorough theoretical analysis of the behavior of the components that make up FGMs be anticipated with great fervour.

The majority of engineering applications, as previously mentioned, require beams and plates. In other words, a variety of applications can benefit from the use of the beam/plate paradigm (for instance, windmill blades can be thought of as beams, while current Armor can be thought of as plates). Currently, laminated composites are the material of choice for

these kinds of applications because of their excellent strength to weight ratio and high stiffness. However, by lessening the interfacial phenomenon, the adoption of FGMs will further improve their capabilities. Therefore, an intriguing and pertinent field of study is the analysis of primary or secondary structural elements that can be idealized as beams (1D) or plates (2D) composed of functionally graded materials. Furthermore, with increase in dimensional complicacy problems are required to be solved with FEA software using their programming capabilities. So, more researches required to develop FEA software programming to make solution process of FG beam problems dimensional complicacy independent. Development of these types of FEA software programming will definitely help us a lot to solve various types crack analysis problems in FG beams and plates.

This study aims to investigate very minutely the influence of various functional gradation parameters, types of loadings and boundary conditions on behaviour of a FG beams by developing a higher order beam formulation. Using this higher order mathematical model, different behavioural output parameters like deformation, axial stress and shear stresses etc can be studied under arbitrary boundary conditions, subjected to static or dynamic load in a thermal and mechanical environment very easily and more accurately. The research will also consider solution of FG beams with dimensional discontinuities using FEA programming to implement the FEA solution process to solve problems FG beams with cracks.

1.3 Research objective

It is a proven fact that FGMs have a lot of potential to be used as an useful and efficient materials in a variety of engineering applications, yet their use is currently restricted because of challenges with production and design. These challenges related to manufacturing and design can be averted greatly by deep understanding of its mechanics and material behavior. In solving problems related to FG beams adopting approximate

method of solution is quite useful and, in that case, devising a suitable numerical method of solution is very much needed keeping balance between desired accuracy and related computational cost. Following a thorough analysis of the most recent research on FG beams and plates, it was found that there are comparatively few studies on the deformation and stresses (axial and shear) of these contemporary composites under simultaneous mechanical and thermal load. Additionally, there are not many studies on numerical analysis of FG beams with various dimensional discontinuities under mechanical and thermal loadings. For all these reasons, researchers are very interested in creating novel formulations and strategies that will make the both analytical as well as numerical analysis of FG beams simpler and lead to a very much acceptable solution.

On the basis of the research requirements stated above, present work proposes a unique method of formulation of a unified higher order differential equation, in the frame work of Third order Shear Deformation Theory (TSDT), and as a function of a single parameter to obtain a single governing equation for the FG beams subjected to thermo-mechanical load and arbitrary boundary condition. The special feature of this technique is that the effect of shear deformation is separately considered by converting the displacement variables into a function of independent variable. Also, to incorporate 6th order of derivative, principle of total potential energy has been adopted through Hamilton's principle instead of elasticity method. Hence if the effect of shear deformation is neglected the theory simplifies to that of classical Euler-Bernoulli beam theory and if time derivative is neglected it gets converted into Timoshenko beam theory. The proposed method follows the approximate solution using B-spline collocation technique using Greville abscissa as collocation points. Hence the present work explores the stress and deformation behavior of FG Timoshenko beams subjected to thermo-mechanical load with arbitrary boundary conditions using B-spline

collocation technique using a mathematical code developed specifically for this research. In the next part of the research, a FEA code has been developed to analyze

1.4 Thesis outline

The contents of this thesis are organized in the following form:

- Chapter 2: *Literature review*

  This chapter summarizes a detailed review on the prominent works reported in the relevant area to identify the research gaps and future scope involving the issue of interest.

- Chapter 3: *Materials and methods*

  This chapter summarizes the classical beam theory (Euler-Bernoulli beam theory), first order beam theory (Timoshenko beam theory) and Third order beam theory (Reddy) and extends them to include material gradations in FGMs. This chapter also explores the technique of B-spline collocation and demonstrates its flexibility and accuracy in solving differential equations of different order; thus, to solve structural problems also that are of higher order. B-spline functions of non-uniform knot spacing have been considered; thus, the effect of change of knot spacing and increase in number of knot spans on the final results has been explored. In the end few case studies of approximate solution of isotropic beam problem under mechanical and thermo-mechanical load has been also addressed.

- Chapter 4: F*unctionally graded beams under purely mechanical load*

  In this chapter a mathematical model has been developed to discusses about the deformation behavior and corresponding stresses induced in a Functionally Graded beam in the frame work of Third order beam theory (TSDT) along with a novel unified formulation technique. To solve the derived governing differential equation a numerical method named, B-spline collocation method, has been adopted for various material gradations. Deformation and stresses; bending (axial) stresses and transverse (shear) stresses, and position of neutral axis are studied for a wide range for different type of volume fractions of constituents.

- Chapter 5: F*unctionally graded beams under thermo-mechanical load*

In this chapter stresses and deformation of FG beams under different thermo-mechanical loading environment has been studied for a various temperature ranges and gradients. Purely thermal and thermo-mechanical load has been considered where temperature has been varied along the beam height. Exact solutions for the deformation and stress have also been obtained for three types of boundary conditions viz.- Clamped-Free (C-F), Simply Supported (S-S) and Propped Cantilever (C-S). The study has been extended to cover wide range of temperature distribution so as to include uniform, linear and non-linear temperature profiles. Deformation and stresses; bending (axial) stresses and transverse (shear) stresses, have been reported for different type of volume fractions of constituents. The buckling problem for C-S & C-C beams has also been reported.

- Chapter 6: *FEA Simulations*

This chapter includes a FEA code to model any beam structure with and without dimensional discontinuity like, incorporation of circular hole and elliptical hole in any beam at any given location to analyze it under all types of loadings and with all types of material gradations.

- Chapter 7: *Conclusions and future scope*

The conclusions drawn from the above chapters and scope for future works are reported in this chapter.

1.5 Closure

This chapter offers an overview of functionally graded materials, which are advanced graded composites that offer increased safety and dependability and are appropriate for numerous essential applications. These materials are inherently free of delamination and stress discontinuity, which gives them an advantage over traditional laminated composites. Many possible uses for these materials are evaluated, and appropriate knowledge of their mechanics for matching uses is anticipated. In this sense, it will be necessary for design processes to analyze functionally graded higher order beams for stress and deformation in a thermo-mechanical environment. Therefore, the aforementioned concept has been chosen as the current work's research goal. This chapter concludes by summarizing the thesis's outline and research goals.

Chapter 2: **Literature Review**

2.1 Introduction

The present era is the era of customised material. Design of various structural components like beams, plates, discs etc are done not only on the basis of topological modifications but also material modifications. Customized materials like fibrous composite materials and the particulate composite materials can be designed varying their constituent properties as well as their process parameters. Though many researches have been done on fibrous composites but particulate composites are yet to explored fully. In the present work a detailed review has been done on the past works in various area of research on Functionally Graded Materials (FGM), a particular type of particulate composite, and the influence of its constitutional properties on the behaviour of various structural components like beams, plates, discs etc under different loading and boundary conditions.

2.2 Categorized review

It is a very well-known fact that to do a research work successfully, a through and versatile literature review is very much essential. In the present work, many literatures like research papers, books, reports etc have been reviewed sincerely to follow the recent trends of research work in this particular field. The literatures which have been review under the present research consists of various research papers published in different renowned journals, many valuable and famous books, research reports and other online documents. To present a detailed report on literature review, it has been assorted into few categories. Few literature reviews have been done on Functionally Graded Material development, study of its properties and utilities. Few literature reviews have been done on structural analysis of FGM components like beams, plates, discs etc under mechanical loading as well as thermo-mechanical loading. Various other research works have also been reviewed on numerical solution of various governing differential equations through B-spline collocation method. Many other research works on FEA analysis of various FGM structural element like beam, plate, shell etc using a FEA commercial programming have also been done.

2.2.1 Research on Functionally Graded Material

Since mid-1980s, with the advent of Functionally Graded Materials (FGMs), we are witnessing a new era in the field of material technology. FGMs, belongs to a class of advanced materials which have continuous variation in properties along a desired direction and in desired fashion. In such materials the composition (volume of constituents) and

hence the structure gradually change over the volume, resulting in corresponding change in the properties of the material that is different from either of the parent material. A thorough overview about FGMs, their manufacturing techniques, modelling and design and applications can be referred in [1-12]. S. Suresh et al [1 - 3] published two papers and a documentary in the year of 1997 and 1998 on Functionally Graded Material and their indentation process where they discussed in detail about the fundamentals of FGM and process of property determination. Next year in 1999 Y. Miyamoto et al [4] published another document in Springer on design, processing and application of various FGM in detail. T. Nakamura et al [5] did a valuable work in the year of 2000 on determination of structural properties of various functionally graded materials using inverse analysis and instrumented analysis method. A detailed work was done by B. Kieback et al [6] on various processing technique of functionally graded material and published in the year of 2003. In the year of 2007 Bhattacharyya et al [7] reported a study on research regarding deflection behaviour of Al/SiC FGM. In their study they also determined stress to strain ratio of the that FGM under various loading and boundary conditions. M. R. Mahamood et al [8] presented many very useful and important information regarding material properties, processing techniques, testing methodologies and various applications of different functionally graded materials in their extensive review report which was published in the year of 2012. In the same year a very precious and specific work was reported by S. Hayun et al [9] regarding an extensive study on microstructure and mechanical properties of silicon carbide processed by Spark Plasma Sintering (SPS) process. In the year of 2014 two detailed reviews were published on thermos-mechanical properties of functionally graded materials. One was by S. S. Rao et al [11] and other one was by V. Birman et al [12].

2.2.2 Research on FGM beams, plates, discs etc under mechanical loading.

Beams, plates and discs are very important structural components that have wide application area. When structures are exposed to severe environments then to sustain such conditions the materials must exhibit superior properties. If we consider a space shuttle, while entering the earth's atmosphere, is exposed to very high temperature gradient through a small thickness. The extreme pressure and temperature gradient requires stringent behaviour prominently significant at the interface. Conventionally, the composites used for such applications fail due to interfacial stress concentrations observed under critical environmental conditions. The ceramic-metal based FGMs are especially suitable for such high temperature gradients with ceramic part exposed to higher temperature while the metal

part ensures the FGM to have its strength. The gradual change of material properties aids in sustaining the stress-concentration and residual stresses developed otherwise. The design of such structural components needs a thorough analysis of load-deflection-stress behaviour under various thermo-mechanical conditions and other related environmental factors. Although considerable research on the functionally graded materials has been reported since their conceptualization, most of the work in the area of functionally graded structures (beams and plates) has been done in last two decades.

Although considerable research on the functionally graded materials has been reported since their conceptualization, most of the work in the area of functionally graded structures (beams and plates) has been done only in last two decades. In the researches on Functionally Graded structure, different types of studies and analysis have been performed by various authors under different types of loadings like mechanical loading, thermal loading and thermo-mechanical loadings. In the present literature review, all the works on FGM structures like beam, plate and discs under mechanical loadings have jot down from reference [13] to [81] in chronology of year of publication. In 2000, Reddy published a work on analysis of a FGM plate under thermo-mechanical loading [13]. In this work he established a governing equation using von-Karman principle and solved it using Navier's solution method. In the same year C. M. Wang and J. Reddy [14] published an important book on relationship between classical solution of deformable beams and plates. In very next year, that is in 2001 B. V. Shankar [15] studied the behaviour of FG Euler-Bernoulli beam using elasticity approach and is considered as the most fundamental work in this realm of FG beams. In this work an exponential variation of modulus of elasticity across the thickness is considered, keeping Poisson's ratio constant; the variations in stress and displacements are monitored and the behaviour of slender and stubby beams under different loading conditions are compared. In year 2002 two important research works were published. One on vibration analysis of a FGM tapered beam by B. K. Lee et al [16]. An innovative work of A. Chakraborty, S. Gopalakrishnan and J. Reddy on development of a new beam element to analyse any FGM beam using finite element method was surfaced in 2003 [17]. In their work they derived a new stiffness matrix considering material properties as a nodal degree of freedom of the element and also made the new element capable to free it from shear locking. Their worked helped a lot in later researchers to analyse their problems of FGM beams using FEA method with least error. Sankar and Zhu [18] did an analysis of a FGM beam in a new approach using the method of Fourier analysis combined

with Galerkin's method for solution and published their work in 2004. A non-linear analysis of a FGM beam under thermo-mechanical loading was performed by M. Tahani et al [19] was performed with First Order Shear Deformation (FSDT) to find out deformation and stresses throughout the FGM beam topology. Their work was published in a renowned journal in the year of 2006. M. Tahani et al extended their [20] work in 2007 into a layer wise non-linear analysis to a FGM plate made with power law of material gradation to find out its deformation and stresses. In the very same year another two important works were published in two renowned journals. One on static and vibration analysis using higher order deformation theory for FG beams which was reported by Aydogdu and Taskin [21] where they used higher order beam theory for the formulation of the problems governing differential equation using Hamilton's principle and solved that governing differential equation for the natural frequencies corresponding to various modes using Navier type solutions. Second one was published by Zhong et al [22] where they reported an analytical method for the formulation of FG beams and solutions are obtained using Airy's stress function. Banerjee et al. [23] did an analytical analysis using non-linear shooting and Adomian Decomposition method to study the large deflection behaviour of compliant cantilever beams. The authors published their work in a very renowned journal named Journal of Non-Linear Mechanics in the year of 2008. In the same year few more works were published on analytical as well as numerical analysis of FGM beams with various boundary and loading conditions with various gradation laws for functional gradation of materials. Those papers were published in different prestigious journals by M. A. Benatta et al [24], R. Kadoli et al. [25], S. Kapuria et al [26] and X. F. Li et al [27]. Kadoli et al. [25] reported the static analysis of FG beams using higher order theory and reported carious cases of axial and shear stress distribution through finite element solution technique. In their work, Kapuria et al. [26] studied the static and dynamic behavior of FG beams using a finite element based third order zig-zag beam modeling theory in which the modulus of elasticity and other parameters were determined using a modified rule of mixtures. As part of their research, the authors put up an experimental setup to confirm and validate the findings for a Ni/Al2O3 FGM that was made by a powder metallurgical method. For the better convergence of the result, they used modified rule of mixture and compared the result with the existing rule of mixture. Li [27] presented a novel unified formulation for the FG Timoshenko beam, which consists of a single fourth order equation that simplifies the three differential equations of displacement variables. After ignoring a few variables, the formulation was analytically reduced to Rayleigh and the Euler-Bernoulli beam while accounting for the effects

of rotating inertia and shear deformation. In the current work, Li's [27] the concept for unification of governing differential equations in terms of a single parameter has been adopted. Li [27] described methodology was modified by Sina et al. [28] to include heat loading of tapered beams through the development of a new beam theory for laminated composites. The authors also extended their work to examine the vibrational features of FG beams in their work. Guinta et al. developed a unified formulation for displacement variables of the cross-section in [31] by utilizing a general N-order approximation. The theory was then applied to FG beams. Their work was published in a renowned journal in the year of 2010. By translating the governing equations to the Fredholm integral equation and extending the mode shapes as power series to achieve the solution, Huang and Li [32] investigated the free vibration characteristics of the axially graded tapered FG (AFG) beam and published their work in the Journal of Sound and Vibration in the same year of 2010.

X. F. Li et al [33] extended their work which they did in 2008 [27] to remodel the governing equation from the view point of higher order beam theory to deal with free and forced vibration of a FGM beam. In their work they incorporated 4^{th} moment of inertia in their unified higher order beam model and expressed all the governing equations in terms of a single parameter 'F'. The authors solved their unified governing equations by successive integration method employing various boundary conditions suitable for a given load case and type of boundary condition. In the present work, theory developed by X. F. Li has been followed and further higher order beam theory has been developed and the governing equations have been unified with help of a common parameter 'F' as X. F. Li did in their work [33]. This work of X. F. Li [33] was published in the year of 2010.

Exact solutions for the free vibration analysis of symmetric FG beams with temperature-dependent (TD) material properties were reported by Mahi et al. [34] in the same year, that is, in 2010. The non-linear temperature distribution throughout the beam height was taken into consideration, along with three different distribution types: power law, exponential, and sigmoid variation. To analyse analytically large deflection of a beam with cantilever and simply-supported boundary conditions G. H. Rahimi et al [35] formulated a suitable governing equation in their work, using Adomian Decomposition method. Their derived formulation was made capable to take account of all geometrical non-linearities and functional variations of FGM. They published their work in the same year of 2010. Simsek [36] used higher order beam theory to study the dynamic behavior of

FG beams. Two different formulations were used, using mid-layer shear rotation and mid-layer slope as variables.

Position of neutral surface in a FGM beam has immense importance in the bending analysis of a FGM beam under various boundary and loading conditions. In [37–39], the impact of geometric nonlinearity has been discussed as a means of explaining relatively substantial deformations in FG beams through the form of von Karman relations in the displacement terms. The neutral axis does not line up with the cross-section's center of gravity because of the differences in material qualities throughout the cross-section. Neutral axis location fluctuation with material gradation has been discussed in [37-39]. H. Yaghoobi et al [37] did a work on determination of neutral surface of a FGM beam with various material gradation laws. In their work they determined bending stress distribution throughout the cross section of a FGM beam with simply supported boundary condition and under uniformly distributed loading. From their work they established the fact that position of neutral surface in a FGM beam has immense role in determination of bending stresses. Their work published in a prestigious journal in the year of 2010. In very next year G. Akhras et al [38] did a dynamic analysis of a FGM plate to study its free vibrations. In their work they applied the spline finite strip method to investigate the stability and vibration behavior of piezoelectric composite plates. Work of G. H. Rahimi et al [35] was carried forward by A. R. Davoodinik et al [39] to study large deflection of tapered beam made of functionally graded material (FGM) with various laws of material gradation along the beam height. In their work, Davoodinik et al [39] used same method derived by Rahimi et al [35] with change in application.

Vibration analysis of an FGM is a very tedious work to do. There is a considerable am ount of mathematical intricacies in deriving a suitable governing equation to find out natural frequencies of a FGM beam under mechanical as well as thermal loading conditions. Two important works were done by two authors in the year of 2011 on vibration analysis of functionally graded beams. H. Hein et al [40] studied free vibration of a non-uniform and axially functionally graded beam with various boundary conditions. In their analysis they investigated vibrations of FGM beams with varying cross-sections using Euler-Bernoulli theory and Haar wavelet matrices. Another work which was done vibration analysis of a FGM beam was work of A Mahi et al [41]. In their work they formulated a mathematical model with help of Higher Order Beam theory and Hamilton’s principle to

study temperature dependent free vibration of a FGM beam with Power Law and Exponential law of material gradation.

Mohanty et al. [42, 43] provided an analysis for the FG beam sitting on Winkler's foundation and the solution using the finite element approach. They then expanded their study to incorporate both static and dynamic stability. J. Reddy [44, 45] published a research paper in the same year of 2011 where, he developed a microstructure based non-linear Euler Bernoulli beam theory to register the effect of size of the microstructures in the functionally graded material. Another work was done on free vibration analysis of a tapered FGM beam in that year 2011. That work was done by Shahaba et al. [46]. In their work they studied free vibration and stability of FG tapered beam for first order shear deformation using finite element technique. Shahba did another work along with Rajshekharan [47] to study free vibration and stability of an Euler tapered FG beam using differential transform element method and the differential quadrature element. Two more works were done in 2012 on vibration analysis of FGM beam. Few governing equations of a geometrically non-linear FG beam were formulated and simplified to a single fourth order equation by Ma et al [48]. In their work they employed the shooting method to get the numerical solution of the equation for examining the pre- and post-buckling properties of clamped and simply supported FGM beams. Next year, that is, in the year of 2013 Loja et al [50] did a numerical analysis on functionally graded sandwich plate structures with piezoelectric skins. In their work they studied static and dynamic behaviours of FG sandwiched plates with piezoelectric skins using the B-spline finite strip technique.

Many more works were published in 2013 on dynamic analysis, like vibration analysis and buckling analysis, of straight and tapered FGM beam with various material gradation laws and under various loading and boundary conditions. Those works have been mentioned from reference number [51] to [57]. Analytical analysis of a FGM tapered beam was performed by D. K. Nguyen et al [51] to determine large deflection of the beam. S Rajshekharan [52] developed a differential transform based dynamic stiffness methodology to do vibration and buckling analysis of a functionally graded beam with non-uniform cross-section and having functional gradation along axial direction. In the same year he did another work [53] on the base of previous work to modify it for functionally graded tapered Timoshenko beams using differential transform-based quadrature method. In order to precisely define the form function in the finite element approach and to analyze the vibration behaviour of a rotating tapered AFG beam, Shahba et al. [54] employed the unit

dummy load method. The buckling and vibration behaviours of FG beams for both temperature-dependent and independent material parameters were investigated by Wattanasakulpong et al. [55]. H. Yaghoobi et al [56] studied analytically the influence of elastic foundation of a functionally graded beam on its large amplitude vibration and post buckling characteristics. D. G. Zhang [57] derived a neutral surface higher-order shear deformation beam theory based on non-linear von Karman stain-displacement relationship to do non-linear bending analysis of FGM beam. They solved the governing equation which they developed in their work by Ritz method to find bending stresses and deflections under various loading and boundary conditions.

Many authors published various important work on the analysis of tapered beam made of functionally graded materials in the year of 2014 [58-61]. A. Mitra et all [58] did a large amplitude vibration analysis of a tapered FGM beam subjected to a harmonic excitation where material variation was considered axially. D. K. Nguyen et al [59] extended his previous work [51] which he published in the year of 2013 to analyse a functionally graded tapered beam for large deflection with material variations along the thickness instead of axial functional gradation. He published another work in the same year of 2014 [60] where he considered end forces on the tapered FGM beam in addition to his previous works [51] & [59]. N T Nguyen et al [61] did static analysis of a functionally graded beam considering both axial and transverse variation of material gradation with respect to the axis of the beam with various loading and boundary conditions. They adopted Euler-Bernoulli beam theory in derivation of the governing equation for static analysis of FGM beams and in their mathematical model they considered power law of material gradation.

Few important researches were published on discs and plates [62, 63] made of functionally graded materials in the year of 2015. H. Çallıoğlu [62] published a work on elastic-plastic stress analysis of rotating disc made of functionally graded material with power law of material gradation. In their investigation they derived the governing equation for their problem considering the rotating velocity of the disc constant. They solved the governing equation with successive integration method and determined elastic as well as plastic stress distribution in the disc. They validated their analytical results with numerical ones which were determined using a FEA software ANSYS. They showed that both the results from analytical process and from software are in good agreement. Another work was reported in that year 2015 by A. Reali and H. Gomez [63] on structural analysis of thin

plate structures made of functionally graded material analytically. In their work they formulated a governing equation on basis of Eiler-Bernoulli beam theory and Kirchoff plate theory. To solve the governing equation the authors adopted Iso-Geometric Analysis (IGA) method where NURBS collocation technique used.

Few more works on FGM tapered beam [64,65] were registered in 2016. All these works were non-linear analysis under the subjection of dynamic loadings. Fang et al [64] performed a dynamic analysis of a rotating axially functionally graded tapered beam to study the effect of various design parameters like, hub ratio, taper ratio, rotational speed ratio, material gradient and rotary inertia on the natural frequency the tapered cantilever FGM beam. In their analysis the authors adopted Chebyshev-Ritz method to solve the problem. Lohar et al [65] also did a very important analytical analysis of an axially functionally graded taper beam to study the characteristic of free vibration of the beam considering it on an elastic foundation. In their work, Lohar et al adopted iterative scheme using relaxation parameters for static analysis and the dynamic part was formulated using Hamilton's principle. The free vibration frequencies were evaluated for different values of taper parameters and foundation thickness. Dimensionless frequency-amplitude surface plotted.

Few research works on analysis of various non-linear structures like variable section bar and beam, variable thickness plates, annular discs [66-69] in the time span of 2017 to 2018. In last few recent years, that is, from 2019 to 2023 miscellaneous work on FGM beams and plates [70-81] regarding dynamic analysis of FGM beam have been done and published in various renowned journals.

2.2.3 Research on FGM beams, plates, discs etc under thermo-mechanical loading.

The behaviours of FG beams in thermal conditions have been extensively studied due to the fact that ceramic-metal FG beams and plates perform best in high/severe temperature environments. It has been noted that the majority of these studies have taken into account the temperature gradient load (across the cross-section), presuming that the temperature distribution is linear or non-linear. One dimensional steady state heat transfer equation must be solved in order to generate a non-linear temperature distribution. There have also been a few situations documented when the temperature is assumed to rise uniformly throughout or to be distributed uniformly over the length. These investigations can be broadly divided into two categories: linked studies (also known as temperature-dependent properties, or

TD) and uncoupled studies (also known as temperature-independent properties, or TID). In the first scenario, material properties depend on both temperature and space; in the second scenario, however, they only change along space when the system's external temperature distribution overlaps.

As FGM structures like beam, plates and discs are readily chosen in the applications with high thermal environment, researches on analysis of FGM structures under thermal loading and thermo-mechanical loading and researches on studies of physical behaviour of FGM structures under thermal and thermo-mechanical loading always been a very important research subject of interest to various researchers. It has been noted that the majority of these studies have taken into account the temperature gradient load (across the cross-section), presuming that the temperature distribution is linear or non-linear. One dimensional steady state heat transfer equation must be solved in order to generate a non-linear temperature distribution. There have also been a few situations documented when the temperature is assumed to rise uniformly throughout or to be distributed uniformly over the length. These investigations can be broadly divided into two categories: linked studies (also known as temperature-dependent properties, or TD) and uncoupled studies (also known as temperature-independent properties, or TID). In the first scenario, material properties depend on both temperature and space; in the second scenario, however, they only change along space when the system's external temperature distribution overlaps.

Many researches on analytical as well as numerical analysis of various FGM structures like FGM bar, beam, plate and disc with material gradation along axial direction and/or transverse direction following material gradation laws under linear and non-linear loading and boundary conditions have been mentioned as reference in this present work. Reddy along with another researcher [82, 83] performed an analysis of a FGM plate made of metal and ceramic analytically under dynamic loading in a thermo-mechanical environment. To derive the governing differential equation for their analysis they used First Order Shear Deformation (FSDT) beam theory and von-Karman’s principle or law. To incorporate thermo-mechanical loading thermo-mechanical coupling was introduced in the formulation. They published their research in the year of 1997. Another two works on two different types of functionally graded structure were done [84, 85] in the year of 2002. One was done by B. V. Shankar and J. T. Tzeng [84] on analytical analysis of beams made of functionally graded materials with material gradation along the thickness of beams under thermo-mechanical loading. In their work they developed governing equations for their

problem taking Poisson's ratio constant and varying other material properties, mechanical as well as thermal, as per the exponential laws of material gradations along thickness of the beam. In the mathematical model they considered variation of temperature across the thickness also exponential. To find out distribution of thermal stresses and deflections in the beam they solved the derived thermoelastic equilibrium equation in closed form. In the same year H. S. Shen [85] did a non-linear bending analysis of rectangular plate made of functionally graded material with material gradation along its thickness. The boundary condition was considered as simply supported and two types of loading was considered in their analysis. One uniformly distributed transverse load and another one sinusoidal varying load in a thermal environment. The material properties were assumed temperature dependent. To develop the mathematical model of the problem they used Reddy higher order beam theory and the differential equations thus formed were solved by a mixed Galerkin-perturbation method. Sundararajan et al. [86] published a work in 2005 non-linear flexural analysis of a functionally graded rectangular skewed plate. In their work they investigated the vibration analysis of FGM plates utilizing TD material characteristics and von Karman non-linearity. A non-linear temperature distribution was also assumed and the effective material properties were calculated using material grading using the Mori-Tanaka method. Another important work was done by S. R. Li et al [87] on thermal post buckling of FGM beam in the frame work of Timoshenko beam theory in next year i.e., in 2006. The authors took into account the effect of shear deformation using geometrically non-linear formulation in the derivation of the governing equation. The beam was subjected to both mechanical and TID thermal loading with temperature distribution profile being non-linear. Tahani et al [88] developed a layer wise theory to determine analytically deflection and stress distribution of a functionally graded plate under cylindrical bending load in a thermal environment. The authors considered power law of material gradation along the thickness of the plate. They published their paper in 2009. In the very next year Kiani et al [89] reported a work on buckling analysis of a functionally graded beam with power law of material gradation across the beam thickness under subjection of various types of thermal loadings and boundary conditions. Three types of thermal loadings were considered. Uniform temperature rise, Linear and non-linear temperature distribution. The boundary conditions which were considered are Clamped, Roller and Simply-supported. To formulate their problem, they adopted Euler-Bernoulli beam theory and solved them by successive integration method in closed form using various boundary conditions.

In order to achieve precise solutions to the buckling problem, Ma has extended their work which they published in 2012[48] to [90]. In their previous work [48], they analysed a shear deformable FGM beam for non-linear static response under mechanical loading only. In work [90], they modified their mathematical model to measure non-linear response under in-plane thermal loadings. Fallah et al [91] reported a work on buckling analysis and non-linear vibration analysis of a FGM beam under thermo-mechanical loading and constrained with an elastic foundation.

For use in sensors and actuators, a different class of FG materials composed of piezoelectric components offers improved dependability and efficiency. Another pertinent field of research is the behaviour of beams composed of FG piezoelectric (FGP) material for specialized applications, such as MEMS. Fu et al. [92] investigated how the FG Euler beam behaved under thermal piezo-electric load in terms of buckling, stability, and free vibration characteristics with nonlinear temperature distribution and temperature-dependent material parameters.

Few works were done by Zhang et al [93], Kani et al [94] and Niknam et al [95] in the year of 2014 on non-linear analysis of FGM beams with constant as well as varying cross-section under mechanical and thermal loading both. In 2026 Paul et al [96], Y. Sun et al [97] and P. Nayak et al [98] did some important work on non-linear post buckling analysis of FGM beams resting on elastic foundations. A non-linear post buckling analysis for temperature-dependent properties and non-linear temperature distribution was reported by Paul and Das [99]. Broyden's algorithm was used by the authors to incorporate the non-linear part of the solution. Various combinations of FGMs were chosen for a comparative analysis. The impact of boundary conditions on the stability of FGM beams with uniform and linear temperature gradients across the cross-section was studied by Nasirzadeh et al. [100]. They simultaneously investigated the thermal and electrical fields' stability criteria for FG beams, reporting their findings over a range of end circumstances and power law indices. Temperature-dependent material properties were taken into consideration in Majumdar and Das's [102] study of thermal buckling under temperature load of clamped beams for both linear and nonlinear temperature distribution across the beam height. An algorithm for solving the nonlinear governing equation by an iterative approach to find critical temperature was succinctly explained. A mathematical model was presented by A Paul et al [103] which one was an improvement on the previously available mathematical models for post buckling analysis of a tapered FGM beam subjected to a heat load

corresponding to uniform temperature rise and steady state heat conduction. P Nayak et al [104] published a research paper in the year of 2020 containing a non-linear analysis of a rotating FGM disc to represent elastic-plastic front of that rotating FGM disc. In their work they considered two materials as constituent particles of FGM, one ceramic another metal where variation of composition of those constituent particles followed the power law of material gradation. They used Principle of Stationary total Potential (PSTP) and Hencky's deformation theory to formulate the governing equation of the problem.

In the year of 2020 a very innovative work was published by D Mahapatra et al [105] on thermo-mechanical analysis of FGM beam using a unified Timoshenko beam theory under the action of mechanical and thermal load both. In their work they followed the work of X. F. Li [33] to derive the governing equations to measure deflection and stress of the FG beam by unifying the elementary governing equations in term of a single parameter 'F'. The authors used Timoshenko beam theory following the path of elasticity method to derive the governing equation. B-spline collocation method was adopted to solve the governing equation. Authors followed various boundary conditions and temperature distribution for the analysis. Few more works published by Nayak et al [106] and R. Javatheri et al [107 & 108] in the same year on non-linear analysis of FG Beams under thermo-mechanical loadings.

2.2.4 Numerical analysis using B-spline collocation method.

As per the above discussion it is evident that various researchers have adopted different techniques, analytical or numerical, in solving the governing equations representing any problem of linear or non-linear analysis of FG beams under mechanical or thermo-mechanical loadings. Different types of numerical methods are there like B-spline Collocation method, NURBS based Iso-geometric method, Galarkin method, FEA method etc. Among all these methods, the most popular numerical method has been the finite element method. The B-spline collocation technique has been employed more frequently in recent years to solve structural issues as well. B-splines are commonly used because of their adaptability and computational effectiveness. In comparison to the Finite Element Method, the collocation technique is much simpler and easier to use for a wide range of differential equation problems. In the following discussions works of few researchers have been mentioned who have adopted B-spline collocation method to solve

governing equations of various FG been analysis problem under mechanical as well as thermal loadings.

Few works on some problems other that analysis of an FG Beam using B-spline collocation [109-111] have been referred in this present work. Chawla et al [109] published a paper in the year of 1975 where he used B-spline collocation method to solve one dimensional heat and mass transfer problem. He published another paper [110] in 1979 where he solved a governing differential equation representing a radiation problem using B-spline collocation method. Another researcher named G Fairweather [111] examined the effectiveness of the spline collocation techniques in solving a differential equation representing governing equation of any boundary value problem. Patlashenko [112] studied the solution process of various one dimensional linear and nonlinear problems under thermal as well as mechanical loadings using cubic B-spline collocation method. Efficiency and accuracy of B-spline collocation method was proved very satisfactory. In [113] Patlashenko extended his work to nonlinear analysis of two-dimensional problems like analysis of laminated panels with help of cubic B-spline collocation method. The spline strip approach was employed by Mizusawa et al. [114, 117] to investigate the vibration properties of thick laminated cylindrical panes and cross-ply laminates. In 1995, Bert et al. [116] applied the method of spline collocation to find approximate solution in statics analysis of beams and plates. Sun et al. [118, 136] reported the application of B-spline collocation to problems of linear elasticity using orthogonal cubic B-spline functions. Kadalbajoo and Yadaw [125, 130] reported a work on comparison study between the B-spline collocation technique, the Finite Element analysis, and the Finite Difference techniques for a two-parameter singularly perturbed boundary value problem. The B-spline collocation method provided better approximation and convergence than the other two techniques. As a general rule, we can assume that for relatively simple geometries like beams and plates, B-spline collocation might be favored. A thorough examination of the literature pertinent to the B-spline collocation method has been covered separately later in this chapter. Wu et al. [124] examined the impact of a non-uniform knot span in the spline collocation procedure applied to a structural problem. The author applied the same concept—radial spline functions—to beam problems and demonstrated that non-uniform knot spacing provides a better approximation. Due to its tendency to diminish the spline's continuity at the knots, multiplicity of the knots could be considered an extra parameter in the study. Vibration analysis of non-uniform beams supported on elastic foundation and of

pre-twisted beams using spline collocation with uniform knot span has been carried out by Hsu [126, 127]. The effect of multiple knots in a structural problem is considered by Provatidis [135] through finite element analysis using cubic B-spline shape functions. Recently, Isogeometric (IG) analysis [137] (using NURBS, which is a refined formulation of B-splines, as shape functions) is increasingly attracting researchers for finding approximate solutions to complex problems. Auricchio et al. [128] have reported the applications of IG collocation technique and applied it to theoretical analysis of many mathematical problems

It is very much difficult to analyze FG beam and beam with various dimensional discontinuities under different types of loadings through analytical formulation process and numerical solution methods. The best alternative method for this case is solving problems of complicated geometry with any FEA software by using its programming module. Many authors have adopted this method [139-142] to solve problems like determination of stress intensity factor (SIF) of any FG beams and plates with various dimensional discontinuity under linear and non-linear loading. Bhandari et al [139] analyzed a FG plate with various material gradations under uniformly distributed static loading using a FEA software in its programming module and published their work in the year of 2013. In 2008 Liu et al [140] reported a systematic approach of FEA analysis of any FGM component through the development of voxels. Ahmed Hassan et al [141] did a work on FEA analysis of an FG object by writing a FEA program and published their work in the year of 2022. In recent year of 2023 Shehab M. B et al [142] did an investigation on free vibration of a cracked FG plate analytically using a mathematical software and also solved the problem through finite element analysis method using a FEA commercial software. They validated the results they got through analytical method using a mathematical code with the results received from FEA analysis using a FEA software.

2.3 Closure

In the above literature review parts of the field of FG beams and FG materials as a whole have been extensively studied. In this review various types of works pertinent to the modeling of different FG structures like FG beams, plates etc and their analysis under various loading and boundary conditions have been compiled. Based on a thorough investigation of the literature, it is believed that gaps still exist in the knowledge related to the formulation of governing equation for more accurate analysis of FG structures with more complexities in structure's topology and functional gradation along with complicated loading and boundary conditions. Additionally, there is a perceived need for techniques to determine whether certain FGM combinations are appropriate for a given application, particularly when thermomechanical stress conditions are present. Furthermore, there aren't many research that address how tapered FG beams behave in hot environments. Therefore, a thorough stress and deformation analysis is required in order to propose design solutions for the development of dependable and sustainable mechanical components. The current study's attempt to examine the stress and deformation of functionally graded Timoshenko beams in a thermo-mechanical environment—with a uniform and tapered section—will undoubtedly help to underpin the design procedures.

Chapter 3: **Fundamental Concepts, Theories and Principles**

3.1 Introduction

Since beams are an essential component of almost all buildings, a thorough examination and synthesis of them is crucial to the overall design of the structures. The various beam models that have been put forth over the past 200 years have enabled design engineers to satisfactorily address a large range of significant structural issues. In beam design, Euler's 1-d beam theory (Classical theory) from the 17th century is still in use. The advancement of sophisticated beam theories has made it possible to build thin-walled beams and complex geometries with acceptable accuracy, opening up new design possibilities for designers. The investigation of the additional difficulties associated with geometrical and material non-linearities is made possible by the higher order beam theories. Nevertheless, in order to achieve the appropriate degree of accuracy, solving these theories involves extensive computations. Therefore, the design engineer carefully considers the available theories in order to strike a balance between the computational demands and the accuracy needed for any given application.

The development of new materials, particularly composites, which offer high strength/stiffness-to-weight ratios for beams has opened up research on the micro- and macro-mechanics of these materials and the related lamination theory for beams and plates. The lamination theory is a modified version of the extended beam theory that takes into account the sequential arrangement of laminates, plies, and layers of materials. This comprises the parameters for axial stretching and twisting in conjunction with bending stiffness. In the final decades of the 20th century, a number of studies on the creation of ideas regarding the behaviour of composite beams and plates were documented in the literature.

The idea of functionally graded materials originated from composites' incapacity to withstand harsh thermo-mechanical conditions. In the setting of smooth modulation of material properties, better beam theories are required for the use of functionally graded materials in beams and plates. It makes obvious sense that FGM-based beams would function similarly to infinitely layered laminated composite beams. Therefore, all that would be needed for the mathematical treatment of FG beams would be a mathematical treatment of the current composite beam/plate theories.
Recent technology advancements have enabled high-speed computer capabilities to support

engineering analytical processes, which call for higher precision in less time and money. Mathematicians and researchers are working to improve the precision of currently available approaches or to develop new ones. Due to the complexity of the geometries and related non-linearities, exact solutions to the engineering challenges are not achievable. But as computing power increases, accurate approximations within a reasonable practical range can be produced, even in complex circumstances. One of the widely used approximation techniques for analysis and design is the finite element technique. There are further approaches such as spectral element method, boundary element method, and finite differences. Because they are easy to use, collocation methods are often used to provide numerical approximations to governing equations.
A differential equation is satisfied, to a certain degree of tolerance, at a limited number of locations known as collocation points in a collocation method. The foundation of a collocation approach is assessing a differential equation's accuracy at a limited number of collocation locations. This technique's primary benefit is its low computational cost and ease of use. However, this technique's application is limited to a relatively confined area due to its low level of precision.

The collocation technique becomes more accurate and appropriate for numerical solutions of complicated governing equations when B-splines are used as approximation polynomials. It has been noted that the application of the B-spline basis function collocation technique to engineering issue solving is growing. B-splines are very well suited for curve fitting applications because of their superior local control and smoothness at the interface characteristics. The objective is to link the low computing cost of collocation with the improved accuracy and smoothness of B-spline basis functions.

It has been noted that there is comparatively very little use of B-spline collocation in obtaining approximations for higher order structural issues. Additionally, there is a strong belief that this technique can be highly useful in providing more precise solutions to structural analysis difficulties.

An innovative approach to the formulation of FG beams has been covered in this chapter. In order to condense the three governing equations into a single equation, Li [27 & 33] suggested taking into account an independent parameter linking the displacement variables. The resulting simplified differential equation resembles the classical beam equation quite a bit. This chapter also includes an in-depth introduction to the B-spline

collocation approach, demonstrating its usefulness in solving structural issues. There have also been discussions of a few case studies to investigate the applicability of this technique to well-established structural challenges. In-house mathematical code and its subroutines have been created to quickly get and analyse the results.

3.2 Modelling of a Beam

A vital part of the majority of structures are beams. These structural components provide resistance against bending as a result of applied loads. Beams are typically made of long, prismatic bars with normal loads applied to the bars' axes. A beam's load carrying capacities are determined by first analyzing the equilibrium needs for the beam as a whole, and then analyzing a portion of the beam for equilibrium conditions. The statics principles are necessary for the analysis of the forces. Thus, specific criteria related to geometry, loading, and material behaviour must be selected in order to construct a beam and monitor the stress distribution inside it as a result of the applied load. Numerous beam models have been used in the past to address engineering issues [148] and offer the kind of reliable, accurate forecasts that are necessary for design. A thorough examination of beam modelling has been covered in the following discussion.

To analyse a beam problem any one of the following two approaches may be adopted.

- *Mechanics of solids approach (elementary)*
  - It uses an assumed deformation mode/ strain distribution and hence yields average stress at a section under a given loading
  - It treats each type of loading separately viz. axial, bending, torsion etc.
  - It is derived under a number of assumptions hence valid for slender members/ restrictive conditions
- *Theory of elasticity approach (refined)*
  - It is general approach valid for any type of external loading with lesser simplifications, requires less intuition/ experience to solve and is nearer to exact/ real distribution of displacement, strain and stress.
  - It is preferred when critical design constraints like minimum weight, minimum cost etc.

All physical problems can be described or presented by a differential equation which is called as governing equation of the problem. These differential equations are

produced in the framework of structural mechanics by integrating the constitutive law, equilibrium equation, and kinematics relationship—the three fundamental equations of continuum mechanics. A partial differential equation is created by combining the kinematics equation (i.e., the relationship between strains and deformations), the constitutive equation (i.e., the relationship between stresses and strains), and the equilibrium equation (i.e., the relationship between the internal reactions and the external loads). Figure 3.1 below represents the steps which are followed to establish the Governing equation of any physical problem along with its solution procedure.

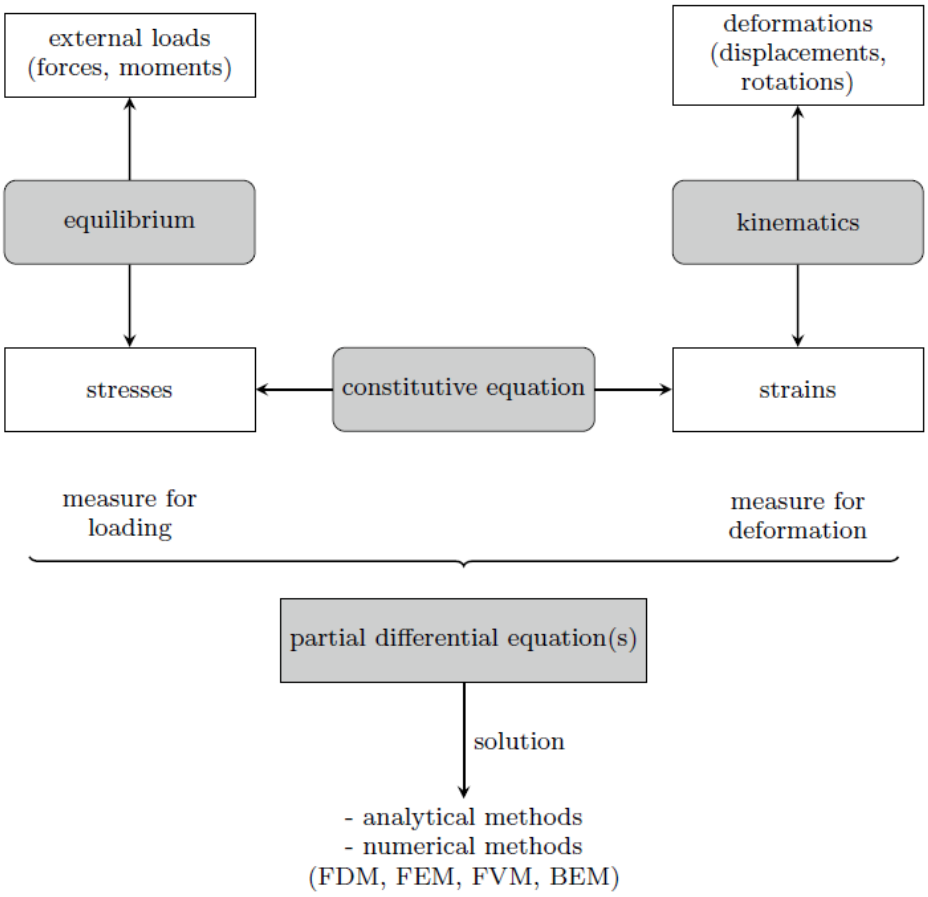

Fig. 3.1: Flowchart to solve a physical problem [155]

In solving a structural problem its material model plays an important role. if we are looking at a three-dimensional beam problem, we must consider six stress components, six strain components, and three displacement components—a total of 15 quantities. In addition to meeting the boundary requirements, these parts also need to meet 15 governing equations that are distributed throughout the body: six stress-strain relations, six strain

displacement relations, three equations of equilibrium, and six equations of compatibility (the latter are derived using the strain displacement relations, so they are excluded). A three-dimensional beam problem may have an extremely complex and challenging direct solution. Therefore, it is wise to simplify the examples by making them two-dimensional. In this sense, there are two different kinds of formulations: plane strain and plane stress. Plane strain analysis, or the latter method, is used to analyse beam difficulties.

To analyse a slender body where other dimensions are very small with respect to the length, generally plain strain model of material property is considered. As the length is very long, it is reasonable to assume longitudinal stain ε_{zz} is zero. So also γ_{xz} and γ_{yz} are zero. Thus, only non-zero strains are ε_{xx}, ε_{yy} and γ_{xy}. The stress-strain constitutive relation for a linear elastic isotropic material under such pre-strain condition is given by

$$\begin{Bmatrix}\sigma_{xx}\\ \sigma_{yy}\\ \tau_{xy}\end{Bmatrix} = \frac{E}{(1-2\nu)(1+\nu)}\begin{bmatrix}1-\nu & \nu & 0\\ \nu & 1-\nu & 0\\ 0 & 0 & \frac{1}{2}-\nu\end{bmatrix}\begin{Bmatrix}\varepsilon_{xx}\\ \varepsilon_{yy}\\ \varepsilon_{xy}\end{Bmatrix} \tag{3.1}$$

Few examples of plain-strain conditions are like bending and torsion of a long shaft which has been schematically represented by figure 3.2 below.

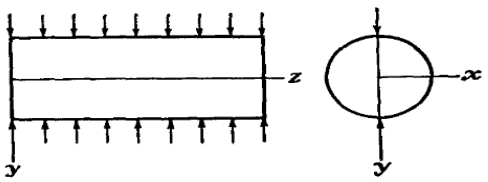

Figure 3.2: Plane Strain Case [151]

3.3 Beam Theories

Many beam models have been formulated over the past two centuries to analyse a variety of structural problems regarding beam design. These beam models are mostly differentiated by the degree of approximations and assumptions made.

3.3.1 Euler-Bernoulli Beam Theory (EBBT)

First widely acceptable beam theory was formulated by Euler and Bernoulli. This beam theory is popularly known as Euler Bernoulli Beam Theory (EBBT) which also called as

Classical Beam Theory (CBT). This beam theory is mainly applicable for long prismatic body derivation and application of which is restricted to the following assumptions

- No deformation in the cross-section, that is cross-section remains rigid after deformation.
- Rotation of cross-section occurs about the neutral axis,
- Neutral surface and the cross-section remain perpendicular to each other after bending,

The classic theories of beam bending distinguish between shear-rigid and shear flexible models. The thin or Euler-Bernoulli beam, also known as the shear rigid-beam, ignores the shear deformation caused by shear forces. According to this theory, as shown in Fig. 3.3, a cross-sectional plane that was perpendicular to the beam axis prior to the deformation continues to be so in the deformed condition.

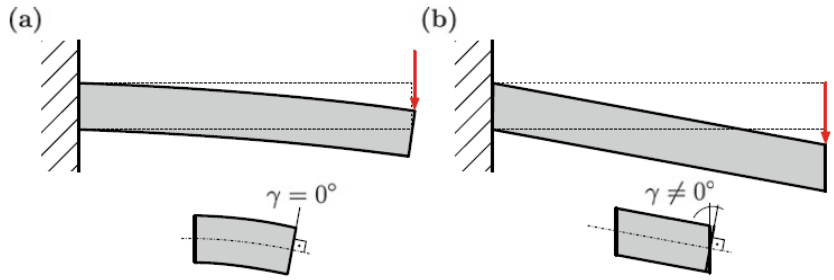

Figure 3.3 Different deformation modes of a bending beam: a shear-rigid; b shear-flexible [155]

According to the first hypothesis, no in-plane deformations are accounted for and, therefore, the in-plane displacements 'v' and 'w' depend upon the axial coordinate 'x' only. This means:

$$\left.\begin{aligned} \varepsilon_{yy} &= \frac{\partial v}{\partial y} = 0 \\ \varepsilon_{zz} &= \frac{\partial w}{\partial z} = 0 \\ \gamma_{yz} &= \frac{\partial v}{\partial z} + \frac{\partial w}{\partial y} = 0 \end{aligned}\right] \tag{3.2}$$

On the basis of the second hypothesis, the out-of-plane or axial displacement $\bar{u}$ is linear versus the in-plane coordinate i.e., $\bar{u} = u + y\phi_z + z\phi_y$, where ϕ_y and ϕ_z are the rotation angles along the y- and z-axis respectively and u is the in mid-plane stretching. It

can be observed that plane (AOB) after deformation will have two types of motion: one is translation in downward direction, w(x) and other is rotation, ϕ_y.

On the basis of the third hypothesis and according to the definition of shear strains, shear deformations γ_{xz} and γ_{xy} are also disregarded i.e., $\gamma_{xz} = \gamma_{xy} = 0$, hence:

$$\begin{bmatrix} \gamma_{xz} = \dfrac{\partial u}{\partial z} + \dfrac{\partial w}{\partial x} = \phi_y + \dfrac{\partial w}{\partial x} = 0 \\ \gamma_{xy} = \dfrac{\partial u}{\partial y} + \dfrac{\partial v}{\partial x} = \phi_z + \dfrac{\partial v}{\partial x} = 0 \end{bmatrix} \Rightarrow \begin{bmatrix} \phi_y = -\dfrac{\partial w}{\partial x} \\ \phi_z = -\dfrac{\partial v}{\partial x} \end{bmatrix} \tag{3.3}$$

If loading is constrained in the x-z plane, the deflection along y direction is negligible, then $\bar{u} = u + z\phi_y$, hence:

$$\bar{u}(x) = u - z\frac{dw}{dx} \tag{3.4}$$

We can then deduce that v=0 since there is no relative motion transverse to the x-z plane. Nonetheless, because the cross-sectional plane stays rigid, the third variable, or displacement along the z-direction, w(x), is independent of the z-coordinate. It suggests that every layer will have the same vertical displacement with respect to the neutral axis and that the bending deformation is mostly dependent on the bending of the beam's centre line. In accordance with EBBT, the three displacement variables are:

$$\begin{bmatrix} \bar{u}(x) = u - z\dfrac{dw}{dx} \\ \bar{v}(x) = 0 \\ \bar{w}(x) = w \end{bmatrix} \tag{3.5}$$

According to EBBT the strains are limited to axial direction only; hence the axial strain will be given by:

$$\varepsilon_{xx} = \frac{d\bar{u}}{dx} = \frac{du}{dx} - z\frac{d^2w}{dx^2} \tag{3.6}$$

The axial stress, σ_{xx} is calculated from axial strain using the constitutive equation:

$$\sigma_{xx} = E\varepsilon_{xx} = E\left(\frac{du}{dx} - z\frac{\partial^2 w}{\partial x^2}\right) \tag{3.7}$$

The stress resultants are obtained by integrating the axial stress over the cross-section:

$$\sigma_{xx} = E\varepsilon_{xx} = E\left(\frac{du}{dx} - z\frac{\partial^2 w}{\partial x^2}\right) \tag{3.8}$$

(i) Axial force (N_x):

$$N_x(x) = \int_A \sigma_{xx} dA = \int_A \left(E\left(\frac{du}{dx} - z\frac{\partial^2 w}{\partial x^2}\right)\right) dA \tag{3.9}$$

(ii) Bending Moment (M_x):

$$M_y(x) = \int_A z\sigma_{xx} dA = \int_A \left(zE\left(\frac{du}{dx} - z\frac{\partial^2 w}{\partial x^2}\right)\right) dA \tag{3.10}$$

For an isotropic beam integrating Eq. 8 & 9 will give:

$$\left.\begin{aligned} N_x &= EA\frac{du}{dx} \\ M_y &= -EI\frac{\partial^2 w}{\partial x^2} \end{aligned}\right] \Rightarrow \begin{aligned} \frac{du}{dx} &= \frac{N_x}{EA} \\ \frac{\partial^2 w}{\partial x^2} &= -\frac{M_y}{EI} \end{aligned} \tag{3.11}$$

Substituting the above Eq. 10 in Eq. 7 we get:

$$\sigma_{xx} = \frac{N}{A} + \frac{M_y z}{I} \tag{3.12}$$

which is the traditional bending equation.

Euler Bernoulli beam theory, however, is riddled with contradictions. It is evident from Eq. 1 that even in the absence of a transverse force in that direction, the normal stress σ_{yy} is not zero. Furthermore, since transverse shear strains are taken to be zero, this theory produces a value of zero for τ_{xz}. When the aspect ratio (L/h) is large, this assumption does not result in substantial inaccuracies; nevertheless, for smaller aspect ratios (L/h), the amplitude of shear stresses is extremely considerable and may not be disregarded. As a result, the Timoshenko beam theory, which takes into account shear strain in the transverse direction—was created. Figure 3.4 below represents how Timoshenko beam theory has been developed by superimposing Euler-Bernoulli beam theory and shear deformation.

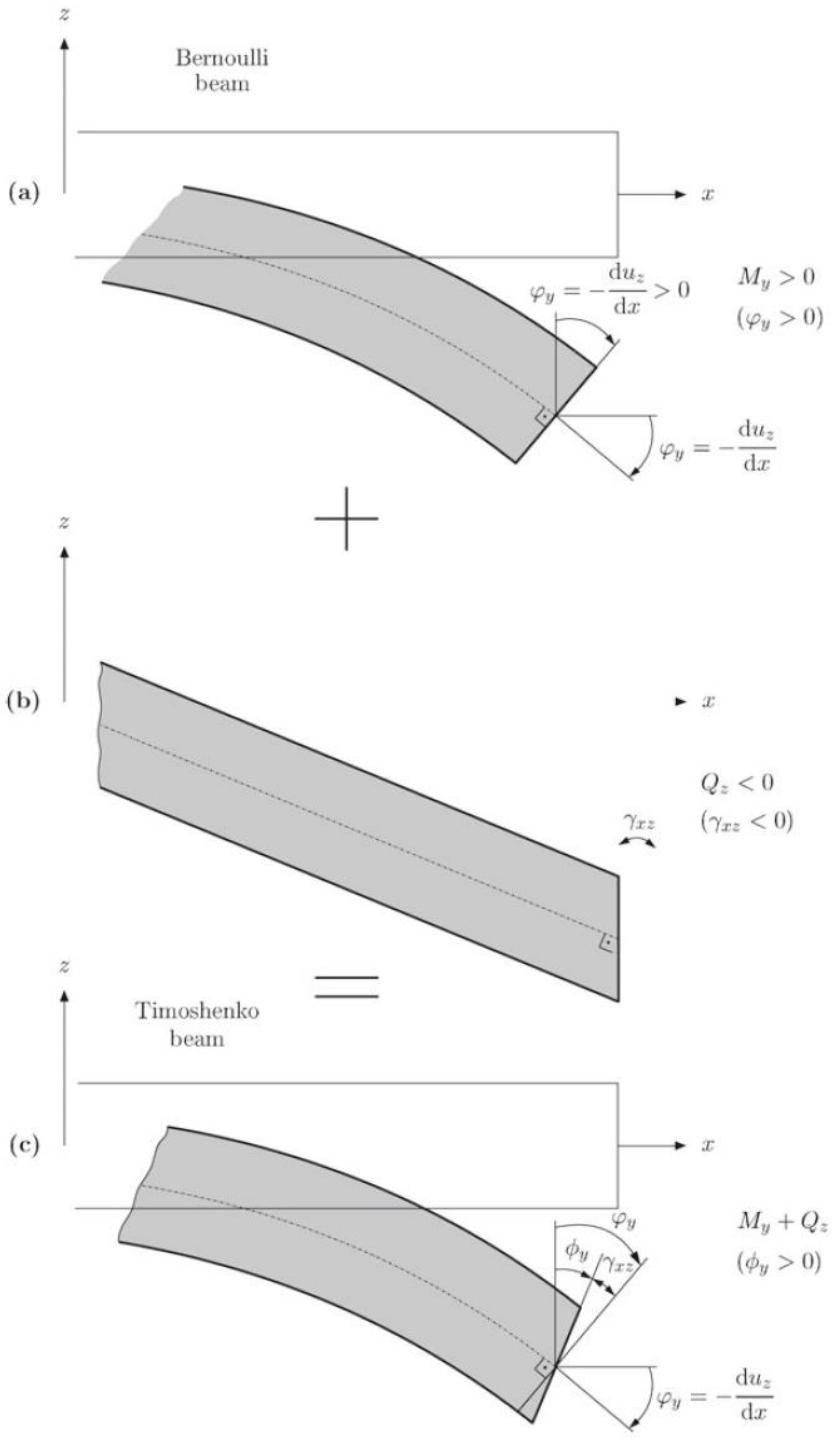

Figure 3.4 Superposition of the Euler–Bernoulli beam (a) and the shear deformation (b) to the Timoshenko beam (c) in the x-z plane [155]

3.3.2 Timoshenko Beam Theory (TBT) or First Order Shear Deformation Theory (FSDT)

Timoshenko beam theory considers the influence of shear deformation along with the axial deformation which has been mentioned in the preceding section. According to

Timoshenko beam theory, a transverse plane rotates more by shear deformation (Fig. 3.4) than it does in EBBT because of the additional shear deformation of the plane. Thus, there may be a relationship between the shear angle, plane rotation, and the slope of the beam's midline:

$$\phi_y = -\frac{dw}{dx} + \gamma_{xz} \tag{3.13}$$

Hence the axial deformation in the axial direction will be given by $\bar{u} = u - z\phi_y$, where ϕ y denotes the rotation of the cross section about the y-axis (see Fig. 3.4). It is assumed in Eq. 3.10 that shear strain and corresponding shear stress are uniform throughout the cross-section and that they are the same at all points. This is not possible, particularly if external loading is applied only to the top surface and there are no loads at the bottom. A proper shear correction factor value, which will be covered later in this section, is used to remedy this inaccuracy. Therefore, the Timoshenko beam's displacement variables are:

$$\left.\begin{aligned} \bar{u}(x) &= u - z\phi_y \\ \bar{v}(x) &= 0 \\ \bar{w}(x) &= w \end{aligned}\right] \tag{3.14}$$

From the strain-displacement relation:

$$\left.\begin{aligned} \varepsilon_{xx} &= \frac{d\bar{u}}{dx} = \frac{du}{dx} - z\frac{d\phi_y}{dx} \\ \varepsilon_{xz} &= \frac{1}{2}\gamma_{xz} \end{aligned}\right] \tag{3.15}$$

The axial and shear stress may be calculated from the constitutive relations:

$$\left.\begin{aligned} \sigma_{xx} &= E\varepsilon_{xx} = E\left(\frac{du}{dx} - z\frac{\partial^2 w}{\partial x^2}\right) \\ \tau_{xz} &= G\gamma_{xz} = G\left(\phi_y + \frac{dw}{dx}\right) \end{aligned}\right] \tag{3.16}$$

The axial force (N_x), bending moment (M_y) and Shear force (V_{xz}) can be written as:

$$N_x(x) = \int_A \sigma_{xx} dA = \int_A \left(E\left(\frac{du}{dx} - z\frac{d\phi}{dx}\right)\right) dA \tag{3.17}$$

$$M_y(x) = \int_A z\sigma_{xx} dA = \int_A \left(zE\left(\frac{du}{dx} - z\frac{d\phi}{dx}\right)\right) dA \tag{3.18}$$

$$V_{xz}(x) = \int_A \tau_{xz} dA = \int_A G\left(\phi_y + \frac{dw}{dx}\right) dA \tag{3.19}$$

Eq. 3.19 can be used to calculate the average shear force for a cross-section that can be used to calculate average shear stress developed in a plane; hence Timoshenko beam theory requires shear correction factors (k_s) to compensate for the error due to this constant shear stress assumption. The shear correction factors depend not only on the material and geometric parameters, but also on the load and boundary conditions.

3.3.3 Higher Order Shear Deformation Theory (HSDT)

Various beam theories are dependent on the fact that how distribution of shear stress in the cross-sectional plane of a beam is considered. This distribution of shear stress influences the deformation of beam. Euler-Bernoulli beam theory considers zero influence of shear stress on the deflection of the beam. In Timoshenko beam theory shear stress distributed uniformly over the cross-section of the beam. In Higher Order beam theories this distribution of shear stress happens according to the higher order polynomial. So, in summery we can say when distribution of shear stress on the cross-section surface is of first order then it is called as First Order Shear Deformation theory (FSDT). When this shear stress distribution is of second order then it is called Second Order Shear Deformation theory (SSDT). Likewise for third order distribution of shear stress on the cross-section is the base of Third Order Shear Deformation (TSDT) theory.

There are many higher order beam theories. The general expression of the axial displacement $u(x, z)$ as a function of domain variables x and z is as follows.

$$u(x, z) = u_0(x) - z\frac{\partial w_0(x)}{\partial x} + \Psi(z)\gamma_0(x) \tag{3.20}$$

Now $\Psi(z)$, which is known as a shape function, may have various expressions with respect to domain variable z according to various beam theories. Following table shown various expressions of shape functions $\Psi(z)$ for various beam theories.

Table 3.1: The shape functions $\Psi(z)$ for various beam theories [62].

Sl No	Beam Theories	Shape Functions
1	First order shear deformation theory (FSDT)	$\Psi(z) = z$
2	Second order shear deformation theory (SSDT)	$\Psi(z) = z\left(1 - \frac{z}{h}\right)$
3	Third order shear deformation theory (TSDT)	$\Psi(z) = z\left(1 - \frac{4z^2}{3h^2}\right)$

4	Trigonometric shear deformation theory (TrSDT)	$\Psi(z) = \frac{h}{\pi}\sin\frac{\pi z}{h}$
5	Exponential shear deformation theory (ESDT)	$\Psi(z) = ze^{-2(z/h)^2}$
6	Hyperbolic shear deformation theory (HSDT)	$\Psi(z) = h\sinh\left(\frac{z}{h}\right) - z\cosh\frac{1}{2}$

Now to depict the fact that how does cross-section of a beam take shape under loading according to the Euler-Bernoulli beam theory, Timoshenko beam theory and Third Order beam theory, following figures, that is figure no 3.5a, b & c have been presented below.

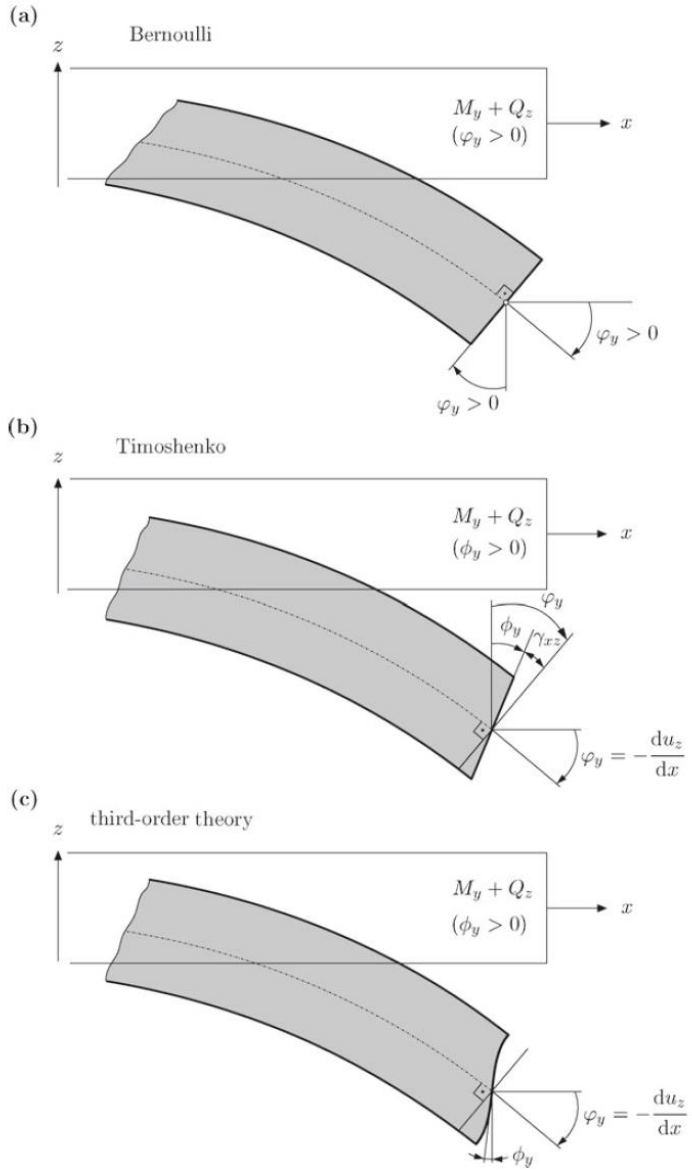

Figure 3.5 Comparison of different beam theories in regards to the deformation in the x-z plane: a) Euler–Bernoulli, b) Timoshenko and c) third-order theory. [155]

In the present work Third Order Shear Deformation Theory (TSDT) has been adopted and detailed of this Higher Order Beam Theory has been discussed in the following chapter.

3.4 Principle of Virtual Work

To establish the state of static equilibrium of any object under various loading and boundary conditions, principle of the virtual work theorem is the best way to express it. It serves as the foundation for the formulation of solids and structural problems and is the first variational concept in mechanics.

According to fundamental physics, virtual work is the sum of all the forces acting on a particle to cause a modest hypothetical displacement while maintaining constant force levels and taking into account all existing restrictions. The same idea can be used to a deformable continuous body, which is supposed to be a group of material particles subject to boundary conditions and with a continuous displacement field existing in the range of infinitesimal deformation. As a result, the total work done on the body is the sum of all the works done on its constituent particles. There are two sorts of this work: internal work resulting from the material structure itself, and external work caused by the applied loads. During the infinitesimal deformation, the applied loads stay constant, but the displacements caused by the external forces dictate the internal forces, which are determined by compatibility and constitutive relations. The algebraic total of internal and exterior work is zero, according to the virtual work principle. Operator δ represents the infinitesimal virtual displacement using the variational formulation. The following beam formulation problem provides a simplified explanation of the idea of virtual work using variational formulation for a continuous media.

Virtual work theorem can be expressed as $\delta W_{Internal} + \delta W_{External} = 0$ where $\delta W_{External}$ is the work done by an external load on the system or body under consideration. It is also known as potential energy of the body stored in. The strain energy which is stored in the body due to straining is denoted as $\delta W_{Internal}$. Now according to the Principle of Stationary Total Potential (PSTP) total energy will remain constant under the action of external forces which is stated or represented as follows.

$$\Pi = (U + V_P) = Constant$$
$$\Rightarrow \delta\Pi = \delta(U + V_P) = 0 \tag{3.21}$$

Here Π represents total energy, U represents strain energy and V_P represents potential energy. To discuss in detail the virtual work theorem let us consider a beam with arbitrary boundary conditions and loading as shown in Fig. 3.6 below.

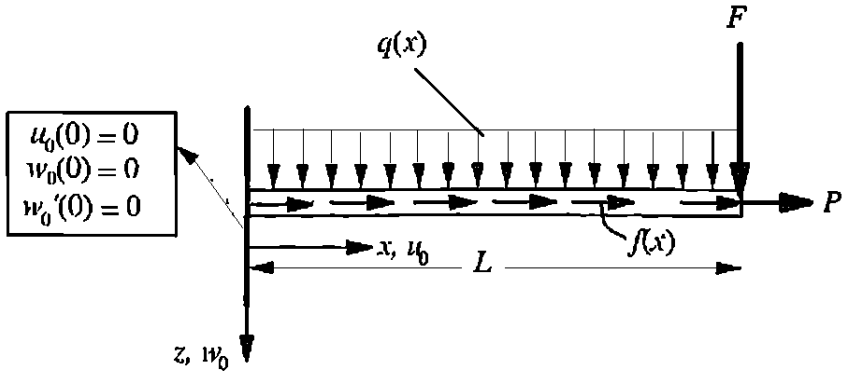

Fig. 3.6: Beam with arbitrary load and Boundary conditions [151]

Assuming one dimensional beam problem corresponding to EBBT, the internal strain energy and external work potential of the system can be written as:

$$U = \frac{1}{2}\iiint_V \sigma_{xx}\varepsilon_{xx}dV \tag{3.22}$$

$$V = -\left[\int_0^L (qw + fu)dx + Fw + Pu\right] \tag{3.23}$$

Using equation 3.21 we get

$$\delta\Pi = \delta U + \delta V = 0 \Rightarrow \iiint_V \sigma_{xx}\delta\varepsilon_{xx}dV - \left[\int_0^L \left(q\delta w + f\delta u\right)dx + F\delta w + P\delta u\right] = 0 \tag{3.24}$$

The first term of Eq. 3.24 can be simplified for a rectangular cross-section beam of constant width 'b' as:

$$\int_0^L\int_A \sigma_{xx}\delta\varepsilon_{xx}dAdx - \left[\int_0^L \left(q\delta w + f\delta u\right)dx + F\delta w + P\delta u\right] = 0 \tag{3.25}$$

Substituting for $\varepsilon_{xx}$and using Eq. 3.6 of EBB theory we get:

$$\int_0^L\int_A \sigma_{xx}\left(\frac{d\delta u}{dx} - z\frac{d^2\delta w}{dx^2}\right)dAdx - \left[\int_0^L \left(q\delta w + f\delta u\right)dx + F\delta w + P\delta u\right] = 0 \tag{3.26}$$

From Eq. 3.8 & 3.9

$$\int_0^L \left(N_x \frac{d\delta u}{dx} - M_y \frac{d^2\delta w}{dx^2} - q\delta w - f\delta u \right) dx - F\delta w - P\delta u = 0 \tag{3.27}$$

After rearranging the terms in accordance with the displacement variables, the above equation can be further reduced using integration by parts, leaving the following governing equations and boundary conditions for the Euler Bernoulli beam:

Governing Equations: for 0<x<L

a) for δu:

$$-\frac{dN_x}{dx} = f \tag{3.28}$$

b) for δw:

$$-\frac{d^2M_y}{dx^2} - q = 0 \tag{3.29}$$

Boundary conditions: at x=0 or x=L

Essential or kinematic boundary conditions		**Natural or force boundary conditions**
u prescribed	or	N_x=P
$\frac{dw}{dx}$ prescribed		M_y=0
w prescribed		V_{xy}=F

The above Eq. 3.28 & 3.29 can be substituted for N_x & M_y using Eq. 3.10 to obtain:

$$-\frac{d}{dx}\left(EA\frac{du}{dx} \right) = f \tag{3.30}$$

$$-\frac{d^2}{dx^2}\left(-EI\frac{d^2w}{dx^2} \right) - q = 0 \tag{3.31}$$

The conventional equation for beam bending that is used in foundational engineering classes is Eq. 3.31. As a result, we have seen that the virtual work method is a helpful tool for determining the governing equations and required boundary conditions. The

aforementioned formulas pertain to an isotropic substance possessing consistent physical characteristics. It is recognized that because this method starts with the most basic equilibrium equations, it will be useful in determining the beam equations for more complex scenarios such as material orthotropy or anisotropy, thermal gradients along length or height, simultaneous mechanical and thermal loading, variable cross sections, etc. The next chapter applies the virtual work concept to obtain the governing equations for a functionally graded material beam subjected to arbitrary boundary conditions. Presenting a description of the anisotropic behaviour and appropriate modelling of FGMs is relevant a priori in order to build a beam equation for FGMs.

3.5 Functional Gradation of Material

When an object is imposed with some loading subjected to a boundary condition the stresses induced in it greatly governed by the structural properties of the material of that object. So, discussion om material properties in detail are very much essential. Now material is of two types in broadest sense. One is natural material and other one is customized material. Most widely used customized material is composite material. Further composite materials are of two types. Fibrous composite material and particulate composite material.

Fibrous composite materials are made of various types of fibres bonded together by a matrix material. Whereas in particulate composite material the reinforcing material is particle of various materials. The particles here also bound by a matrix material also. Common examples of particulate composite material are Metal matrix Composite (MMC), Functionally Graded Material (FGM) etc. In the present work Functionally Graded Materials have been considered. So, a detailed discussion would be taken place on functionally graded material.

A functionally graded material is modelled by gradation of particles of various materials as per a pre-defined function. This process of functional gradation is mainly done by two ways- (i) by Rule of Mixture and by (ii) By Mori-Tanaka rule.

Rule of Mixture can be presented as follows:

$$P(z) = P_1 V_1 + P_2 V_2 = P_1 (1 - V_2) + P_2 V_2 \tag{3.30}$$

Where, volume fraction of the first particle is represented by V_1 and the second particle volume fraction is represented by V_2 which is equal to $(1-V_1)$. P_i are any material property of the constituent materials or particles.

Particularly appropriate examples for the Mori-Tanaka technique are those with a well-defined continuous matrix and a discontinuous particulate phase. The bulk modulus, B, and the shear modulus, G, are related using this method:

$$\left.\begin{aligned}\frac{B-B_1}{B_2-B_1}&=\frac{V_2}{1+(1-V_2)\frac{B_2-B_1}{B_1+\frac{4}{3}G_1}}\\ \frac{G-G_1}{G_2-G_1}&=\frac{V_2}{1+(1-V_2)\frac{G_2-G_1}{G_1+f_1}}\end{aligned}\right] \tag{3.31}$$

where $f_1=\frac{G_1(9B_1+8G_1)}{6(B_1+2G_1)}$ Once the values of B and G are calculated, they can be used to find Young's modulus and Poisson's ratio as below:

$$E=\frac{9BG}{3B+G} \tag{3.32a}$$

$$\nu=\frac{3B-2G}{2(3B+G)} \tag{3.32b}$$

The effective thermal conductivity, K and coefficient of thermal expansion, α are given by:

$$\frac{K-K_1}{K_2-K_1}=\frac{V_2}{1+(1-V_2)\frac{K_2-K_1}{3K_1}} \tag{3.33a}$$

$$\frac{\alpha-\alpha_1}{\alpha_2-\alpha_1}=\frac{1/B-1/B_1}{1/B_2-1/B_1} \tag{3.33b}$$

As previously stated, the aforementioned criterion ignores the specific phase interactions involved at the microstructural level in favour of bulk features. The effective qualities of FGMs fluctuate in the gradation direction because the volume fraction of each phase varies progressively in that direction. It is possible to suppose that the volume fraction will initially fluctuate continuously over the thickness in accordance with one of

three distributions: power law (P-FGM), sigmoid law (S-FGM), or exponential law (E-FGM).

According to power law the volume fraction is given by:

$$\left.\begin{aligned} P(z) &= P_1V_1 + P_2V_2 = P_1(1-V_2) + P_2V_2 \\ V_2(z) &= \left(\frac{z}{h}+\frac{1}{2}\right)^{\beta} \end{aligned}\right] \tag{3.34}$$

where β is the exponent of variation.

When a single power law function is applied in some circumstances (such as multi-layered composites), stress concentration occurs close to an interface where the material is continuous but changes quickly. In these situations, the volume fraction corresponding to two power law functions make the distribution of stress smooth. This kind of composition is known as the sigmoid function (S-FGM), and it is described as follows:

$$\left.\begin{aligned} V_2(z) &= \frac{1}{2}\left(1+\frac{2z}{h}\right)^{\beta} \; for\left(-\tfrac{h}{2} \le z \le 0\right) \\ V_4(z) &= 1-\frac{1}{2}\left(1-\frac{2z}{h}\right)^{\beta} \; for\left(0 \le z \le \tfrac{h}{2}\right) \end{aligned}\right] \tag{3.35}$$

The rule of mixture is defined for S-FGM as:

$$\left.\begin{aligned} P(z) &= P_1V_1 + P_2V_2 = P_1(1-V_2) + P_2V_2, for\left(-\tfrac{h}{2} \le z \le 0\right) \\ P(z) &= P_1V_3 + P_2V_4 = P_1(1-V_4) + P_2V_4, for\left(0 \le z \le \tfrac{h}{2}\right) \end{aligned}\right] \tag{3.36}$$

Another rule of mixture is there which is often preferred by many researchers and engineers due to its simplicity in formulation. This is known as exponential law of material gradation and is expressed as follows.

$$\left.\begin{aligned} P(z) &= Ce^{D\left(z+\frac{h}{2}\right)} \\ C &= P_2 \\ D &= \frac{1}{h} ln\left(\frac{P_1}{P_2}\right) \end{aligned}\right] \tag{3.37}$$

Above mentioned three laws of material gradation have been presented graphically in figures 3.7a, b, c below.

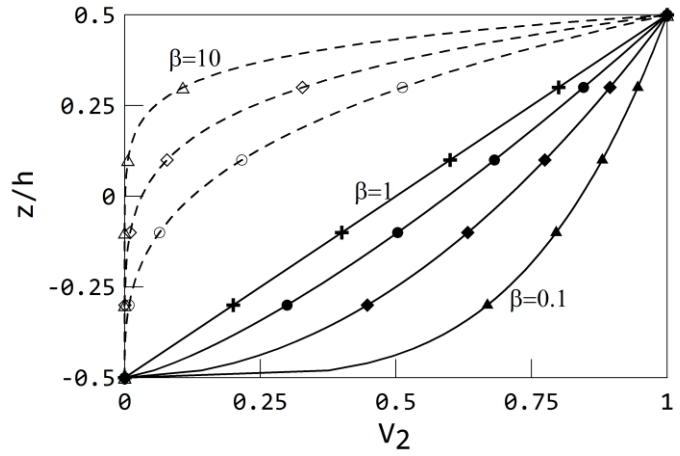

Fig. 3.7 (a)

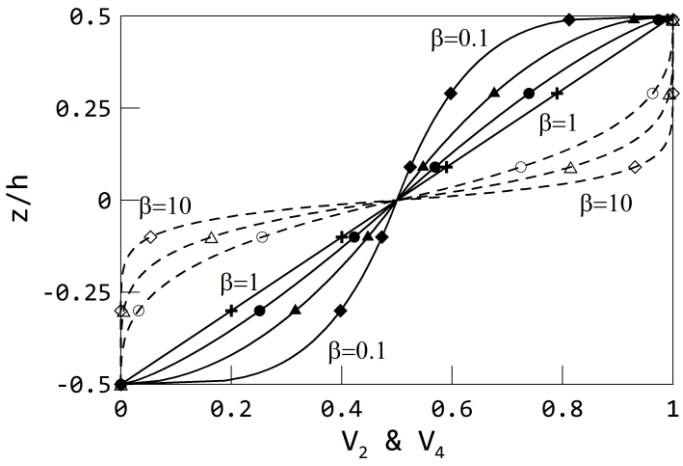

Fig. 3.7 (b)

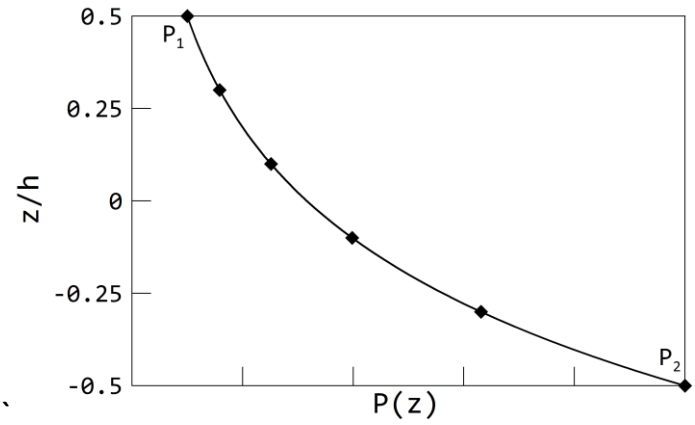

Fig. 3.7 (c)

Fig. 3.7: Various profiles for phase distribution a) P-FGM, b) S-FGM, c) E-FGM [144]

3.6 B-Spline Collocation Technique

3.6.1 B-spline basis function

The term Spline is originated from a flexible tool used by draftsmen and shipbuilders to draw curves via predetermined places known as knots in a way that makes the curve and its derivatives continuous even at the joints. The concept of spline was originally developed in the 17th century during the building of boats and ships. The lengthy curves on a boat were inscribed on wood using a thin, flexible steel or wood strip that was initially known as a spline. On a level surface, the spline is bent and secured in place by several hooked metal weights known as "ducks". This fact has been depicted in figure 3.8 below. The uniform stress distribution across the ducks contributes to the smoothness, which reduces the drag of the vessel in the water. The plotting of spline curves has been replaced by tools like "French curves," however ship prototypes still employ this method.

Figure 3.8: Hooked weights, called “ducks,” accurately secure a spline – here, no more than a thin strip of balsa – for tracing the hull of a sailing vessel. Source: Edson International [109]

Mathematically, higher degree polynomials that may be continuous over the domain and their derivatives are required if we have to trace a smooth curve. Higher degree polynomial expression handling, however, is costly and time-consuming. Thus, piece-wise polynomials were conceptualized. This indicates that many polynomials (of smaller degree) formed over sub-domains can approximate the function rather than utilizing a single polynomial for the full domain. We refer to these polynomials as piece-wise polynomials. The piece-wise polynomials have to be differentiable to some extent and sufficiently smooth at the connecting points. Spline curves have both of these characteristics.

B-splines are the most flexible and smooth among all the spline curve types, including cubic splines, Bezier curves, and B-splines. As a result, they work well as piece-wise polynomials in curve fitting. A spline function with minimal support in terms of a certain degree, smoothness, and domain partition is called a B-spline. The basis function of a B-spline is its fundamental component. It's depicted in the parametric space "t." They rely on a set of non-decreasing coordinates in parametric space known as a knot-vector and are described in terms of the order or degree of the curve. Given the knot vector, it is:

$$T = \left[t_0,\ t_1,\ t_2 \ldots\ldots,\ t_{n+k+1}\right] \tag{3.38}$$

where, n+1 = no. of control points and 'k' is order of the polynomial spline. The b-spline basis of 'k_{th}' order is defined recursively using the relation:

$$N_{(i,k)} = \frac{t - t_i}{t_{i+k-1} - t_i} N_{(i,k-1)} + \frac{t_{i+k} - t}{t_{i+k} - t_{i+1}} N_{(i+1,k-1)} \tag{3.39}$$

In order to use the above relation, we need to define the smallest basis function i.e. of first order:

$$N_{i,1} = \begin{cases} 1, t_i < t < t_{i+1} \\ 0, otherwise \end{cases} \tag{3.40}$$

Using (n+1) control points B0, B1... Bn, a B-spline function is defined as:

$$B(t) = \sum_{i=0}^{n} N_{i,k}(t).B_i \tag{3.41}$$

Since the B-spline equation above is parametric in terms of "t," a mathematical curve can be constructed by identifying the vertices' coordinates and using Ni,k as the basis or weighting function for the polygon. Standard textbooks contain information on the features of the B-spline basis; nonetheless, a few pertinent properties are briefly covered here.

The knot vector, T, the number of control points (n+1), and the order (k) of the b-spline basis function determine the nature of B-spline functions. A Bezier curve will closely resemble the final curve if the number of control points (polygon vertices) is equal to the order of the basis. On the other hand, the curve breaks out into several parts known as spans when the number of control points increases, providing the curve more local control and flexibility. Various B-splines with different Besis Functions have been shown in figure 3.9 below.

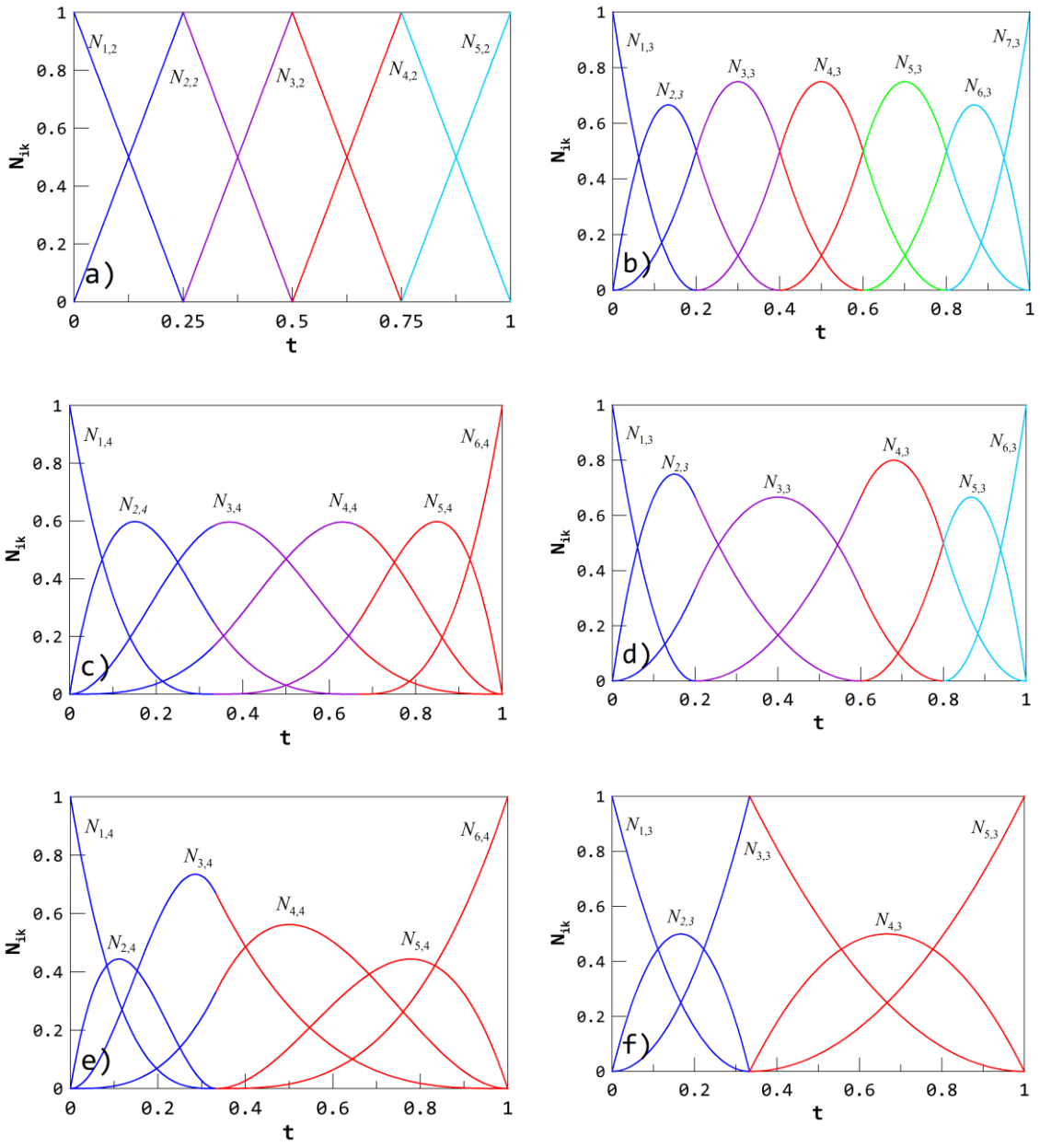

Figure 3.9(a-f) B-spline basis functions: open uniform and non-uniform type with various order and knot vectors [110]

Various Knot Vectors and Order Values corresponding to the above figures have been mentioned below.

Open-uniform	*a)*	*k=2*	*[0 0 1 2 3 4 4]*	*or*	*[0 0 0.25 0.5 0.75 1 1]*
	b)	*k=3*	*[0 0 0 1 2 3 4 5 5 5]*		*[0 0 0 0.2 0.4 0.6. 0.8 1 1 1]*
	c)	*k=4*	*[0 0 0 0 1 2 3 3 3 3]*		*[0 0 0 0 0.333 0.667 1 1 1]*
Open-non-uniform	*d)*	*k=3*	*[0 0 0 1 3 4 5 5 5]*	*or*	*[0 0 0 0.2 0.6. 0.8 1 1 1]*
	e)	*k=4*	*[0 0 0 0 1 1 3 3 3 3]*		*[0 0 0 0 0.333 0.333 1 1 1]*
	f)	*k=3*	*[0 0 0 1 1 3 3 3]*		*[0 0 0 0.333 0.333 1 1 1]*

A careful knot vector selection is always required because the knot vector has an impact on the final B-spline curve. Knot vectors can be classified as either periodic or open, with each type having a uniform and non-uniform variation. Only open uniform and open non-uniform knot vectors are taken into consideration in this study. An open uniform knot vector has many "k" knots at both ends and uniform spacing between them; non-uniform knots can have many knots in between in addition to the ends or inconsistent spacing. As may be seen in figure 3.9(a-f), non-uniform knot vectors result in poorer curve continuity. When plotting Figure 3.9f, the existence of several knots results in a discontinuity. For example, in Figure 3.9, each segment/span is represented by four spline functions. These basic functions are combined using the vertex coordinate through equation 4, and the number of polynomials is equal to the order of the spline. Equation 4 gives a B-spline curve of order k (polynomial of degree k-1) with continuous derivatives of order 1, 2, 3,..., k-2 over the whole curve [112]. The number of smoothness criteria between the segments at the interface will be given by: Suppose two 4th order B-spline curves are meeting at an interface (a knot). The 4th order curve is a 3rd degree polynomial. This example will help us grasp the continuity property of B-splines.

1	C^0	$B(t)_j=B(t)_{j+1}$
2	C^1	$B'(t)_j=B'(t)_{j+1}$
3	C^2	$B''(t)_j=B''(t)_{j+1}$
:	:	:
:	:	:
k-1	C^{k-2}	$B^{k-1}(t)_j=B^{k-1}(t)_{j+1}$

As a result, a 4th order (3rd degree) curve will have three smoothness requirements and be C_2 continuous throughout. For an open uniform knot vector, the aforementioned condition is true. The continuity of the B-spline curve, on the other hand, diminishes at interfaces if the knot vector is non-uniform and there are numerous knots; this is represented by C^{k-s-1}, where "s" is the number of knots at the interface. As a result, the number of smoothness criteria increases to k-s.

The resulting B-spline is divided into pieces or segments by the knot vector, or spline curve, which takes the shape of spans or segments when the number of control points exceeds the spline order. The number of spans in the knot vector equals the number of curve segments. Furthermore, the order, k, is equal to the number of non-zero basis functions in a given span. For example, if the spline has four orders and six control points, its three segments will match the knot vector [0 0 0 0 1 2 3 3 3 3], or 0-1, 1-2, and 2-3. Four explicit non-zero basis functions (polynomials) will correspond to each span, and only four control points will contribute to the curve formation for that span (and the other spans as well). With the help of matrix representation, this system is readily understood. Equation 3.41 can be expressed as follows:

$$B(t) = [B_i][N] \tag{3.42}$$

where [N] is a square matrix of order equal to number of control points, and [Bi] is the coordinate vector. For the 4th order b-spline considered above, the matrix [N] using equation 3.39 and 3.40 will be:

$$\begin{bmatrix} (1-t)^3 & 0 & 0 \\ \left(3t-4.5t^2+1.75t^3\right) & 0.25(2-t)^3 & 0 \\ \left(1.5t^2-0.9167t^3\right) & \left(4.5t-3t^2+0.5833t^3-1.5\right) & 0.1667(1-t)^3 \\ 0.667\,t^3 & \left(2.25t^2-0.5833t^3-2.25t+0.75\right) & \left(15.75t-6.75t^2+0.9167t^3-11.25\right) \\ 0 & 0.25(t-1)^3 & \left(-23.25t+11.25t^2-1.75t^3+15.75\right) \\ 0 & 0 & (t-2)^3 \end{bmatrix} \tag{3.43}$$

It is evident from the above that $B_1B_2B_3B_4$ will impact the first span while the other two points will not affect the first span; similarly, the other spans use $B_2B_3B_4B_5$ and $B_3B_4B_5B_6$ accordingly, if $[B_i]=[B_1B_2B_3B_4B_5B_6]$ to have a knot vector [0 0 0 0 1 2 3 3 3].

Figure 3.9 makes clear how flexible the B-spline basis is. However, the following conditions [112] can be used to regulate the flexibility of the resulting B-spline curve using these basis functions in equation 3:

a) By changing basis function types and knot vector types

b) By changing basis function's order

c) By changing positioning of the control polygon vertices

d) By using multiple vertices polygon

B-splines curves made of various knot vector combinations and convex hull vertices combinations are displayed in Figure 3.10. A fourth order B-spline curve with six control points and no coinciding knots in the knot vector is shown in Figure 3.10a [Open uniform knot vector [0 0 0 0 1 2 3 3 3 3], and unique vertices.] Given that the knot vector has three spans, the B-spline curve has three segments, which are, respectively, $B_1B_2B_3B_4$, $B_2B_3B_4B_5$ and $B_3B_4B_5B_6$. The effect of a coincident knot in the knot vector is depicted in Figure 3.10b [b) non-uniform knot vector with multiple coincident knots [0 0 0 0 1 1 2 2 2 2]. Since there are still six vertices (control points) in the knot vector, there are only two spans in the curve—the intermediate span being a zero-span because of knot multiplicity. When the knot vector is uniform but there is a multiple vertex (coincidence control point) at B_3, the resulting curve is displayed in Figure 3.10c [c) Two coincident vertex points at B_3 & open uniform knot vector [0 0 0 0 1 2 3 4 4 4 4]. The curve is obviously drawn in the direction of the coinciding vertex. The fact that only the middle part of curve 3.10c is impacted, with the other segments remaining unaffected, is another significant characteristic of the B-spline curve. The combined effect of many coincident vertices and knot multiplicity is evident in figure 3.10d [d) Multiple knots as well as multiple vertex (at B_3) [0 0 0 0 1 1 2 3 3 3 3], leading to a C_0 continuity at B_3. However, adding a new vertex must result in an increase in the number of knots in the knot vector; in other words, if a coincident vertex is considered to be added, then the knot vector must contain numerous knots, and vice versa.

3.6.2 Collocation technique

The numeric solution of an initial or boundary value problem that is a linear combination of coordinate function with linear coefficients can be obtained through the development of a collocation approach. At a limited number of locations known as collocation points, it entails satisfying a differential equation to a certain degree of tolerance. Therefore, the collocation approach relies on assessing a differential equation's accuracy at a limited number of collocation locations. Examine the following differential equation:

$$f\left(x, y, y'\right) = 0 \tag{3.44}$$

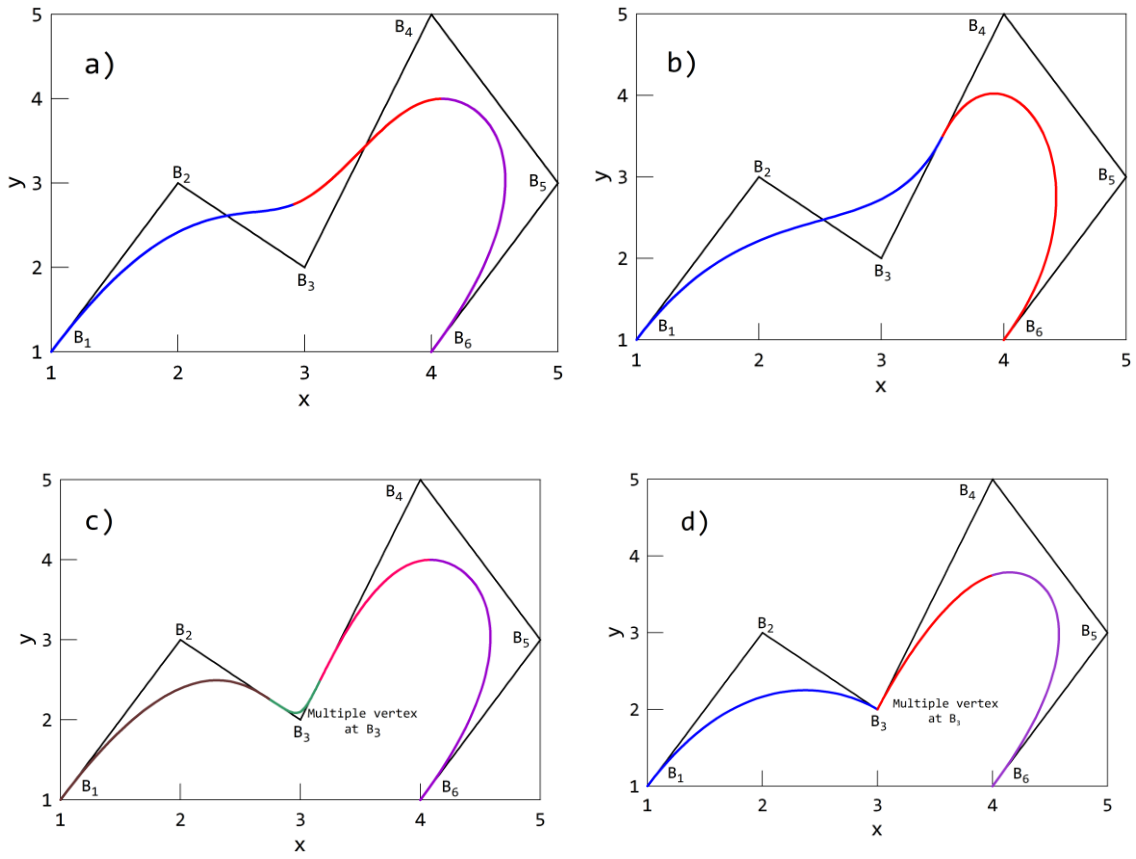

Figure 3.10(a-d): B-spline curves with various control [110]

By mentioning boundary conditions as $y(a) = y_1$ and $y(b) = y_2$, indicates domain of the problem is [a, b]. This approach starts with the assumption of an approximation polynomial (or a trial solution). Typically, this method starts with a suitable selection of fundamental functions $\{\phi_1, \phi_2, \phi_3, \ldots, \phi_n\}$ joined together in a generalized form as follows: $Y = \sum_{i=1}^{n} C_i \phi_i$. The boundary conditions must be met by this approximation solution, but extra equations are needed to get the unknown coefficients, C_i. Therefore, it is necessary to determine a collection of collocation points in the domain [a, b] so that the differential equation can be satisfied by the approximation polynomial Y. Therefore, the approximation needs to meet both the boundary conditions and the differential equation at the nodes (collocation sites). Since "n" is a quality parameter in this case, an increase in its value must result in an increase in accuracy and a decrease in error.

Depending on the nature of the problem, several fundamental functions (ϕ_i) may be chosen. A wise choice of these functions could aid in a speedy convergence of the solution. Choosing the right collocation points is another crucial step in achieving quick convergence. Therefore, this technique's primary benefit is its simplicity, which results in

a low computational cost. However, this technique's application is limited to a relatively confined area due to its low level of precision.

Using piecewise polynomials can significantly improve the technique's accuracy, and B-splines provide an excellent workaround. Many technical difficulties have been solved recently thanks to the combination of B-splines' flexibility and smoothness and collocation's inexpensive cost. The main benefit of the B-spline basis is its smoothness (being differentiable) and extremely high degree of continuity at the interfaces, even though they are piecewise polynomials. The B-spline collocation method is briefly described in the following paragraphs.

3.6.3 B-Spline Collocation method

From the above discussion it is quite evident that to solve any differential equation through any approximate solution method like collocation method a piece wise polynomial is essential as an approximate function and B-spline is a very good polynomial as an approximate solution. To make a B-spline function very useful for any approximate solution, it is required to evaluate properly the B-spline curve's order, the type of knot vector, and the number of control points that result from these factors. In order for the B-spline curve to be differentiated when substituted, if the order of the differential equation is known, it must be greater. For example, if the differential equation is of second order, the order of the B-spline curve must be three (2nd degree polynomial) or more. In order to provide enough resolution to approximate the problem's solution, choosing the right knot vector is also crucial. The number of B-spline curve segments in the problem domain is determined by the number of spans in the knot vector; each segment is made up of a compilation of k basis functions. The number of control points in the B-spline function equals the number of coefficients needed for the approximation function. The total number of coefficients will be k.l if the knot vector with l intervals is used to generate the kth order B-spline.

The number of smoothness criteria at the knots is (k-s) and hence depends on the multiplicity "s" since the continuity at the knots at the interfaces of segments (internal knots) equals C^{k-s-1}. Let $\mathfrak{N}i$ represent the coordinate vector's dimension or the number of control points. At each internal knot, let $\boldsymbol{\vartheta}i$ represent the number of smoothness conditions, which is equal to (k-s). Therefore, the number of coefficients of piecewise polynomials of degree "l," which is equivalent to the number of control points, can be written as follows:

$$\mathrm{N} = kl - \sum \vartheta_i \tag{3.45}$$

If the knot vector is open uniform type, then the number of smoothness condition at each internal knot is equal to (k-1); for l spans there are l-1 internal knots, hence the number of control points reduces to:

$$\mathrm{N} = k.l - (l-1)(k-1) = l + k - 1 \tag{3.46}$$

This leads to $\mathfrak{N}$ unknowns that are to be determined for which an equal number of equations are required. If there are 'm' boundary conditions, which provide 'm' simultaneous equations; the number of equations still required will amount to $\mathfrak{N}$-m. These equations will be obtained from collocation points. Hence the number of collocation points required is equal to $\mathfrak{N}$-m.

Numerous collocation schemes are employed based on the collocation points chosen; the most well-known ones are the Greville, orthogonal, and nodal collocation schemes [135]. Whereas the points for orthogonal collocation are determined using the Gaussian-Legendre quadrature approach, often known as Gauss points, the nodes or collocation points for nodal collocation coincide with the intermediate knot points. The order of the differential equation, the continuity of the curve, and the order of the B-spline basis are used to determine how many Gauss points are needed for each interval. For a 1-, 2-, or 3-point orthogonal collocation, the corresponding Gauss points in the normalized domain [-1, 1] are $[0], \left[\pm\frac{1}{\sqrt{3}}\right] and \left[0, \pm\sqrt{\frac{3}{5}}\right]$. Collocation points are determined using the Greville abscissa method based on a knot vector, T = [t_0, t_1, t_2……, t_{n+k+1}], as follows:

$$x_i = \frac{1}{n}(t_i + t_{i+1} + \cdots + t_{i+n-1}) \tag{3.47}$$

where (i=0, 1… g-n), g is the total number of knots in knot vector.

As Greville abscissa collocation is straightforward and maintains accuracy, it is used in this work for all approximations. To further streamline the process, we can assume (generally) that $t_0 = 0$ and $t_{n+k+1} = L$ in order to combine the parametric and real spaces. As a result, we can assume t = x [135] or that the parametric and domain variables coincide. The B-spline collocation can be summarized by taking the subsequent actions to get the approximate solutions:

a) A suitable knot vector and order of B-spline must be assumed

b) The basic functions using equations 1&2 are then calculated

c) By using Greville abscissa, the abscissa coordinates of the control points are calculated

d) Using equation 4 the b-spline curve equations and their derivatives can be calculated

e) The equations obtained in step d can be substituted in the governing differential equation

f) Substituting the equations of step e in the boundary conditions will provide necessary equations for solution

g) The collocation points obtained in step c may be substituted in the differential equation to get the remaining equations

h) The simultaneous equations obtained may be solved to obtain the ordinate coordinates of the control points

i) These ordinate coordinates can be substituted in equation 3 to obtain the required approximate solution

j) The percentage error and RMS error may be calculated so as to quantify the approximations for desired accuracy

k) If the error is not within permissible limits then two approaches may be adopted:

i) increase the number of spans in the knot vector

ii) increase the order of the b-spline basis function

To execute above sequence of jobs of B-spline collocation method, a MATLAB code has been developed along with few subroutines. The above method has been applied to solve a fourth order isotropic beam problem in the following paragraphs. To ensure a precise match, the findings are compared with existing literature.

3.6.4 Case Studies on Isotropic Beam Problem, 4th order differential equation

An isotropic rectangular cross-section beam is considered for analysis. Its governing equation is a one dimensional fourth order boundary value problem [144] given by:

$$EI\frac{d^4w}{dx^4} + q = 0 \tag{3.48}$$

where "q" is a mechanical load with known boundary conditions, "w" is the beam's transverse deflection, and "EI" is the beam's flexural resistance. The beam's boundary condition as follows could be taken into consideration:

Table-3.2: Various Beam Boundary Conditions

Sl. No.	Type of boundary condition	Corresponding conditions
a)	Clamped-Free (C-F)	$(i)w(0)=0,(ii)\frac{\partial w}{\partial x}(0)=0,(iii)\frac{\partial^2 w}{\partial x^2}(\mathrm{L})=0,(iv)\frac{\partial^3 w}{\partial x^3}(\mathrm{L})=0$
b)	Clamped-Simply supported (C-S)	$(i)w(0)=0,(ii)\frac{\partial w}{\partial x}(0)=0,(iii)\frac{\partial^2 w}{\partial x^2}(\mathrm{L}),(iv)w(\mathrm{L})=0$
c)	Clamped-Clamped (C-C)	$(i)w(0)=0,(ii)\frac{\partial w}{\partial x}(0)=0,(iii)\frac{\partial w}{\partial x}(\mathrm{L})=0,(iv)w(\mathrm{L})=0$
d)	Simply supported-Simply supported (S-S)	$(i)w(0)=0,(ii)\frac{\partial^2 w}{\partial x^2}(0)=0,(iii)\frac{\partial^2 w}{\partial x^2}(\mathrm{L})=0,(iv)w(\mathrm{L})=0$

3.6.4.1 Case study 1: Isotropic beam subjected to only mechanical load

To solve Equation 13 numerically, an analysis is conducted on a rectangular beam with homogeneous dimensions along the span. Its width is believed to be unity, its height to be 0.125 meters, and its length to be 0.5 meters. Assume that the beam is made of steel with a Young's modulus of 210 GPa. A uniformly distributed load of 10kN/m is applied to the beam. An approximation polynomial of sixth order B-spline basis function is used to solve Equation (13). To keep things simple, the knot vector is chosen to have a single span, which is provided by:. According to Equation 8, if l is the number of span, then l+k-1 is the number of control points. Because there are four boundary conditions in this scenario, $\mathfrak{N}$ = 6, and we thus require two collocation points.

In order to numerically solve Equation 3.48, a rectangular beam of uniform dimensions throughout the span is considered for analysis. Its length is assumed to be 0.5m, its height is 0.125m and width is assumed to be unity. Let the material of the beam be steel whose Young's modulus is taken as 210GPa. The beam is loaded with a uniformly distributed load of 10kN/m. In order to solve Equation (3.48) a sixth order B-spline basis function is considered as approximating polynomial. For simplicity the knot vector is

selected so as to have a single span of knot vector given by: $T = [0\ 0\ 0\ 0\ 0\ 0\ 1\ 1\ 1\ 1\ 1\ 1]$. From Equation 3.45, if the number of spans is l, then the number of control points is l+k-1. Hence in this case $\mathfrak{N} = 6$, and since we have four boundary conditions, we need two collocation points.

A mathematical code is used to solve the governing Equation (3.48) using the boundary conditions listed in Table 3.2, which correspond to different end circumstances. The results are presented in Figure 3.11 (a-d). Subsequently, the outcomes are confirmed using the reference results found in the literature [112, 138]. Table 3.3 displays the deflections under mechanical load for various end circumstances, along with a comparison of the obtained results with conventional findings in the literature.

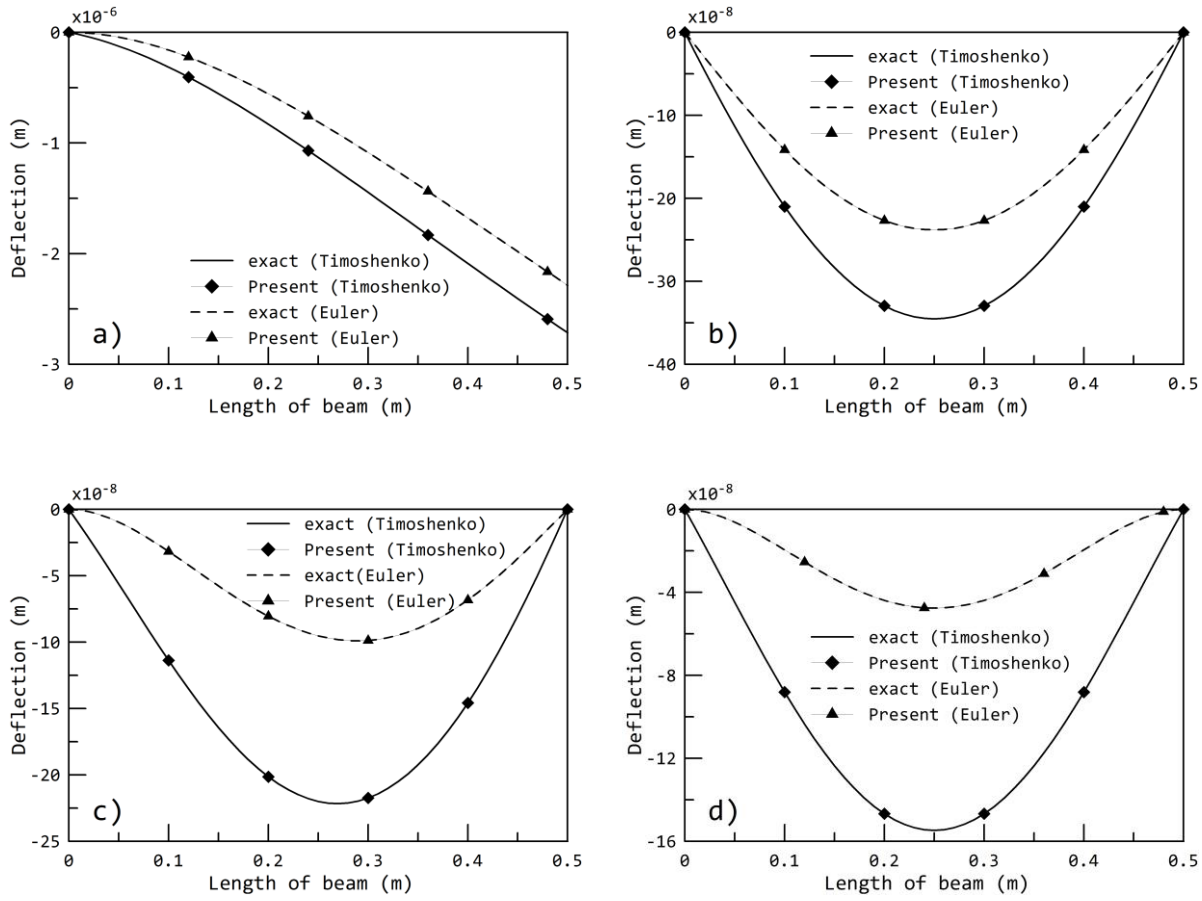

Figure 3.11 Deflection of beam (l/h=4) using B-spline collocation and its validation a) C-F, b) S-S, c) C-S, d) C-C [138]

A noteworthy finding in figure 3.11 above is that the Timoshenko and Euler deflections differ significantly at smaller aspect ratios (l/h=4). The disparity between the two plots must get less as the aspect ratio is increased. Figure 3.12 confirms the same.

The foregoing figures and Table 3.3 make it evident that the B-spline collocation technique can be highly successful in providing high-accuracy approximation solutions (the difference between the produced and standard results varies in the range of 10–13 RMS error %). This technique's degree of accuracy suggests that it can also manage intricate loadings and non-linearities, particularly for beams and plates.

Table-3.3: Error analysis of B-spline collocation for beam sunder purely mechanical load

End Condition	Type of beam	Order of B-spline	No. of internal knots	RMS Error %
C-F	Euler-Bernoulli	6	0	5.27×10^{-13}
	Timoshenko	6	0	1.50×10^{-12}
S-S	Euler-Bernoulli	6	0	9.23×10^{-14}
	Timoshenko	6	0	2.55×10^{-14}
C-S	Euler-Bernoulli	6	0	4.45×10^{-13}
	Timoshenko	6	0	4.07×10^{-13}
C-C	Euler-Bernoulli	6	0	4.78×10^{-13}
	Timoshenko	6	0	3.63×10^{-13}

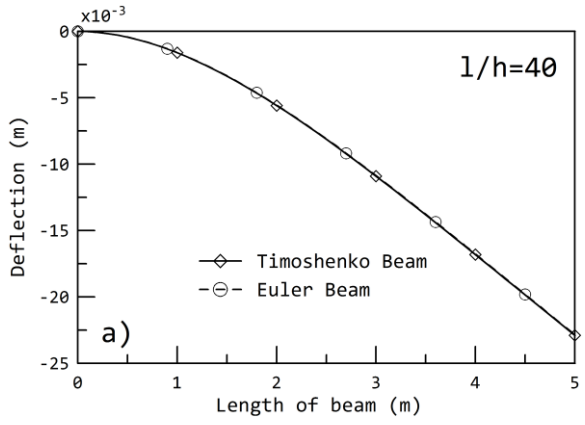

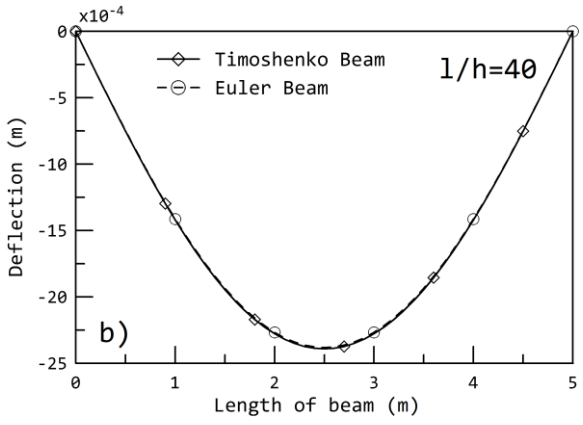

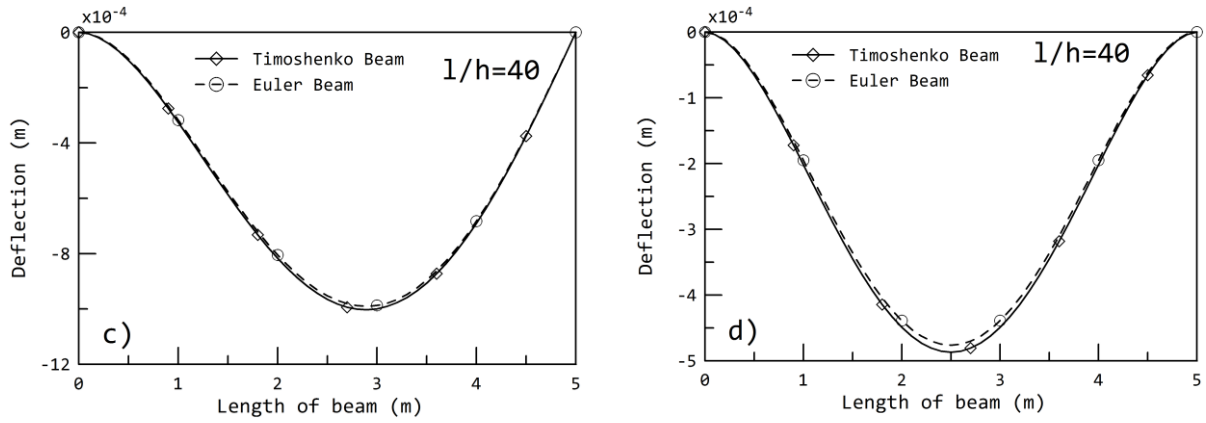

Figure 3.12 Comparison of Euler and Timoshenko deflection using B-spline collocation and its validation a) C-F, b) S-S, c) C-S, d) C-C [138]

Since the current method is parametric, studies may also be conducted over a range of beam length values. Therefore, by lengthening the beam to 5 meters, the aspect ratio (l/h ratio) of the beam is increased to 40. The resulting deformation of the beam under the load of 10 kN/m is displayed in Figure 3.12. Shear deformation's effect is noticeable when l/h<10 and disappears when aspect ratio increases. Figure 3.12 (a-d) provides verification of the same outcome. Therefore, the parametric representation of the B-splines aids in obtaining additional understanding of the issue at hand. The following part examines the computational analysis of beams that are exposed to thermo-mechanical loading.

3.6.4.2 Isotropic beam subjected to only thermo-mechanical load

This section examines the scenario where a thermal load is applied to the beam. To verify the findings, an issue from [138] is used. An evenly distributed load of intensity "q" is applied to a propped beam, which is clamped at the left end and simply supported at the right. Additionally, a linear temperature distribution provided by: is applied to the beam.

$$T = T_b + (T_t - T_b)\left[\frac{z}{h} + \frac{1}{2}\right] \tag{3.49}$$

where Tb and Tt are temperature of bottom and top surface respectively which is defined initially and ‘h’ is height of beam cross-section.

It is noted that the boundary conditions are altered yet the governing differential equation stays the same even with the thermal load included. The moment distribution along the length of the beam is notably altered by the thermal load. By combining the

mechanical and thermal moments in Table 3.2's end conditions, the boundary condition for this problem can be found.

Table-3.4: Modifications on boundary conditions for thermos-mechanical loads

Sl. No.	Type of boundary condition	Corresponding conditions
a)	Clamped-Free (C-F)	$(i)w(0)=0,(ii)\frac{\partial w}{\partial x}(0)=0,(iii)\frac{\partial^2 w}{\partial x^2}(\mathrm{L})+T_{moment}=0,(iv)\frac{\partial^3 w}{\partial x^3}(\mathrm{L})=0$
b)	Clamped-Simply supported (C-S)	$(i)w(0)=0,(ii)\frac{\partial w}{\partial x}(0)=0,(iii)\frac{\partial^2 w}{\partial x^2}(\mathrm{L})+T_{moment}=0,(iv)w(\mathrm{L})=0$
c)	Clamped-Clamped (C-C)	$(i)w(0)=0,(ii)\frac{\partial w}{\partial x}(0)=0,(iii)\frac{\partial w}{\partial x}(\mathrm{L})=0,(iv)w(\mathrm{L})=0$
d)	Simply supported-Simply supported (S-S)	$(i)w(0)=0,(ii)\frac{\partial^2 w}{\partial x^2}(0)+T_{moment}=0,(iii)\frac{\partial^2 w}{\partial x^2}(\mathrm{L})+T_{moment}=0,(iv)w(\mathrm{L})=0$

Table-3.5: Variation of temperatures in beam

Case	Temperature (^{0}C)		
	Top Surface	Bottom Surface	Ambient Temp.
Case1a	31	33	30
Case1b	31	35	30
Case1c	31	37	30
Case2a	33	31	30
Case2b	35	31	30
Case2c	37	31	30

The behavior of this type of beam is examined under thermomechanical loads, and Equation (3.48) is resolved by substituting the boundary conditions found in Table 3.4 and employing the B-spline collocation method. The thermal load—that is, the variations in the temperatures of the top and bottom surfaces—is maintained at a constant 10 kN/m. We've looked at two different kinds of boundary conditions: i) Clamped-Free and ii) Clamped-Simply supported. Because of the sliding/free end constraint, the impact of internal forces resulting from temperature rise is minimal in both scenarios. For the sake of conciseness, the change in characteristics with temperature is also not taken into account. Three different

forms of thermal loading have been taken into consideration, as listed in Table 3.5, in order to track changes in deflection as the temperature gradient in the beam progressively grows. For steel, the coefficient of thermal expansion (α) has been determined to be 24x10-6/0C. The remaining information and process are the same as in the purely mechanical load example from earlier. Following a comparison of the results with those in [129], an exact match is established, as illustrated in Figure 3.13. On purpose, the mechanical and thermal moments are kept in opposition to one another. Because of this, the beam's deflection changes dramatically as the temperature gradient increases. Thus, Figure 3.13(a–b) clearly illustrates how heat load has an impact on beam behavior.

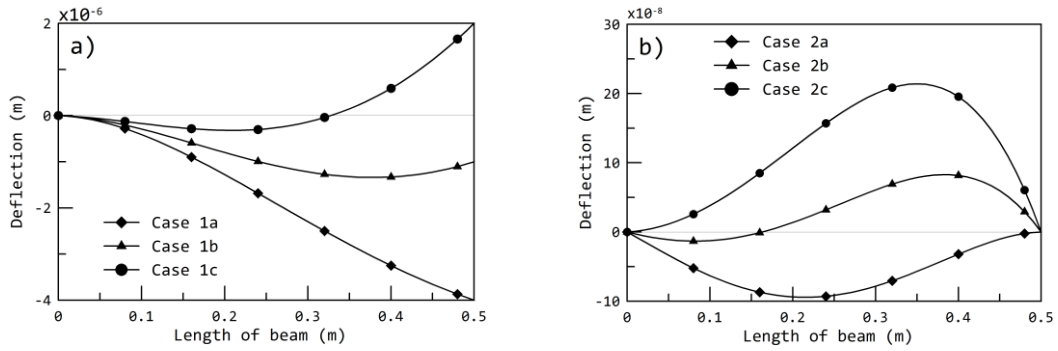

Figure 3.13: Deflection under thermo-mechanical load a) C-F b) C-S [138]

Table-3.6: Error analysis of B-spline collocation for beam under thermo- mechanical load

End Condition	Type of beam	Case	Order of B-spline	No. of internal knots	RMS Error %
C-F	Timoshenko	Case 1a	6	0	5.22×10^{-4}
		Case 1b	6	0	1.28×10^{-3}
		Case 1c	6	0	1.55×10^{-3}
C-S	Timoshenko	Case 2a	6	0	1.21×10^{-4}
		Case 2b	6	0	3.45×10^{-4}
		Case 2c	6	0	5.82×10^{-6}

3.7 Closure

This chapter has covered a variety of beam model types and their formulations. Additionally, a summary of functionally graded material modelling has been included. The idea of the B-splines collocation approach is then investigated in order to get an approximate numerical solution of differential equations of different orders that are pertinent to structural issues. The accuracy of the method is then established by verifying the relevant results with existing literature. Using this technique, a great degree of precision has been found by numerically solving a few case studies of structural analysis issues.

The following conclusions can be summarized:

- The piece-wise closed form solution can be obtained quickly and with little computational cost using the B-spline collocation method.
- The methodology has a high degree of accuracy and may be used to complex scenarios as well.
- B-splines' parametric character makes it easy to investigate the given problem for a variety of dimensions.
- It can be deduced from the structural problems addressed that this technique can also be efficiently used to study the effect of geometric and material non-linearities.

Chapter 4: **Unified Higher Order Formulation under Mechanical load**

4.1 Introduction

Since the mid-1980s, with the advent of Functionally Graded Materials (FGMs), we have been witnessing a new era in the field of material technology. FGMs belong to a class of advanced materials that have continuous variation in properties along a desired direction and in a desired fashion. Compositions (volume of constituents) and hence the properties gradually change over the volume of such materials, resulting in a corresponding change in the properties of the material that is different from either of the parent materials. Functionally graded materials eliminate the sharp interfaces existing in composite materials and structures, where failure is usually initiated. Due to their customized behavior, FGMs may have very wide applications. If their manufacturing cost is reduced by improving the processes, then it may revolutionize the design process as a whole. A thorough overview of FGMs, their manufacturing techniques, modeling and design, and applications can be found in [1–10]. In [11] and [12], an exhaustive review of the modeling and analysis of functionally graded materials and their applications has been reported under mechanical as well as thermos mechanical loading.

Although considerable research on functionally graded materials has been reported since their conceptualization, most of the work in the area of functionally graded structures (beams and plates) has been done only in the last two decades. Analysis of a beam structure is based on few well-known theories. Most primitive theory among these is Euler-Bernoulli (Classical beam theory, CBT) beam theory. Then it was modified by Timoshenko and it is known as First Order Shear Deformation Theory (FSDT). There was another modification done by Levinson termed as Second Order Shear Deformation Theory (SSDT) after that many modifications have been done by many scientists. In the present work the analysis of the FGM beam is based on Reddy-Bickford derived Higher Order Shear Deformation Theory (HSDT) theory which is a Third Order Shear Deformation Theory (TSDT) to have a clear picture of the developments. Conventionally, CBT is suitable for slender beams with large values of aspect ratio, and as such, the effect of transverse shear deformation can be ignored. In FSDT, a constant state of transverse shear strain with respect to thickness is assumed; however, this theory requires a shear correction factor to accommodate for vanishing shear stresses at the top and bottom fibers of the beam. It has been established

that this theory gives satisfactory results for small aspect ratios as well. Second-order shear deformation theory is rarely adopted, and theories higher than third-order shear deformation theory are rarely used because, compared to the efforts required, the accuracy gained is difficult to justify. The third-order beam theory, also known as higher-order beam theory, adopts a displacement field such that it develops a parabolic shear strain across any cross-section, requiring no shear correction factor. Later, new theories like Carrera Unified Formulation (CUF) have also emerged to generalize the theories to a wider spectrum. The same concept has been adopted and reported by many researchers in the case of FG beams as well, and a categorical description is put forth in the successive paragraphs.

4.2 Higer Order beam formulation with given functional gradation

In the present work a beam has been considered which is made of a functionally graded material. Let us consider, the length of the beam is 'L' and it has a rectangular cross-section of width 'b' and height 'h'. It has been shown in figure 1 below. The x-axis is oriented in the axial direction along the mid-plane of the unbent beam, and the positive z-axis is directed upwards and perpendicular to the x-axis.

Let axial and transverse deflections of the beam be represented by 'u' and 'w, respectively, whereas angular or rotational deflection of the cross-section at the mid-plane is represented by 'ϕ'. To account for the variable values at mid plane a subscript of value 0 has been used in this work. Further, in the present work, 'w' and 'γ' have been used to denote or represent the transverse deflection and the shear deformation respectively which are assumed to be functions of 'x' and are uniform for a cross-section. In this work, higher order beam theory is considered according to which the top and bottom surfaces of the beam are free from shear traction. To arrive at such boundary condition, we assume the following condition for shear deformation (γ_{xz}) [33]:

$$\gamma_{xz} = \left(1 - \frac{4z^2}{h^2}\right)\gamma_0 \tag{4.1}$$

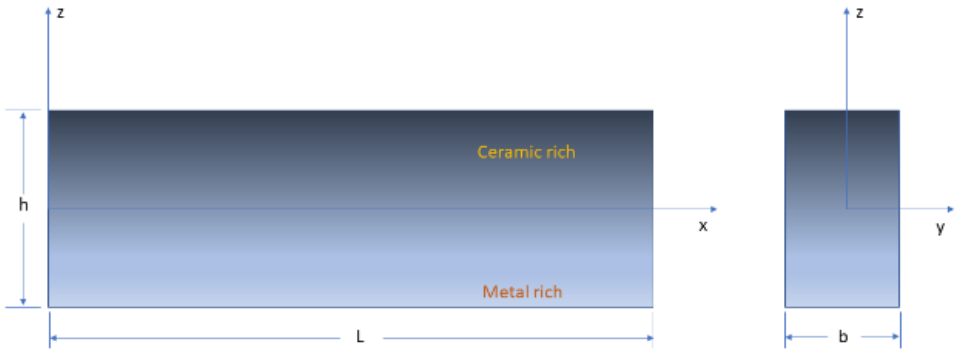

Fig. 4.1. Diagram of a Functionally Graded Beam with co-ordinate system [138]

For small deformations we can write [33]:

$$\gamma_{xz} = \frac{\partial u}{\partial z} + \frac{\partial w}{\partial x} \tag{4.2}$$

Integrating both sides with respect to 'z', the expression for deformation 'u' is obtained as

$$u(x,z) = \int \left(\left(1 - \frac{4z^2}{h^2}\right)\gamma_0 - \frac{\partial w}{\partial x} \right) dz \tag{4.3}$$

$$u(x,z) = u_0(x) + \left(z - \frac{4z^3}{3h^2}\right)\gamma_0 - z\frac{\partial w}{\partial x} \tag{4.4}$$

$$u(x,z) = u_0(x) + z\phi_0 - \frac{4z^3}{3h^2}\left(\phi_0 + \frac{\partial w}{\partial x}\right) \tag{4.5}$$

The above Eq. (4.5) is obtained by substituting, $\phi_0 = \frac{du}{dz}$ and $\gamma_0 = \phi_0 + \frac{dw}{dx}$in Eq. (4.2).

Knowing that $\varepsilon_{xx} = \frac{\partial u}{\partial x}$ we can write:

$$\varepsilon_{xx} = \frac{\partial u_0}{\partial x} + z\frac{\partial \phi_0}{\partial x} - \frac{4z^3}{3h^2}\left(\frac{\partial \phi_0}{\partial x} + \frac{\partial^2 w}{\partial x^2}\right) = \varepsilon_{xx}{}^{(0)} + z\varepsilon_{xx}{}^{(1)} + z^3\varepsilon_{xx}{}^{(3)} \tag{4.6}$$

$$\gamma_{xz} = \left(1 - \frac{4z^2}{h^2}\right)\left(\phi_0 + \frac{\partial w}{\partial x}\right) = \gamma_{xz}{}^{(0)} + z^2\gamma_{xz}{}^{(2)} \tag{4.7}$$

where,

$$\varepsilon_{xx}^{(0)} = \frac{\partial u_0}{\partial x}$$

$$\varepsilon_{xx}^{(1)} = \frac{\partial \phi_0}{\partial x}$$

$$\varepsilon_{xx}^{(3)} = -c_1\left(\frac{\partial \emptyset_0}{\partial x} + \frac{\partial^2 w}{\partial x^2}\right)$$

$$\gamma_{xz}^{(0)} = \emptyset_0 + \frac{\partial w}{\partial x}$$

$$\gamma_{xz}^{(2)} = -c_2\left(\emptyset_0 + \frac{\partial w}{\partial x}\right)$$

$$c_1 = \frac{4}{3h^2}, c_2 = \frac{4}{h^2}$$

To derive the governing equations of motion for an FG beam, Hamilton's Principle is applied as shown below.

$$\delta L = \delta(U + K + V) = 0 \tag{4.8}$$

$$\left.\begin{aligned} \delta U &= \int_0^t \int_0^L \int_A (\sigma_{xx}\delta\varepsilon_{xx} + \tau_{xz}\delta\gamma_{xz})\, dA dx dt \\ \delta K &= \int_0^t \int_0^L \int_A \rho(z)(\dot{u}\delta\dot{u} + \dot{w}\delta\dot{w})\, dA dx dt \\ \delta V &= -\int_0^t \int_0^L q\delta w dx dt \end{aligned}\right\} \tag{4.9}$$

Substituting the expressions for U, K and V in Eq. (4.8) and assuming,

$$N_x = \int_A \sigma_{xx} dA, \quad M_x = \int_A z\sigma_{xx} dA$$

$$P_x = \int_A z^3\sigma_{xx} dA, \quad Q_x = \int_A \tau_{xz} dA,$$

$$R_x = \int_A z^2\tau_{xz} dA \ \text{and}\ I_k = \int_A z^k \rho(z) dA,$$

We get the following governing equation

$$\int_0^t \int_0^L \left(N_x \delta {\varepsilon_{xx}}^{(0)} + M_x \delta {\varepsilon_{xx}}^{(1)} + P_x \delta {\varepsilon_{xx}}^{(3)}\right) dxdt$$
$$+ \int_0^t \int_0^L \left(Q_x \delta {\gamma_{xz}}^{(0)} + R_x \delta {\gamma_{xz}}^{(2)}\right) dxdt \quad (4.10)$$
$$+ \int_0^t \int_0^L I_k((\dot{u}\delta\dot{u} + \dot{w}\delta\dot{w}))\, dxdt - \int_0^t \int_0^L q\delta w dxdt = 0$$

Integrating by parts and categorically separating the variables, the following governing equations and boundary conditions are derived.

$$\frac{\partial \mathrm{N_x}}{\partial \mathrm{x}} = \mathrm{I_0}\frac{\partial^2 \mathrm{u_0}}{\partial \mathrm{t}^2} + {\mathrm{I_1}}^*\frac{\partial^2 \varphi_0}{\partial \mathrm{t}^2} - \mathrm{c_1 I_3}\frac{\partial^3 \mathrm{w}}{\partial \mathrm{x}\,\partial \mathrm{t}^2} \quad (4.11)$$

$$\frac{\partial \bar{M}_\mathrm{x}}{\partial \mathrm{x}} - \bar{\mathrm{Q}}_\mathrm{x} = {\mathrm{I_1}}^*\frac{\partial^2 \mathrm{u_0}}{\partial \mathrm{t}^2} + {\mathrm{K_2}}^*\frac{\partial^2 \varphi_0}{\partial \mathrm{t}^2} - \mathrm{c_1}{\mathrm{I_4}}^*\frac{\partial^3 \mathrm{w}}{\partial \mathrm{x}\,\partial \mathrm{t}^2} \quad (4.12)$$

$$c_1\frac{\partial^2 \mathrm{P_x}}{\partial \mathrm{x}^2} + \frac{\partial \bar{Q}_\mathrm{x}}{\partial \mathrm{x}} + \mathrm{q} = \mathrm{c_1 I_3}\frac{\partial^3 \mathrm{u_0}}{\partial \mathrm{x}\,\partial \mathrm{t}^2} + \mathrm{c_1}{\mathrm{I_4}}^*\frac{\partial^3 \varphi_0}{\partial \mathrm{x}\,\partial \mathrm{t}^2} - {\mathrm{c_1}}^2\mathrm{I_6}\frac{\partial^4 \mathrm{w}}{\partial \mathrm{x}^2\,\partial \mathrm{t}^2} + \mathrm{I_0}\frac{\partial^2 \mathrm{w}}{\partial \mathrm{t}^2} \quad (4.13)$$

Boundary Conditions ($at\ x = 0$ & $at\ x = L$)

$$N_x - I_0\frac{\partial u_0}{\partial t} - I_1\frac{\partial \phi_0}{\partial t} + c_1 I_3\left(\frac{\partial \phi_0}{\partial x} + \frac{\partial^2 w}{\partial x \partial t}\right) = 0 \quad (4.14)$$

$$\bar{M}_x - {I_1}^*\frac{\partial u_0}{\partial t} - {K_2}^*\frac{\partial \phi_0}{\partial t} + c_1{I_4}^*\frac{\partial^2 w}{\partial x \partial t} = 0 \quad (4.15)$$

$$c_1\frac{\partial P_x}{\partial x} + \bar{Q}_x - c_1 I_3\frac{\partial^2 u_0}{\partial t^2} - c_1{I_4}^*\frac{\partial^2 \phi_0}{\partial t^2} + {c_1}^2 I_6\frac{\partial^3 w}{\partial x \partial t^2} + I_0\frac{\partial w}{\partial t} = 0 \quad (4.16)$$

To simplify the above equations, the following substitutions have also been incorporated:

$$\bar{M}_x = M_x - c_1 P_x, \quad \bar{Q}_x = Q_x - c_2 R_x,$$

$$I_j^* = I_j - c_1 I_{j+2}, \quad K_2^* = I_2 - 2c_1 I_4 + c_1^2 I_6$$

Substituting $\sigma_{xx} = E(z).\varepsilon_{xx}$ in expressions for Nx and $\bar{M}_x$ and simplification thereafter, we get

$$N_x = E_0\frac{\partial u_0}{\partial x} + {E_1}^*\frac{\partial \phi_0}{\partial x} - c_1 E_3\frac{\partial^2 w}{\partial x^2} \quad (4.17)$$

$$\bar{M}_x = \frac{{E_1}^*}{E_0}N_x + \left(A^* - \frac{{E_1^*}^2}{E_0}\right)\frac{\partial \phi_0}{\partial x} - \left(c_1 E_4^* - \frac{c_1 E_1^* E_3}{E_0}\right)\frac{\partial^2 w}{\partial x^2} \quad (4.18)$$

$$P_x = \frac{E_3}{E_0} N_x + \left({E_4}^* - \frac{E_1^* E_3}{E_0} \right) \frac{\partial \phi_0}{\partial x} - \left(c_1 E_6 - \frac{c_1 E_3^{*2}}{E_0} \right) \frac{\partial^2 w}{\partial x^2} \tag{4.19}$$

$$\bar{Q}_x = G_0^* \left(\phi_0 + \frac{\partial w}{\partial x} \right) \tag{4.20}$$

The following assumptions have been made for the simplification of the above equations.

$$E_j = \int_A z^j E(z) dA$$

$$G_j = \int_A z^j G(z) dA$$

$$E_s^* = E_s - c_1 E_{s+2}$$

$$A^* = E_2 - 2c_1 E_4 + c_1^2 E_6$$

$$G_0^* = G_0 - 2c_2 G_2 + {c_2}^2 G_4$$

$$K^* = I_2 - 2c_1 I_4 + c_1^2 I_6$$

$$I_s^* = I_s - c_1 I_{s+2}$$

(Where, s =1,2,4)

The expression for Nx (Eq. 4.17) is used to eliminate uo to arrive at the following expressions. Further, it is assumed that the resultant axial force will be zero (for statically determinate cases), so by substituting Nx=0 in the above equations obtained after eliminating u0, we arrive at final governing equations for an FG beam in the framework of higher-order beam theory.

$$\bar{A}^* \frac{\partial^2 \phi_0}{\partial x^2} - c_1 \bar{E}_4^* \frac{\partial^3 w}{\partial x^3} - G_0^* \left(\phi_0 + \frac{\partial w}{\partial x} \right) = \bar{K}^* \frac{\partial^2 \phi_0}{\partial t^2} - c_1 \bar{I}_4^* \frac{\partial^3 w}{\partial x \partial t^2} \tag{4.21}$$

$$\begin{aligned} G_0^* \left(\frac{\partial \phi_0}{\partial x} + \frac{\partial^2 w}{\partial x^2} \right) + c_1 \left(\bar{E}_4^* \frac{\partial^3 \phi_0}{\partial x^3} - c_1 \bar{E}_6 \frac{\partial^4 w}{\partial x^4} \right) + q \\ = c_1 I_3 \frac{\partial}{dx} \left(\frac{I_1^*}{I_0} \frac{\partial^2 \phi_0}{\partial t^2} + \frac{c_1 I_3}{I_0} \frac{\partial^3 w}{\partial x \partial t^2} \right) + c_1 I_4^* \frac{\partial^3 \phi_0}{\partial x \partial t^2} \\ - c_1^2 I_6 \frac{\partial^4 w}{\partial x^2 \partial t^2} + I_0 \frac{\partial^2 w}{\partial t^2} \end{aligned} \tag{4.22}$$

Where,

$$\overline{A^*} = A^* - \frac{E_1^{*2}}{E_0}$$

$$\overline{E_4^*} = \left(E_4^* - \frac{E_1^* E_3}{E_0}\right)$$

$$\overline{K^*} = K^* - \frac{I_1^{*2}}{I_0}$$

$$\overline{I_4^*} = I_4^* - \frac{I_1^* I_3}{I_0}$$

$$\overline{E_6} = E_6 - \frac{E_3^{*2}}{E_0}$$

Li et al. [33] have also derived similar equations, but they have neglected the higher-order terms considering E6 and I6. The derivation in their work has been approached using the theory of elasticity approach, and hence the scope of incorporation of these (E6 and I6) terms could not be made. Moreover, the boundary conditions are also affected. In the present work, the derivation of the above governing equation is followed from the first principles using Hamilton's principle, which also enables us to derive the relevant expressions for boundary conditions. The above formulation can be compared with that of [33], and the above equations are reduced to the same equations by ignoring E6 and I6.

4.3 Unification of governing equations with a common parameter

A significant finding of [27, 33] is to reduce the above two equations into a single governing equation by considering an independent parameter 'F' such that domain variables i.e., w and $\emptyset_0$ are functions of 'F' such that it satisfies the governing equations. In the present work, similar substitution is made after appropriate modification as below and substituted in the governing equation to obtain a single expression for higher-order beam theory, taking into account the higher order terms.

$$w = F - \frac{\bar{A}^*}{G_0^*}\frac{\partial^2 F}{\partial x^2} + \frac{\bar{K}^*}{G_0^*}\frac{\partial^2 F}{\partial t^2} \tag{4.23A}$$

$$\phi_0 = -\frac{\partial F}{\partial x} - \frac{c_1 \bar{E}_4^*}{G_0^*}\frac{\partial^3 F}{\partial x^3} + \frac{c_1 \bar{I}_4^*}{G_0^*}\frac{\partial^3 F}{\partial x \partial t^2} \tag{4.23B}$$

After substituting Eq. (4.23) to Eq. (4.21 and 4.22) the governing equation for FG beams is simplified to:

$$\left(E_2 - \frac{E_1^2}{E_0}\right)\frac{\partial^4 F}{\partial x^4} - \left\{\left(I_2 - \frac{I_1^2}{I_0}\right) + \frac{I_0 \bar{A}^*}{G_0^*}\right\}\frac{\partial^4 F}{\partial x^2 \partial t^2} + I_0 \frac{\partial^2 F}{\partial t^2} + \frac{I_0 \bar{K}^*}{G_0^*}\frac{\partial^4 F}{\partial t^4} = q \qquad (4.24)$$

It can be observed that the above equation is exactly similar to the equation derived in reference [105] when the terms E6 and I6 are neglected. The above equation represents the single governing equation for FG beams in the framework of higher order beam theory. Once the parameter 'F' is calculated, the other dependent variables can be easily determined, which can be used to calculate the stresses and strains in the beam for various loading and boundary conditions. We may also calculate the shear forces and bending moments caused by the external loads using the equations discussed in previous paragraphs.

Additionally, by substituting $c_1 = 0$ and $c_2 = 0$ in the above equation, we arrive at Timoshenko beam theory for FG beams [27], which can be further reduced to Rayleigh and Euler beam theory by considering infinite shear modulus. To distinguish the current study and work of Li [33] for higher order beam theory, the terms containing E6 are multiplied with an arbitrary constant whose value is taken as zero or one; when it is zero, it suffices to Li's work, while its value is one it represents the present study.

Now, to find out expression for axial deflection we need use the following expression

$$N_x = \int_A \sigma_{xx} dA \qquad (4.25)$$

Where,

$$\sigma_{xx} = E(z)\epsilon_{xx}$$

Now, from equation (4.6) we can write

$$\varepsilon_{xx} = \frac{\partial u_0}{\partial x} + z\frac{\partial \phi_0}{\partial x} - \frac{4z^3}{3h^2}\left(\frac{\partial \phi_0}{\partial x} + \frac{\partial^2 w}{\partial x^2}\right)$$

Substituting above expression in equation (4.25) we get the expressions for u_0, ε_{xx}, σ_{xx} can be obtained in terms of w & $\emptyset_0$, as shown below

$$\frac{\partial u_0}{\partial x} = \frac{N_x}{E_0} - \frac{E_1^*}{E_0}\frac{\partial \phi_0}{\partial x} - \frac{c_1 E_3}{E_0}\frac{\partial^2 w}{\partial x^2} \qquad (4.26)$$

Integrating both sides, assuming that the resultant axial force vanishes, and using the boundary conditions, we can obtain the equation for u0, which can be further substituted in Eq. (4.5) to obtain axial deformation, strains and stresses as below.

$$u = \left(z - c_1 z^3 - \frac{E_1^*}{E_0}\right)\phi_0 + c_1\left(\frac{E_3}{E_0} - z^3\right)\frac{\partial w}{\partial x} \tag{4.27}$$

$$\varepsilon_{xx} = \frac{\partial u}{\partial x} = \left(z - c_1 z^3 - \frac{E_1^*}{E_0}\right)\frac{\partial \phi_0}{\partial x} + c_1\left(\frac{E_3}{E_0} - z^3\right)\frac{\partial^2 w}{\partial x^2} \tag{4.28}$$

$$\sigma_{xx} = E(z)\varepsilon_{xx} = E(z) \times \left\{\left(z - c_1 z^3 - \frac{E_1^*}{E_0}\right)\frac{\partial \phi_0}{\partial x} + c_1\left(\frac{E_3}{E_0} - z^3\right)\frac{\partial^2 w}{\partial x^2}\right\} \tag{4.29}$$

$$\tau_{xz} = G(z)\gamma_{xz} = G(z)\left(1 - \frac{4z^2}{h^2}\right)\left(\phi_0 + \frac{\partial w}{\partial x}\right) \tag{4.30}$$

Now if we substitute expression of 'w' and 'ϕ_0' in the equations (4.27) to (4.30) we will get relation between field variables, i.e., axial deformation u (x, z), axial strain ε_{xx}, axial stress σ_{xx}, and in-plain shear stress τ_{xz} in terms of parameter 'F'.

In the Eq. (4.29) and Eq. (4.30), the modulus of elasticity follows a power law distribution across the height of the beam, and Poisson's ratio is assumed to be a constant. The solution to the above problem is approached using the B-spline Collocation technique. The variation of the modulus of elasticity is made according to the power law distribution given by

$$E(z) = E_b + (E_t - E_b)\left(\frac{z}{h} + 0.5\right)^{\beta} \tag{4.31}$$

The subscript 'β' refers to the power law index whereas the subscripts 'b' and 't' represent bottom and top fiber respectively. The variation of the modulus of elasticity for various values of the power law index is plotted in Figure 2. The variation of the modulus of rigidity will be similar to the elasticity modulus due to the assumption of constant Poisson's ratio. Modulus of rigidity is calculated from the relation:

$$G(z) = \frac{E(z)}{2(1+\mu)} \tag{4.32}$$

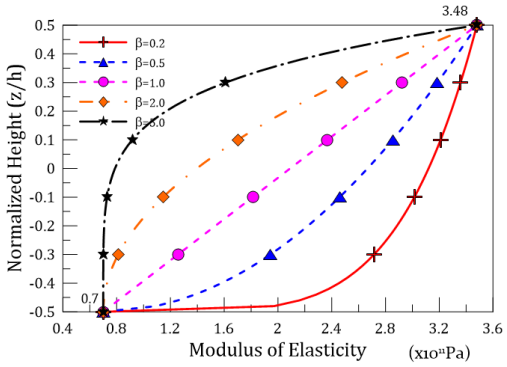

Fig. 4.2. Modulus of Elasticity variation as per power law index, β along the height. [138]

4.4 Exact Solution by successive integration and using boundary conditions

In the preceding section governing equation of a FG Timoshenko beam for arbitrary loading and boundary condition has been derived. It is a fourth order ordinary differential equation in terms of an independent variable, F. In order to determine the domain variables of the problem and subsequently the stresses in the beam, F is to be required to be determined. For obtaining solution of the problem as above boundary conditions must be specified initially. In the present work five types of boundary conditions are considered for study and are mentioned in Table-1. The conventional beams like cantilever, simply supported or clamped may be formed by suitable combinations of these boundary conditions, for example:

a) Cantilever beam *(C-F_r)*

b) Simply supported beam *(S-S) or (S-S_{SL})*

c) Propped beam *(C-S) or (C-S_{SL}) or (C-C_{SL})*

d) Fixed beam *(C-C)*

Table 4.1: Boundary Conditions with value of DOFs

i)	Clamped (C)	$u=0 \quad w=0 \quad \phi=0$
ii)	Movable clamped (C_{SL})	$N_x=0 \quad w=0 \quad \phi=0$
iii)	Simply supported (S)	$u=0 \quad w=0 \quad M_y=0$
iv)	Movable simply supported (S_{SL})	$N_x=0 \quad w=0 \quad M_y=0$
v)	Free (F_r)	$N_x=0 \quad M_y=0 \quad V_{xz}=\frac{dM_y}{dx}=0$

Integration of the governing equation of FG beam (Equation 4.24) after neglecting the time derivative parts we get the following solution:

$$F = \frac{q}{D_{11}^*}\frac{x^4}{24} + C_1\frac{x^3}{6} + C_2\frac{x^2}{2} + C_3 x + C_4 \tag{4.33}$$

where Cj (j=1,2,3,4) are constants to be determined from the end conditions and $D_{11}^* = \left(E_2 - \frac{E_1^2}{E_0}\right)$. It is hence observed that the method follows the conventional integration technique as the material gradient is varying only along the cross-section while remaining constant along the beam axis. In the present study four combinations of boundary conditions as defined above are considered as above to find the exact solution for a FG Timoshenko beam. The beams are subjected to an external uniform mechanical pressure of 'q' kN/m intensity throughout the span on its top surface. The resulting deformations and stresses are then observed for a wide range of parameters as discussed below.

Various Boundary conditions

4.4.1 Clamped-Free (C-F_r)

For a cantilever beam slope and deflection at the fixed end are zero while shear force and bending moment at the free end are zero. Hence, we have the following end conditions for a C-Fr beam-

$$w(0) = \phi(0) = 0, M_y(l) = V_{xz}(l) = 0 \tag{4.34}$$

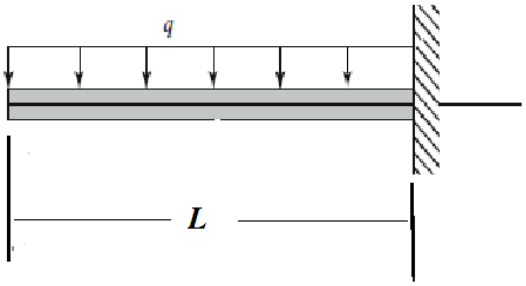

Fig. 4.3: Cantilever FG Beam (C-F_r) [138]

Using Eq. 4.23A and B in Eq. 4.34 the boundary condition is converted into following form:

$$\left(F - \frac{\bar{A}^*}{G_0^*}\frac{d^2F}{dx^2}\right)_{x=0} = \left(-\frac{dF}{dx} - \frac{c_1\bar{E}_4^*}{G_0^*}\frac{d^3F}{dx^3}\right)_{x=0} = \left(\left(\bar{A}^* + c_1\bar{E}_4^*\right)\frac{d^2F}{dx^2}\right)_{x=l} = \left(\left(\bar{A}^* + c_1\bar{E}_4^*\right)\frac{d^3F}{dx^3}\right)_{x=l} = 0 \tag{4.35}$$

The above conditions can be used to obtain four simultaneous linear equations in C_j (j=1,2,3,4) which can be solved easily to obtain the coefficients and thereby the independent variable, F. Once F is determined, the actual domain variables and stresses can be easily obtained as shown below:

$$w = \frac{q}{24D_{11}^*}\left(x^4 - 4lx^3 + 6l^2x^2\right) - \frac{q}{2G_0^*}\frac{\bar{A}_0^*}{D_{11}^*}\left(x^2 - 2lx\right) + \frac{q}{D_{11}^*}\frac{c_1\bar{E}_4^*}{G_0^*}xl \tag{4.36}$$

$$\phi = \frac{q}{6D_{11}^*}\left(-x^3 + 3lx^2 - 3l^2x - \frac{c_1\bar{E}_4^*}{G_0^*}x\right) \tag{4.37}$$

$$u = -\frac{B_{11}}{A_{11}}\phi = \frac{q}{6D^*}\frac{B_{11}}{A_{11}}\left(x^3 - 3lx^2 + 3l^2x\right) \tag{4.38}$$

$$u = -\frac{B_{11}}{A_{11}}\phi = \frac{q}{6D^*}\frac{B_{11}}{A_{11}}\left(x^3 - 3lx^2 + 3l^2x\right) \tag{4.39}$$

$$\sigma_{xx} = \frac{qE(z)}{2D^*}\left(\frac{B_{11}}{A_{11}} + z\right)\left(x^2 - 2lx + l^2\right) \tag{4.40}$$

$$\sigma_{xx} = \frac{qE(z)}{2D^*}\left(\frac{B_{11}}{A_{11}} + z\right)\left(x^2 - 2lx + l^2\right) \tag{4.41}$$

$$\sigma_{xz} = \frac{q}{D^*}(l - x)\left[\int_{-h/2}^{z} zE(z)dz + \frac{B_{11}}{A_{11}}\int_{-h/2}^{z} E(z)dz\right] \tag{4.42}$$

For isotropic beams D*=EI, K_{55} = ksGA and stretching-bending coupling coefficient B11=0, hence for isotropic materials the above equations are reduced to:

$$\left.\begin{aligned} w &= \frac{q}{24EI}\left(x^4 - 4lx^3 + 6l^2x^2\right) - \frac{q}{2k_sGA}\left(x^2 - 2lx\right) \\ \sigma_{xx} &= \frac{q}{2I}\left(x^2 - 2lx + l^2\right)(z) = \frac{M_y z}{I} \end{aligned}\right] \tag{4.43}$$

The above can be easily verified from standard textbooks and relevant literature. In a similar way we can write direct solutions corresponding to other end conditions also.

4.4.2 Clamped-Simply supported (C-S)

For a propped cantilever beam (C-S) slope and deflection at the fixed end are zero while transverse deflection and bending moment at the roller end are zero. Similar to procedure followed above and the given end conditions for a C-S beam we obtain:

$$w(0) = \phi(0) = 0, w(l) = M_y(l) = 0 \tag{4.44}$$

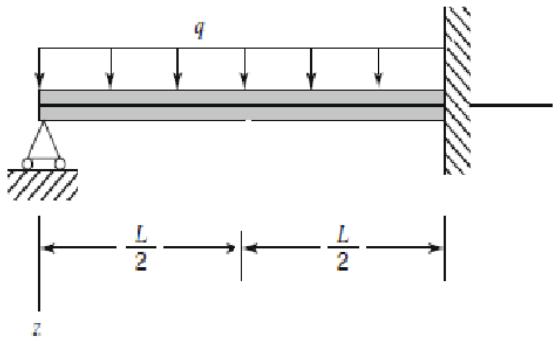

Fig. 4.4: Propped FG Beam (C-S) [138]

$$\left(F-\frac{D^*}{K_{55}}\frac{d^2F}{dx^2}\right)_{x=0}=\left(\frac{dF}{dx}\right)_{x=0}=\left(F-\frac{D^*}{K_{55}}\frac{d^2F}{dx^2}\right)_{x=l}=\left(D^*\frac{\partial^2F}{\partial x^2}\right)_{x=l}=0 \tag{4.45}$$

$$\xi.w=\frac{q}{144D^*}\left(2x^4l^2-5x^3l^3+3x^2l^4\right)+\frac{q}{24K_{55}}\left(x^4-4x^2l^2-2x^3l+5l^3x\right)-\frac{qD^*}{2K_{55}^2}\left(x^2-lx\right) \tag{4.46}$$

$$\sigma_{xx}=\frac{E(z)}{\xi}\left(\frac{B_{11}}{A_{11}}-z\right)\left\{\frac{q}{24D^*}\left(4x^2l^2-5xl^3+l^4\right)-\frac{q}{2K_{55}}\left(x^2-lx\right)\right\} \tag{4.47}$$

$$\xi.\sigma_{xz}=\left[\frac{q}{24D^*}\left(8xl^2-5l^3\right)+\frac{q}{2K_{55}}\left(2x-l\right)\right]\left\{\int_{-h/2}^{z}zE(z)dz-\frac{B_{11}}{A_{11}}\int_{-h/2}^{z}E(z)dz\right\} \tag{4.48}$$

Where,

$$\xi=\frac{l^2}{3}+\frac{D^*}{K_{55}}$$

If we neglect the effect of shear deformation in the above analysis for C-S beam hence the corresponding beam will become Euler-Bernoulli beam (EBB). For such beams the value of K55 will be infinite hence the value of ξ=l2/3 which will simplify them to those for EB beams. Further if the beam is assumed to be isotropic by substituting D*=EI, K55=ksGA and B11=0 as in the previous case. It has been observed that the resulting equations for isotropic beam with C-F boundary condition, then the resulting equations for transverse deflection, axial and shear stress are exactly similar to that in standard books [Shames 152].

4.4.3 Simply Supported-Simply Supported (S-S)

A similar analysis as above for S-S or S-SSL type boundary condition whose at least one end is roller supported is discussed in this section. The boundary conditions associated with such beam are:

$$w(0)=M_y(0)=0, w(l)=M_y(l)=0 \tag{4.50}$$

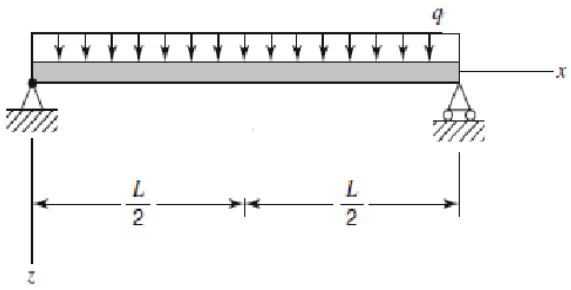

Fig. 4.5: Simply Supported FG Beam (S-S) [138]

$$\begin{aligned}\left(F-\frac{D^*}{K_{55}}\frac{d^2F}{dx^2}\right)_{x=0}&=\left(D^*\frac{\partial^2F}{\partial x^2}+\frac{B_{11}}{A_{11}}N_T-M_T\right)_{x=0}=0\\ \left(F-\frac{D^*}{K_{55}}\frac{d^2F}{dx^2}\right)_{x=l}&=\left(D^*\frac{\partial^2F}{\partial x^2}+\frac{B_{11}}{A_{11}}N_T-M_T\right)_{x=l}=0\end{aligned} \tag{4.51}$$

The final expressions obtained for transverse deflection and stresses after solution and simplification of the linear simultaneous equations are obtained as:

$$\left(F-\frac{D^*}{K_{55}}\frac{d^2F}{dx^2}\right)_{x=0}=\left(\frac{dF}{dx}\right)_{x=0}=\left(D^*\frac{d^2F}{dx^2}\right)_{x=l}=\left(D^*\frac{d^3F}{dx^3}\right)_{x=l}=0 \tag{4.52}$$

$$w=\frac{q}{24D^*}\left(x^4-2x^3l+xl^3\right)-\frac{q}{2K_{55}}\left(x^2-xl\right) \tag{4.53}$$

$$\sigma_{xx}=\frac{E(z)}{2D^*}\left(\frac{B_{11}}{A_{11}}-z\right)\left\{q\left(x^2-lx\right)\right\} \tag{4.54}$$

$$\sigma_{xz}=\frac{q}{2D^*}(l-2x)\left[\int_{-h/2}^{z}zE(z)dz-\frac{B_{11}}{A_{11}}\int_{-h/2}^{z}E(z)dz\right] \tag{4.55}$$

4.4.4 Clamped-Clamped (C-C)

For a fixed-fixed (C-C) beam, slope and deflection at both the ends is zero. Hence the related end conditions are:

$$w(0)=\phi(0)=0, w(l)=\phi(l)=0 \tag{4.56}$$

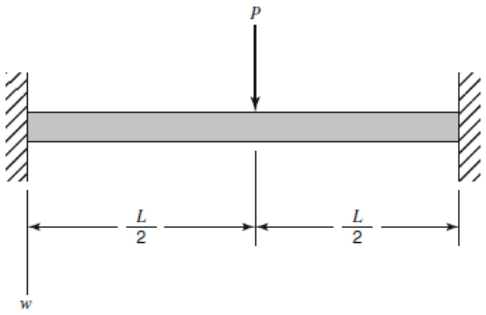

Fig. 4.6: Fixed FG Beam (C-C) [138]

$$\left(F-\frac{D^*}{K_{55}}\frac{d^2F}{dx^2}\right)_{x=0}=\left(\frac{dF}{dx}\right)_{x=0}=\left(F-\frac{D^*}{K_{55}}\frac{d^2F}{dx^2}\right)_{x=l}=\left(\frac{dF}{dx}\right)_{x=l}=0 \tag{4.56}$$

$$w=\frac{q}{24D^*}\left(x^4-2x^3l+x^2l^2\right)-\frac{q}{2K_{55}}\left(x^2-xl\right) \tag{4.57}$$

$$\sigma_{xx}=\frac{E(z)}{2D^*}\left(\frac{B_{11}}{A_{11}}+z\right)\left\{q\left(x^2-lx\right)\right\} \tag{4.58}$$

$$\sigma_{xz}=\frac{q}{2D^*}(l-2x)\left[\int_{-h/2}^{z} zE(z)dz-\frac{B_{11}}{A_{11}}\int_{-h/2}^{z}E(z)dz\right] \tag{4.59}$$

4.5 Numerical solution using B-spline collocation technique

Now to solve the governing equation as stated in Eq. 4.24 a numerical method named as B-spline Collocation method has been adopted in this work. A detailed discussion has already been taken place in Chapter 2 about the B-spline collocation technique. According to this technique a B-spline function is needed to be considered as a trial solution for the parameter 'F' and need to substitute in the governing equation, i.e., Eq. 4.24. The resulting equation is then forced to satisfy the governing equation at collocation points given by Greville abscissa. Here in the present study a B-spline function of sixth order basis function has been considered (as the governing equation is a fourth order differential equation so the degree of polynomial needed is 5th.)

It can be assessed that the number of collocation points required will be equal to the difference between the number of control points of the B-spline curve and the number of boundary conditions. In the present case, a sixth-order B-spline function with no intermediate knots is used. Hence, we have six coefficients to be determined. As there are 4 boundary conditions available, we require only 2 collocation points to develop six linear equations that can be solved easily to find the coefficients.

In the next section, the solution is approached using the B-spline collocation technique; a detailed discussion of the process is reported by Mahapatra et al. [105] for reference. A mathematical code developed for the above formulation is used to obtain computational results.

4.6 Results and Discussions

In the present work, new higher-order unified formulations have been derived for the determination of deflection, axial stress and shear stress, as mentioned in the previous section. Now the results generated using these formulae have been validated, as discussed below.

4.6.1 Verification of results

To verify the results with standard literature references, we consider the data as discussed in a numerical example of cantilever beam in Li et al. [33]. The considered beam is of length L = 0.5m, depth h = L/3 and width of unit length. Aluminium (Al) has been considered at the bottom and Silicon Nitride (Si3N4) has been considered at the top as the constituent materials for the functionally graded material for this beam, whose properties have been mentioned below.

$$E_b = E_{Al} = 70GPa, E_t = E_{(Si_3N_4)} = 348GPa$$

A constant value of Poisson's ratio is assumed over here as 0.3. The value of the power law index is assumed to be equal to 1. It has been assumed that at the top of the beam, a pressure load of 1kN/m is being imposed uniformly. The axial and shear stresses are normalized as follows:

$$\sigma_{x,norm} = \frac{\sigma_{xx}A}{ql}, \quad \tau_{xz,norm} = \frac{\tau_{xz}A}{ql}$$

The normalized axial and shear stresses are calculated at different locations in the span of the beam and are presented in Figures.

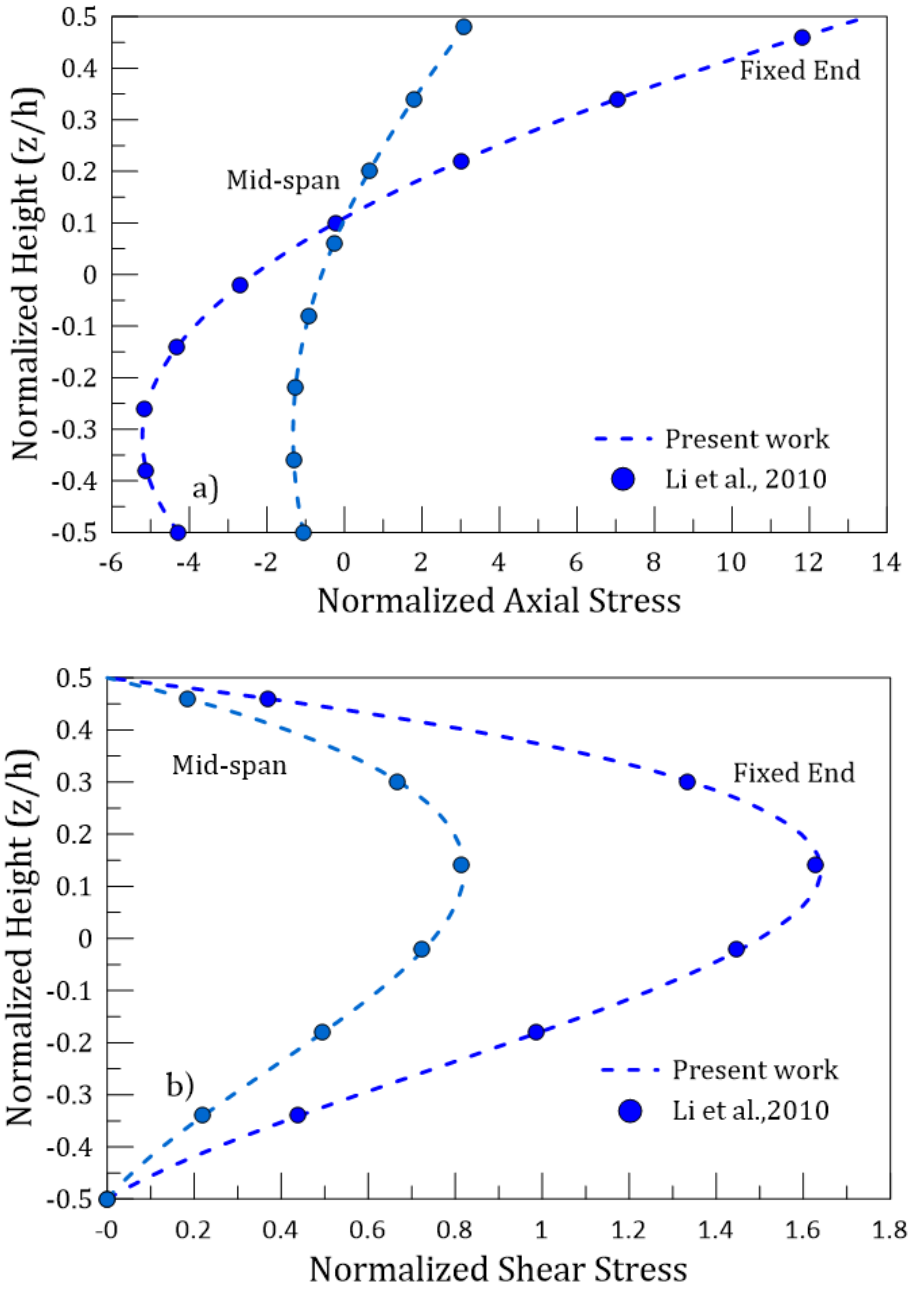

Fig. 4.7: Verification of present work, a) normalized axial stress b) normalized shear stresses (ignoring E6)

As can be observed from Figure 4.7, the results of this study match exactly those of Li et al. [33] while ignoring the higher order terms that contain E6. The significance of the terms containing E6 on the behaviour of FG beams is explored in successive paragraphs.

A comparison of normalized axial and shear stresses for higher-order beam theory used in [33] with the higher-order beam theory of the present work (considering E6) reveals that the effect of E6 is negligible for axial stresses; however, from Figure 4.8, it can be clearly observed that the effect of consideration of the higher order terms has a moderate

effect (approximately 4.083%) on shear stresses and a very small difference of 0.836% in the normalized axial stresses.

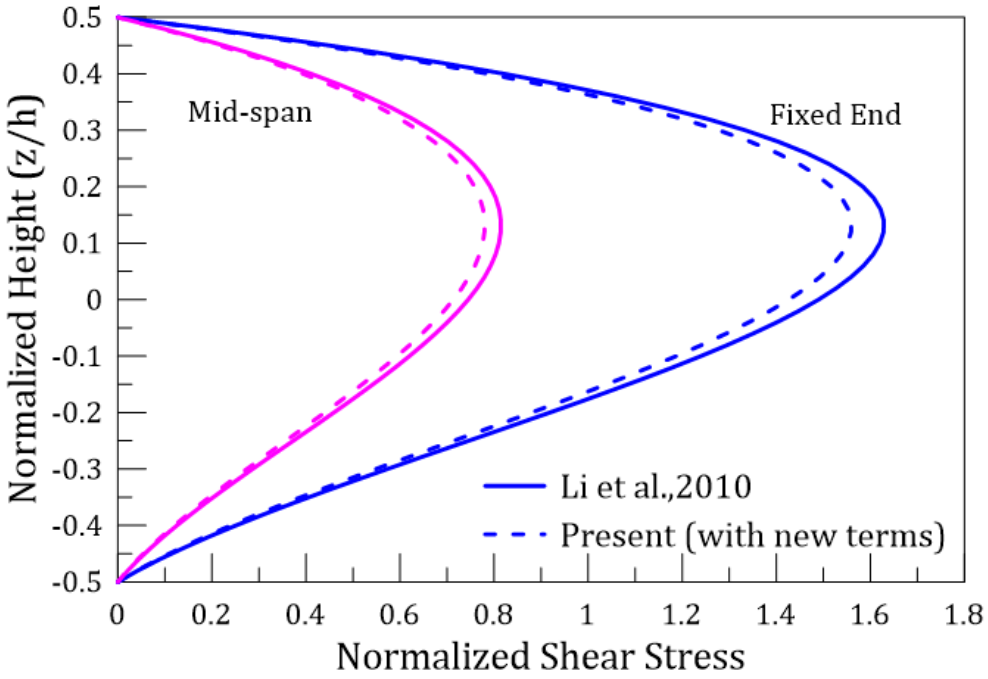

Fig. 4.8: Comparison plots for effect of higher order terms on shear stress

4.6.2 Other numerical experiments

In this section, the behaviour of FG beams for different cases of material distribution (using different index values) and the effect of shear modulus on the stresses are discussed. In Figure 4.9a & b, the normalized axial and shear stresses at the fixed end of the beam are respectively plotted for different values of the power law index ranging from (0, 0.2, 1, 2, and 5). Hence, a comparative study of axial and shear stresses in FG beams with an equivalent isotropic beam can be observed. The asymmetry in the material composition results in behavioural variations, as reported in Figure 4.9. With the increase in index value, the maximum axial stress (at the top and bottom fibers) varies considerably as compared to the isotropic case. The maximum shear stress also increases with increasing index up to a certain maximum, then decreases.

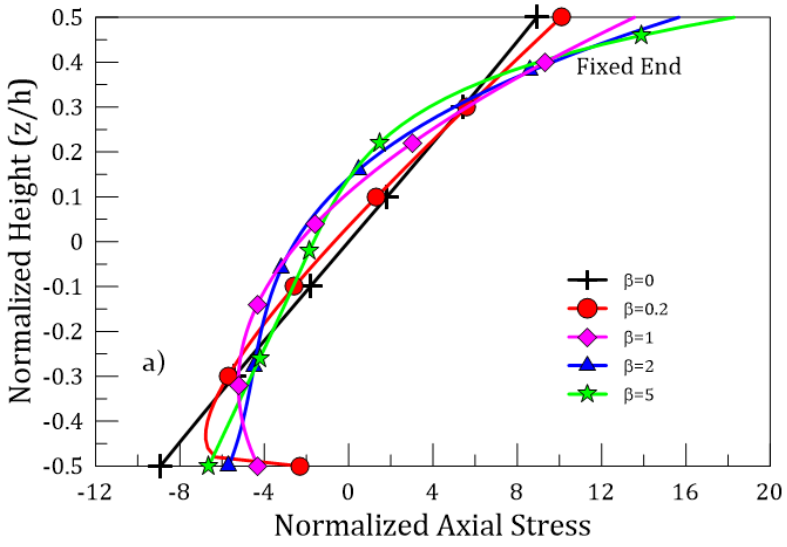

(a)

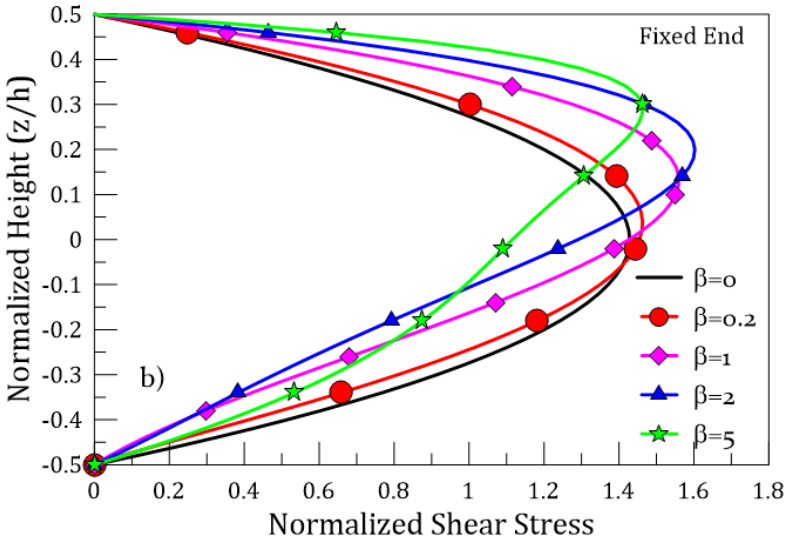

(b)

Fig. 4.9: Effect of material gradation on stresses (fixed end), a) Normalized axial stresses b) Normalized shear stresses

The study of the effect of material gradient on deflection and stresses of an FG beam can be further extended using three dimensional plots that give better visualization and understanding. Figure 4.10(a-c) reports the 3D plots corresponding to the beam and can be referred to for the study of the effect of material index on the beam behaviour.

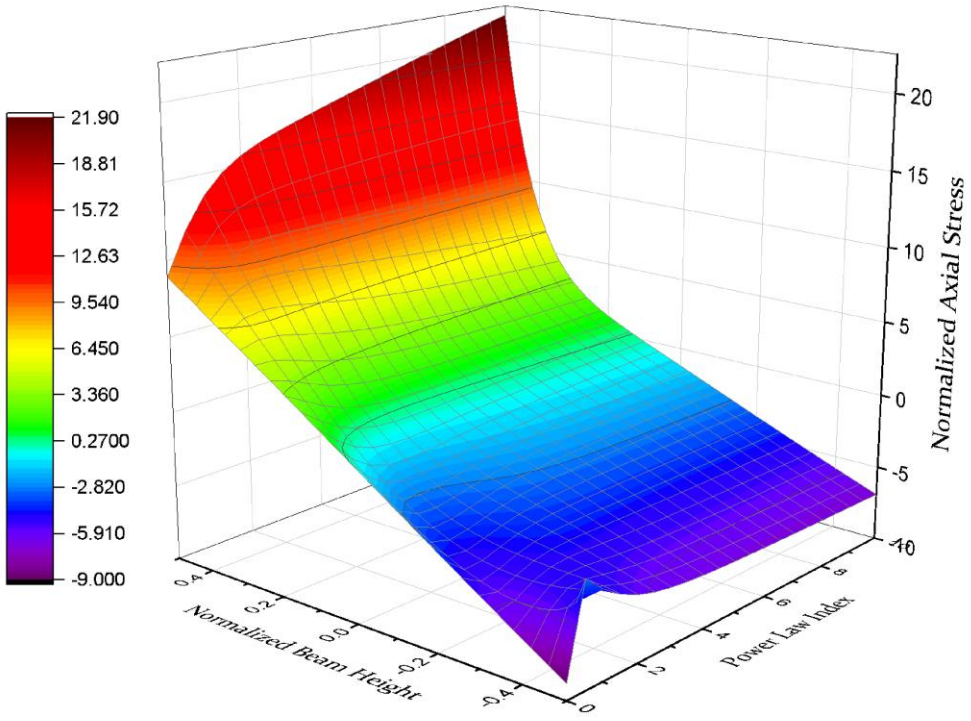
21.90
18.81
15.72
12.63
9.540
6.450
3.360
0.2700
-2.820
-5.910
-9.000
Normalized Axial Stress
20
15
10
5
0
-5
-10
Normalized Beam Height
0.4
0.2
0.0
-0.2
-0.4
Power Law Index
0
2
4
6
8

(a)

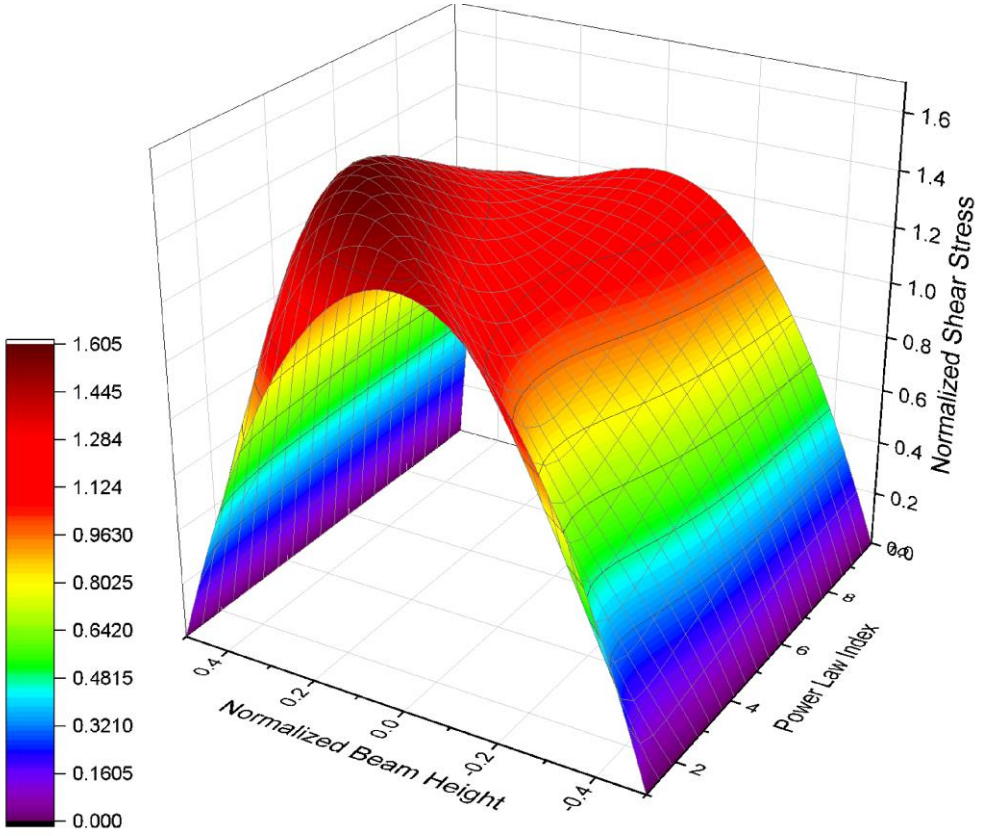
1.605
1.445
1.284
1.124
0.9630
0.8025
0.6420
0.4815
0.3210
0.1605
0.000
Normalized Shear Stress
1.6
1.4
1.2
1.0
0.8
0.6
0.4
0.2
0.0
Normalized Beam Height
0.4
0.2
0.0
-0.2
-0.4
Power Law Index
0
2
4
6
8

(b)

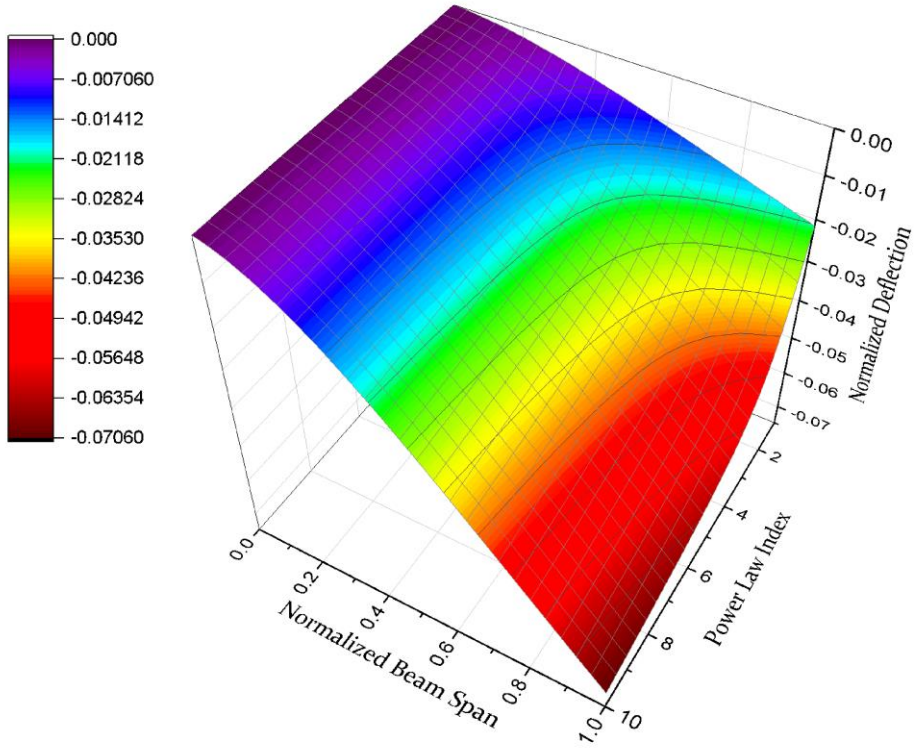

(c)

Fig. 4.10: 3D plots to visualize the effect of material gradation on beam behaviour a) Normalized axial stress, b) Normalized shear stress, c) Deflection

In Figure-4.10, comparative plots for different beam theories are reported for axial and shear stresses for different values of aspect ratio. For Euler's theory the shear modulus is considered to be infinite while for Timoshenko theory the value of c1 is assumed to be zero. To distinguish the current study and Li [33] for higher order beam theory, the terms containing E6 are multiplied with an arbitrary constant whose value is taken as zero/ one; when it is zero, it suffices to Li's work while its value is one for present study. The normalized transverse deflection is calculated using the relation:

$$\bar{w} = \frac{wh^3 E_b}{qL^4}$$

In Figure-4.11(a & b), the deflection of cantilever corresponding to various beam theories is plotted for two aspect ratios of 3 and 10. It can be observed that for L/h=3, there is a significant difference in deflection corresponding to Euler's theory, while, Li's work

and present deflections are almost equal, differences being negligible. Timoshenko deflection only marginally varies from the higher order cases. However, for L/h=10, all types of deflections are practically indistinguishable. The results are in line with the previous similar reported studies.

It can be observed from Figure-4.11(c & d) that the axial stresses calculated by all the beam theories are nearly equally for both aspect ratios. The normalized axial stress values are proportionally increasing for increasing aspect ratios while the variation is of same profile. However, shear stresses are significantly different for the various theories considered as in Figure-6(e&f). The shear stresses are zero for Euler's theory due to infinite value of shear modulus while for other theories, the observed values of shear stresses are parabolically obtained with zero shear at top and bottom surfaces. The values of shear stresses obtained using higher order beam theory [33] are slightly higher than that of Timoshenko theory and the results obtained using the present work are in between the stresses obtained by Timoshenko beam [27] and higher order beam theory reported in [33].

Average percentage difference between the results, with and without the inclusion of higher order terms (i.e., present work and cited literature) for normalized axial stress is 0.8355% and for normalized shear stress, it is 4.083% (For details, please refer appendix).

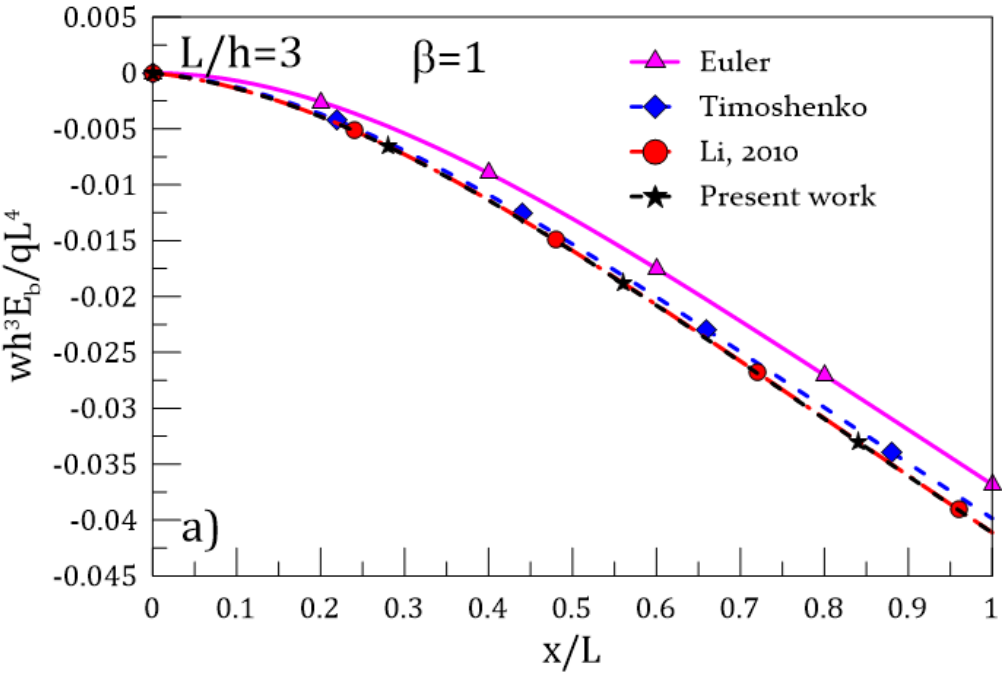

(a)

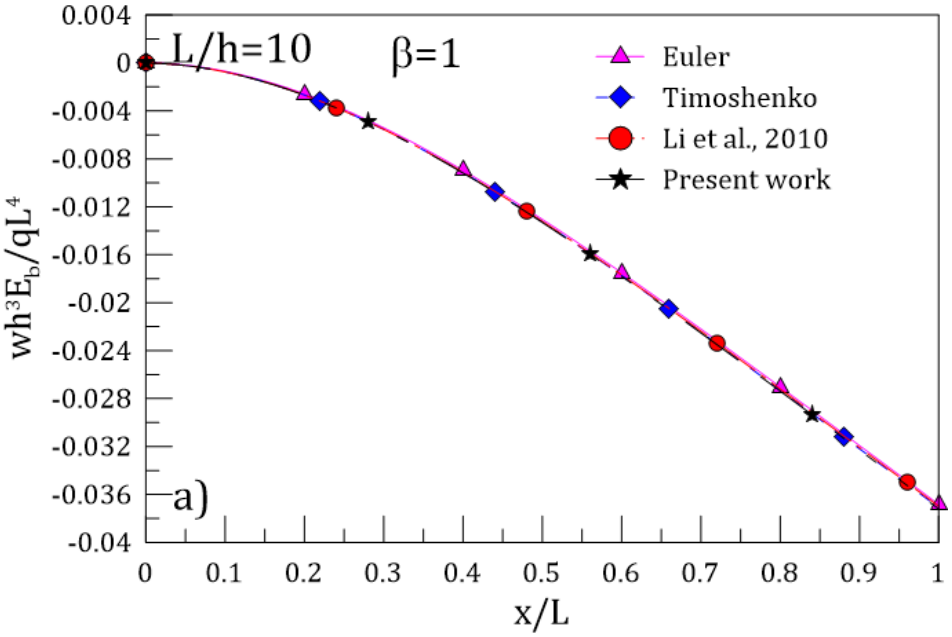
L/h=10
β=1
Euler
Timoshenko
Li et al., 2010
Present work
a)
wh^3E_b/qL^4
x/L
0.004
0
-0.004
-0.008
-0.012
-0.016
-0.02
-0.024
-0.028
-0.032
-0.036
-0.04
0
0.1
0.2
0.3
0.4
0.5
0.6
0.7
0.8
0.9
1

(A)

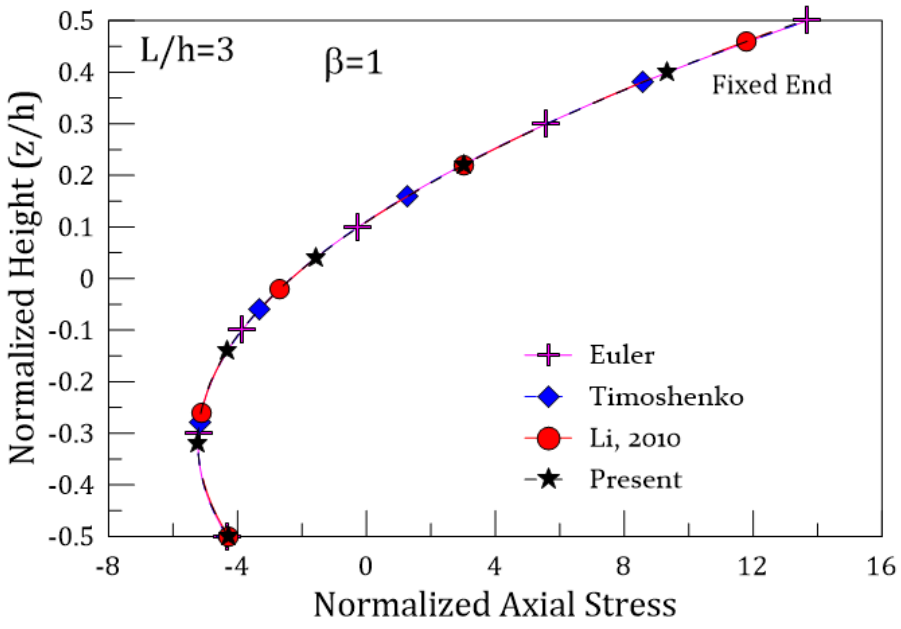
L/h=3
β=1
Fixed End
Euler
Timoshenko
Li, 2010
Present
Normalized Height (z/h)
Normalized Axial Stress
0.5
0.4
0.3
0.2
0.1
0
-0.1
-0.2
-0.3
-0.4
-0.5
-8
-4
0
4
8
12
16

(b)

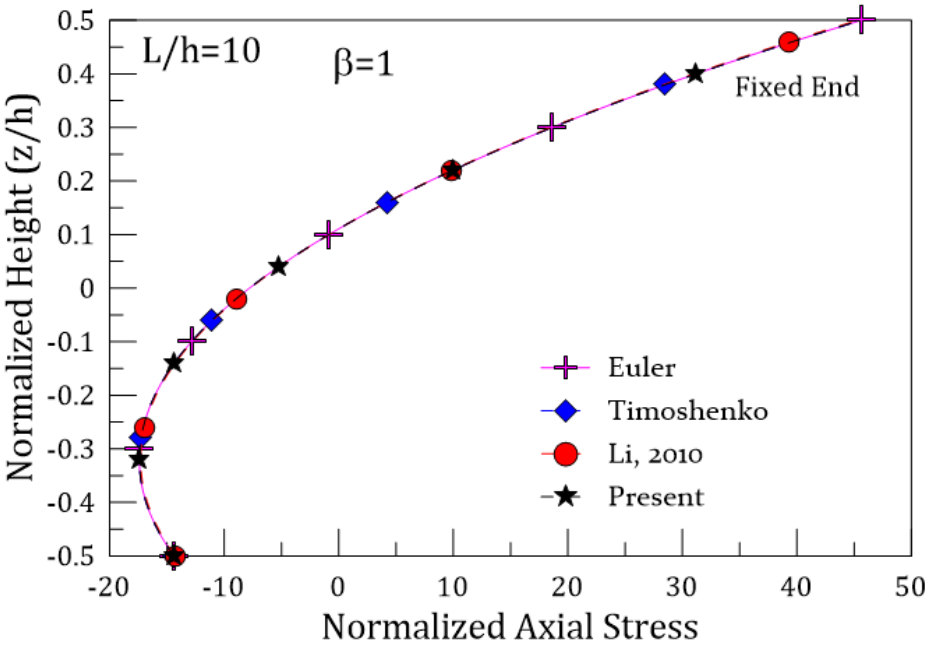
L/h=10
β=1
Fixed End
Euler
Timoshenko
Li, 2010
Present
Normalized Height (z/h)
Normalized Axial Stress
0.5
0.4
0.3
0.2
0.1
0
-0.1
-0.2
-0.3
-0.4
-0.5
-20
-10
0
10
20
30
40
50

(b)

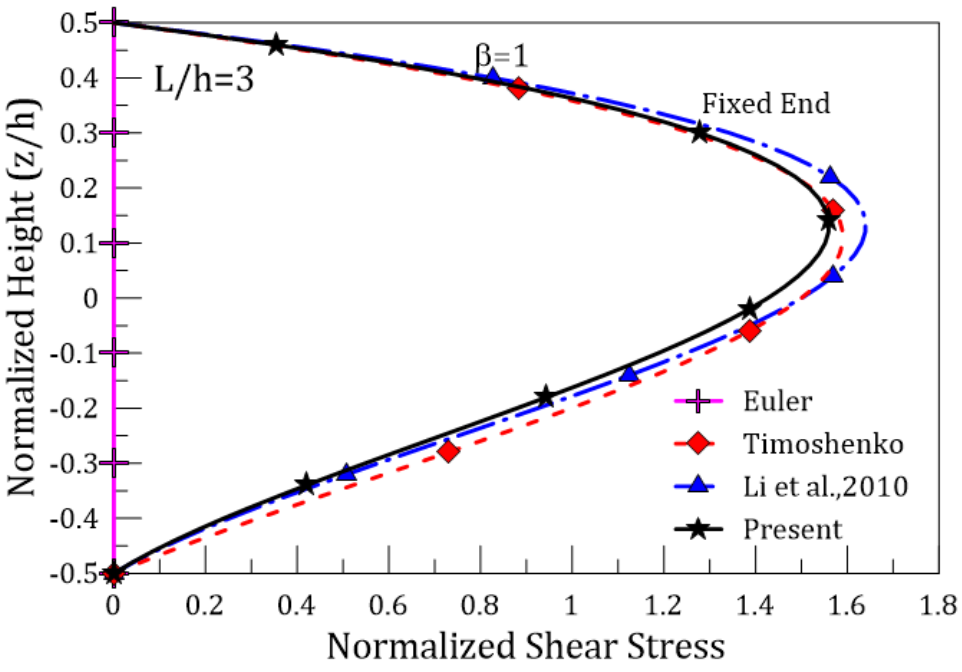
L/h=3
β=1
Fixed End
Euler
Timoshenko
Li et al.,2010
Present
Normalized Height (z/h)
Normalized Shear Stress
0.5
0.4
0.3
0.2
0.1
0
-0.1
-0.2
-0.3
-0.4
-0.5
0
0.2
0.4
0.6
0.8
1
1.2
1.4
1.6
1.8

(c)

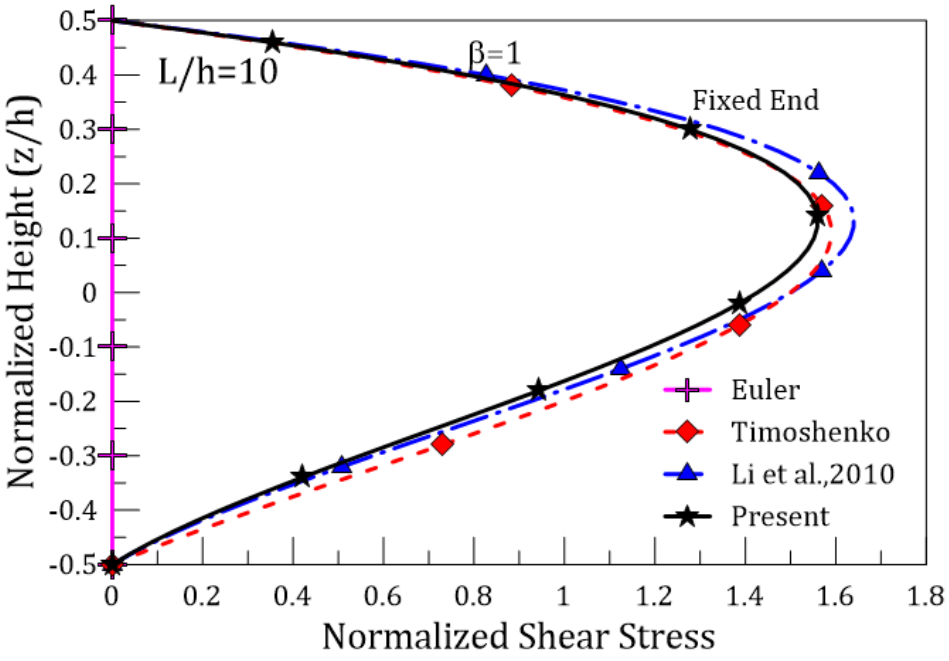

(c)

Fig. 4.11: Comparison of various results according to various beam theories for L/h ratio 3 &10 – (a) Beam Deflection for L/h=3 &10, (b) Normalized Axial Stress for L/h=3&10, and (c) Normalized Shear Stress for L/h=3&10

To continue further with the numeric experiments, normalized transverse deflection are studied as a function of material gradient index. The maximum deflection that is obtained is a function of index value as reported in literature. Hence to observe such effects in the present case along with the effect of aspect ratio using various beam theories is reported in Figure 4.12. For an in-depth observation, the study has been categorized as two cases; Case-A: when ceramic is on the top surface, Case-B: metal surface is in top with the external uniformly distributed load acting on the top surface in downward direction. It can be expected that changing the loading surface will also have substantial effect on the behaviour of beam for a given material composition.

It can be clearly observed from Figure-4.12a of case A that for thick stubby beams there is a clear difference in the maximum transverse displacement corresponding to Euler, Timoshenko and higher order theories. This difference is small for lower gradients, that increases as the value of index β increases for L/h=3. This difference in normalized transverse displacement reduces as the aspect ratio increases; for L/h =10, the difference is practically insignificant as in Figure-4.12b of case A. Another noticeable observation in Figure-4.12 (a & b) of case A is that the slope of the curve (rate of increase in maximum

deflection) decreases as the material gradient increases. This can be explained by the fact that the percentage of metal (less stiff component) increases as the value of β increases, (when β=0 then material at top surface is 100%, for β=1, both components are 50% and further increase in β increases the composition of metal). It can be observed that the effect of material gradient is more significant for values up to β=2; the effect is less significant for higher index values.

In the next study, i.e. Case-B, the beam is inverted to expose the metal part to the external load applied at top surface. For β=0, i.e. for isotropic material made of metal, the deflection is maximum and as the stiffer component fraction increases with the value of β the deflection decreases considerably. This can be observed in Figure-4.12 a & b of case B for aspect ratio 3 and 10. Similar to the previous case the difference in the Euler and higher order displacements is significant for lower aspect ratio and is practically insignificant for aspect ratio greater than 10.

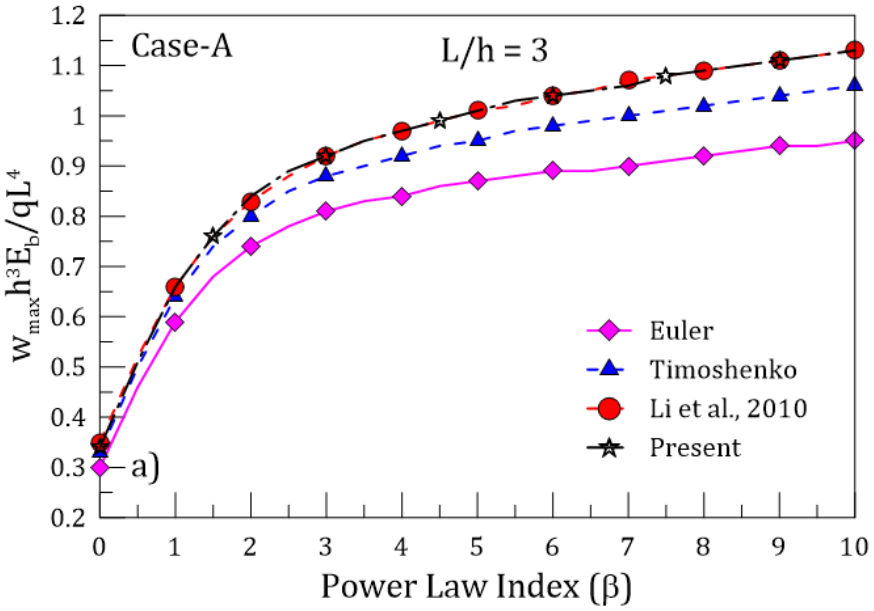

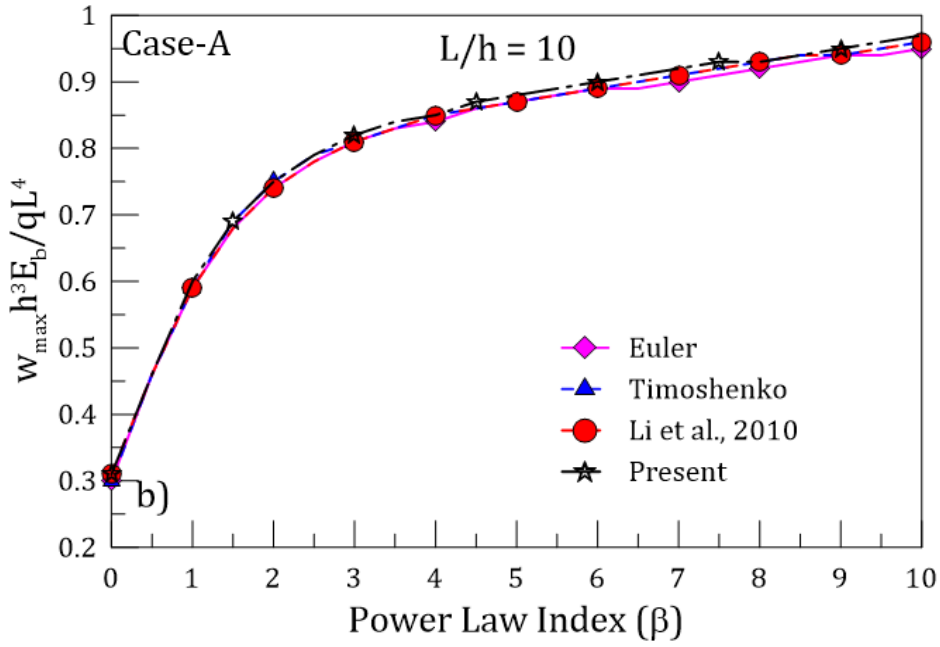
Case-A
L/h = 10
Euler
Timoshenko
Li et al., 2010
Present
b)
$w_{max}h^3E_b/qL^4$
Power Law Index (β)

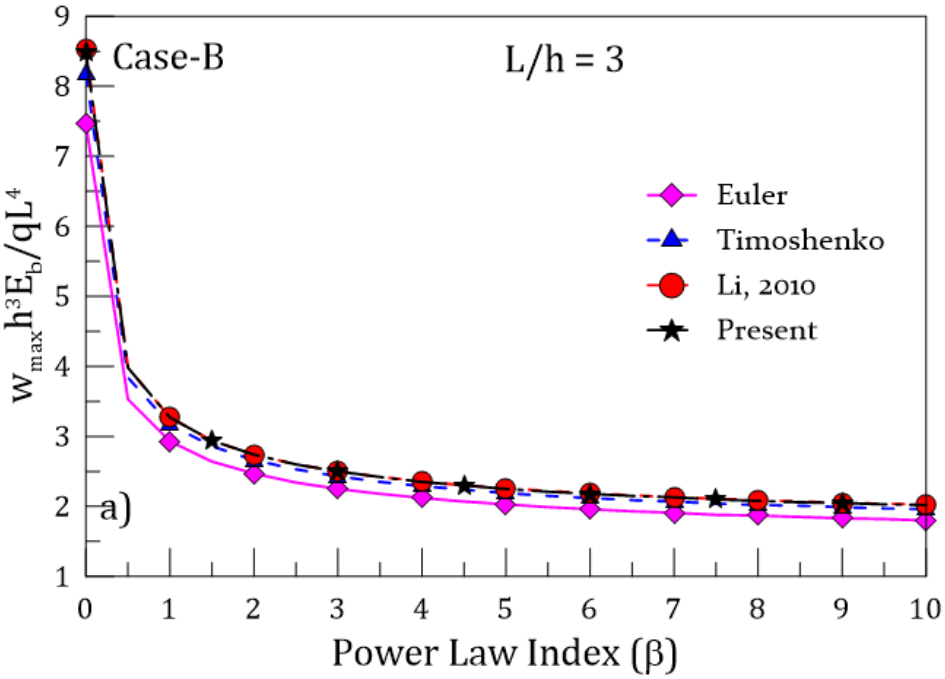
Case-B
L/h = 3
Euler
Timoshenko
Li, 2010
Present
a)
$w_{max}h^3E_b/qL^4$
Power Law Index (β)

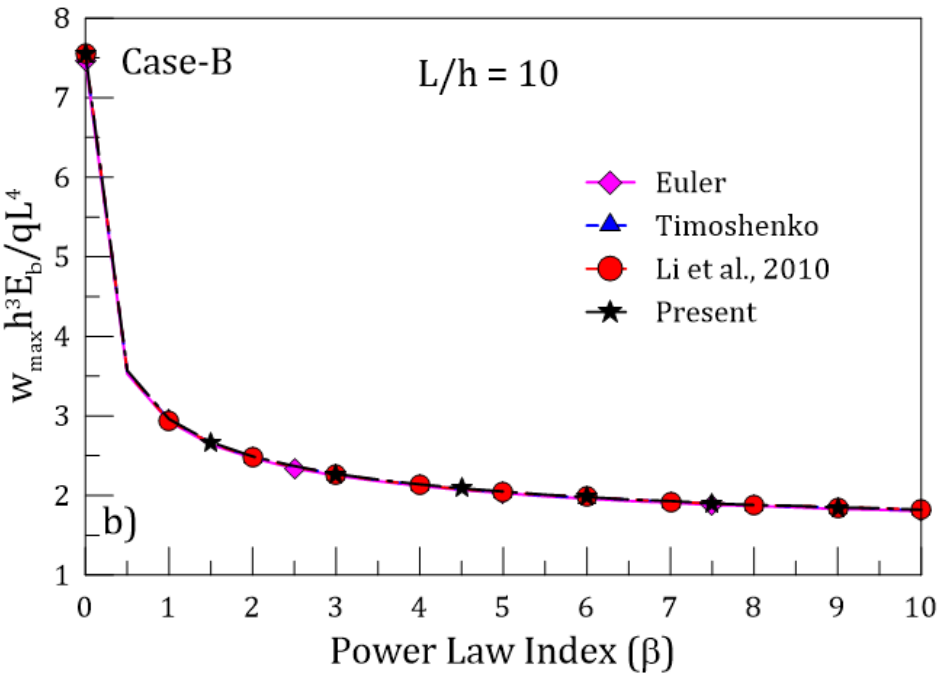

Fig. 4.12. Dimensionless maximum transverse deflection as a function of material gradient index for Case A: Metal at base and Ceramic at top and Case B: Metal at top and Ceramic at base.

Another study has been done where three discrete combinations of materials have been selected to observe the variation in beam behaviour due to arbitrary ratio of material properties. The material properties of selected materials are mentioned in Table-4.2. The combination of materials with ration of material properties is mentioned in Table-4.3.

Table 4.2. Structural Properties of the reinforcing particles [33]

Sl. No.	Material	Modulus of Elasticity	Poisson's Ratio
1.	Aluminum	70GPa	0.30
2.	Silicon Nitride	348GPa	0.24
3.	Silicon Carbide	440GPa	0.27
4.	Steel	210GPa	0.30

Table4.3. Combination of various reinforcing particles for analysis under mechanical load

Set	Materials	Ratio of Modulus of Elasticity
Set-A	Aluminum+ Silicon Nitride	(348GPa /70GPa) ~5
Set-B	Aluminum+ Silicon Carbide	(440GPa /70GPa) ~7
Set-C	Aluminum+ Steel	(210GPa /70GPa) ~3

The three combinations can be observed to have a discrete ratio of modulus of elasticity (3, 5 and 7). The behaviour of such beams corresponding to β=1 has been plotted in Figure-4.13 to observe the variations and relate the same to ratio of material properties. The behaviour of such beams corresponding to β=1 under uniformly distributed load for a comparative study is mentioned in Figure-4.13.

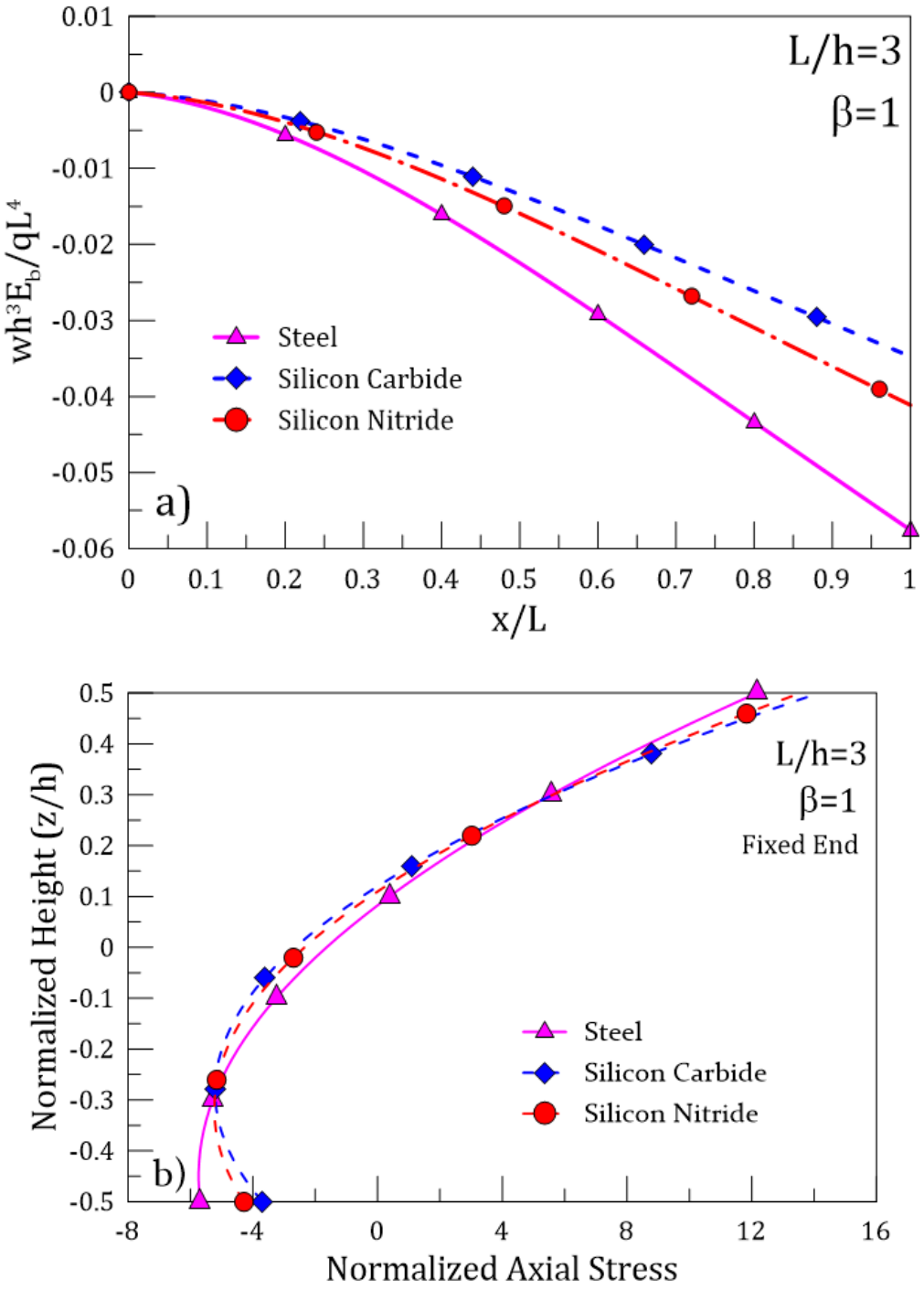

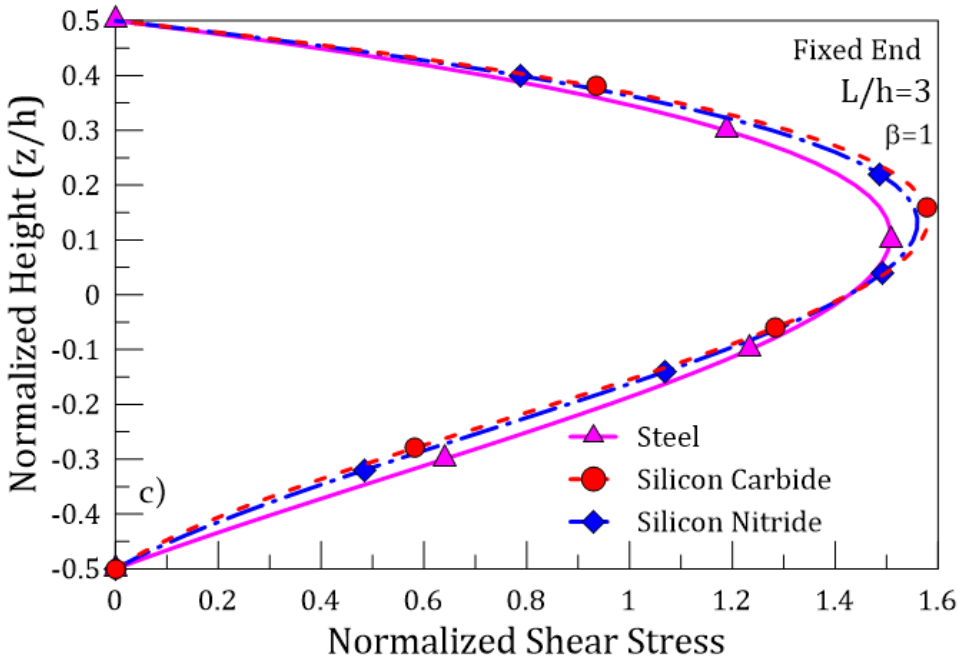

Figure-4.13 Comparative plots for various combinations of materials with aluminium a) Normalized Transverse Deflection b) Normalized Axial Stress c) Normalized Shear Stress

The deflection of cantilever beam is plotted in Figure-4.13a. From the figure it can be observed that composition corresponding to Set-B is stiffer and that validates the elasticity moduli ratio. However, when we observe the stresses, the variation is as shown in Figure-4.13b for axial stress and 9c for shear stress. The stresses are found to be higher for higher moduli ratios. In the present case, the normalized tensile stresses at top surface are higher for Set-B for moduli ratio 7 while the compressive stresses are on the lower side for the same set of materials. On the contrary, for Set-B with moduli ratio 3, the maximum tensile stress at top fibre is lower and compressive stress at lower surface are higher than the other sets. Another observation from Figure-4.13b is that the steepness (curvature) of the axial stress curves increases with increase in moduli ratio. Figure-9c shows the normalized shear stress plots for the three combinations of materials. It is clear that shear stress is higher for Set-B with higher moduli ratio, which can also be inferred from the axial stress values. This discussion is pertinent to the design plan of FG beams.

The study is further extended to include simply supported boundary condition (bending moment and deflection are zero at the supports) for FG beam. In Figure 4.14, deflection and stress plots corresponding to simply supported boundary condition are presented. It is observed that the differences in axial stress and shear stress are similar in trend as for cantilever support. The percentage difference in axial stresses for a cantilever

beam is about 1.2% for isotropic beam and 1.9% for FG beam. On the other hand, the difference in shear stress is 7.7% for isotropic beam and 8.0% for FG beam (details can be referred in appendix)

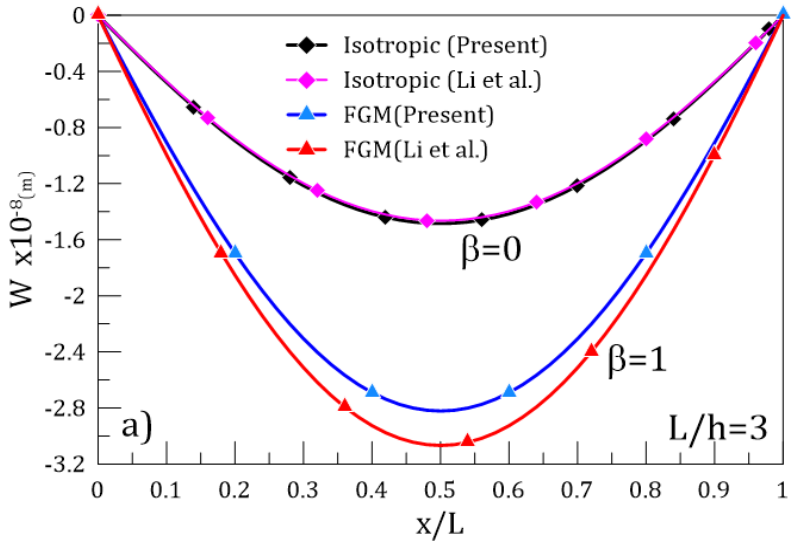

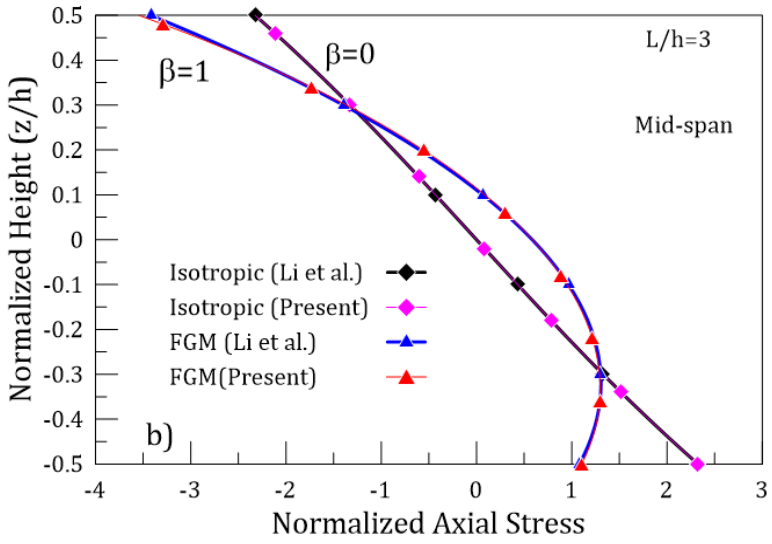

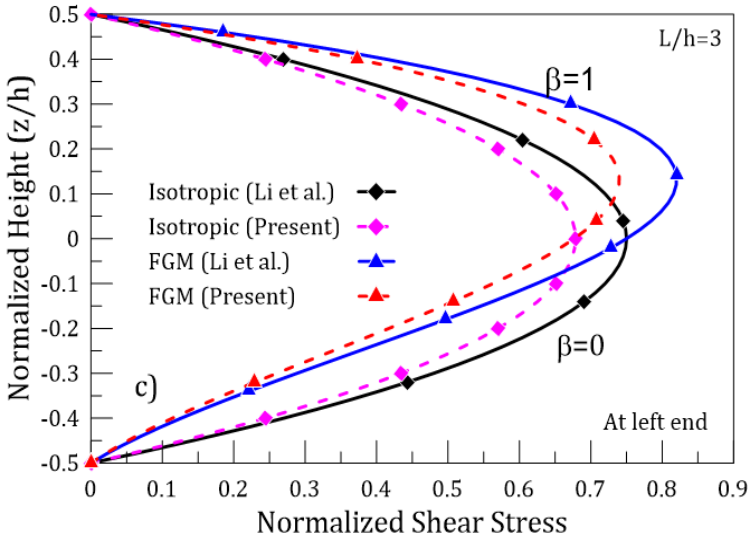

Figure-4.14 Comparison of the isotropic and FG beam behaviour with/without higher order terms a) deflection, b) normalized axial stress, c) normalized shear stress

4.7 Closure

Using Hamilton's principle, a higher-order beam formulation is derived to obtain a single governing equation for functionally graded beams by incorporating higher-order terms that were not considered in previous similar work. The unification of three developed equations into a single equation is done by considering a parameter that is a function of domain variables. The solution to the governing equation is approached using the approximation technique of B-spline collocation. A cantilever functionally graded beam with grading along the cross-section is studied for its behavioural properties under the action of a distributed mechanical load. The variation of modulus of elasticity and modulus of rigidity is considered by power law, and Poisson's ratio is considered to be a constant. The collocation points are calculated using Greville abscissa. It is observed that the new higher order terms have a moderate effect (approximately 4%) on the shear stress calculations compared to the similar report cited in the literature and only 0.8% on normalized axial stresses. The normal stresses are negligibly affected by the new terms considered for cantilever beams. The difference in values corresponding to simply supported end conditions is slightly on the higher side; 1.8% for axial stress and 8% for shear stresses. The study is then extended to explore the effect of material gradient, aspect ratio, and moduli ratio on transverse deformation, normalized axial stresses, and normalized shear stress variations.

Chapter 5: **Unified Higher Order Formulation under Thermo-Mechanical load**

5.1 Introduction

The development of functionally graded materials as high-grade composite materials has fundamentally changed engineering and several aspects of material technology research. Due to the progressive change in their properties, which is the core of FGMs, naturally occurring FGMs like bamboo, human bones and teeth, etc., exhibit excellent qualities in their behaviour. However, FGM was developed to stop composites from delaminating under thermo-mechanical stress conditions. In order to achieve high temperature strength and toughness and to avoid stress concentration or residual stresses, the most typical FGM is composed of a refractory ceramic and metal. The FGMs have continuous or gradual changes in characteristics, hence there is no interface problem, in contrast to typical composites which have sharp interfaces leading to failures.

Structures are made up of plates and beams. When structures are subjected to harsh environments, the materials must possess excellent qualities in order to withstand such situations. When a space shuttle enters the earth's atmosphere, it is subjected to a very high temperature gradient via a very thin layer of air. The enormous gradient in pressure and temperature necessitates strict behaviour that is particularly important near the interface. The ceramic half of ceramic-metal based FGMs is exposed to greater temperatures while the metal part guarantees the FGM maintains its strength, making them particularly ideal for such extreme temperature gradients. The stress-concentration and residual stresses that would have otherwise generated are sustained by the gradual change in material characteristics. Such structural components must be designed after a careful investigation of load-deflection-stress behaviour under various thermomechanical conditions.

After an exhaustive review of the published works in the area of thermo-mechanical analysis of FG beams it has been observed that studies pertinent to simultaneous thermal and mechanical loading has been relatively less. Considering the scope of applications of beams in wide areas of severe/ critical standards the possibility of beams exposed to amalgamated thermal and mechanical loading cannot be foreseen. In other words when FG beam is subjected to constant mechanical load in thermal environment the study of

deformation and stresses with changes in temperature distribution can be quite significant in its design analysis and synthesis.

In this chapter the effect of change of temperature distribution on stress and deformation behaviour of an FG Timoshenko beam loaded with a constant mechanical load and a temperature gradient in transverse direction is reported. The governing equations derived in the previous chapter for FG beams have been extended to include the thermal strains due to applied temperature gradients. The effect of transverse shear strains is also considered. As the formulation is derived using the unified approach as reported by Li [27] in which a single governing equation is derived by reducing the three differential equations of displacement variables into a single fourth order equation. Poisson's ratio is assumed to be a constant and material properties are assumed to be independent of temperature change. Such formulation in the area of thermo-mechanical analysis is unique and has been reported for the first time in literature.

Exact solutions are obtained assuming beam to be subjected to various boundary conditions. Numerical solution using B-spline collocation is also used to study the deformation and stresses so as to compare the same with exact results and thus to verify the precision of the technique for thermo-mechanical loading conditions. The combination of materials as discussed in previous chapter i.e. Aluminium/Steel (metal-metal), Stainless Steel/ Silicon Nitride(metal-ceramic) and Stainless Steel/ Zirconia (metal-ceramic) as FGM-1, FGM-2 & FGM-3 have been also considered in the present study of thermo-mechanical loading under linear and non-linear distribution of temperatures.

5.2 Governing equation of FG beam under thermo-mechanical load

This section discusses the formulation of the beam taken into account to include thermal gradients across the beam cross-section. The thermal force and thermal moment produced by the temperature gradient applied to the beam result in thermal bending. When an isotropic material is used, a beam's uniform temperature rise does not result in bending; nevertheless, if thermal strains are restricted, thermal buckling, also known as bowing, results. However, with functionally graded materials, the beam bends for any kind of temperature change, even for a uniform rise. The change in coefficient of thermal expansion brought on by the material grading of FGM's component parts is what causes bending. The mechanical load and the amount of mechanical pressure present will determine the amount of deformation that results.

This section discusses the governing equation for a uniformly loaded FG beam that is exposed to a temperature gradient. The dimensions and coordinate system used in the previous chapter are presumptively the same. The methodology is still the same; the only difference is that in addition to mechanical strains, thermal strains caused by temperature gradients must also be taken into account. The strains are deducted from the mechanical strains since it is recognized that thermal strains only cause stresses when they are restricted. The remaining criteria and technique are the same as those previously taken into account.

Based on higher order beam theory:

$$u(x,z) = u_0(x) + z\phi_0 - \frac{4z^3}{3h^2}\left(\phi_0 + \frac{\partial w}{\partial x}\right) \tag{5.1}$$

$$\varepsilon_{xx} = \frac{\partial u_0}{\partial x} + z\frac{\partial \phi_0}{\partial x} - \frac{4z^3}{3h^2}\left(\frac{\partial \phi_0}{\partial x} + \frac{\partial^2 w}{\partial x^2}\right) = {\varepsilon_{xx}}^{(0)} + z{\varepsilon_{xx}}^{(1)} + z^3{\varepsilon_{xx}}^{(3)} \tag{5.2}$$

$$\varepsilon_{thermal} = \alpha(z)\{T(z) - T_0\} \tag{5.3}$$

$$\gamma_{xz} = \left(1 - \frac{4z^2}{h^2}\right)\left(\phi_0 + \frac{\partial w}{\partial x}\right) = {\gamma_{xz}}^{(0)} + z^2{\gamma_{xz}}^{(2)} \tag{5.4}$$

where,

$$\varepsilon_{xx}^{(0)} = \frac{\partial u_0}{\partial x}$$

$$\varepsilon_{xx}^{(1)} = \frac{\partial \emptyset_0}{\partial x}$$

$$\varepsilon_{xx}^{(3)} = -c_1\left(\frac{\partial \emptyset_0}{\partial x} + \frac{\partial^2 w}{\partial x^2}\right)$$

$$\gamma_{xz}^{(0)} = \emptyset_0 + \frac{\partial w}{\partial x}$$

$$\gamma_{xz}^{(2)} = -c_2\left(\emptyset_0 + \frac{\partial w}{\partial x}\right)$$

$$c_1 = \frac{4}{3h^2}, c_2 = \frac{4}{h^2}$$

Here α(z) is the coefficient of thermal expansion and T(z) is the temperature profile; both of these depends on the material configuration given by volume composition of parent materials.

The constitutive law for the material for linear thermo-elastic conditions is given by-

$$\begin{aligned} \sigma_{xx} &= E(z).\{\grave{o}_{xx} - \grave{o}_{thermal}\} \\ &..... = E(z).\left\{\frac{du}{dx} + z\frac{d\phi_0}{dx} - \frac{4z^3}{3h^2}\left(\frac{d\phi_0}{dx} + \frac{d^2w}{dx^2}\right) - \alpha(z)\left(T(z)\text{-}T_0\right)\right\} \end{aligned} \tag{5.5}$$

$$\tau_{xz} = G(z).\gamma_{xz} = G(z).\left(1 - \frac{4z^2}{h^2}\right)\left(\phi + \frac{dw}{dx}\right) \tag{5.6}$$

To derive the governing equations of motion for an FG beam, Hamilton's Principle is applied as shown below.

$$\delta L = \delta(U + K + V) = 0 \tag{5.7}$$

$$\left.\begin{aligned} \delta U &= \int_0^t \int_0^L \int_A (\sigma_{xx}\delta\varepsilon_{xx} + \tau_{xz}\delta\gamma_{xz})\, dA dx dt \\ \delta K &= \int_0^t \int_0^L \int_A \rho(z)(\dot{u}\delta\dot{u} + \dot{w}\delta\dot{w})\, dA dx dt \\ \delta V &= -\int_0^t \int_0^L q\delta w dx dt \\ \delta W &= \frac{1}{2}\int_0^t \int_0^L N_T \delta\left(\frac{dw}{dx}\right)^2 dx\, dt \end{aligned}\right\} \tag{5.8}$$

Substituting the expressions for U, K and V in Eq. (8) and assuming,

$$N_x = \int_A \sigma_{xx} dA, \quad M_x = \int_A z\sigma_{xx} dA \tag{5.9}$$

$$P_x = \int_A z^3 \sigma_{xx} dA, \quad Q_x = \int_A \tau_{xz} dA, \tag{5.10}$$

$$R_x = \int_A z^2 \tau_{xz} dA \; and I_k = \int_A z^k \rho(z) dA, \tag{5.11}$$

In the above equations, N_T represents the thermal force; M_T is the thermal moment given by-

$$N_T = \int_{-h/2}^{h/2} E(z).\alpha(z).\Delta T(z).dA \tag{5.12}$$

$$M_T = \int_{-h/2}^{h/2} z.E(z).\alpha(z).\Delta T(z).dA \tag{5.13}$$

We get the following governing equation

$$\begin{aligned} &\int_0^t \int_0^L \left(N_x \delta {\varepsilon_{xx}}^{(0)} + M_x \delta {\varepsilon_{xx}}^{(1)} + P_x \delta {\varepsilon_{xx}}^{(3)}\right) dxdt \\ &\quad + \int_0^t \int_0^L \left(Q_x \delta {\gamma_{xz}}^{(0)} + R_x \delta {\gamma_{xz}}^{(2)}\right) dxdt \\ &\quad + \int_0^t \int_0^L I_k((\dot{u}\delta\dot{u} + \dot{w}\delta\dot{w}))\, dxdt \\ &\quad - \int_0^t \int_0^L q\delta w dxdt - \int_0^t \int_0^L N_T \delta\left(\frac{dw}{dx}\right)^2 dx\, dt = 0 \end{aligned} \tag{5.14}$$

Integrating by parts and categorically separating the variables, the following governing equations and boundary conditions are derived.

$$\frac{\partial \mathrm{N_x}}{\partial \mathrm{x}} = \mathrm{I_0}\frac{\partial^2 \mathrm{u_0}}{\partial \mathrm{t}^2} + \mathrm{I_1}^*\frac{\partial^2 \varphi_0}{\partial \mathrm{t}^2} - \mathrm{c_1 I_3}\frac{\partial^3 \mathrm{w}}{\partial \mathrm{x}\,\partial \mathrm{t}^2} \tag{5.15}$$

$$\frac{\partial \bar{M}_\mathrm{x}}{\partial \mathrm{x}} - \bar{\mathrm{Q}}_\mathrm{x} = \mathrm{I_1}^*\frac{\partial^2 \mathrm{u_0}}{\partial \mathrm{t}^2} + \mathrm{K_2}^*\frac{\partial^2 \varphi_0}{\partial \mathrm{t}^2} - \mathrm{c_1 I_4}^*\frac{\partial^3 \mathrm{w}}{\partial \mathrm{x}\,\partial \mathrm{t}^2} \tag{5.16}$$

$$c_1\frac{\partial^2 \mathrm{P_x}}{\partial \mathrm{x}^2} + \frac{\partial \bar{Q}_\mathrm{x}}{\partial \mathrm{x}} + N_T\frac{\partial^2 w}{\partial x^2} + \mathrm{q} = \mathrm{c_1 I_3}\frac{\partial^3 \mathrm{u_0}}{\partial \mathrm{x}\,\partial \mathrm{t}^2} + \mathrm{c_1 I_4}^*\frac{\partial^3 \varphi_0}{\partial \mathrm{x}\,\partial \mathrm{t}^2} - \mathrm{c_1}^2\mathrm{I_6}\frac{\partial^4 \mathrm{w}}{\partial \mathrm{x}^2\,\partial \mathrm{t}^2} + \mathrm{I_0}\frac{\partial^2 \mathrm{w}}{\partial \mathrm{t}^2} \tag{5.17}$$

Boundary Conditions ($atx = 0$ &$atx = L$)

$$N_x - I_0\frac{\partial u_0}{\partial t} - I_1\frac{\partial \phi_0}{\partial t} + c_1 I_3\left(\frac{\partial \phi_0}{\partial x} + \frac{\partial^2 w}{\partial x \partial t}\right) - N_T = 0 \tag{5.18}$$

$$\bar{M}_x - I_1^*\frac{\partial u_0}{\partial t} - K_2^*\frac{\partial \phi_0}{\partial t} + c_1 I_4^*\frac{\partial^2 w}{\partial x \partial t} - M_T = 0 \tag{5.19}$$

$$c_1\frac{\partial P_x}{\partial x} + \bar{Q}_x - c_1 I_3\frac{\partial^2 u_0}{\partial t^2} - c_1 I_4^*\frac{\partial^2 \phi_0}{\partial t^2} + c_1^2 I_6\frac{\partial^3 w}{\partial x \partial t^2} + I_0\frac{\partial w}{\partial t} = 0 \tag{5.20}$$

To simplify the above equations, the following substitutions have also been incorporated:

$\bar{M}_x = M_x - c_1 P_x, \quad \bar{Q}_x = Q_x - c_2 R_x,$

$I_j^* = I_j - c_1 I_{j+2}, \quad K_2^* = I_2 - 2c_1 I_4 + c_1^2 I_6$

Substituting $\sigma_{xx} = E(z).\varepsilon_{xx}$ in expressions for Nx and $\bar{M}_x$ and simplification thereafter, we get

$$N_x = E_0\frac{\partial u_0}{\partial x} + E_1^*\frac{\partial \phi_0}{\partial x} - c_1 E_3\frac{\partial^2 w}{\partial x^2} - N_T \tag{5.21}$$

$$\bar{M}_x = \frac{E_1^*}{E_0}N_x + \left(A^* - \frac{E_1^{*2}}{E_0}\right)\frac{\partial \phi_0}{\partial x} - \left(c_1 E_4^* - \frac{c_1 E_1^* E_3}{E_0}\right)\frac{\partial^2 w}{\partial x^2} - M_T \tag{5.22}$$

$$P_x = \frac{E_3}{E_0}N_x + \left(E_4^* - \frac{E_1^* E_3}{E_0}\right)\frac{\partial \phi_0}{\partial x} - \left(c_1 E_6 - \frac{c_1 E_3^{*2}}{E_0}\right)\frac{\partial^2 w}{\partial x^2} \tag{5.23}$$

$$\bar{Q}_x = G_0^*\left(\phi_0 + \frac{\partial w}{\partial x}\right) \tag{5.24}$$

The following assumptions have been made for the simplification of the above equations.

$$E_j = \int_A z^j E(z) dA$$

$$G_j = \int_A z^j G(z) dA$$

$$E_s^* = E_s - c_1 E_{s+2}$$

$$A^* = E_2 - 2c_1 E_4 + c_1^2 E_6$$

$$G_0^* = G_0 - 2c_2 G_2 + {c_2}^2 G_4$$

$$K^* = I_2 - 2c_1 I_4 + c_1^2 I_6$$

$$I_s^* = I_s - c_1 I_{s+2}$$

(Where, s =1,2,4)

The expression for Nx (Eq. 5.17) is used to eliminate uo to arrive at the following expressions. Further, it is assumed that the resultant axial force will be zero (for statically determinate cases), so by substituting Nx=0 in the above equations obtained after eliminating u0, we arrive at final governing equations for an FG beam in the framework of higher-order beam theory.

$$\bar{A}^* \frac{\partial^2 \phi_0}{\partial x^2} - c_1 \bar{E}_4^* \frac{\partial^3 w}{\partial x^3} - G_0^* \left(\phi_0 + \frac{\partial w}{\partial x} \right) = \bar{K}^* \frac{\partial^2 \phi_0}{\partial t^2} - c_1 \bar{I}_4^* \frac{\partial^3 w}{\partial x \partial t^2} \tag{5.25}$$

$$\begin{aligned} G_0^* \left(\frac{\partial \phi_0}{\partial x} + \frac{\partial^2 w}{\partial x^2} \right) + c_1 \left(\bar{E}_4^* \frac{\partial^3 \phi_0}{\partial x^3} - c_1 \bar{E}_6 \frac{\partial^4 w}{\partial x^4} \right) + N_T \frac{\partial^2 w}{\partial x^2} + q \\ = c_1 I_3 \frac{\partial}{dx} \left(\frac{I_1^*}{I_0} \frac{\partial^2 \phi_0}{\partial t^2} + \frac{c_1 I_3}{I_0} \frac{\partial^3 w}{\partial x \partial t^2} \right) + c_1 I_4^* \frac{\partial^3 \phi_0}{\partial x \partial t^2} \\ - c_1^2 I_6 \frac{\partial^4 w}{\partial x^2 \partial t^2} + I_0 \frac{\partial^2 w}{\partial t^2} \end{aligned} \tag{5.26}$$

where,

$$\overline{A^*} = A^* - \frac{{E_1^*}^2}{E_0}$$

$$\overline{E_4^*} = \left(E_4^* - \frac{E_1^* E_3}{E_0} \right)$$

$$\overline{K^*} = K^* - \frac{{I_1^*}^2}{I_0}$$

$$\overline{I_4^*} = I_4^* - \frac{I_1^* I_3}{I_0}$$

$$\overline{E_6} = E_6 - \frac{{E_3^*}^2}{E_0}$$

The above equation is the governing equation for FG beams under thermo-mechanical load. It contains only two variables (ϕ & w). As discussed in the last chapter an independent parameter 'F' is considered to further simplify the above equation. The consideration of such independent variable was first introduced by Li [33] to FG beams under mechanical load and it is extended to consider the thermo-mechanical loading conditions. As per the authors knowledge this technique is for thermo-mechanical loading conditions is unique and applied for the first time in the present research. Substituting the following expression for ϕ and w the governing equation is obtained as:

$$w = F - \frac{\bar{A}^*}{G_0^*}\frac{\partial^2 F}{\partial x^2} + \frac{\bar{K}^*}{G_0^*}\frac{\partial^2 F}{\partial t^2} \tag{5.27A}$$

$$\phi_0 = -\frac{\partial F}{\partial x} - \frac{c_1 \bar{E}_4^*}{G_0^*}\frac{\partial^3 F}{\partial x^3} + \frac{c_1 \bar{I}_4^*}{G_0^*}\frac{\partial^3 F}{\partial x \partial t^2} \tag{5.27B}$$

After substituting Eq. (5.23) to Eq. (5.21 and 5.22) the governing equation for FG beams is simplified to:

$$\left(E_2 - \frac{E_1^2}{E_0}\right)\frac{\partial^4 F}{\partial x^4} + N_T\left(\frac{\partial^2 F}{\partial x^2} - \frac{\bar{A}^*}{G_0^*}\frac{\partial^4 F}{\partial x^4} + \frac{\bar{K}^*}{G_0^*}\frac{\partial^4 F}{\partial t^4}\right) - \left\{\left(I_2 - \frac{I_1^2}{I_0}\right) + \frac{I_0 \bar{A}^*}{G_0^*}\right\}\frac{\partial^4 F}{\partial x^2 \partial t^2} + I_0\frac{\partial^2 F}{\partial t^2} + \frac{I_0 \bar{K}^*}{G_0^*}\frac{\partial^4 F}{\partial t^4} = q \tag{5.28A}$$

In case of other boundary conditions with at one sliding support i.e. for C-Fr, C-S_{SL}, S-S_{SL} beams, the term 'N_T' can be assumed to be negligible and can be ignored.

$$D_{11}^* \frac{d^4 F}{dx^4} - q = 0 \tag{5.28B}$$

The bending moment and shear force will take the form-

$$\overline{M}_x = \frac{{E_1}^*}{E_0} N_x + \left(A^* - \frac{{E_1^*}^2}{E_0}\right)\frac{\partial \phi_0}{\partial x} - \left(c_1 E_4^* - \frac{c_1 E_1^* E_3}{E_0}\right)\frac{\partial^2 w}{\partial x^2} - M_T \tag{5.29}$$

$$\bar{M}_x = \left(\frac{E_1^*}{E_0} N_x - M_T\right) + (\bar{A}^*)\frac{\partial \phi_0}{\partial x} - \left(\overline{E_4^*}\right)\frac{\partial^2 w}{\partial x^2} \tag{5.30}$$

Substituting for 'w' and phi

$$\bar{M}_x = \left(\frac{E_1^*}{E_0} N_x - M_T\right) - \left(\bar{A}^* + c_1\overline{E_4^*}\right)\frac{\partial^2 F}{\partial x^2} \tag{5.31}$$

$$\bar{Q}_x = G_0^*\left(\phi_0 + \frac{\partial w}{\partial x}\right) = \left(\bar{A}^* + c_1\overline{E_4^*}\right)\frac{\partial^3 F}{\partial x^3} \tag{5.32}$$

It can be observed that the governing equation for both purely mechanical load and thermos-mechanical load corresponding to the three boundary conditions (C-Fr, C-SSL, S-SSL) is same; only the boundary conditions are updated for the latter case. The boundary conditions we have for these cases:

Table 5.1: Various boundary conditions of FG Beam under thermal load

Beam		x=0	x=l
a) Cantilever beam	(C-Fr)	u=0, w=0, ϕ =0	Nx=0, Mx=0, Qxz=0
b) Simply supported beam	(S-S_{SL})	u=0, w=0, Mx=0	u=0, w=0, Mx=0
c) Propped beam	(C-S_{SL})	u=0, w=0, ϕ =0	u=0, w=0, Mx=0

It is observed that only bending moment terms are modified in the boundary condition, due to thermal moment caused by temperature gradient. Once the independent variable 'F' is determined, the other dependent variables can easily be determined. Exact solution of Equation 5.32 is derived for each of the above three boundary conditions after considering the beam to be loaded with constant mechanical load in thermal environment is presented in next section. In the latter half of the chapter the case of non-zero axial force has been taken to study the buckling behaviour of C-C and S-S beams.

Poisson's ratio is assumed to be a constant. As the material gradient is assumed to vary along the cross-section height hence the term D_{11}* is constant, here in case of uniform cross-section beams. The above equation is hence open for the any type of material

gradation law, temperature gradient and three boundary conditions mentioned above. In the next section different temperature gradients assumed in the study and their formulation is discussed.

5.3 Various temperature profiles

The top surface is assumed to be at temperature, Tt while the bottom surface temperature is Tb. Here it is assumed that Tt<Tb, so as to have a thermal moment opposite in sense to mechanical moment. Both Tt and Tb are greater than the ambient temperature T0. Three temperature profiles are considered in the present study- a) uniform temperature rise (UTR), b) linear temperature distribution (LTD) and b) non-linear temperature distribution (NLTD). Generally, the temperature distribution in a component is determined using steady state heat conduction equation assuming the heat flow to be one-dimensional along the beam height. In a limiting case when beam is slender the temperature distribution can be approximated to be linear along the beam height.

5.3.1 Uniform Temperature Rise

The beam is uniformly heated in such a way that all the points along any cross-section are raised by an equal amount above the ambient temperature. In this case $\Delta T=T(z)-T_0$ will cause thermal expansion in each layer and the relative expansion of the layers cause bending of the beam.

5.3.2 Linear temperature distribution

The two surfaces (top and bottom) of the beam are assumed to be at an initial temperature higher than the surroundings and the temperature distribution is assumed to follow a linear distribution according to the expression-

$$T\left(z\right)=T_b+\left(T_t-T_b\right).\left(\frac{z}{h}+\frac{1}{2}\right) \tag{5.33}$$

If both the temperature Tt and Tb are kept at same value then the latter part of above equation becomes zero and will reduce to the case of uniform temperature rise. Ven thermal expansion as the constituents have different expansion coefficients.

5.3.3 Non-linear temperature distribution

Assuming there is no heat generation and heat flows uni-directionally from bottom layer to top layer such that it follows steady state one dimensional heat conduction equation given by:

$$\frac{d}{dz}\left(K(z)\frac{dT}{dx}\right)=0, T_{(-h/2)}=T_b, T_{(h/2)}=T_t \tag{5.34}$$

In the above equation K(z) is the thermal conductivity of FGM at any point along the cross-section. The variation of thermal conductivity is also assumed to vary according to rule of mixtures. The above equation can be solved using polynomial series solution [25, 26, 28] and assuming that the first seven terms (Np) of the series provide accurate solutions, the temperature profile across the beam height is given by:

$$T=T_b+\frac{(T_t-T_b)}{R}\left[\sum_{i=0}^{N_p}\frac{(-1)^i}{i\beta+1}\left(\frac{K_{tb}}{K_b}\right)^i\left(\frac{1}{2}+\frac{z}{h}\right)^{i\beta+1}\right] \tag{5.35}$$

where-

$$R=\sum_{i=0}^{N_p}\frac{(-1)^i}{i\beta+1}\left(\frac{K_{tb}}{K_b}\right)^i$$

and $K_{tb} = K_t - K_b$

5.4 Solution of governing equations

Equation 5.28(A&B) represents the governing equation of a higher order theory for shear deformable FG beam subjected to mechanical loads in thermal environment. It is also observed that for those beam end conditions in which the axial force is negligible, the bending moment is a function of thermal load and moment as given by Equation 5.30. This is applicable for three end conditions viz. – a) cantilever or clamped-free (C-Fr); b) propped cantilever or clamped-simply supported (C-SSL) and c) Simply Supported-Simply supported (S-SSL). In order to have zero axial force one of the ends must be free to move in horizontal direction; hence the present study focuses on these end conditions only. In order to include other end conditions, the effect of the axial force can be taken into account that is however a non-linear analysis and beyond the scope of present study. However, a case study considering the limiting conditions of non-linearity is approached to study the buckling problem of clamped-clamped and clamped-simply supported beams using the above equation to find a satisfactory match.

In this section solution of the above governing equation is approached using direct integration and also using numerical technique of B-spline collocation. The collocation technique is found to give very precise results when compared to the exact solution.

5.4.1 Exact solution by direct integration

Integration of the governing equation of FG beams (Equation 5.28B) leads to the following solution:

$$F = \frac{q}{D_{11}^*}\frac{x^4}{24} + C_1\frac{x^3}{6} + C_2\frac{x^2}{2} + C_3x + C_4 \tag{5.36}$$

where Cj (j=1,2,3,4) are constants to be determined from the end conditions. In the present study the three boundary conditions free of axial forces are considered as above to find the exact solution for thermo-mechanical loading of FG Timoshenko beams. The beams are subjected to an external uniform mechanical pressure of 'q' kN/m intensity throughout the span and are also subjected to various types of temperature distributions superimposed on the beam. The resulting deformations and stresses are then observed for a wide range of parameters.

5.4.2 Various end conditions-Clamped-Free (C-F$_r$)

For a cantilever beam slope and deflection at the fixed end are zero while shear force and bending moment at the free end are zero. Hence, we have the following end conditions for a C-F beam:

$$w(0) = \phi(0) = 0, M_x(l) = Q_{xz}(l) = 0 \tag{5.37}$$

The above boundary condition (Equation 5.36) can be substituted by Equations 5.27A-B, 5.31 and 5.32 respectively to obtain the following:

$$\begin{aligned}&\left(F - \frac{\bar{A}^*}{G_0^*}\frac{d^2F}{dx^2}\right)_{x=0} = \left(-\frac{dF}{dx} - \frac{c_1\bar{E}_4^*}{G_0^*}\frac{d^3F}{dx^3}\right)_{x=0} = \\ &\left((\bar{A}^* + c_1\bar{E}_4^*)\frac{d^2F}{dx^2} - \frac{E_0^*}{E_0}N_T - M_T\right)_{x=l} = \left((\bar{A}^* + c_1\bar{E}_4^*)\frac{d^3F}{dx^3}\right)_{x=l} = 0\end{aligned} \tag{5.38}$$

Substituting the Equations 5.36in Equation 5.38 to obtain four simultaneous linear equations in Cj (j=1,2,3,4) which can be solved easily to obtain:

$$F = \frac{q}{24D^*}(x^4 - 4lx^3 + 6l^2x^2) - \frac{q}{2G^*}\frac{1}{D^*}(2c_1\bar{E}_4^*lx + \bar{A}_0^*l^2) + \ldots\ldots \tag{5.39}$$

$$\ldots\ldots\ldots\frac{1}{2(\bar{A}_0^* + c_1\bar{E}_4^*)}\left(\frac{E_1^*}{E_0}N_T - M_T\right)\left(x^2 + 2\frac{\bar{A}_0^*}{G_0^*}\right)$$

Correspondingly after substitution of 'F', we can easily obtain the following expressions.

$$w = \frac{q}{24D_{11}^*}(x^4 - 4lx^3 + 6l^2x^2) - \frac{q}{2G_0^*}\frac{\bar{A}_0^*}{D_{11}^*}(x^2 - 2lx) + \frac{q}{D_{11}^*}\frac{c_1\bar{E}_4^*}{G_0^*}xl\ldots\ldots$$
$$\ldots\ldots + \frac{x^2}{2(\bar{A}_0^* + c_1\bar{E}_4^*)}\left(\frac{E_1^*}{E_0}N_T - M_T\right) \quad (5.40)$$

and using Equations 5.5:

$$\sigma_{xx} = \frac{E(z)}{2D^*}\left(\frac{B_{11}}{A_{11}} - z\right)\left\{q(x^2 - 2lx + l^2) - \left(\frac{B_{11}}{A_{11}}N_T - M_T\right)\right\} + \frac{E(z)\,N_T}{A_{11}} - E(z)\alpha(z)\Delta T(z) \quad (5.41)$$

Using the axial stresses obtained in Equation 5.6, shear stresses can easily be derived by integrating:

$\sigma_{xz} = \int_{-\square/2}^{z}\frac{d\sigma_{xx}}{dx}dz$

Hence an expression for shear stress is obtained as:

$$\sigma_{xz} = \frac{q}{D^*}(l - x)\left[\int_{-h/2}^{z} zE(z)dz - \frac{B_{11}}{A_{11}}\int_{-h/2}^{z} E(z)dz\right] \quad (5.42)$$

The above Equations 5.39, 5.40-5.42 represent respectively the transverse deflection, normal stresses and shear stresses in a FG Timoshenko Beam subjected to thermo-mechanical load with C-F boundary conditions. It is clear from the Equation 5.40- 5.41 that in the absence of mechanical load (q=0) the transverse deflection and axial stresses are non-zero. On the other hand, if thermal load is zero (i.e. surface temperatures are equal to ambient temperature) then the equations 5.40, 5.41 exactly resembles that of Reference [16]. For isotropic beams D_{11}*=EI, G_0*= GA and E_1*=0, hence for isotropic materials the above equations are reduced to:

$$w = \frac{q}{24EI}(x^4 - 4lx^3 + 6l^2x^2) - \frac{q}{2GA}(x^2 - 2lx) - \frac{x^2M_T}{2EI} \quad (5.43)$$

$$\sigma_{xx} = \frac{qz}{2I}(x^2 - 2lx + l^2) + \frac{M_Tz}{I} + \frac{N_T}{A} - E\alpha(T - T_0) \quad (5.44)$$

For isotropic beams the last two terms of Equation 5.44 are equal and hence cancel each other and terms with thermal moment are obtained. The above equations can be easily verified from standard available text-books of solid mechanics.

5.4.3 Approximate solution using B-spline collocation technique

Now to solve the governing equation 5.27B, B-spline Collocation method has been adopted in this work. A detailed discussion has already been taken place in Chapter 3 and 4 about the B-spline collocation technique, hence it is not discussed again. Using this technique, a trial solution for the parameter 'F' is assumed as B-spline shape function that will be substituted in the governing equation, i.e., Eq. 5.27B. The resulting equation is then forced to satisfy the governing equation at collocation points given by Greville abscissa. Here in the present study a B-spline function of sixth order basis function has been considered (as the governing equation is a fourth order differential equation so the degree of polynomial needed is 5th.)

It can be assessed that the number of collocation points required will be equal to the difference between the number of control points of the B-spline curve and the number of boundary conditions. In the present case, a sixth-order B-spline function with no intermediate knots is used. Hence, we have six coefficients to be determined. As there are 4 boundary conditions available, we require only 2 collocation points to develop six linear equations that can be solved easily to find the coefficients.

In the next section, the solution is approached using the B-spline collocation technique; a detailed discussion of the process is reported by Mahapatra et al. [105] for reference. A mathematical code developed for the above formulation is used to obtain computational results.

5.5 Results and Discussions

In the present work, new higher-order unified formulations have been derived for the determination of deflection, axial stress and shear stress under purely thermal and thermo-mechanical loading conditions, as mentioned in the previous section. Now the results generated using these formulae have been validated, as discussed below.

5.5.1 Verification of results

To validate the results of the above a simply supported beam is considered whose length, l=100mm and height, h=10mm to have l/h ratio 10. The material of FGM is assumed to vary according to an exponential function. The modulus of elasticity and coefficient of thermal expansion vary according to the function, $E(z) = E_0 e^{\beta z}$ and $\alpha(z) = \alpha_0 e^{\gamma z}$ assuming Poisson's ratio to be a constant, υ=0.25 and q=0. The plane strain case is

considered and accordingly value of E and α is taken. An exponential temperature gradient given by $\theta(z) = \Delta T e^{\kappa z}$ where ΔT=100^{0}C and κ=+230m-1 for temperature gradient $\frac{\theta(\square)}{\theta(0)} = 10$ for the given height. To consider the effect of relative values of coefficient of thermal expansion and modulus of elasticity, it is assumed that $\alpha_0 = \frac{E_0}{10^4}$ while the values of β & γ are varied according to Table-5.2 that relates to the Figure-5.1.

It can be observed from the figures below that the present method exactly matches with the results in literature and validates the current method for study. From the present study the important observations made are: a) The neutral axis shifts towards the stiffer side in case of thermal loads also, b) maximum axial stress are obtained near the neutral axis, c) from figure 1c and 1e it is observed that when the temperature gradient is in opposite sense relative to the material gradation, which significantly reduces the thermal stresses, d) the deflection of the beam is much higher when the stiffness and thermal coefficient vary in the same direction as that of temperature (figure 2b) which further increases for higher value of thermal coefficient, e) the deflection largely reduces when the temperature gradient is opposite to the expansion coefficient and elastic moduli.

Table 5.2: Properties of FG beam considered for validation under thermal load

Case	*E_0 GPa*	*E_h GPa*	*β m^{-1}*	*γ/β*
b	1	1	0	0
c	10	1	$-\kappa$	1
d	1	10	κ	1
e	10	1	$-\kappa$	1.5
f	1	10	κ	1.5
g	1	10	κ	-1

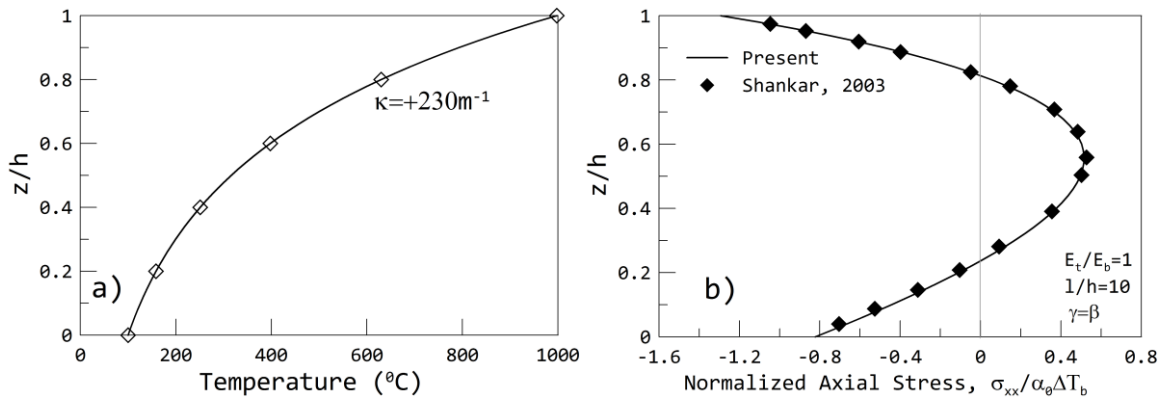

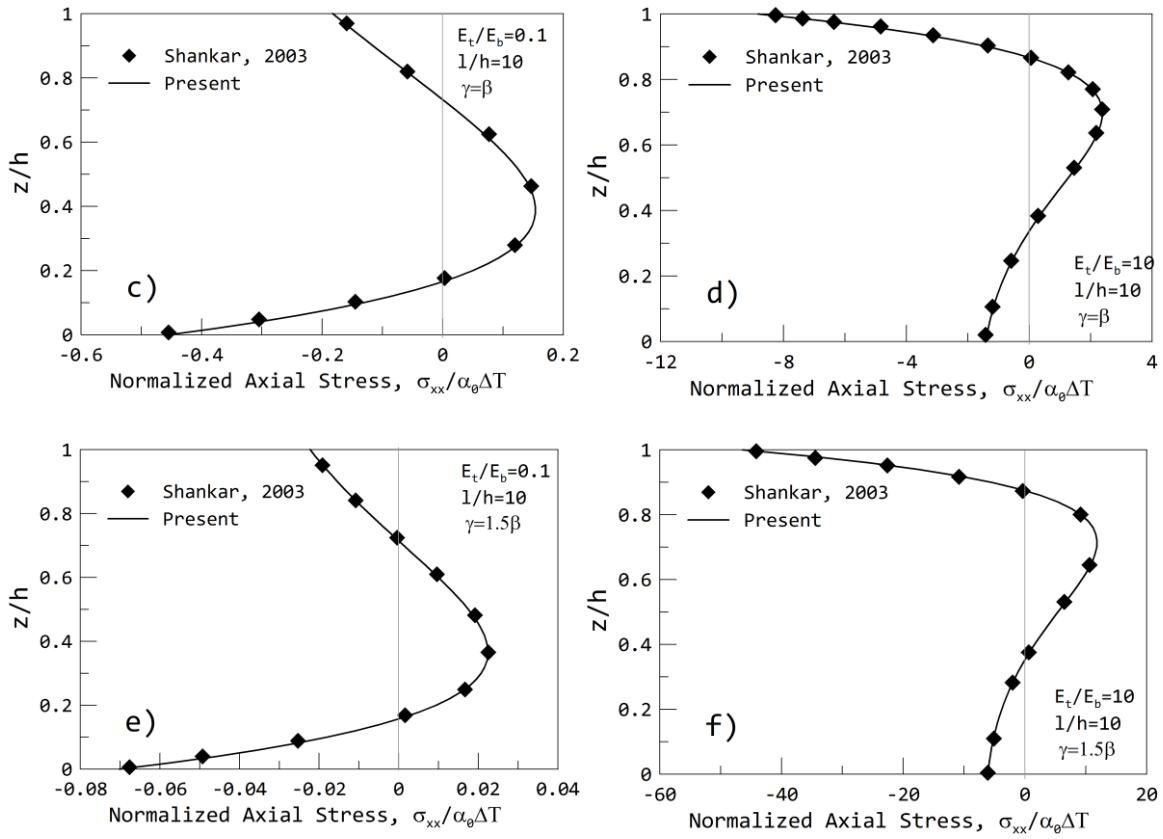

Figure 5.1(a-f): E-FGM simply-supported beam subjected to purely thermal load and its verification

5.5.2 Other numerical experiments

To have a deeper insight on the behaviour of a FG beams when it is subjected to mechanical load and the temperature distribution across the beam height is varied, a number of numerical results based on the above analysis are presented in this section. In order to provide a clear perspective, the study has been categorized into different cases so that the behaviour of FG beam is studied by varying one of the parameters (relevant to FGM) with a progressive rise of temperature and temperature independent (TID) properties. The range of temperatures considered in the present study is comparatively small hence variation of properties with temperature is not considered in the present study.

The parameters that are of interest are: a) volume fraction of constituents governed by rule of mixture, b) comparison of different material combinations for constituents and hence material properties, c) comparison of various beams theories for the same aspect ratio (l/h), and d) uniform temperature rise, linear and non-linear temperature profiles. A comparison of variation in load parameters namely purely mechanical/ purely thermal/ thermo-mechanical behavior has also been considered for different set of temperature

ranges. For various numerical experiments, FGM-1 is assumed as Aluminum and Silicon Nitride while FGM-2 is considered as Stainless steel and Zirconia.

For computational purpose a beam of length L=1m and height h=0.1m, temperature of the surroundings $T_0=30^0C$ (stress-free state) and uniform pressure of intensity q=10kN/m has been assumed. The material properties are mentioned in Table-5.2. The temperature of the top and bottom surfaces is kept at constant values assuming steady state conditions and observations are made for different sets of temperature as mentioned in Table-5.4.

The axial stresses and shear stresses are normalized using the following relations-

$$\sigma_{norm}=\frac{(\sigma_{xx}bh)}{ql+N_T};\tau_{norm}=\frac{(\sigma_{xz}bh)}{ql+N_T} \tag{5.45}$$

Table-5.3 Structural and thermal properties of reinforcing particles

Material	Poisson's Ratio	Modulus of Elasticity (GPa)	Coefficient of Thermal Expansion $10^{-6}(^0C^{-1})$	Thermal Conductivity $(Wm^{-1}K^{-1})$
Steel	0.3000	207	12.3	51.90
Aluminum	0.3300	69	23.6	222.00
Stainless Steel	0.3262	201.04	12.330	15.379
Silicon Nitride	0.2400	348.43	5.8723	13.7230
Zirconia	0.2882	244.27	12.766	1.7000

Table-5.4 Symbols for temperature distribution adapted in the graphs

Temperature	**Symbol**	**Temperature**	**Symbol**	
	Uniform		**Linear**	**Nonlinear**
$T_t=31^0C$, $T_b=31^0C$	TU_1	$T_t=31^0C$, $T_b=31^0C$	TL_1	TNL_1
$T_t=33^0C$, $T_b=33^0C$	TU_2	$T_t=31^0C$, $T_b=33^0C$	TL_2	TNL_2
$T_t=35^0C$, $T_b=35^0C$	TU_3	$T_t=31^0C$, $T_b=35^0C$	TL_3	TNL_3
$T_t=37^0C$, $T_b=37^0C$	TU_4	$T_t=31^0C$, $T_b=37^0C$	TL_4	TNL_4

To study the effect of volume composition of the constituent materials on thermo-mechanical behavior of FG beam, the following study is reported. A cantilever beam with FGM-1(with metal at bottom and ceramic at top) composition is considered with dimensions as above. The successive studies take into account, the volume fractions using

power law theory. 50% of both the constituents is taken, hence index value is considered to be one. It is observed (Figure 5.2 and 5.3) that even with the slightest rise in temperature of surface (above ambient temperature), results in appreciable variations in the deformation and stress features of FG beam. For example, when the given FG beam is kept near a heat source such that the temperature of bottom surface rises by 2^0C and the temperature of top surface rises by 1^0C from the ambient, then the thermal gradient induces a net moment (due to the difference in coefficient of thermal expansion of the layers) that deflects the beam in upward direction. Thus, even for a small rise in temperature from the surrounding an FG beam shows a special behaviour that must be understood for further design and development.

In Figure 5.3 (a-c) the deflection, normal and shear stresses are plotted for a given temperature rise and no mechanical load. The same results are compared with reported literature and found a satisfactory match in deflection and normal stresses; thus, results are again verified (even for power law distribution). From Figure 5.3c, it is observed that the shear stress values are negligibly small, the reason for the same is that the effect of thermal strain on shear strain is ignored in the fundamental derivations, and this may be considered as a future scope.

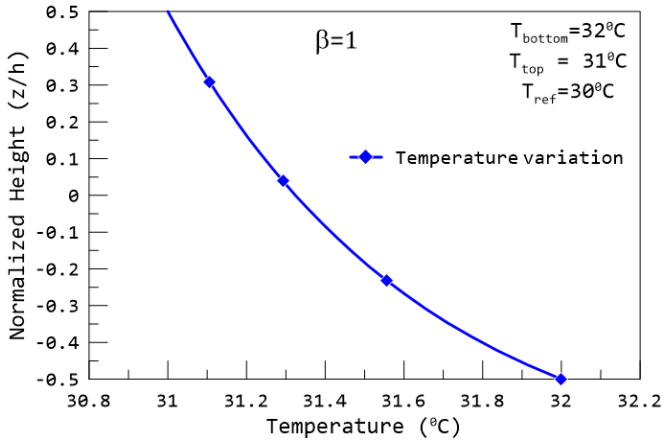

Figure-5.2 Nonlinear Temperature variation due to functional grading

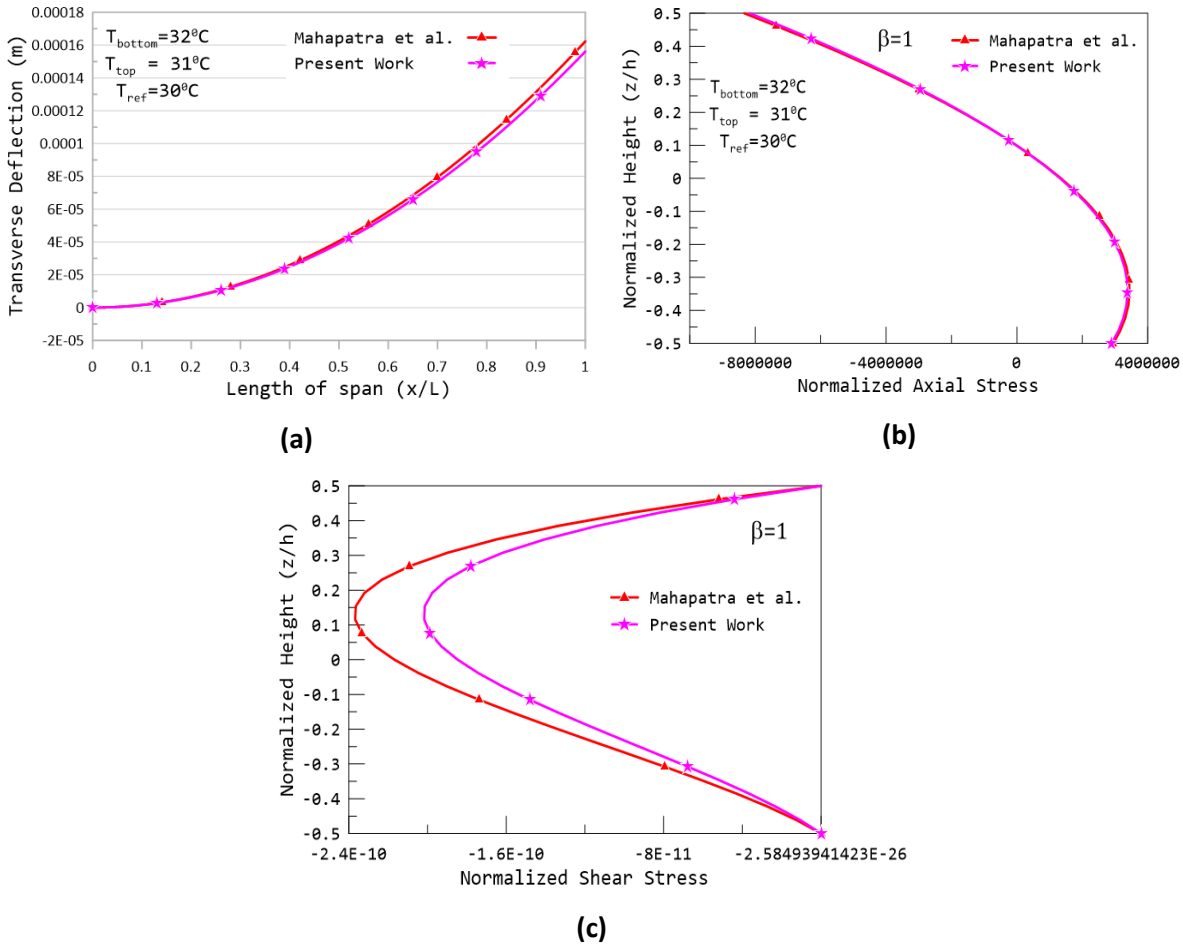

Figure-5.3(a-c): Purely Thermal Load
a) deflection, b) normalized axial stress, c) normalized shear stress
(For a small temperature gradient and material gradient using power law)

In order to have a broader view of such changes in their behaviour, the values of temperatures for uniform, linear and non-linear distribution must be judiciously selected and suitable combinations of materials must be selected to obtain desired properties. A number of case studies are discussed in elaborate in the successive paragraphs.

In the next study a metal-ceramic combination (FGM-1) is again considered for observing the characteristics of FG beam under purely thermal load and linear temperature variation as shown in Table 5.5. Aluminium with higher value of coefficient of thermal expansion is at the bottom, as compared to ceramic (Silicon Nitride), which is at the top. The case-1 gives a deflection in upward direction as expected, and also for case-2 and case-3, the deflection can be predicted a priori. However, the normal stresses have to be observed more carefully.

Table-5.5: Symbols for temperature distribution adapted in the graphs (5.4)

Cases	T_b	T_t	T_0
Case-1	31	30	30
Case-2	35	31	30
Case-3	31	35	30

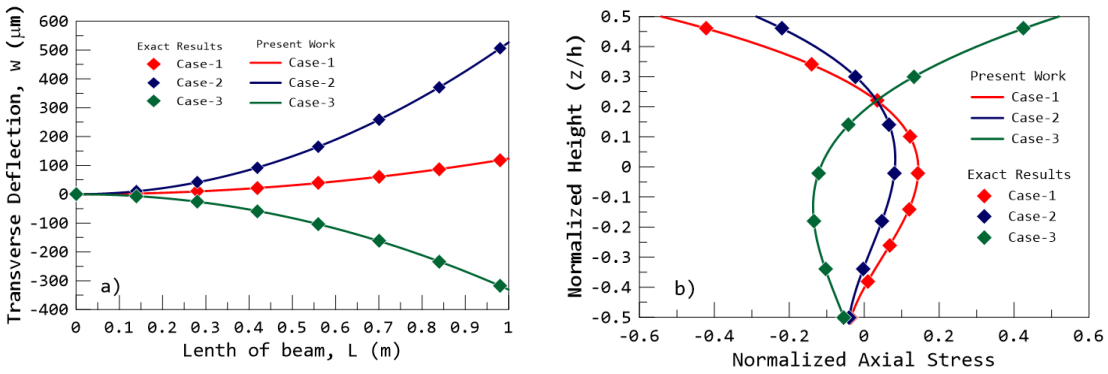

Figure-5.4: Purely Thermal Load with flipped gradients
a) deflection, b) normalized axial stress

In Figure 5.4b, the case-1 can be visualized as following. Aluminium with greater thermal expansion will expand, however the top ceramic does not. The differential expansion between the top and bottom creates a thermal moment as already discussed. To maintain continuity, the bottom layers will not be allowed to expand freely resulting in compressive thermal stress at bottom. However, the continuity requirement and thermal moment bends the beam upwards resulting in compressive mechanical stresses at the top fiber. The stresses in the fibres near the centre line are tensile (whose intensity will depend on the thermal expansion coefficient ratio). Similarly in case-2, both top and bottom fiber will expand but for different temperature gradients, resulting in thermal moment. The thermal compressive stress at the bottom is very small as compared to the mechanical strains. This is because of requirement to maintain geometric continuity. However, it may be noted that the net stress at the top decreases. The reason is due the differential expansion of top and bottom fiber which is only responsible for causing stress. The more the difference in expansion coefficient, more will be the resulting stress. In case-3, the direction of thermal moment is reversed.

Table-5.6 Symbols for temperature distribution adapted in the graphs (5.5)

Cases	E_b/E_t	α_b/α_t	ΔT_b	ΔT_t
Case-1	1	**10**	20	10
Case-2	10	**1**	20	10

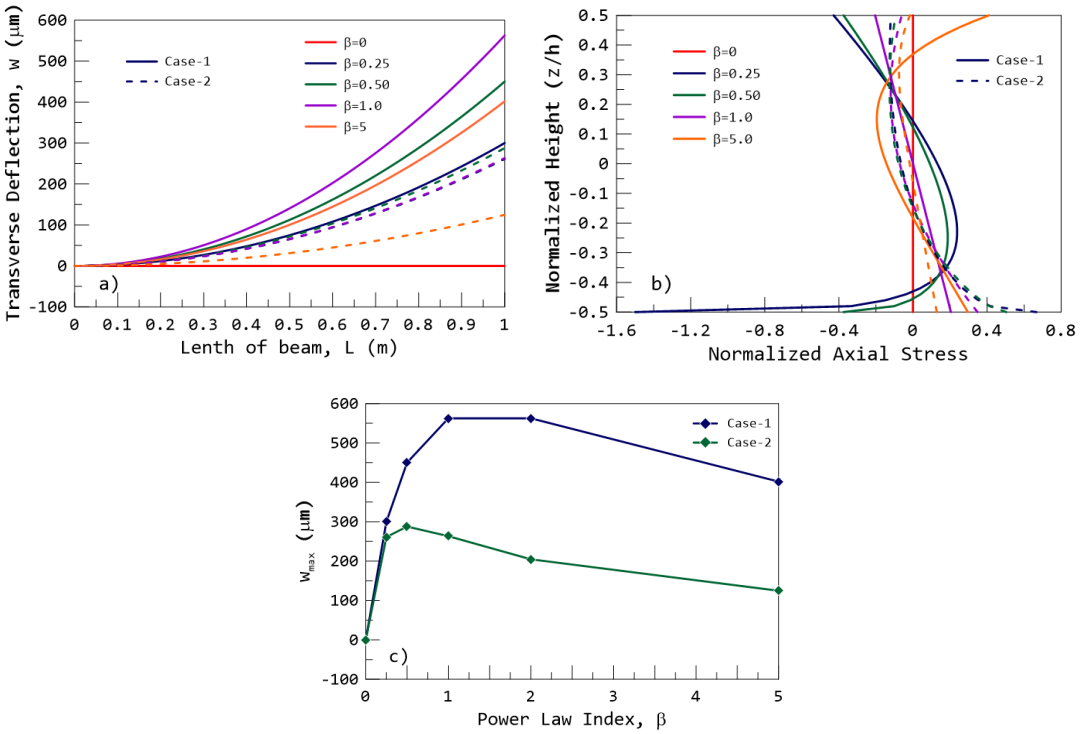

Figure-5.5 a) deflection, b) normalized axial stress, c) normalized shear stress when temperature of bottom layer is more than that of top layer as per table-5.6

To study the effect of combination of materials, a unique study has been planned in which arbitrary set of parameters have been considered to generalise the results.

For FGM-1 and FGM-2 comparison

Table-5.7 Symbols for temperature distribution adapted in the graphs (5.6)

Cases	Material Combination	E_b/E_t	α_b/α_t	ΔT_t (^{0}C)	ΔT_b (^{0}C)
Case-1.1	FGM-1	1/5	4	1	5
Case-1.2	FGM-1	1/5	4	5	1
Case-2.1	FGM-2	4/5	1	1	5
Case-2.2	FGM-2	4/5	1	5	1

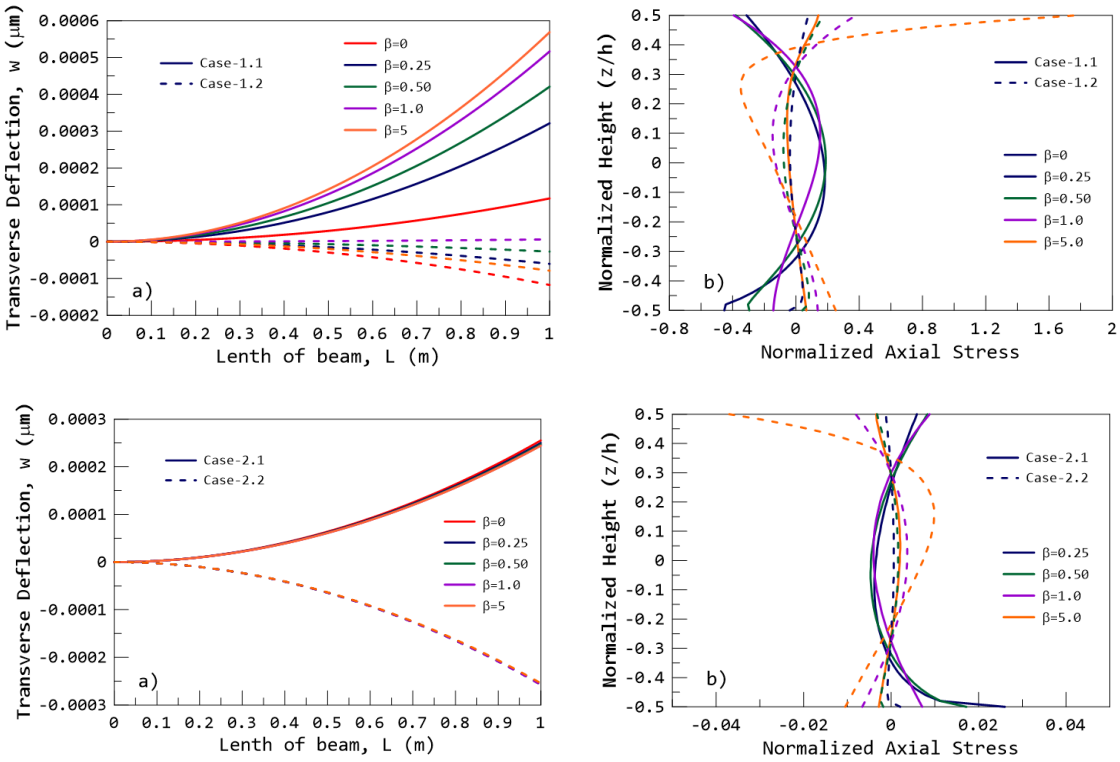

Figure-5.6 Comparison of a) deflection, b) normalized axial stress, c) normalized shear stress of FGM1 and FGM2 when temperature of bottom layer is more than that of top layer

5.6 Closure

In this chapter a detailed study has been performed to understand and exhibit influence of thermal and thermos-mechanical loads on the structural behaviours of an FG beam made with different types of material gradations and subjected to various types of boundary conditions. Though many works have already been done on analysis of FG beams under thermal and thermo-mechanical loading by various of authors, in the present work FG beams have been reanalysed in frame work of a newly developed higher order unified beam theory. To validate the newly developed mathematical model work of Li at al [27, 33], work of Wattanasakulpong et al [55] and work of Mahapatra et al [70, 105] have been referred. It has been shown that the present mathematical model can be used to validate the results of the problems solved by the above-mentioned authors in their works with exclusion of higher terms which have been incorporated in the present mathematical model. It has been vividly described in this chapter and also in the previous chapter that, exclusion of higher terms which have been considered in the present work to derive the governing differential equations influences few results, especially in plane shear stresses, considerably. Few further problems have been solved thereafter.

Chapter 6: **FEA Analysis using APDL Programming**

6.1 Introduction

In chapter 4 and 5 a FGM beam has been investigated for the determination of transverse displacement 'w', normalized axial stress 'σ_{xx}' and normalized shear stress 'τ_{xz}' with respect to normalized domain variable, i.e., $\left(\frac{x}{L}\right)$. To determine these parameters a unified higher order mathematical model has been derived from 'Principle of Stationary Total Potential (PSTP)' point of view by using Hamilton's principle. The governing equation thus derived has been solved using a numerical method known as B-spline colocation method to find the expression of the unification parameter 'F' in terms of the domain variable. Further substituting this 'F' in the expression of 'w', 'σ_{xx}' and 'τ_{xz}' value of these output parameters have been determined at different normalized domain positions, i.e., at different values of $\left(\frac{x}{L}\right)$.

Though the above-mentioned process has been validated with many published results but to establish more firmly the authenticity of this newly developed formulation or mathematical model under the frame work of 'Unified Higher Order Beam Theory', another validation has been done using a very renowned numerical method known as Finite Element Analysis (FEA) method. This FEA method has been executed with a FEA software.

A FEA software has many modules. To validate the results determined by Unified Higher Order beam formulations using a mathematical code the same problem has been solved by Finite Element Analysis (FEA) method using programming Module module of a FEA software by executing a FEA program. This FEA program has been developed in this present work in few parts. One part of the program is to generate a model of beam with 'n' numbers of layers according to few input parameters like, length of the beam 'L', width of the beam 'b', height of the beam 'h' and number of layers 'n'. Next part of the FEA Code generates material properties for each layer as per a material gradation law and impart those properties at each layer successfully. In the present work Eq. 3.30 has been incorporated in the FEA Code to generate material properties as per the power law of material gradation for each layer out of the given properties of two constituent materials. Last part of the FEA Code has been developed to mesh the topology automatically against input value of number

of elements wished by the user in all the directions. This part of the program also let user to impose boundary conditions and loadings with minimum effort.

In the following sections few problems have been solved with the Unified Higher Order Beam Theory using the Mathematical Code as well as through Finite Element Analysis (FEA) method using a FEA Programming and their results have been compared.

6.2 Validation of APDL Programming by solving few problems

6.2.1 A FGM cantilever beam subjected to a given UDL

In this problem a FGM beam has been considered of length 1m, width 0.1m and thickness also 0.1m. A Uniformly Distributed Load (UDL) of 1000 N/m has been imposed on the beam over its throughout length. The beam is made of a FGM in combination of Aluminium and Silicon Nitride where Aluminium at the bottom layer and Silicon Nitride at the top layer. Properties of Aluminium and Silicon Nitride have been taken from table 1.0. The gradation of material has been done as per power law and properties have been calculated by Eq. 31 and Eq. 32. This problem definition has been taken from the work of X. F. Li et al [33].

To validate the FEA program/code, two output parameters have been evaluated. One transverse deflection 'w' and other one is axial stress 'σ_{xx}'. Prior the final simulation grid independence has been checked. To check the grid independence a mesh control parameter factor which has been named as MCP, has been incorporated in the program. This MCP value has been set 1 in the first trial and then 0.5 in the second trial. To check the grid independence, the reference output parameter which has been considered is the maximum transverse deflection at free end.

Following is the geometry of a FGM beam created as per the above-mentioned dimensional values using the FEA code or Macro with 50 layers (Figure 6.1a and b).

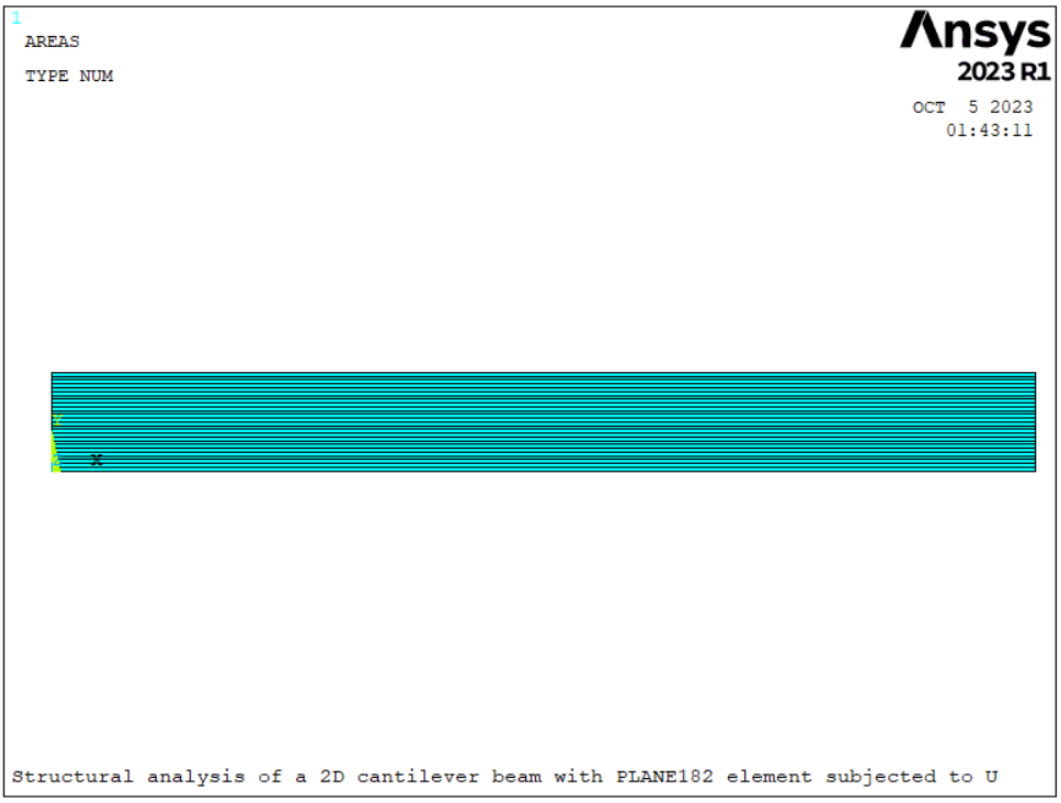

Figure-6.1a FGM Beam Geometry generated using the FEA Program

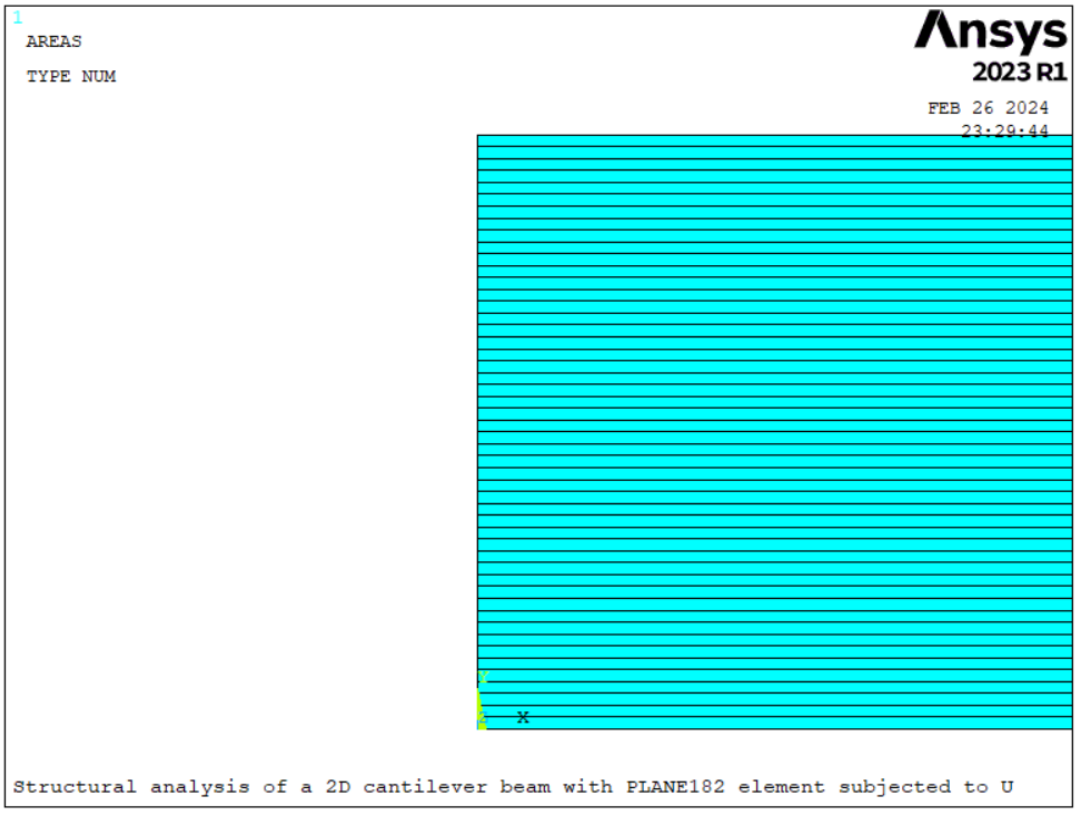

Figure-6.1b Enlarged view of the FGM Beam Geometry generated using the FEA Program

Now to set the proper value of Mesh Control Parameter (MCP) this problem has been solved with various combination of MCP values and for each case maximum deflection and maximum axial stress have been calculated. Here MCPv' and 'MCPh' means mesh control parameter along horizontal or axial direction of the FGM beam and vertical direction respectively. The reference value for controlling size of elements of the FGM beam here has been taken as height of each layer. So, if MCP value is set 1 for any direction of the beam then the size of the element in that direction would be equal to the thickness or height of each layer.

For the present problem length of the beam has been considered 1 meter. Height and width of the FGM beam has been considered $\frac{1}{10}$ th of the length of the beam. Therefore, the height and width of the FGM beam become 0.1 m each. Total 50 number of layers have been considered in this FGM beam for gradation along height of the beam. So, thickness of each layer for the present case would be $\frac{1}{50} = 0.002\ mm$.

Therefore, if 'MCPv' is taken as 1 and 'MCPh' is taken as 2 then size of each element along vertical direction is equal to the thickness of each layer and size along axial direction of the beam is 2 times the size of thickness of each layer. In the present problem following four combinations of the 'MCPv' and 'MCPh' values have been considered and with each combinations the problem has been solved for maximum transverse deflection and maximum axial stress.

Table 6.1: Maximum transverse deflection and maximum axial stress for various MCP values

MCPv	MCPh	Nodes	Elements	Max Defection	Max Stress
1	2	12801	12500	0.085896 mm	4.2273 Mpa
1	1	25551	25000	0.086111 mm	4.2389 Mpa
0.5	1	50601	50000	0.085924 mm	4.2552 Mpa
0.5	0.5	101101	100000	0.086110 mm	4.2567 Mpa

From the above table 6.1 it is very much clear that with 'MCPv' and 'MCPh' values 1 each, results of maximum transverse deflection and maximum axial stress are quite acceptable as reducing the values of 'MCPh' and 'MCPv' further, results of maximum transverse deflection and maximum axial stress do not improve much. So, it has been decided to do all the simulations ahead with 'MCPv' and 'MCPh' values as 1 as this combination generates lesser number of nodes.

Following figures (figure 6.2a, b and c) shows the enlarged meshed views of the FGM beam with above mentioned combinations of ‘MCPv’ and ‘MCPh’ values.

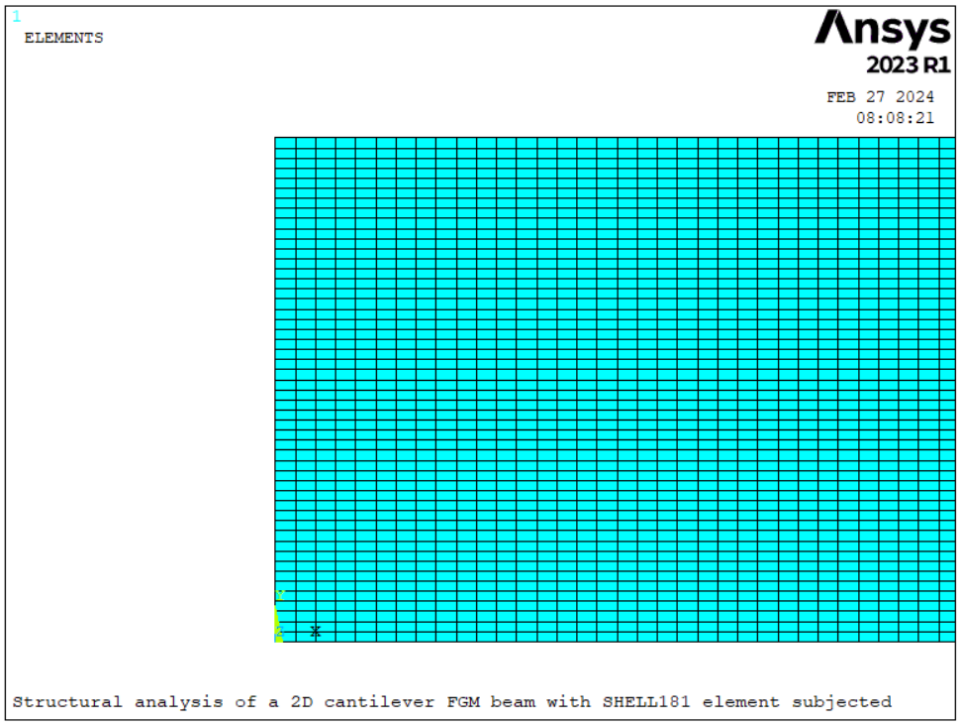

Figure-6.2a Enlarged Meshed view of the FGM Beam Geometry generated using the FEA Program considering ‘MCPv’ and ‘MCPh’ values 1 and 2 respectively.

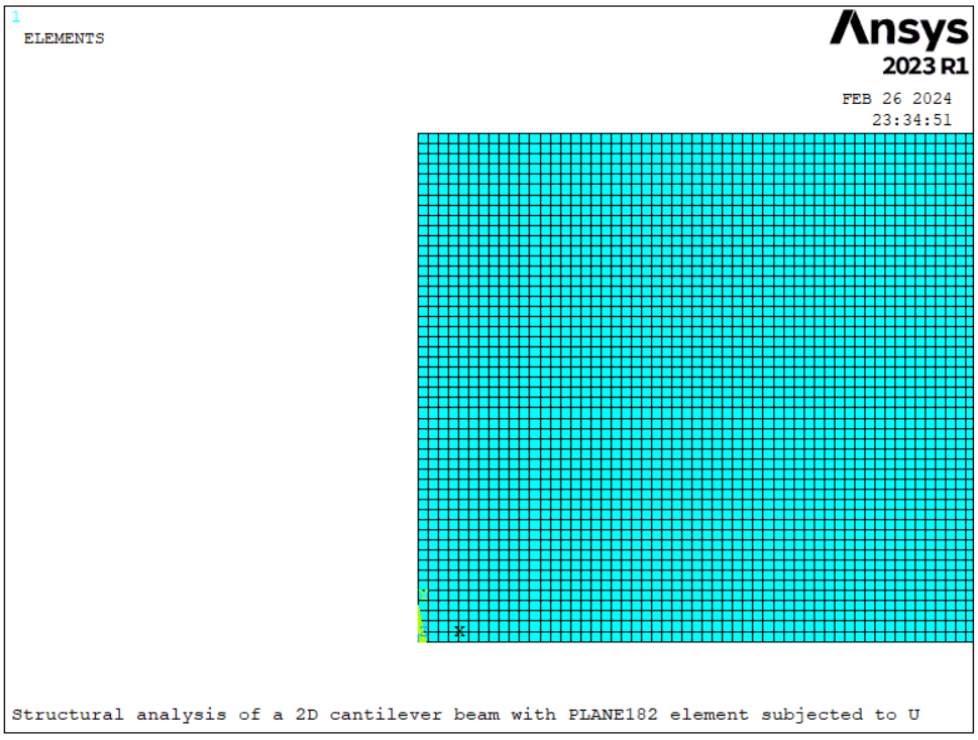

Figure-6.2b Enlarged Meshed view of the FGM Beam Geometry generated using the FEA Program considering ‘MCPv’ and ‘MCPh’ values 1 each.

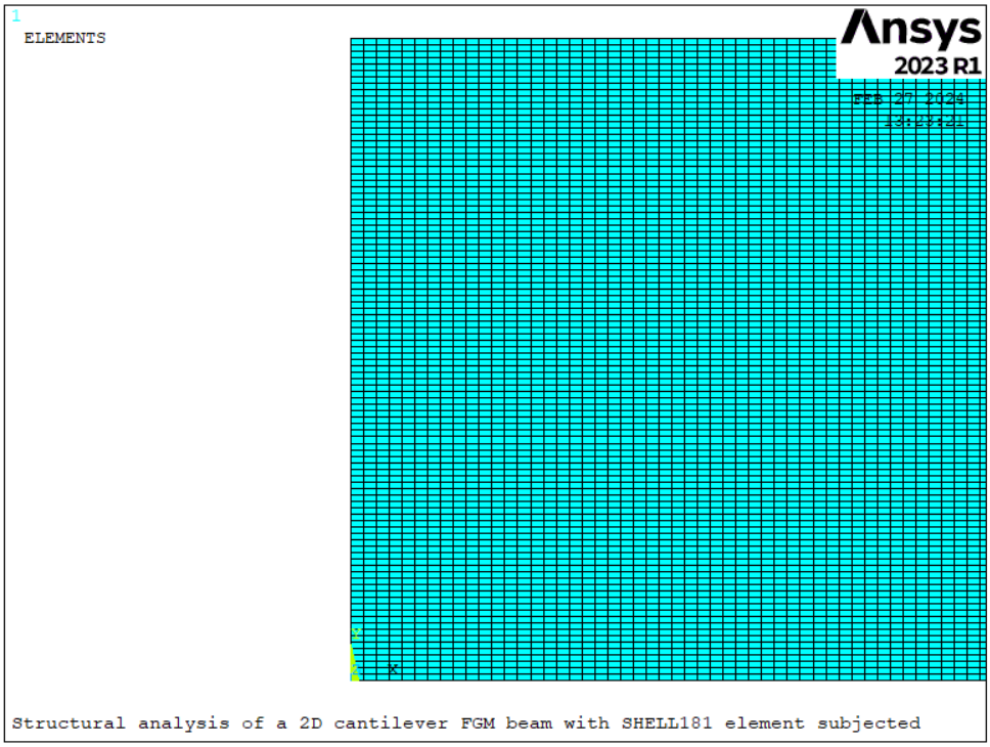

Figure-6.2c Enlarged Meshed view of the FGM Beam Geometry generated using the FEA Program considering 'MCPv' and 'MCPh' values 0.5 and 1 respectively.

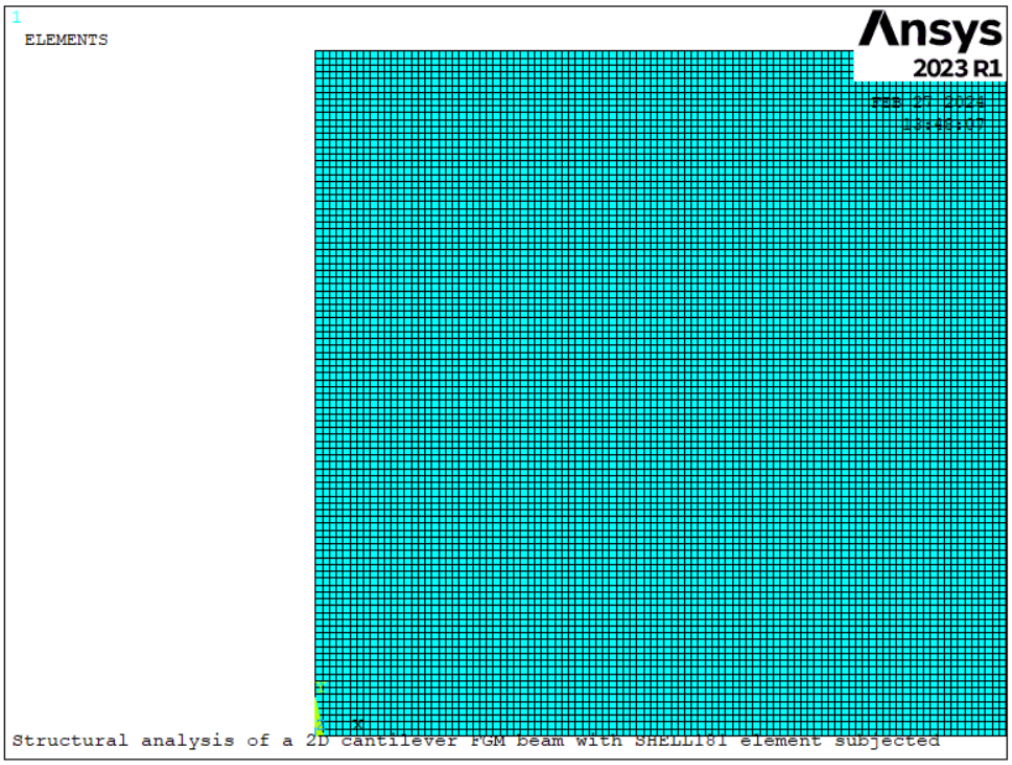

Figure-6.2d Enlarged Meshed view of the FGM Beam Geometry generated using the FEA Program considering 'MCPv' and 'MCPh' values 0.5 each.

Following figures shows the enlarged meshed views of the FGM beam with above mentioned combinations of ‘MCPv’ and ‘MCPh’ values.

Now, among the above configurations further simulations have been completed with the configuration corresponding to the ‘MCPv’ and ‘MCPh’ values 1 each. In this simulation SHELL181 element has been used and material properties have been generated for each of the 50 layers using power law of material property gradation and have been assigned with separate material property number. After calculating material property values for each layer of the beam, those have been assigned properly to each layer.

In this problem boundary conditions and loading have been imposed on nodes and for that purpose a suitable APDL Macro has been written to select proper nodes to apply displacement values and loading values.

Following is the figure of the FGM beam with clamped boundary condition at the left most nodes, that is, at nodes having ‘X’ coordinate value 0 with displacement parameter vales as Ux = 0, Uy = 0, Uz = 0, Rx = 0, Ry = 0 and Rz = 0, that is, All Degree of Freedom (ALL DOF) = 0.

To apply load nodes at ‘Y’ coordinate value ‘h’ have been selected using a APDL Macro and the number of those nodes have been counted and labelled with a suitable name. Afterward total load has been divided by those number of nodes, that per unit load has been imposed at each of the above nodes.

Loading and boundary conditions have been depicted in figure numbers 6.3 and b.

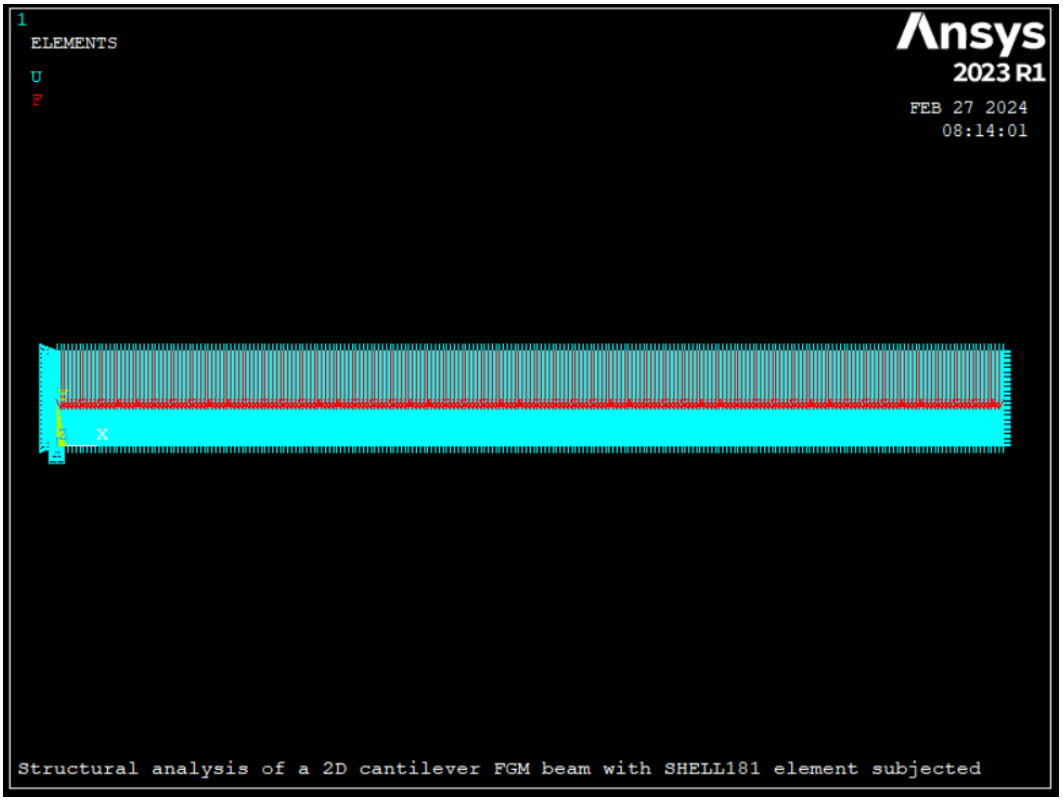

Figure-6.3a Loading and Boundary Condition imposed using the FEA code.

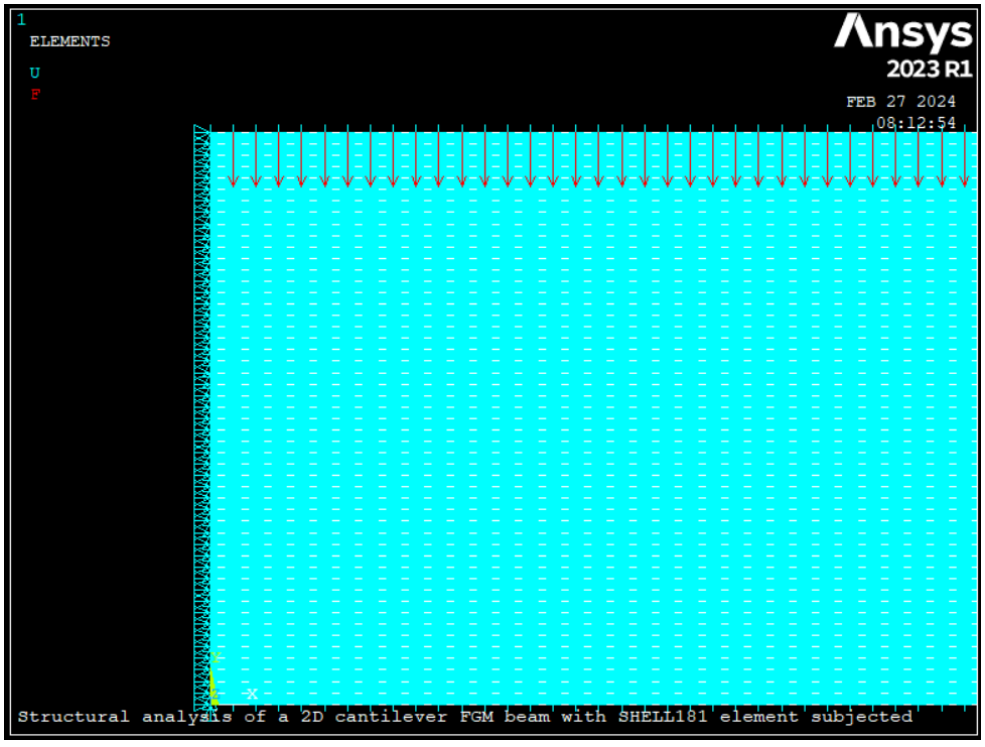

Figure-6.3b Enlarged view of imposed Loading and Boundary Condition shown in fig. 6.3a

After imposing loading and boundary conditions solution has been done and transverse deflections of the beam at various nodes on the mid line or elastic curve along the length

of the beam have been listed. Then a graph has been plotted between the x-coordinate of the nodes and the deflection values which has been presented in **figure 6.4** below.

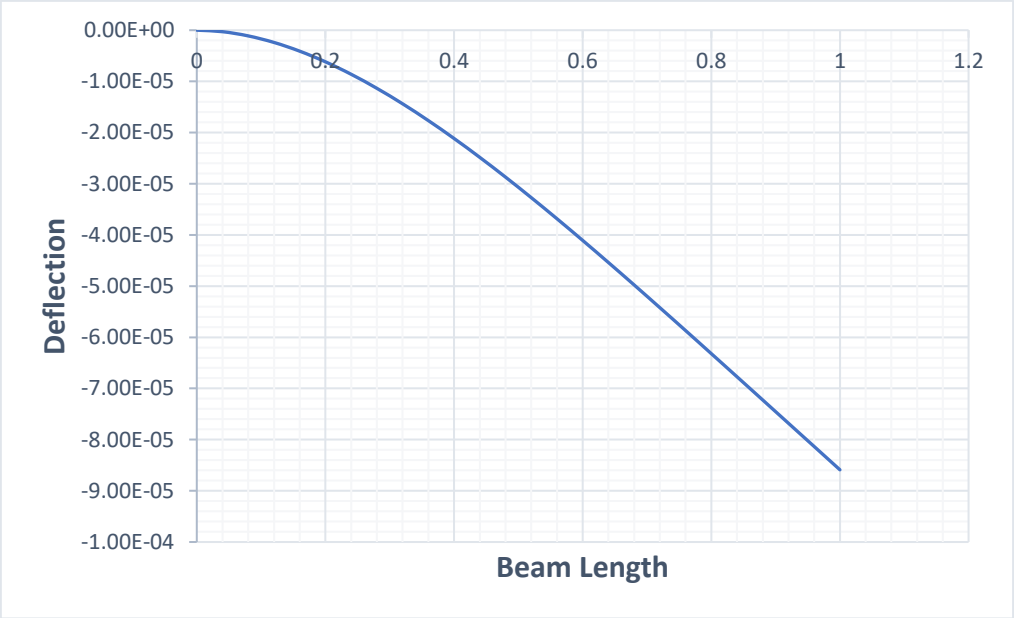

Figure-6.4 Variation of transverse deflection of elastic curve at y=h/2 along the length of the FGM beam.

Now axial stress values at various nodes on the left most side of the beam, that is, at the x-coordinate value zero have been listed. Here also a graph between y-coordinates of the nodes and axial stress values in Pascal has been plotted and presented below.

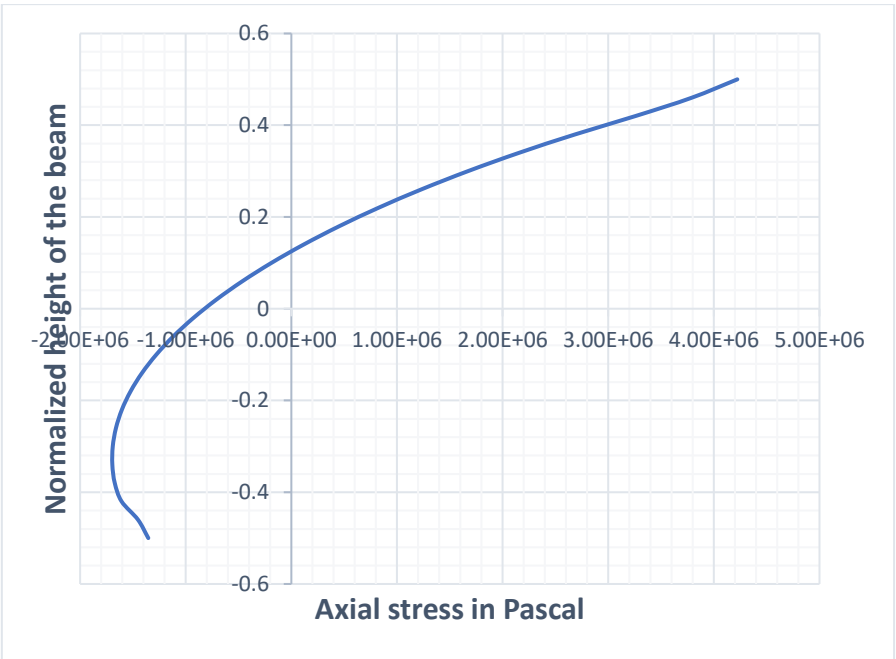

Figure-6.5 Variation of axial stress along the height of the FGM beam at x=0.

Besides graph plotting contour plotting has also been done for the deflection distribution and axial stress distribution as shown below.

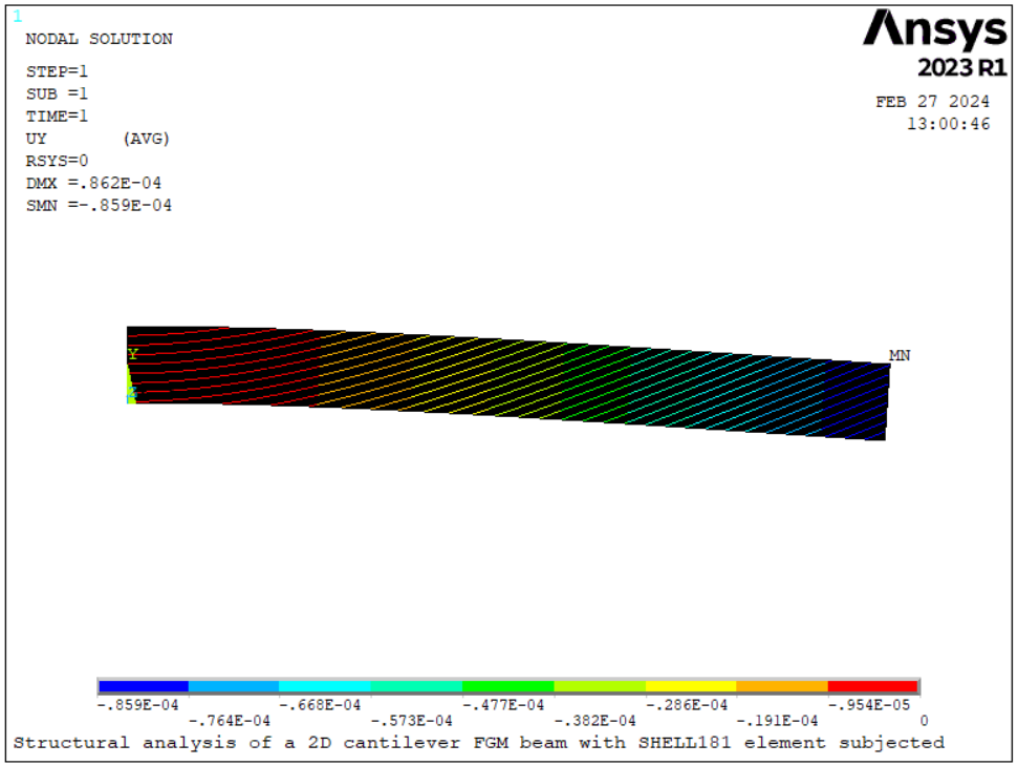

Figure-6.6 Contour plotting of the transverse deflection along the length in the FEA program.

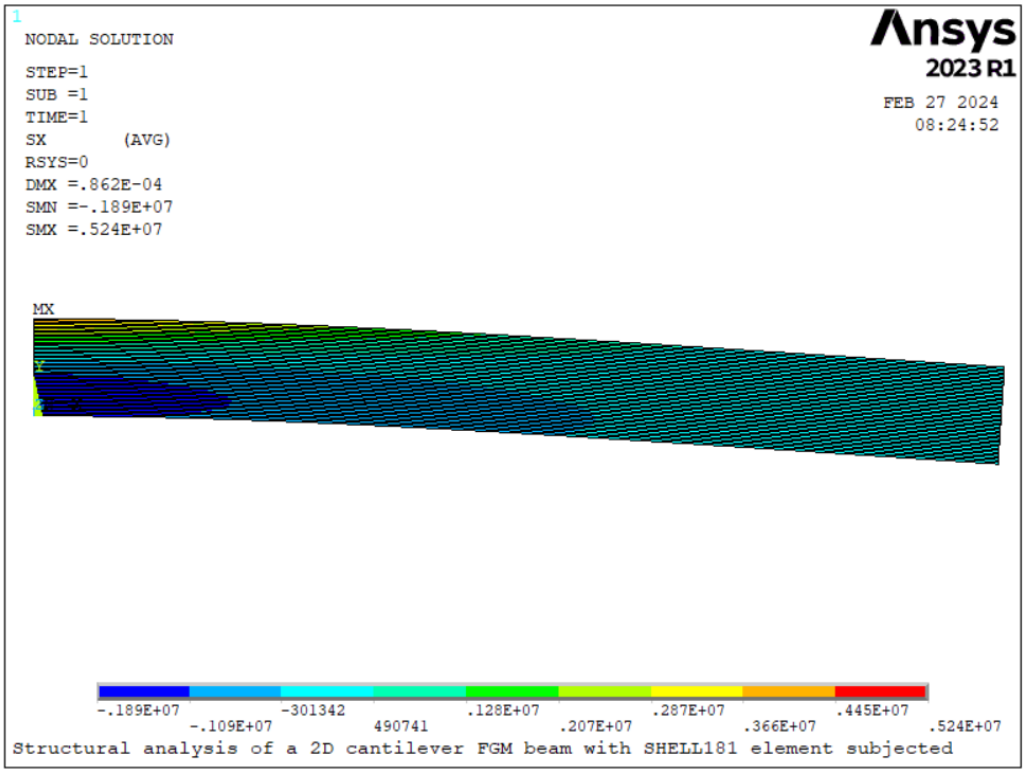

Figure-6.7a Contour plotting of the Axial stress distribution in the FEA program.

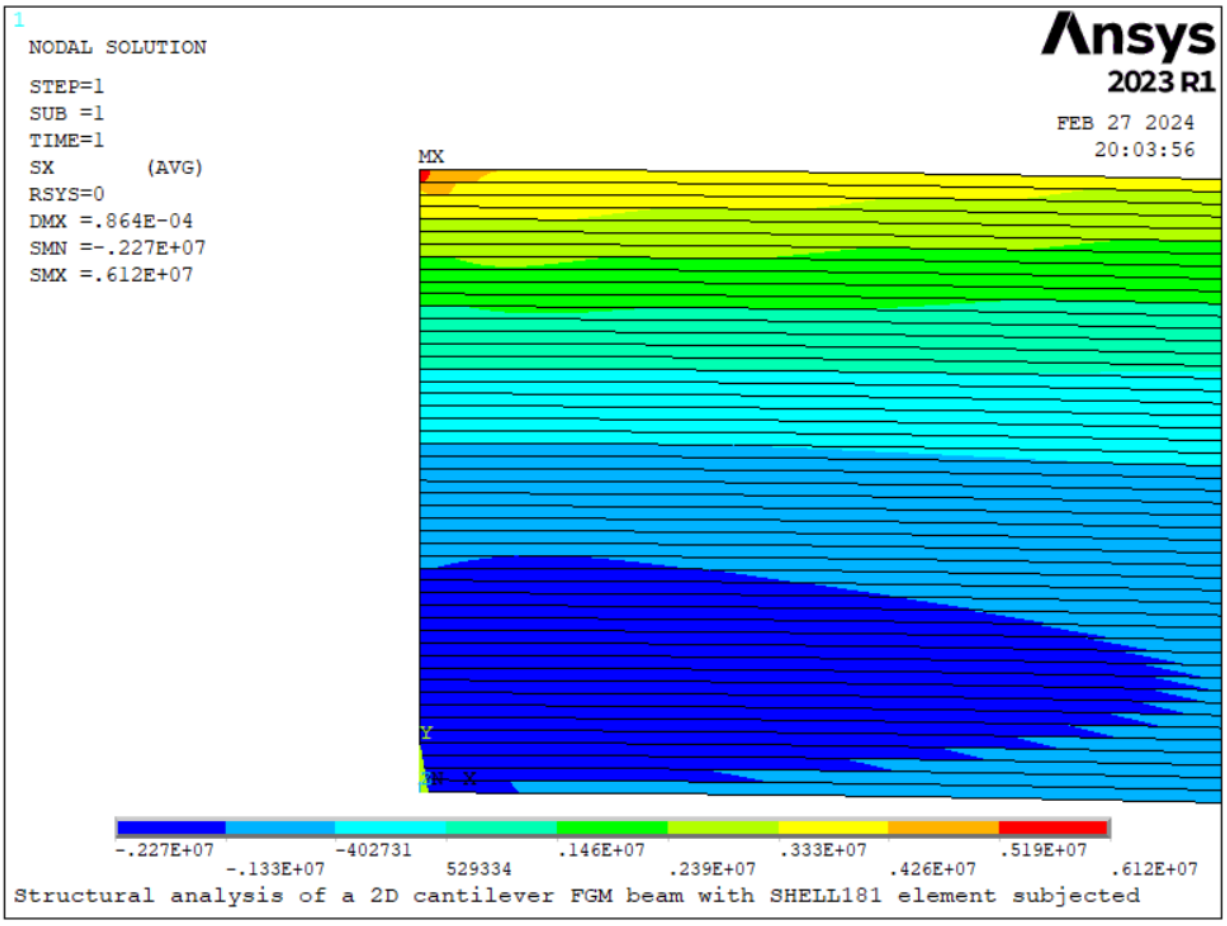

Figure-6.7b Enlarged view of the contour plot shown in figure 6.7a

Now to validate the method of determination of transverse deflections at various nodes on the central curve or elastic curve of the FGM beam along its length with help of FEA method using the APDL code developed in this work, all the values of transverse deflections have been compared with the results of transverse deflection determined by the Unified Higher Order Beam theory developed in this present work using a MATLAB code which has also been written in this present work.

As the problem solved here has been taken from the work of X. F. Li [33], all the results of transverse deflection have also been compared with result of the work of X. F. Li [33]. To compare all these results three set of data have been plotted in a single graph against axial distance of the beam measured from fixed end. The graph which has been plotted has been shown below.

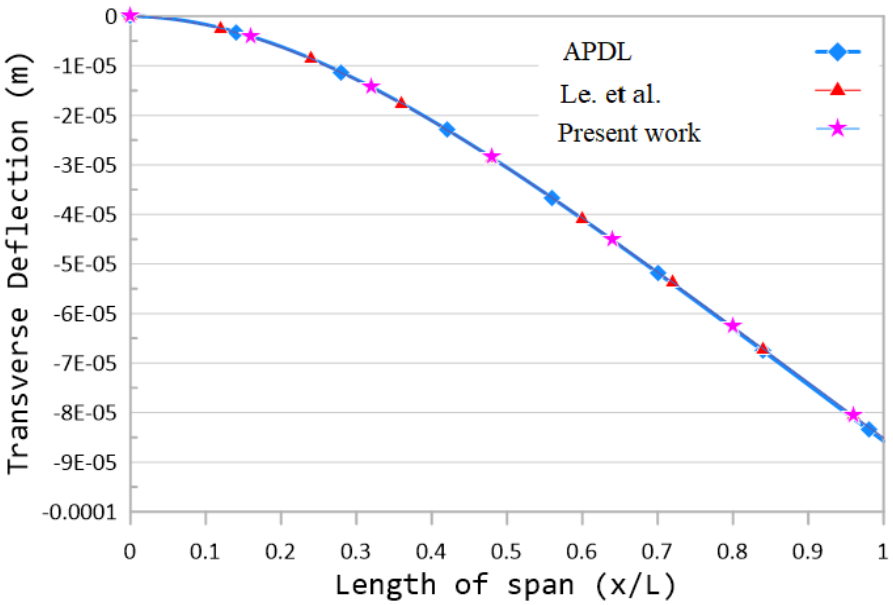

Figure-6.8a Comparison of deflections determined using ANSYS APDL program with MATLAB results and with the results from the work of X. F. Li [33].

Similar to the transverse deflections, axial stress at various nodes on the vertical edge at the left most position, that is, at x=0 determined with help of FEA method using the APDL code developed in this work, have been compared with the results of axial stresses determined analytically using the MATLAB code which is also developed in this present work. All the results of axial stresses have also been compared with result of the work of X. F. Li [33]. Following is the graph showing all the above-mentioned results together.

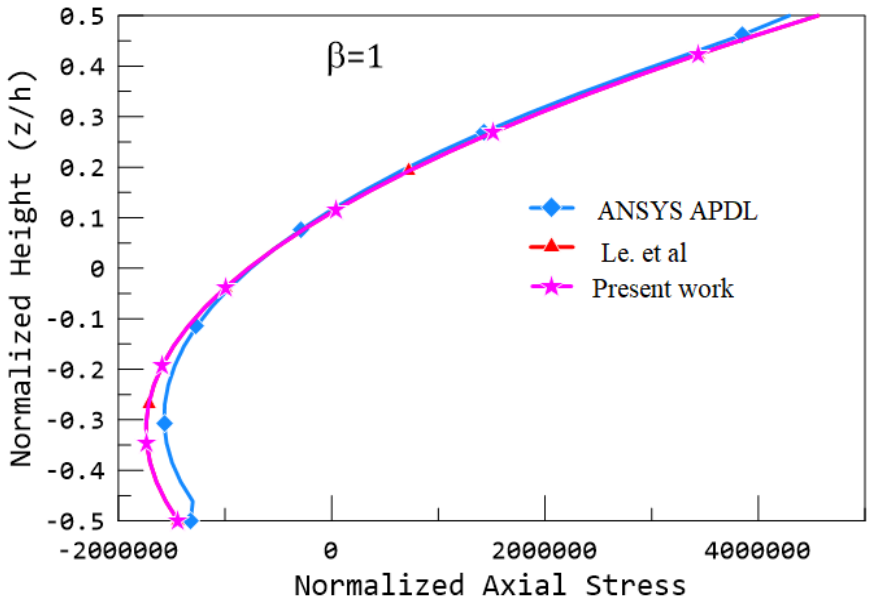

Figure-6.8b Comparison of axial stress using ANSYS APDL program with MATLAB results and with the results from the work of X. F. Li [33].

6.2.2 A FGM simply supported beam subjected to a given UDL

To validate the ANSYS APDL program developed in this work, another problem of a FGM beam with transverse loading has been solved with the APDL program developed in this work. The problem definition has been stated below which has been taken from the work of X. F. Li [33].

In this problem a FGM Simply-supported beam has been considered of length 1m, width 0.1m and thickness also 0.1m. A Uniformly Distributed Load (UDL) of 1000 N/m has been imposed on the beam over its throughout length. The beam is made of a FGM in combination of Aluminium and Silicon Nitride where Aluminium at the bottom layer and Silicon Nitride at the top layer. Properties of Aluminium and Silicon Nitride have been taken from table 1.0. The gradation of material has been done as per power law and properties have been calculated by Eq. 31 and Eq. 32.

Above problem has been solved for the output parameters i.e., transverse deflection 'w' and axial stress 'σ_{xx}' using the APDL program. The APDL program automatically generates the FGM beam with 'n' number of layer as user input. Here 50 number of layers have been considered. After generating the topology of the FGM beam the APDL program can automatically calculate material properties for each layer and can assign them at each layer as discussed for the case of cantilever beam. This program also imposes boundary conditions and loading at required nodes after selecting them automatically as per the user input. Following are the figures depicting the loading and boundary conditions on the beam.

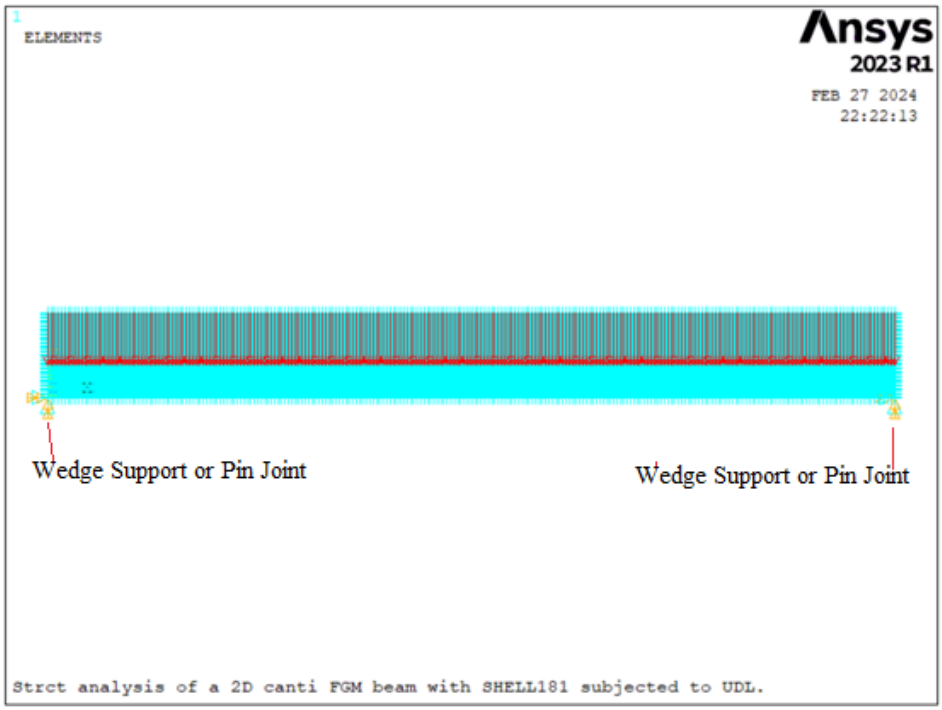

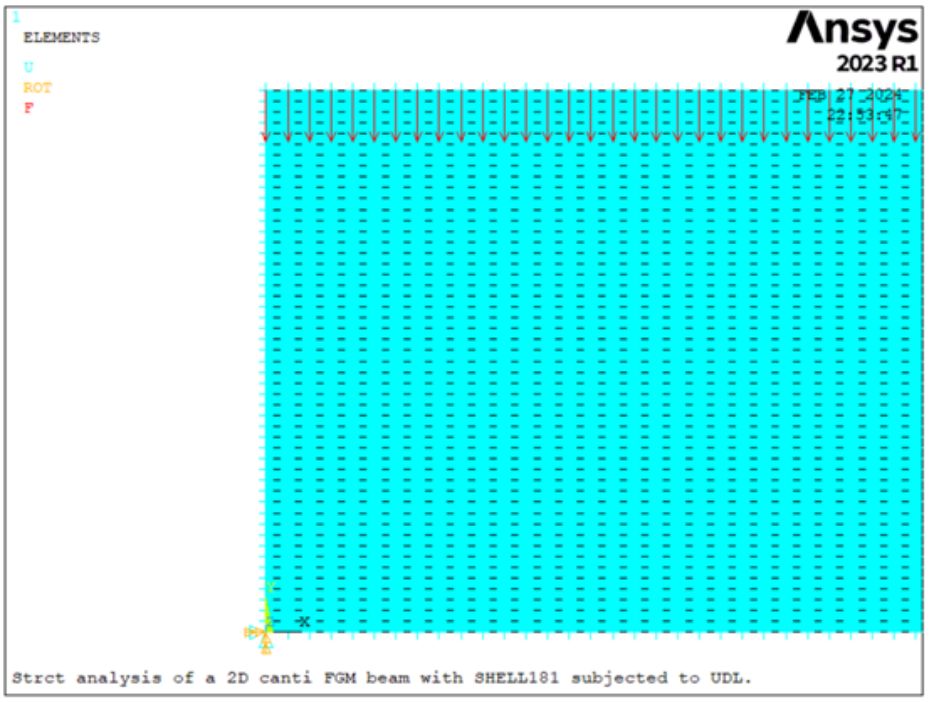

Figure-6.9 (a) Full view of the total beam with Wedge support as boundary condition and loading as UDL **(b)** Enlarged view of imposed Loading and Boundary Condition.

After imposing loading and boundary conditions solution has been done and transverse deflections of the beam at various nodes on the mid line or elastic curve along the length of the beam have been listed. Then a graph has been plotted between the x-coordinate of the nodes and the deflection values which has been presented below.

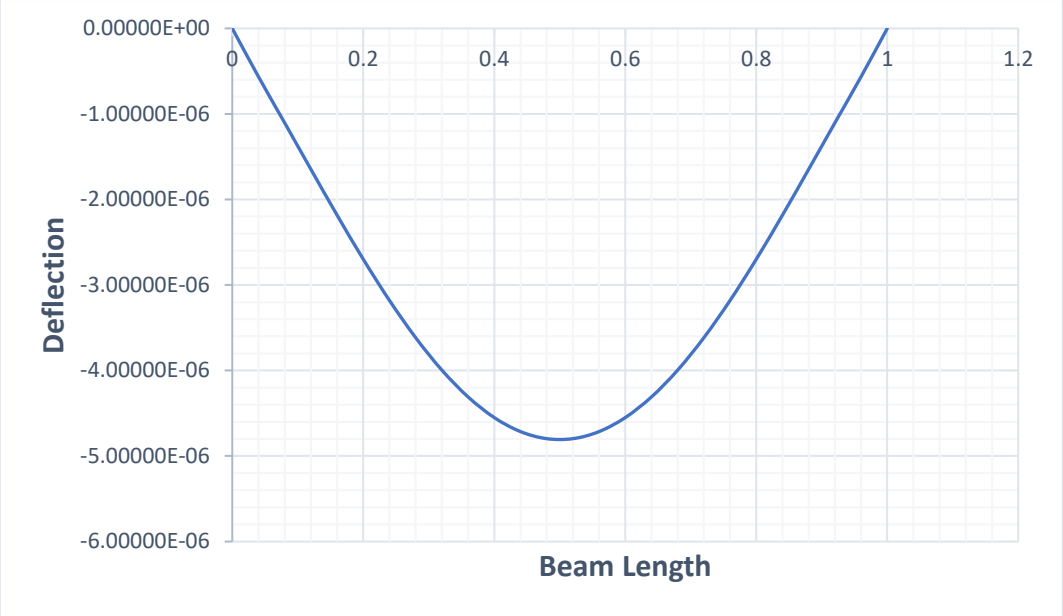

Figure-6.10 Variation of transverse deflection of elastic curve at y=h/2 along the length of the FGM beam.

Now axial stress values at various nodes on the axis of symmetry of the mid surface of the beam, that is, at the x-coordinate value L/2 have been listed. Here also a graph between y-coordinates of the nodes and axial stress values in Pascal has been plotted and shown below.

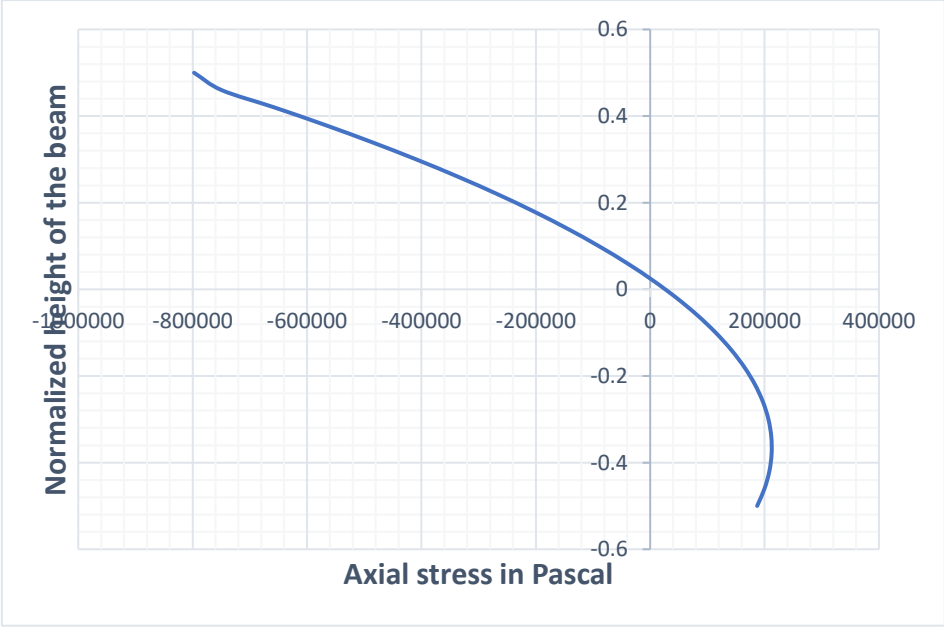

Figure-6.11 Variation of axial stress along the height of the FGM beam at mid surface i.e at x=L/2.

Besides graph plotting contour plotting has also been done for the deflection distribution and axial stress distribution as shown below.

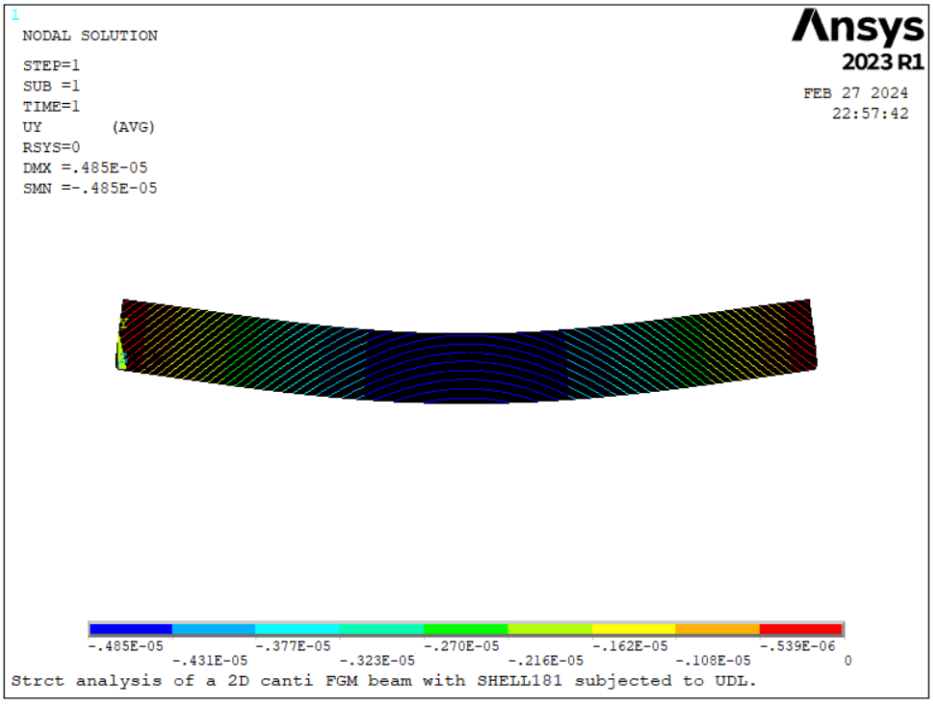

Figure-6.12 Contour plotting of the transverse deflection along the length of the simply-supported beam.

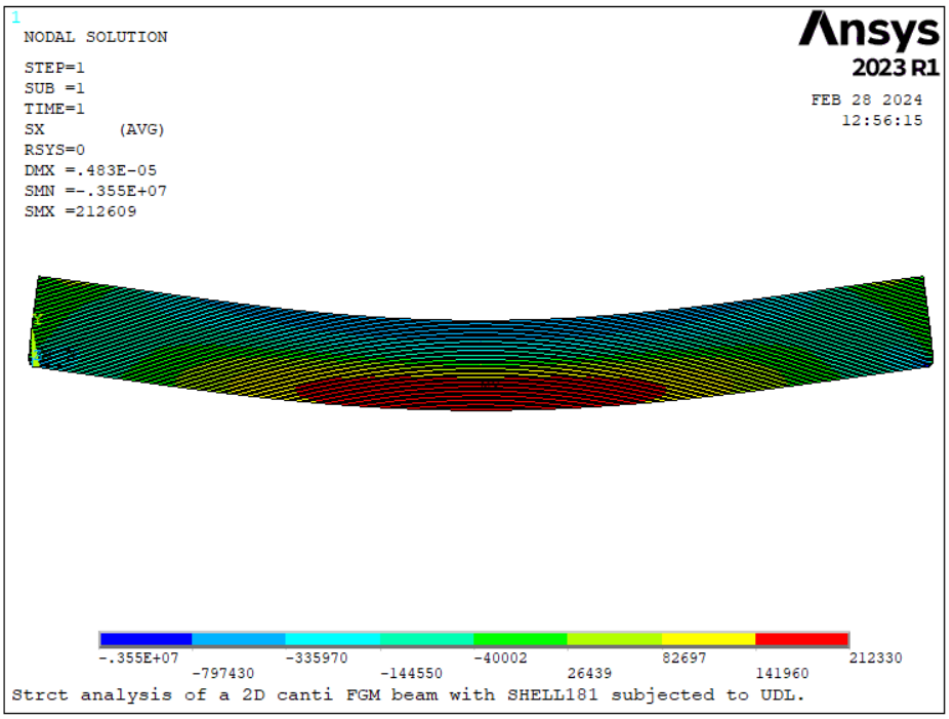

Figure-6.13a Contour plot of the Axial stress distribution of a simply-supported FGM beam under UDL.

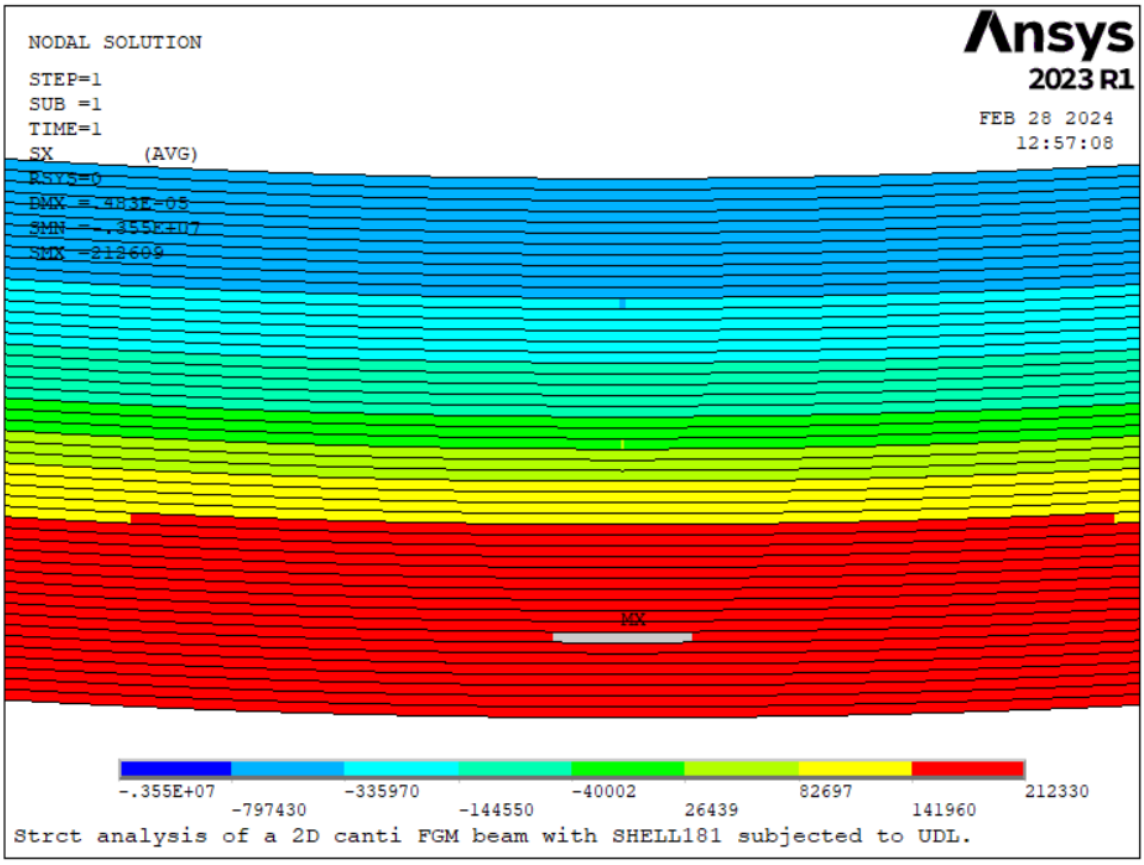

Figure-6.13b Enlarged view of above contour plot as shown in figure 6.13a.

The output parameters i.e., transverse deflection 'w' and axial stress 'σ_{xx}' which have been determined above using FEA method through APDL program developed in the present work have also been compared with the values calculated by the derived Unified Higher Order Beam theory and solved using B-spline collocation method in the present work through a MATLAB code.

As the problem solved here has been taken from the work of X. F. Li [33], all the results of transverse deflection and axial stress have also been compared with result of the work of X. F. Li [33]. To compare all these results three set of data have been plotted in a single graph against axial distance of the beam measured from fixed end. The graph which has been plotted has been shown below.

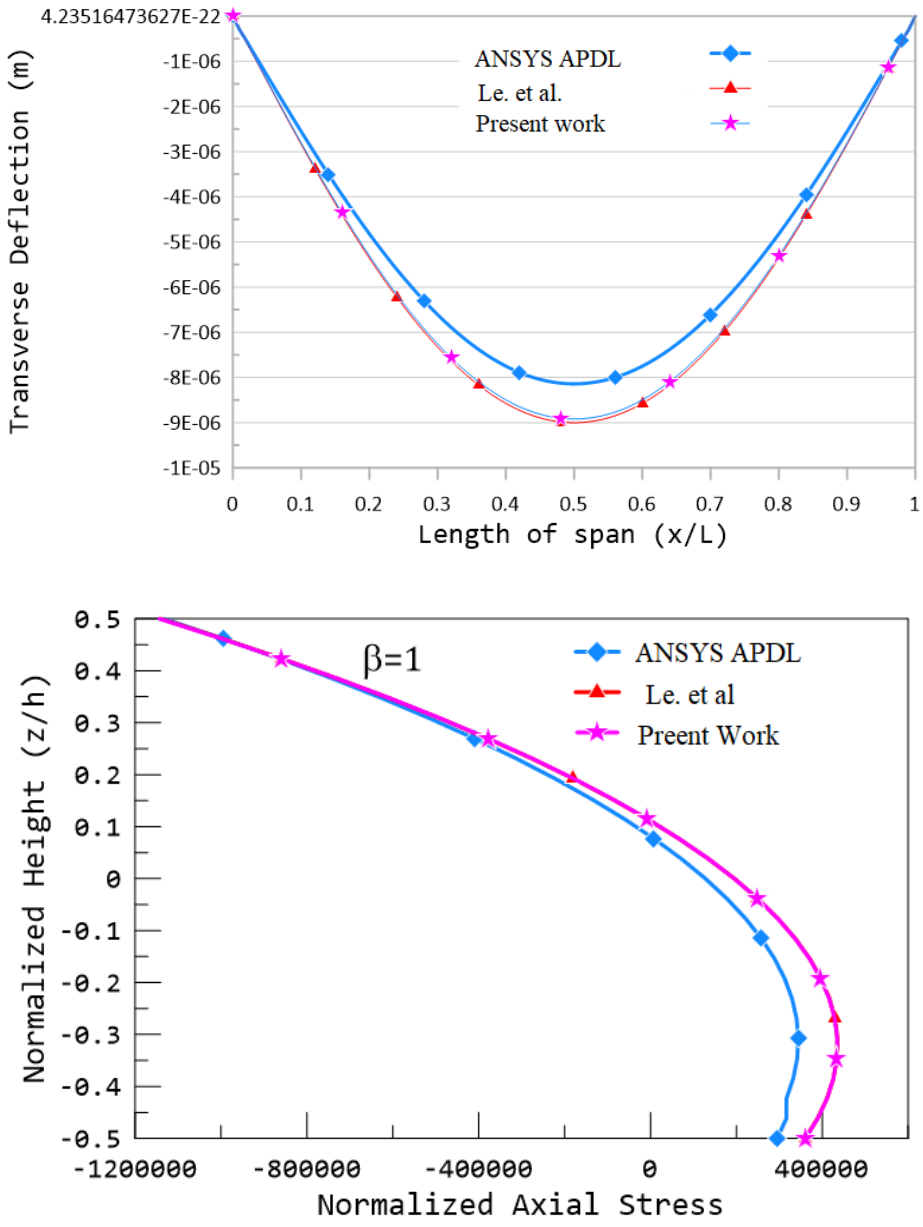

Figure-6.14 Comparison of FEA code derived results with results from code for Hinged condition a) deflection, b) normalized axial stress

6.3 Solving few critical problems using a FEA software programming

Structural analysis of any non-uniform and irregular bodies made of functionally graded materials (FGM) is very difficult using a mathematical program. Because it is extremely difficult to derive a governing equation for an irregular body, for example, beams and bars with various dimensional discontinuities like holes of various sizes and shapes, notches with various dimensions etc in the frame work of Unified Higher Order Beam Theory. So, it is a wise decision to analyse an irregular body using FEA method using a FEA software

through its programming module. Before proceeding in the development of a FEA Code for beams and bars with holes and notches, few FEA Codes have been developed to solve few problems from a few published research papers [27], [33], [138] and validated their results. These have been shown in section 6.2 in detail.

After validating basic FEA codes for FGM beams and bars without any discontinuity and having 'n' number of layers, these programs have been modified to incorporate various discontinuities like circular holes and elliptical holes with different dimensions. These FEA codes can also incorporate the holes at user defined positions in the beams and bars.

To examine the efficiency and capability of the FEA codes, few problems of beams and bars with circular holes and elliptical holes have been solved in this section. In the first problem a short beam/bar of length 100mm and cross-section 10mmx10mm has been considered. This beam/bar has been incorporated with a hole of 5mm diameter at the centre of the beam/bar and has been imposed with an axial load of 1kN at extreme right end with extreme left end fully fixed. Here one thing is worthy to mention over here that, as in this validation process only axial force is imposed so this layered structure would be considered as a Bar though it is termed as a Beam.

Now before the solution of the above-mentioned problem is performed, proper value of Mesh Control Parameter 'MCP' for the grid independent solution has been determined. It has been shown in the previous section that, MCP value of '1' has given a grid independent solution successfully. But in the present problem due to incorporation of the hole, denser meshing is required. To determine the mesh independent solution total five MCP values have been tested. These are 1, 0.5, 0.25, 0.2 and 0.125.

Here one thing is worthy to mention that for the purpose of validation only single material has been used in this problem, that is, steel with modulus of elasticity (E) 210 GPa, Poisson's ratio 0.3 and Density 7800 kg/m^3. Though topology of the beam/bar has been created with 50 layers but each layer has been assigned with material properties of steel only. Then maximum stress has been determined which is occurred at the vicinity of the hole and this maximum value of stress is compared with the analytically determined maximum value of stress considering the standard value of 'Stress Concentration Factor' (SIF). Following is the figure of the topology of the beam/bar with hole generated using the APDL program.

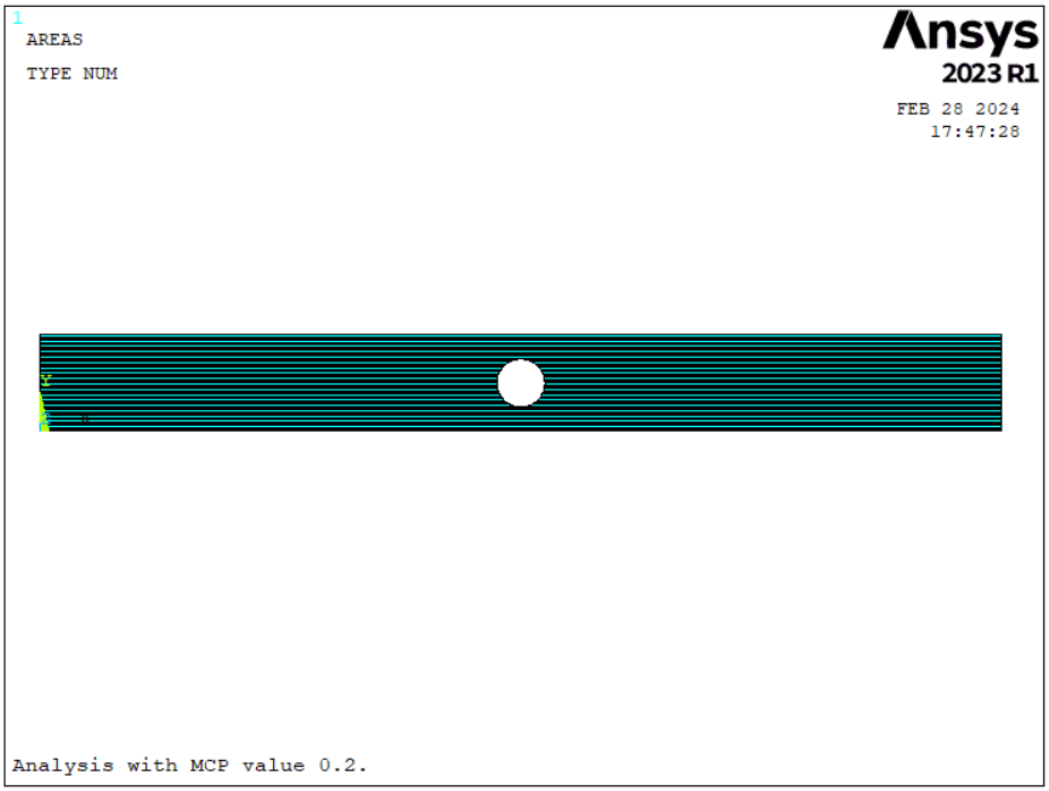

Figure-6.15a Layered beam/bar generated by the FEA code with a hole at center.

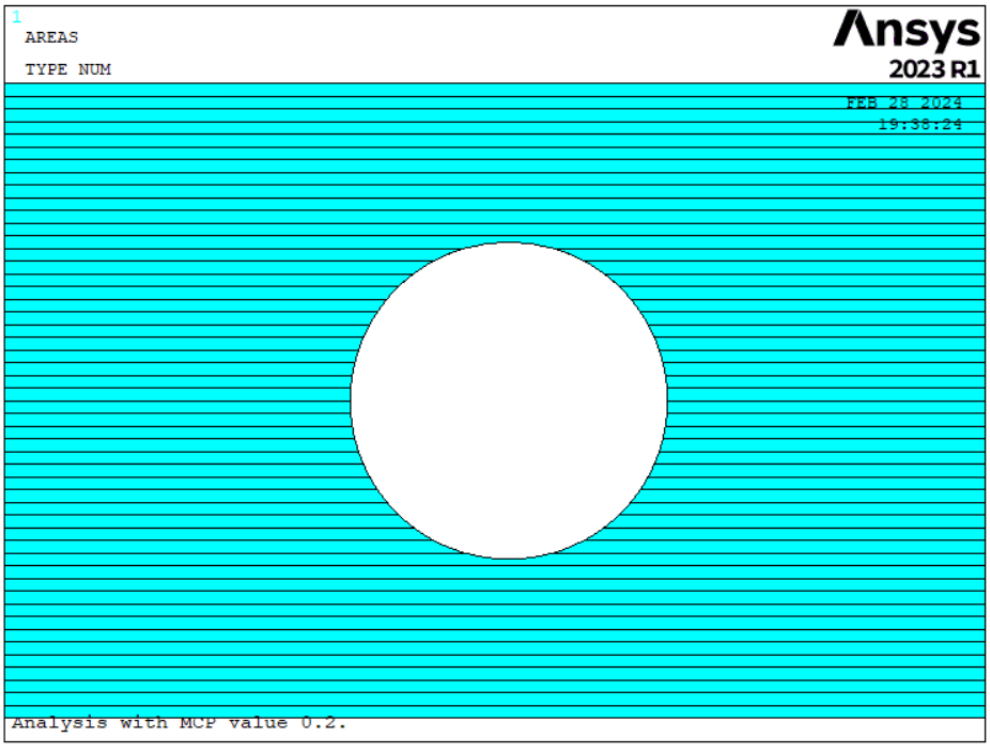

Figure-6.15b Enlarged view of the layered beam/bar generated by the FEA code with a hole at center

Now, to determine required value of MCP (Mesh Control Parameter) for the mesh independent solution maximum axial stresses have been calculated for each value of MCP. Following is the meshed view with MCP 0.2.

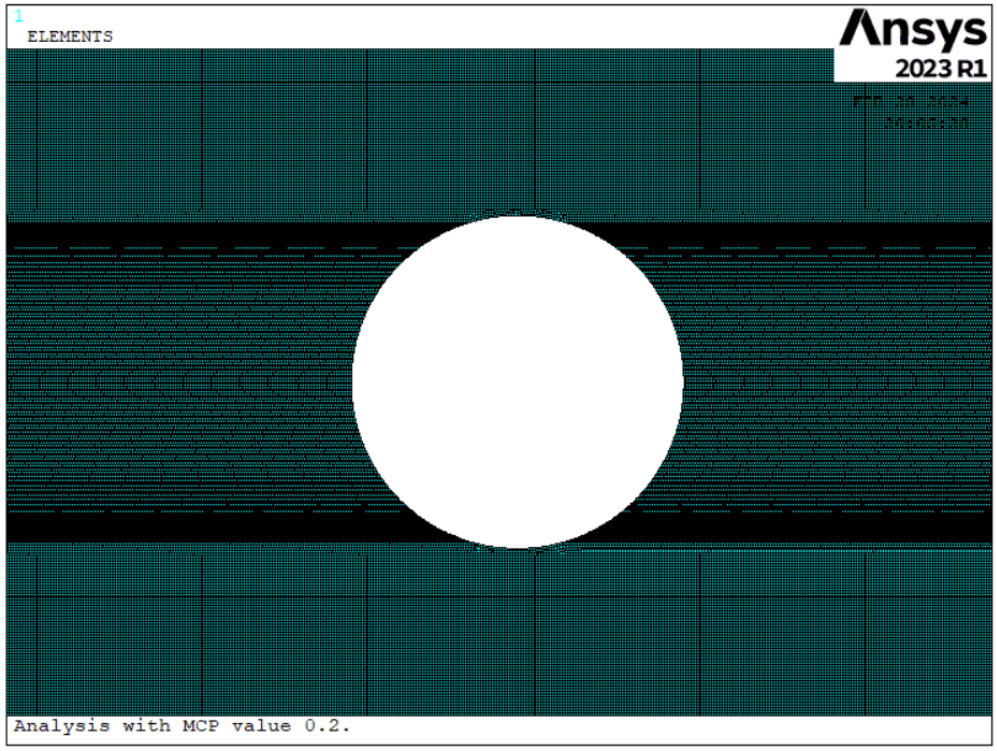

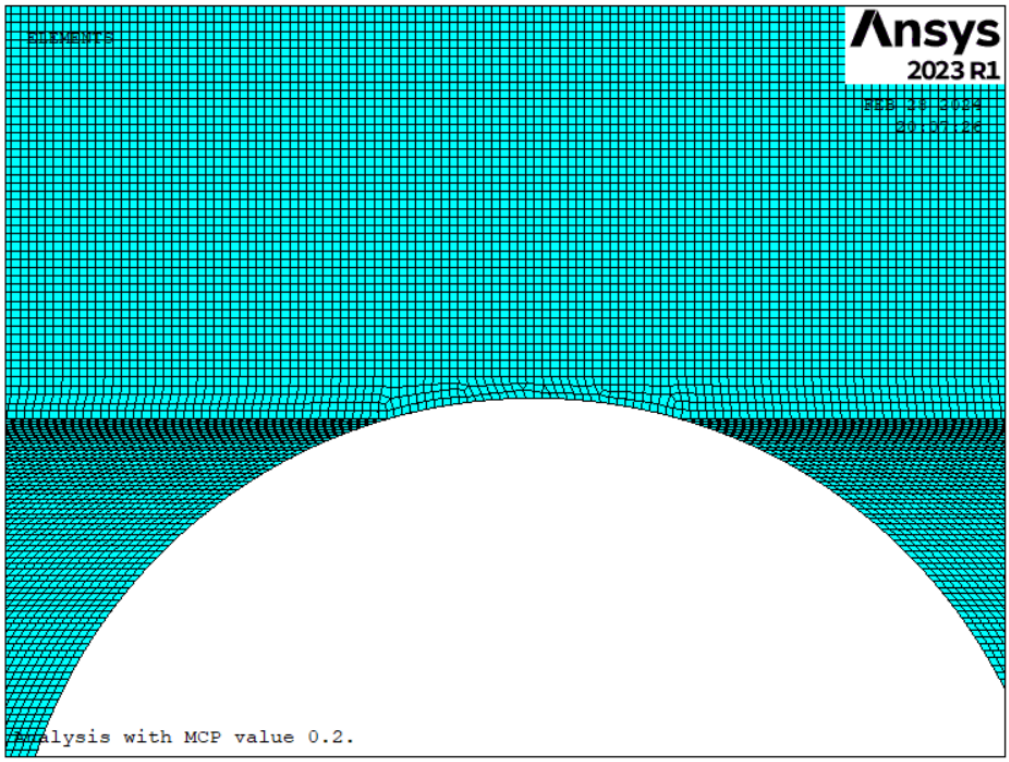

Figure-6.16 (a) Meshed view of the beam/bar with hole **(b)** Enlarged view of the mesh near hole position.

From the above meshed view, it is clear that MCP value perfectly controls the meshing around the circular hole and a perfect structed mesh has been done as per the curvature of the hole. After successful meshing, loading and boundary condition been imposed. Under boundary condition, each node of the left most edge has been assigned with all degree of freedom equal to zero, i.e Ux=0, Uy=0, Uz=0, Rx=0, Ry=0 and Rz=0. To impose load, number of nodes at the right most edge have been counted first and then total load value have been divided by this number of nodes to get load for each node. Following is the figure of the beam/bar with loadings and boundary conditions imposed.

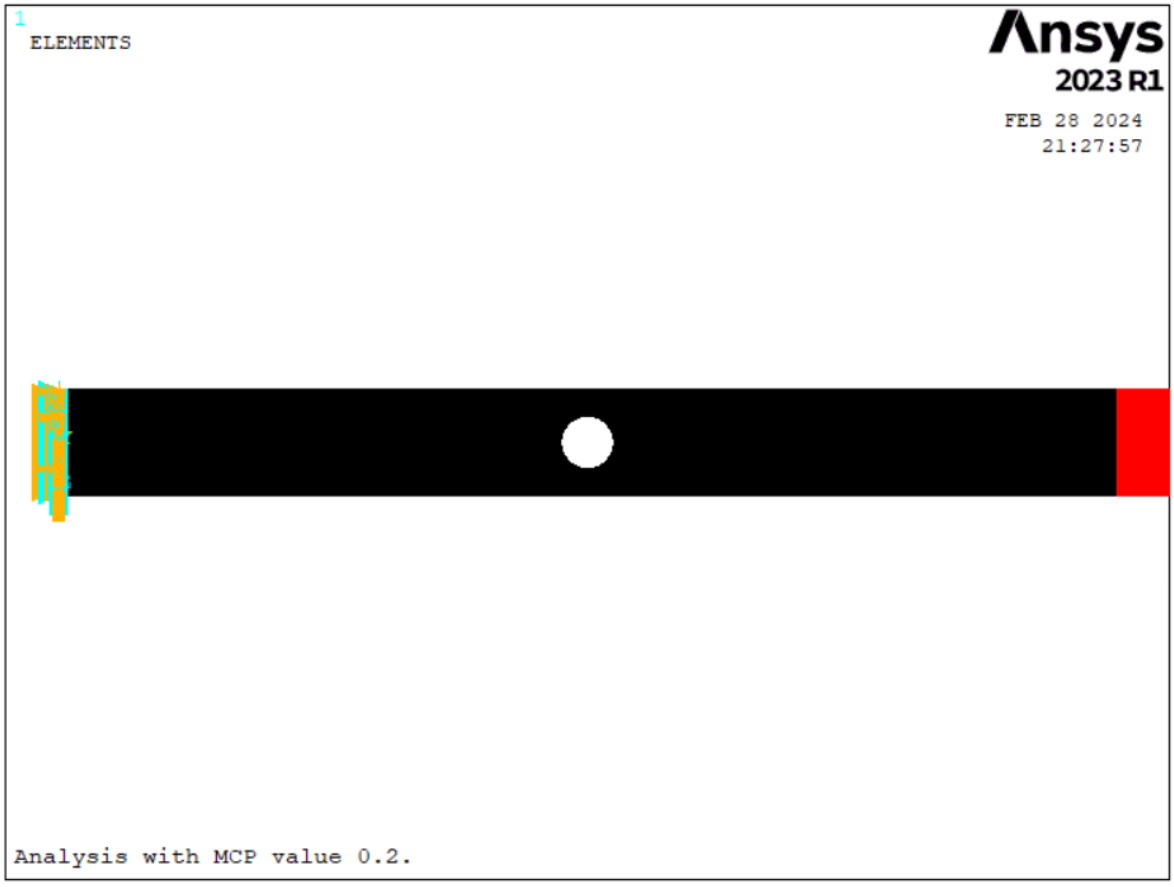

Figure-6.17 Beam/bar with hole subjected to boundary condition and loading.

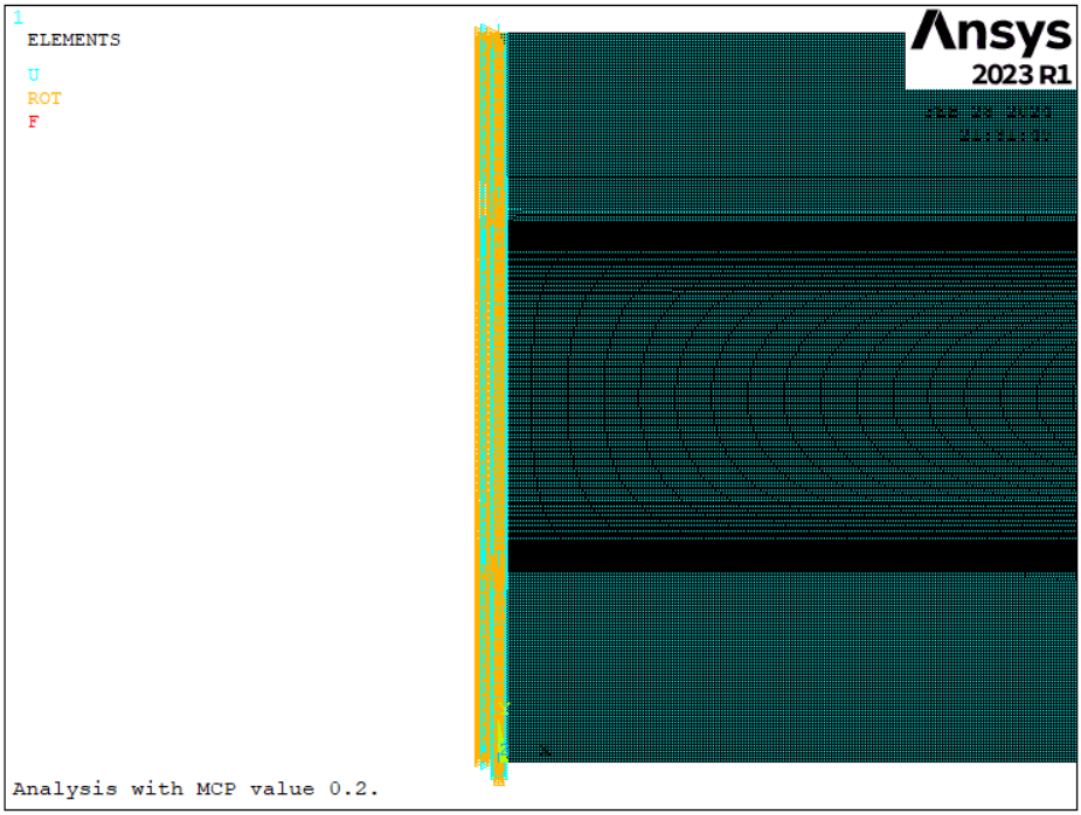

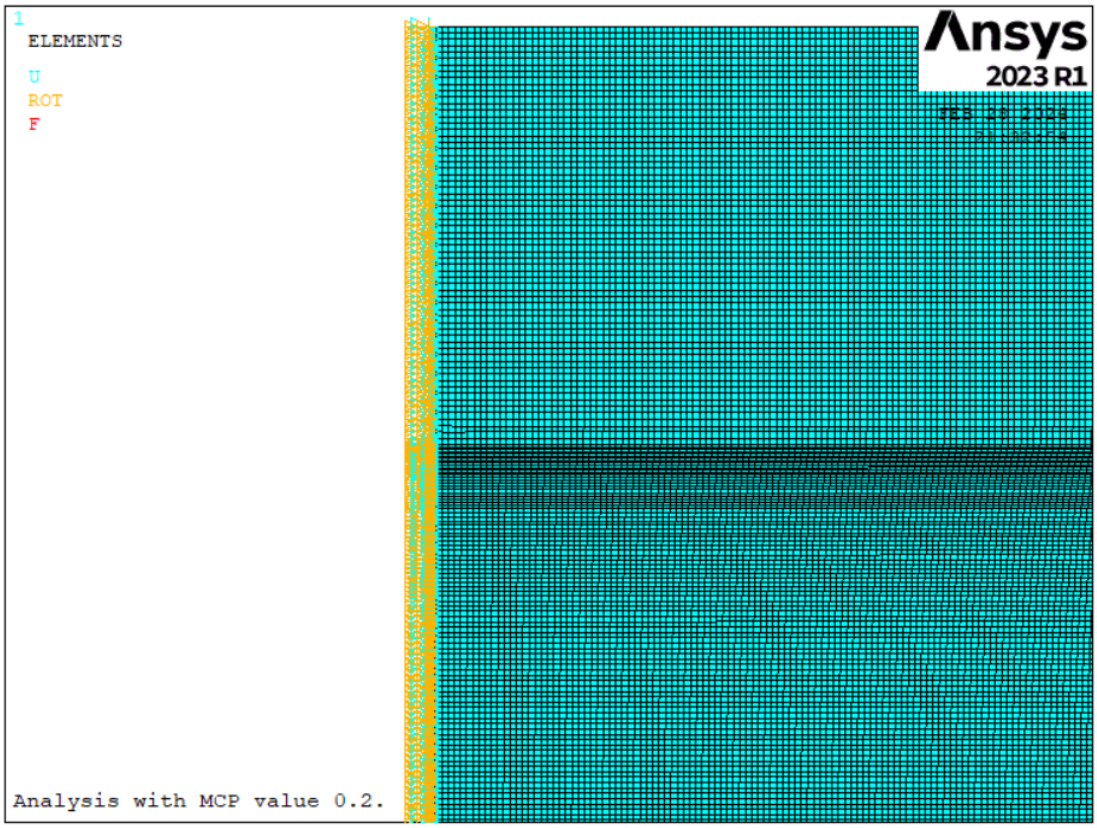

Figure-6.18 a, b Enlarged views of the imposed boundary condition on the nodes at the left most edge.

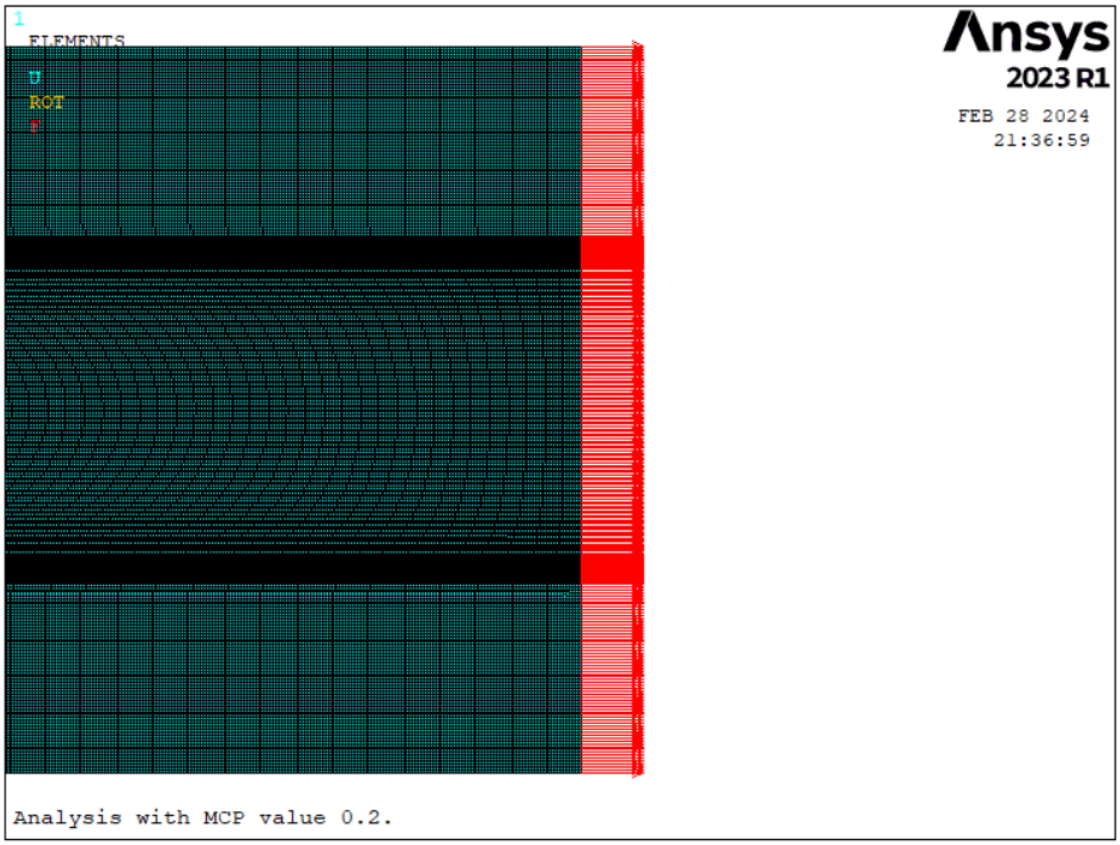

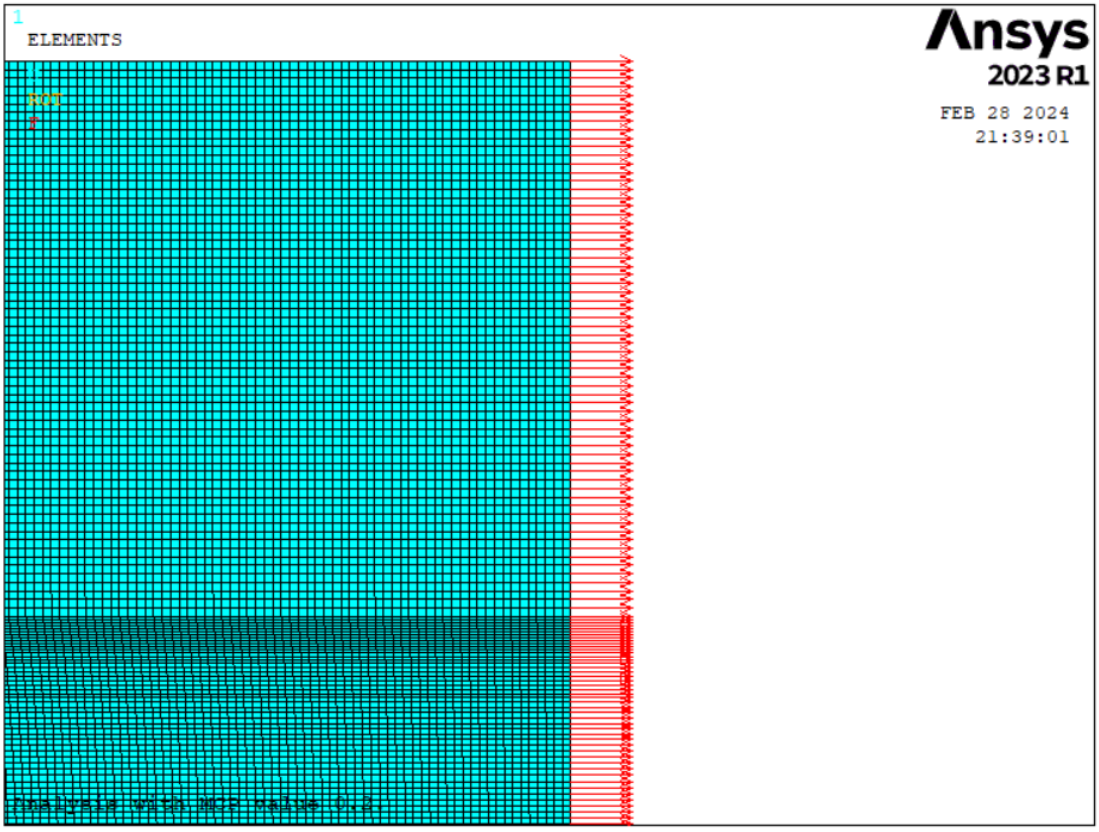

Figure-6.19 a, b Enlarged views of the imposed loadings on the nodes at the right most edge.

After imposing loading and boundary conditions the problem has been solved and maximum stress at the vicinity of the hole has been noted. In this problem simulation has been done for various mesh sizes controlled by a parameter named as 'Mesh Control Parameter' (MCP). MCP values which have been used for this problem are 1.0, 0.5, 0.25, 0.2 and 0.125. For each value of MCP maximum stress in the beam/bar with hole which is occurred near hole has been noted and compared with the theoretical value of the maximum stress calculated analytically and with help of standard value of Stress Intensity Factor (SIF).

As per the given data regarding dimensions of the beam/bar structure the nominal stress that would be generated in the beam/bar near hole is

$$\sigma_x = \frac{Load}{Cross - sectional\ area\ at\ hole}$$

$$= \frac{1000N}{(Width - Hole\ dia) \times Thickness}$$

$$= \frac{1000\ N}{(10-5) \times 10\ mm^2} = 20\ \ N/mm^2$$

Now Stress Concentration Factor has been selected from a standard graph as shown below

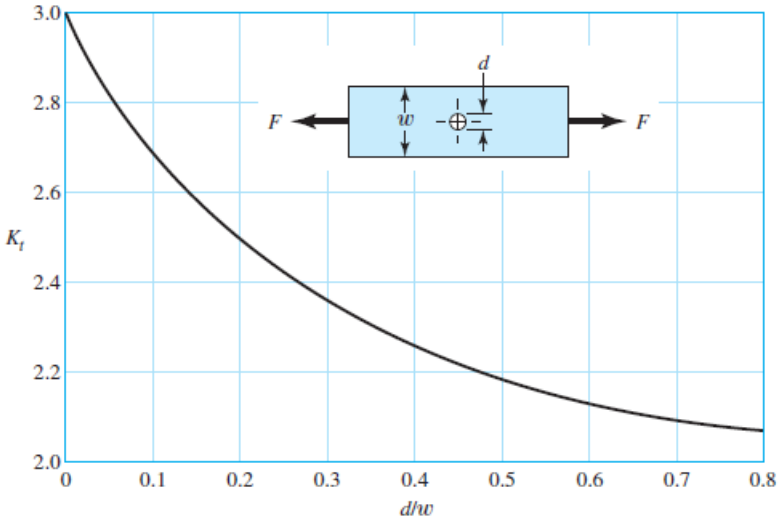

Figure-6.20 Graph of theoretical Stress Concentration Factor K_t for Rectangular Beam/Bar with Transverse Hole in Tension or Compression [149]

From the given problem the value of $\left(\frac{d}{w}\right)$ is $\frac{5}{10} = 0.5$. So, the value of Stress Intensity Factor K_t is corresponding to the graph above is 2.15.

Therefore, the maximum value of axial stress at the hole-area becomes

$$\sigma_x = 20MPa \times K_t = 20 \times 2.15 = 43\ MPa$$

Now, maximum stress in the beam/bar at hole region has been determined numerically using an APDL program for different mesh density controlled by different MCP values. These values of maximum stresses for each MCP values have been summarized in a table shown below.

Table 6.2: Maximum transverse deflection and maximum axial stress for various MCP values

Max. Stress in MPa by APDL	**MCP**	**Element size equal to**	**No of Elements**	**No of Nodes**	**%error**
40.5609	1.00	Height of each layer (h_n)	37704	38336	5.67
41.0131	0.50	Half of h_n	132840	134070	4.62
41.973	0.25	One fourth of h_n	495860	498282	2.39
42.7849	0.20	One fifth of h_n	758931	761947	0.5
42.8012	0.125	One eighth of h_n	975447	993985	0.46

From the values shown in the table it is quite clear that the APDL program calculates more or less same maximum stress value with error less than 1% with mesh fineness corresponding to MCP values 0.2 and 0.125. As MCP value of 0.125 generates considerably larger number of nodes than that of MCP value 0.2 with a negligible improvement in the value of maximum stress, all the further simulations for structural analysis of beams/bars with various type of circular as well as elliptical holes. MCP value would be considered as 0.2. Following is the figure of stress distribution of the beam/bar with a central hole as mentioned in the problem stated above.

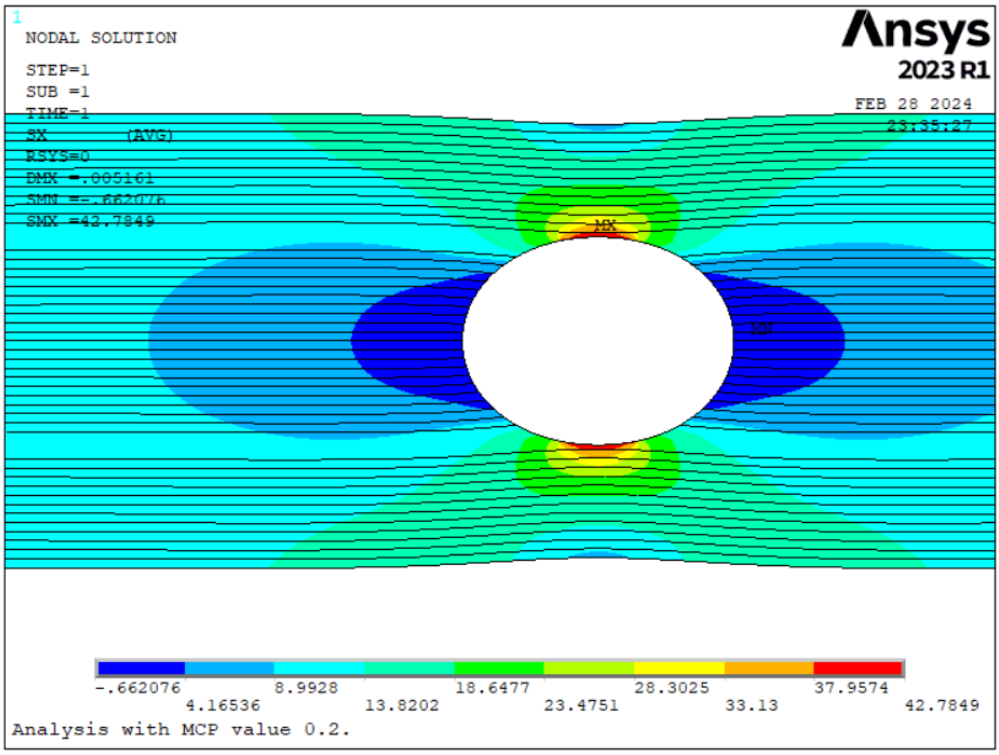

Figure-6.21 Axial stress distribution around the circular hole in the layered beam made of steel.

After validating the APDL program developed for the FEA analysis of any FGM beam/bar with circular and elliptical holes in it, various cases have been solved below.

Case I: In this problem a FGM Bar of length 100 mm and made of an isotropic material steel has been considered. Width and height of the bar has been considered as 10 mm. There is an elliptical hole of following mentioned dimensions at the centre of the bar. It is subjected with an axial load of 1000 N at the right extreme edge equally distributed along the edge length. The dimensions of the elliptical holes are as follows

Table 6.3: Dimensions of the elliptical holes placed at centre of the layered beam/bar

Sl No.	Hole no.	Length along the axis of the beam/bar	Length along the perpendicular of the axis of the beam/bar
1	1	4mm	3mm
2	2	3mm	4mm
3	3	5mm	3mm
4	4	3mm	5mm
5	5	10mm	5mm

All the configurations of the bar object have been constructed using the APDL program designed in this work. The APDL program developed here is so general that it can create any of the above-mentioned configurations very easily and with minimum time. Following

are two figures of the bar/beam created by the APDL program with hole configurations 3 and 4 mentioned above.

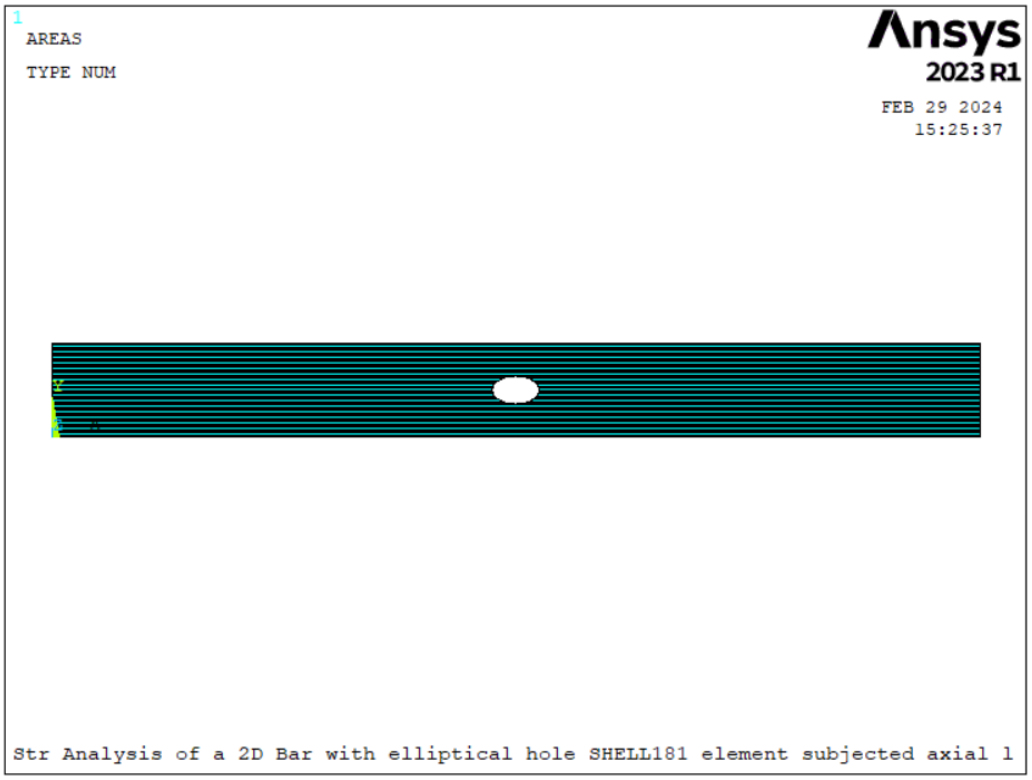

Figure-6.22a A layered beam with an elliptical hole at center as per configuration 3 of table 6.3.

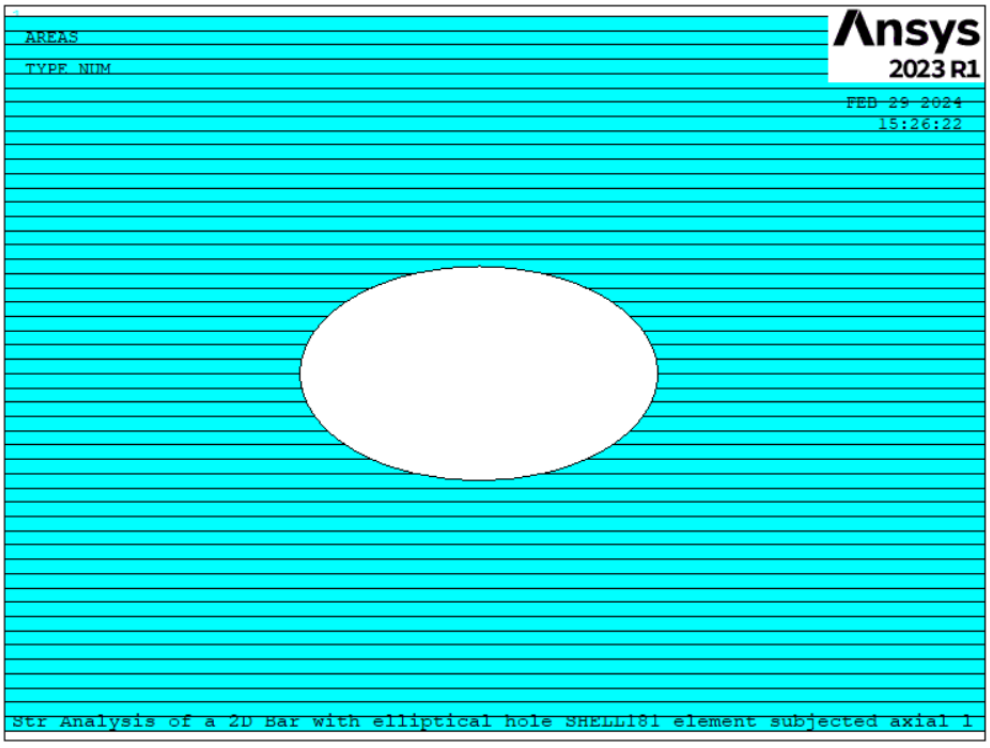

Figure-6.22b Enlarged view of fig 6-18a showing layers prominently along with the elliptical hole.

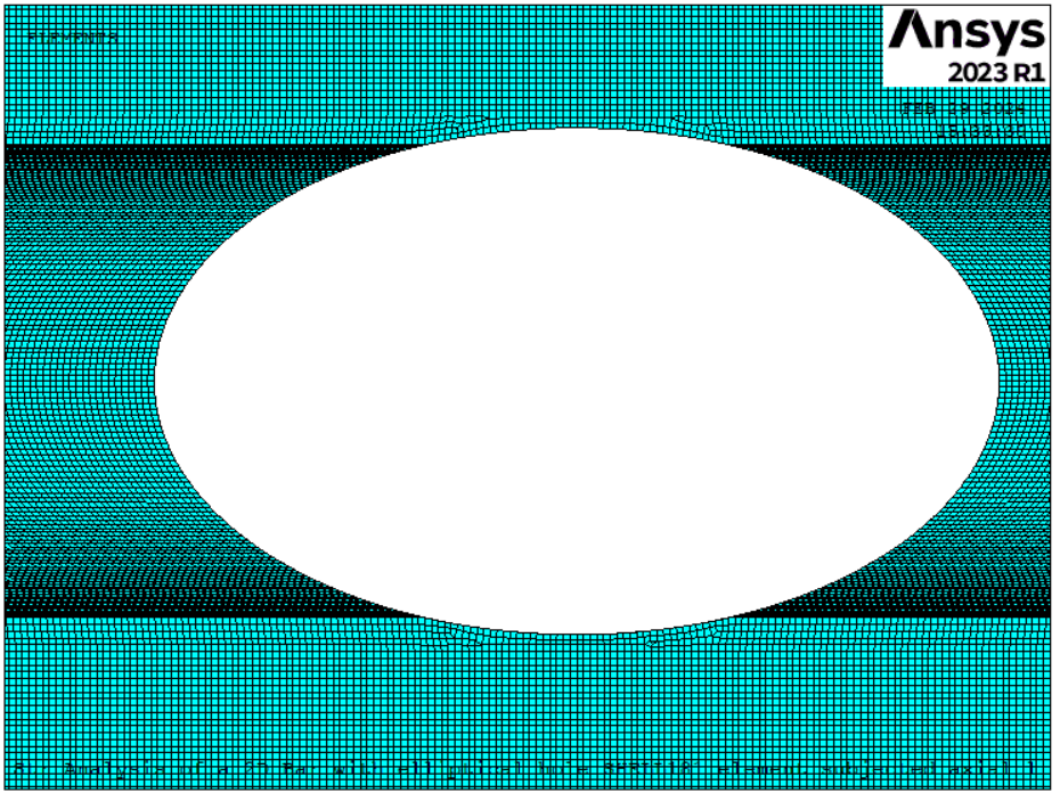

Figure-6.23a Structured meshing of the layered beam/bar with the elliptical hole.

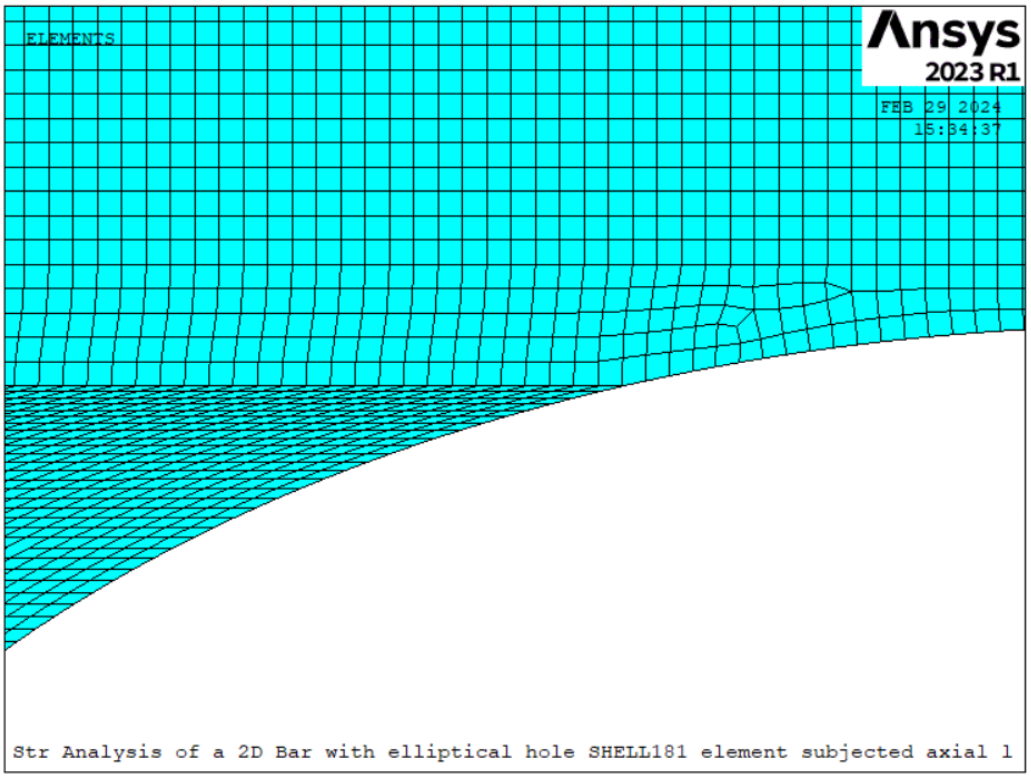

Figure-6.23b Enlarged view of the above meshing clearly showing the SHELL elements near hole.

Upon successful meshing, boundary condition and loading have been imposed on the proper nodes. Nodes on the left most edge have been constrained with all degree of freedom and an axial load has been imposed on each node at right most edge. This has been depicted in the figure below.

Figure-6.24 Imposition of boundary condition and loading on the layered bar/beam with elliptical hole.

After imposition of load and boundary conditions the problem has been solved and following is the contour plot of axial stress distribution near the hole-region.

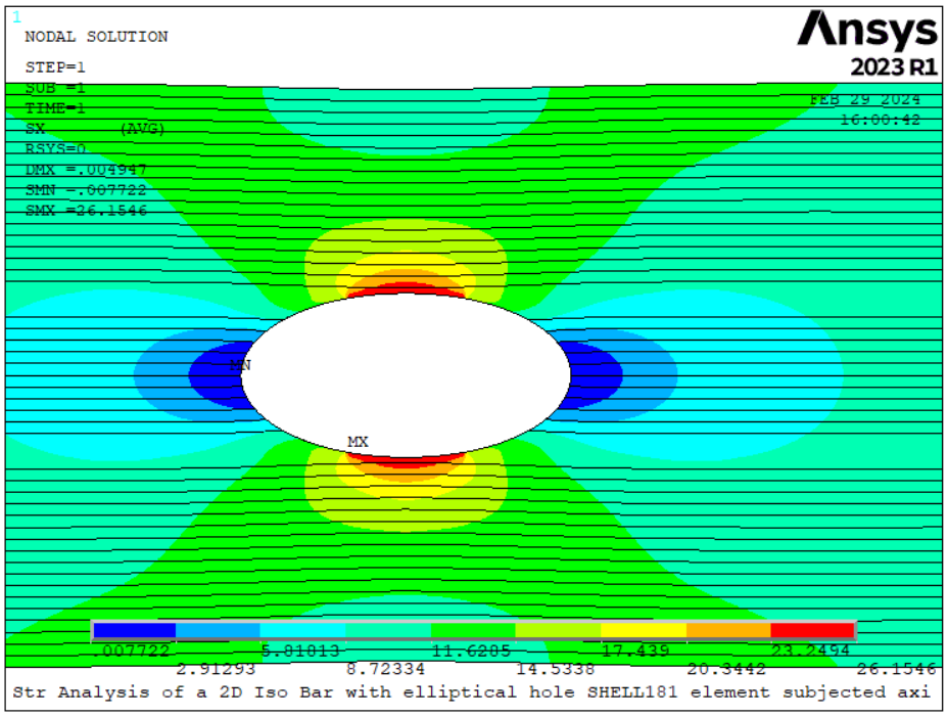

Figure-6.25 Contour plot of the axial stress distribution in the beam with hole configuration 3.

Now simulation has been done using the APDL program with hole configuration 4 as mentioned in table 6.3. Following is the axial stress distribution.

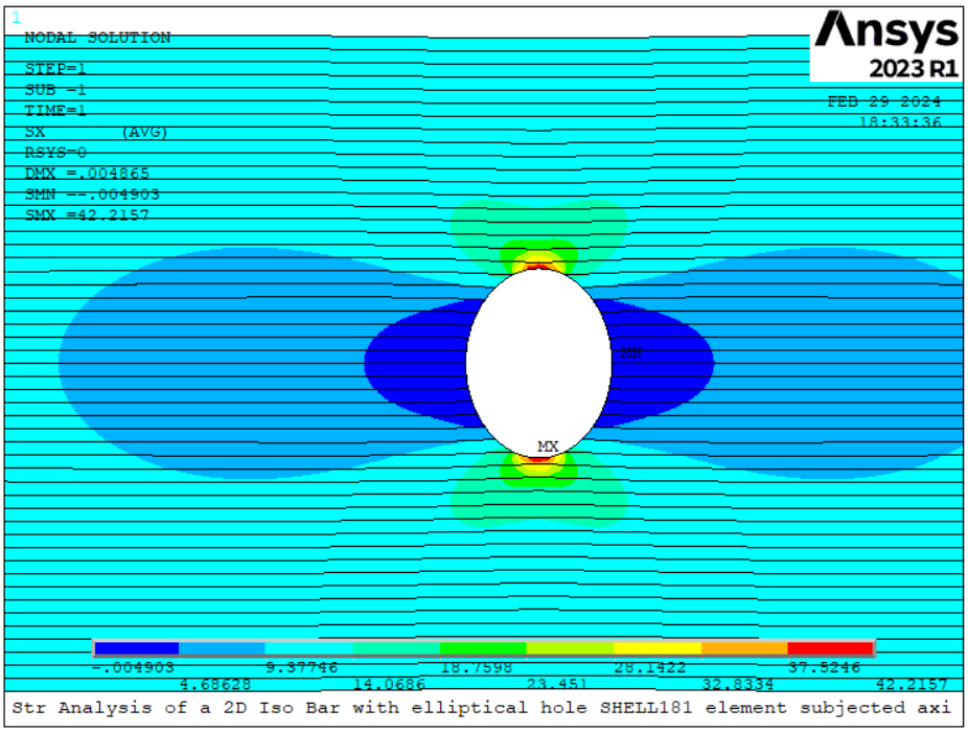

Figure-6.26 Contour plot of the axial stress distribution in the beam with hole configuration 4.

In the following table axial stress results for all the hole configuration as mentioned in the table 6.3 have been summarized.

Table 6.4: Maximum axial stresses generated around the elliptical holes of various configurations.

Dimension of the elliptical hole (mm)		**Nominal stress (MPa)**	**Max. Stress (MPa) (by APDL Program)**	**stress concentration numerically (Kn)**	**MCP**
X-axis length	Y-axis length				
4	3	14.29	28.2952	1.98	0.20
3	4	16.67	37.3744	2.24	
5	3	14.29	26.1546	1.83	
3	5	20	42.2157	2.11	
10	5	20	37.4695	1.87	

In the present problem though the geometry of the beam/bar has been created in layer wise with 50 layers but each layer has been assigned with a single material steel to make it isotropic. In the next case or problem same beam/bar has been considered but with circular hole of various dimeters placed at the centre of the beam and with varying materials between top and bottom layers.

Case II: In this case two materials have been considered. Top layer is made of 100% Silicon Nitride (Si_3N_4) and bottom layer is made of 100% Aluminium (Al). In between top layer and bottom layer these two materials have been mixed up as per laws of volume mixture following power law of mixture. The material properties of Silicon Nitride (Si_3N_4) and Aluminium (Al) have been taken from table 4.1 [38] and material properties of the in between layers have been calculated in the APDL code as per Power law of mixture. These material properties have been assigned to each layers automatically by the APDL programming. For this case a load of 1000 N has been imposed axially at the nodes of extreme right end or edge. Nodes on the extreme left edge has been imposed with the boundary condition of zero degree of freedom. As the loading for this case has been considered as axial one so it will be termed as bar and its geometrical configuration would be same as the above problems of isometric material, that is, length 100mm and section 10 × 10mm. For this case two types of circular holes with diameter 3mm and 5mm have been considered at the centre of the bar. As mentioned above, the material property variations

have been made as per power law and five different values of the power law index, that is five different values of 'β' have been considered here. Following table shows all the design variants with various combinations of hole diameter and power law index 'β'.

Bar geometry: 100mm × 10mm × 10mm. Hole position: (50mm, 5mm) from lower left end.

Table 6.5: Various design variants of the problem mentioned in Case II.

Design Variant	Hole Dia (mm)	Power law index (β)
1	3mm	0.25
2		0.50
3		1
4		2
5		5
6	5mm	0.20
7		0.25
8		0.50
9		1
10		2
11		5
12	6mm	1
13	7mm	1
14	8mm	1

Following are the results of maximum deflection and maximum axial stress out of the above simulation using APDL program.

Table 6.6: Maximum deflection and axial stress corresponding to various design variants of Case II.

Design Variant	Hole Dia (mm)	Power law index (β)	Maximum deflection (mm)			Maximum axial stress (MPa)
			X	Y	Vector sum	
II.1	3mm	0.25	0.0140064	0.049028	0.051005	32.9527
II.2		0.50	0.012789	0.049775	0.051392	36.8393
II.3		1	0.010453	0.041743	0.043031	31.652
II.4		2	0.00802	0.029895	0.030952	32.6395
II.5		5	0.005566	0.015703	0.01666	32.7165
II.6	5mm	0.25	0.01525	0.051959	0.054151	37.4362
II.7		0.50	0.01365	0.052361	0.054111	42.0727

II.8		1	0.011323	0.044712	0.046124	39.6843
II.9		2	0.008838	0.032785	0.033955	43.6052
II.10		5	0.006239	0.01792	0.018996	45.0093
II.11	6mm	1	0.011785	0.04604	0.047518	49.3647
II.12	7mm	1	0.01324	0.050354	0.052065	57.5252
II.13	8mm	1	0.014507	0.053396	0.055332	63.408

Above results which have been tabulated can be categorized into two parts. One is the study of influence of power law index of the material gradation on deflection and axial stress generated in the FG beam with a given size of hole at centre of the beam. Next category of result is the impact of hole diameter for a given power law index value of the material gradation on maximum deflection and axial stress. Here one thing is necessary to mention that, for both the above-mentioned categories beam has been subjected to an axial loading with opposite end being fixed. So, though it is being mentioned as a Beam, but it is working in this case, that is, in case II as a Bar.

Two above mentioned categories of results have been presented below by few graphs.

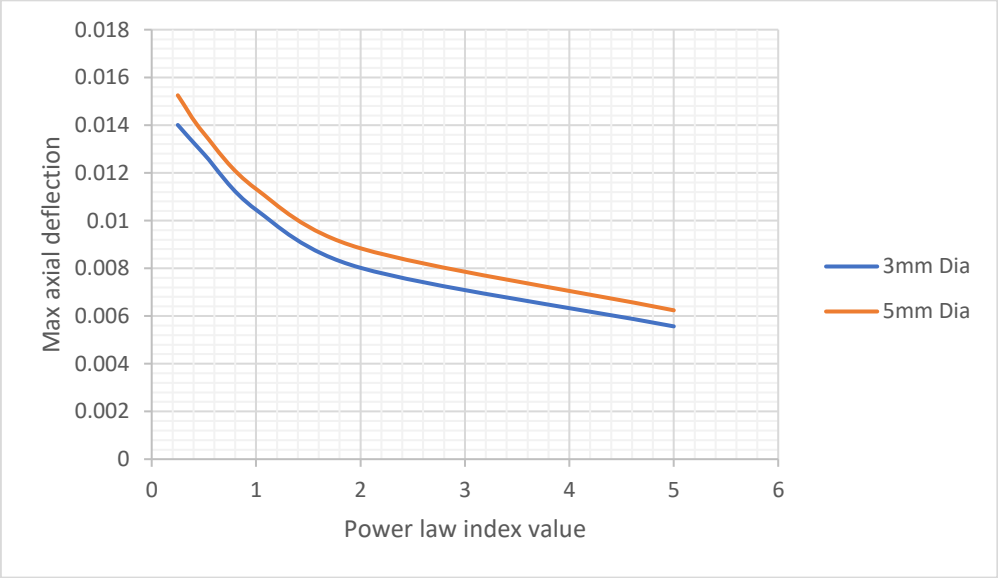

Figure-6.27 Influence of power law indices on maximum axial deflection under axial load of a beam with two types of hole diameters, 3mm and 5mm.

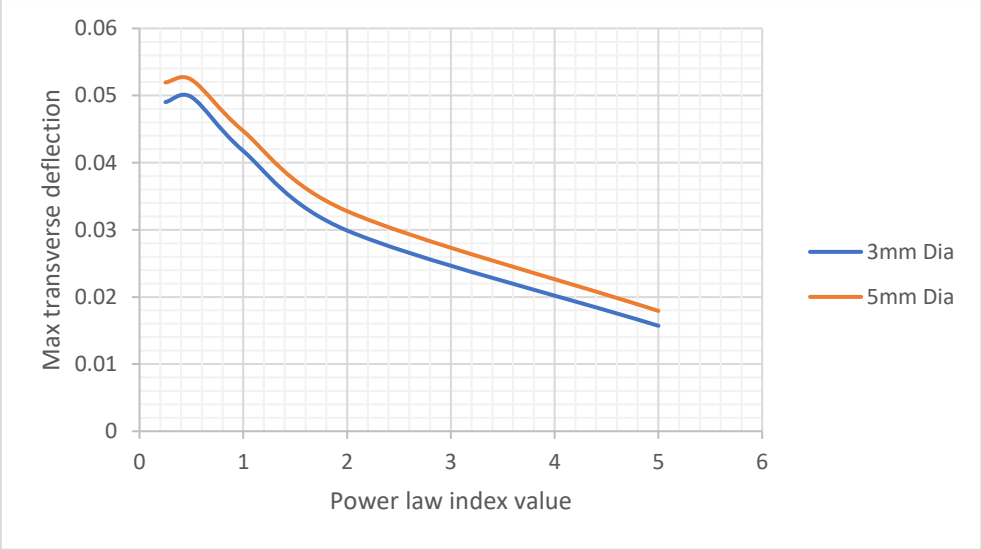

Figure-6.28 Influence of power law indices on maximum transverse deflection under axial load of a beam with two types of hole diameters, 3mm and 5mm.

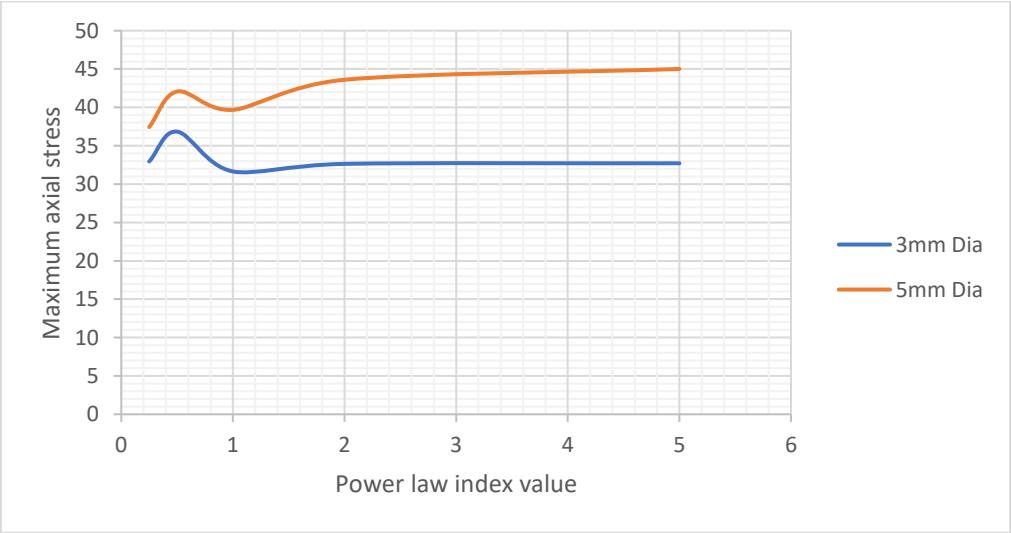

Figure-6.29 Influence of power law indices on maximum normal stress under axial load of a beam with two types of hole diameters, 3mm and 5mm.

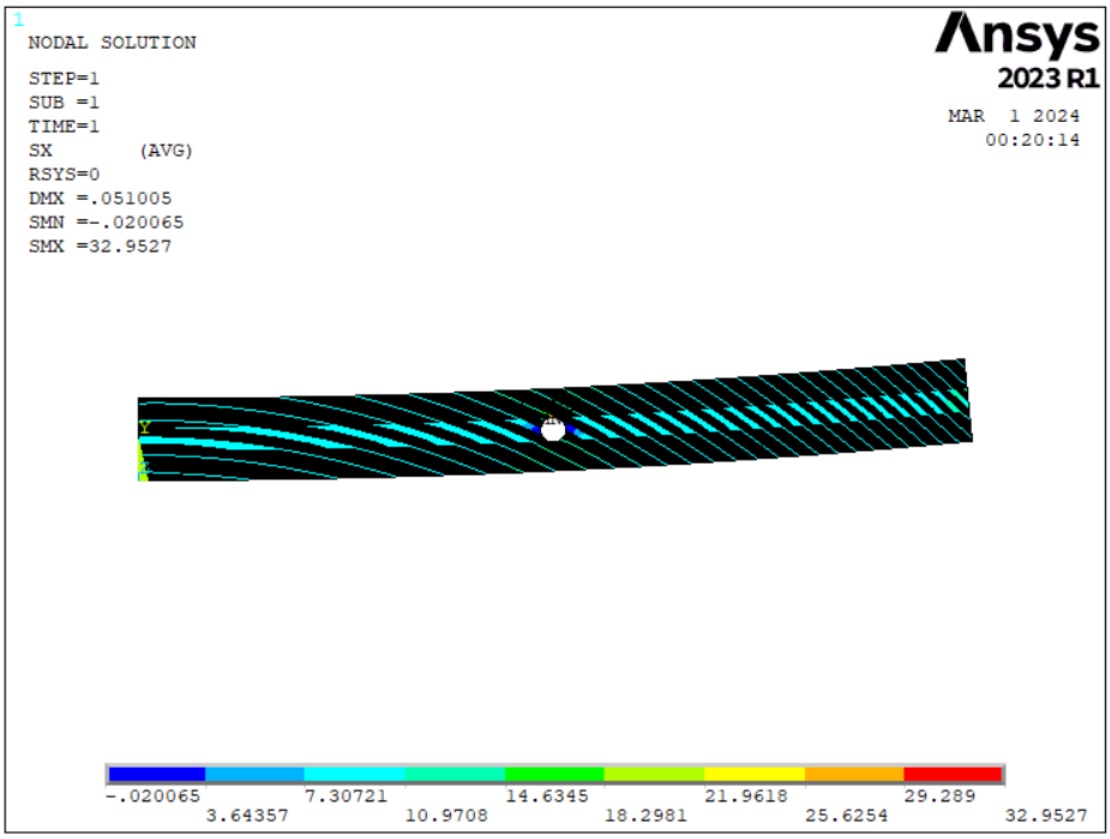

Figure-6.30a Contour plot of deflection as per Design Variant II.1 mentioned in table 6.6.

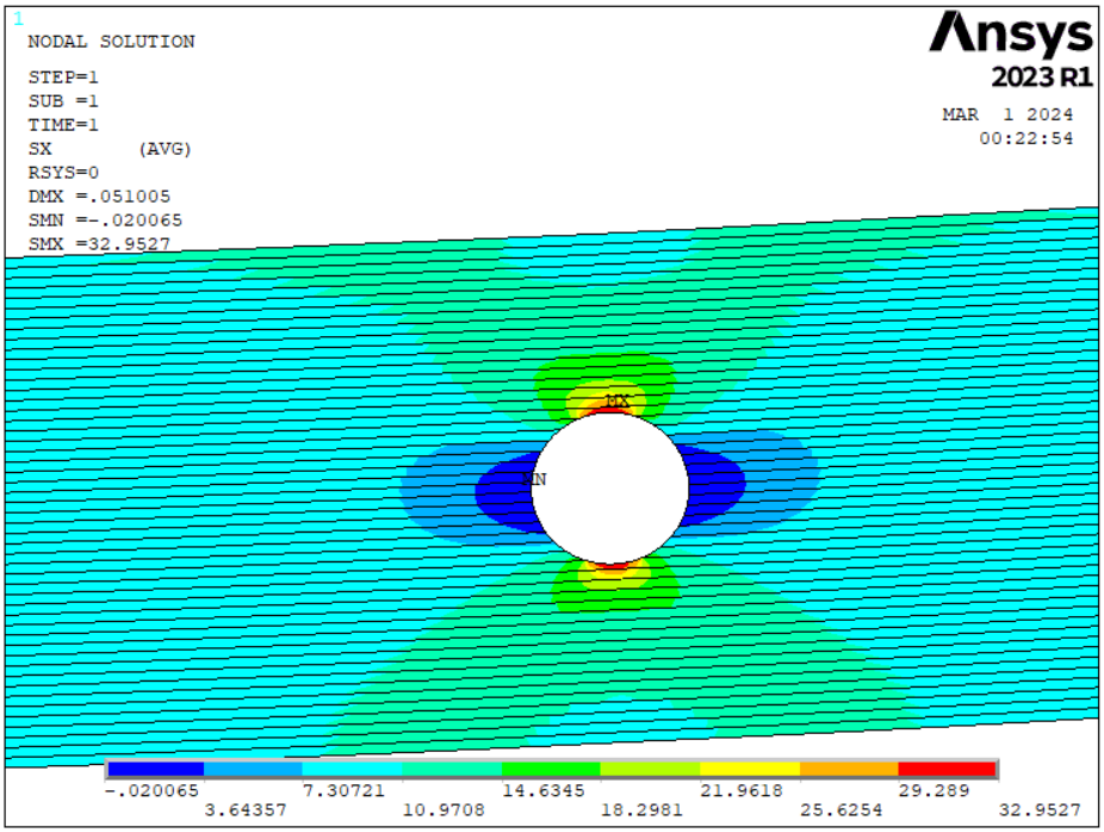

Figure-6.30b Contour plot of axial stress as per Design Variant II.1 mentioned in table 6.6.

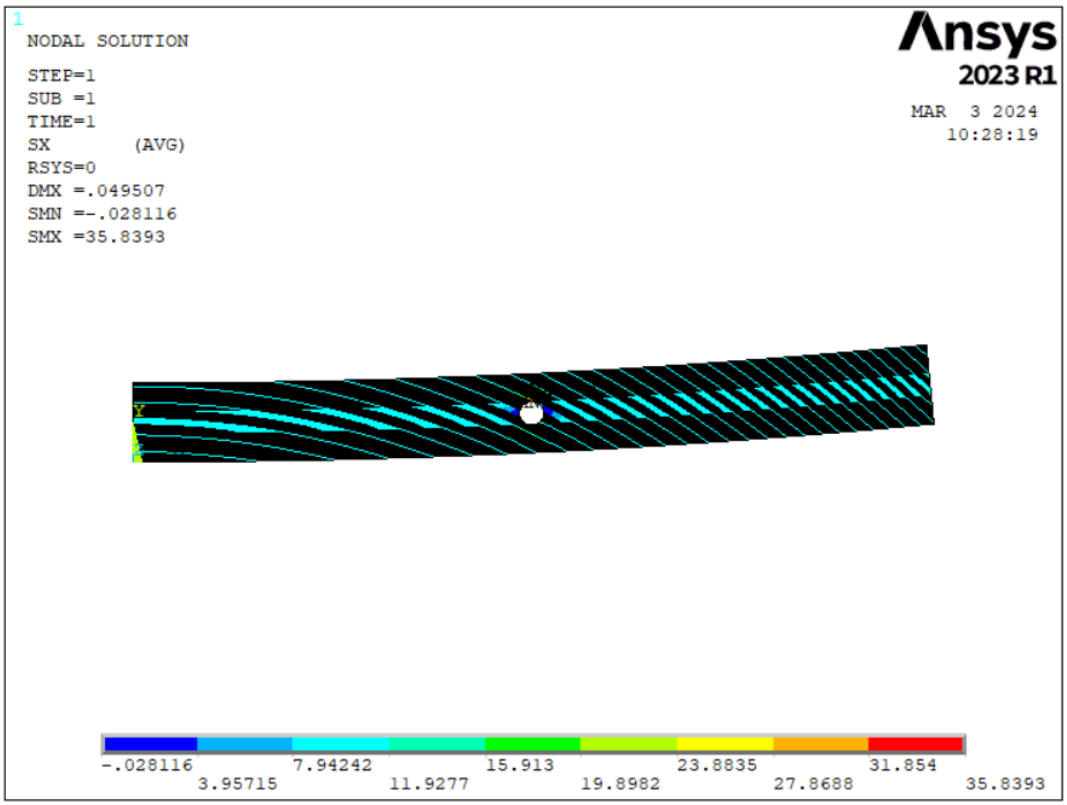

Figure-6.31a Contour plot of deflection as per Design Variant II.2 mentioned in table 6.6.

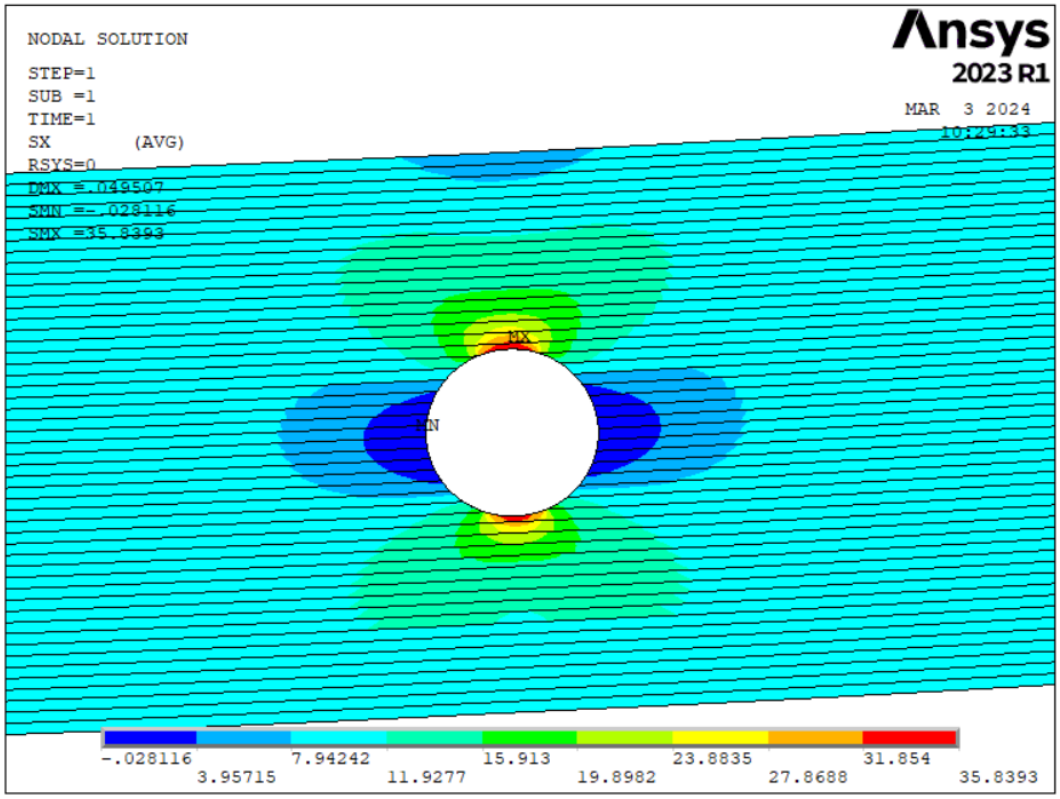

Figure-6.31b Contour plot of axial stress as per Design Variant II.2 mentioned in table 6.6.

Similarly, many other design variants can be simulated with ease and accuracy within minimum time.

6.4 Closure

It is evident from the above discussion that to analyse a beam or bar structure made of a functionally graded material with various types of material gradations, with various types of loadings and with various types of dimensional discontinuities, it is not possible every time to approach mathematically by solving few governing differential equations with help of with few boundary conditions. Derivation of governing differential equations for any structural problem where topology of the structure is complicated, is a very tedious job. For those cases solving problems with finite element method through any well-established FEA software like ANSYS is very helpful. In this work few problems with dimensional discontinuities have been simulated with ANSYS APDL programming. Solving numerical problem with ANSYS APDL programming give immense flexibility to simulate problems with a large number of design variants in minimum time and with maximum accuracy. Before ANSYS APDL programming has been adopted for solving problems of FG bars and beams with various types of holes, it has been validated with results of previously solved FG beam problems analytically using MATLAB programs.

Chapter 7: Conclusions & scope for future work

7.1 Introduction

Because of their innate ability to gradually change their characteristics, functionally graded materials can be highly helpful in situations where interfacial stress concentration causes delamination failure. A sharp change in direction at the contact causes this concentration of stress. Therefore, FGMs can be a very acceptable alternative when joining materials whose characteristics vary greatly in order to produce a composite and avoid failure under temperature or load-related critical circumstances.

Numerous application domains, including as windmill and helicopter blades, cutting tools, turbomachine blades, and beam-like structures, can all be optimized as beams. It is anticipated that using beams with functionally graded qualities will increase their dependability and safety. In a similar vein, graded material tapered beams can be used in applications like as aerospace and biomedicine, where a high stiffness-to-weight ratio is necessary. It follows that in order to maximize the design and development processes, it will undoubtedly be necessary to investigate the behaviour of functionally graded beams. Therefore, in the design synthesis and analysis of such components, the principles of beam modelling to account for deformation and stresses, and incorporating the gradient in characteristics, become extremely important. Consequently, it has been determined that a pertinent and fascinating research field is the examination of the stress and deformation behaviour of FG beams under thermo-mechanical load.

In this research a unified higher order beam theory has been formulated using the principle of virtual work theorem through Hamilton's principle in the frame work of third order shear deformation theory. The resulting equations are coupled in terms of stiffness coefficients along with generalized boundary conditions are obtained. The derived governing equation solved numerically using B-spline collocation method under mechanical and thermal loads both. The grading is assumed to be along the cross-sectional height by considering the variations of elasticity, rigidity modulus, expansion coefficient and thermal conductivity while Poisson's ratio is assumed to be a constant. The formulation has been simplified into a single governing equation by assuming an independent parameter to relate the displacement variables. This method has been suggested by Li [33] for purely mechanical

load, and this work extends the same to thermo-mechanical conditions. The solution to the equations is approached both analytically and numerically to study the behaviour of such beams under purely mechanical, purely thermal and thermo-mechanical loading conditions. The axial and shear stresses and their variations with respect to various parameters have been studied to draw a number of important conclusions that will serve to refine the design and optimization processes of these components. Furthermore, a FEA code has been developed to solve FG beam problems with holes and other types of dimensional discontinuities under various types of loadings and boundary conditions.

7.2 Conclusions

In this section conclusions have been drawn in few categories associated with types of loads and method of analysis, that is mathematically and by software.

7.2.1 Functionally graded beams under mechanical load

a) The grading has a significant impact on the beam's deformation and stress properties. The behavior of the beam adopts the properties of the bottom material as the index value increases.

b) It is noted that the neutral axis moves in the direction of the more elastic material. For a given index value, the neutral axis is the furthest from the geometrical center and decreases asymptotically as β increases.

c) For C-C beams, the impact of a change in material composition is negligible, but for S-SSL beams, it is noticeable.

d) Non-uniform loading can also be solved using this mathematical model.

e) Analysis of FG beams using the unified higher order beam theory, which is the novelty of this present work, shows that the results on defection and axial stresses are very much in compliance with the results determined by Li et al [33] and D. Mahapatra et al [138]. But the value of shear stress differs by more than 4%.

7.2.2 Functionally graded beams under thermo-mechanical load

a) Independent of mechanical loading, the deflection of the FG beam caused by the transverse thermal gradient begins at even the smallest increase in surface

temperature above the surrounding value. This is caused by variations in the component materials' attributes, particularly their expansion coefficient.

b) The directions of the temperature and material property gradients have a significant impact on how the FG beams respond. When the expansion coefficient and temperature gradient are pointing in the same direction, there are increased stresses.
c) There will be significant deflections and stresses if the gradients of heat conductivity, elasticity modulus, and expansion coefficient coincide. For this reason, such circumstances should always be avoided in design.
d) The behavior of the beam is significantly different for linear and non-linear temperature profiles for the same temperature differential between the top and bottom surfaces.
e) The thermal conductivity of the parent materials is critical to the behavior of the FG beam in the event of nonlinear temperature profiles. The temperature profile will be more nonlinear the greater the differential in thermal conductivity. Therefore, even for thick beams, a linear temperature profile may be assumed if the elements' differences in thermal conductivity are negligible.
f) All the above conclusions are based on the analysis of FG beams using the unified higher order beam theory derived in the present work in the environment mechanical as well as thermal load as mentioned before. Now, it has been observed that under thermal load also the results on shear stress differs considerably with the previous work of different authors [27,33,138].

7.2.3 Functionally graded beams with dimensional discontinuities

a) It has been observed that, it is very much difficult and cumbersome to analyze beams and plates with dimensional discontinuities using the formulated higher order beam theory formulations.
b) To overcome the above-mentioned problem few FEA codes have been generated using a FEA commercial software. These codes are capable to generate layered model of FG beams with user input variables like, geometrical parameters, number of layers, material properties of the constituent particles and meshing parameters.
c) Same problems of FG beams as considered for solving with the unified higher order beam theory using a mathematical software have been solved with the newly

developed FEA code. The results of transverse deflections and axial stresses are in good compliance with the analytical results.

d) Few more problems of beams with circular and elliptical holes under axial as well as transverse loadings have been solved.

7.3 Scope for the future

The current study examines the stress and deformation behavior of uniformly tapered FG Timoshenko beams under both thermomechanical and simply mechanical loading scenarios. In order to characterize the precise behavior of FG beams, both exact and approximate solutions have been obtained for the investigation of the reaction to variations in material composition, type of end constraint, temperature profiles, material gradient laws, etc. To expand the work on a larger scale, there are still several unexplored areas. The following can be used to summarize the possible future work:

- In the present study uniform mechanical load is assumed. However, the non-uniform loading may be also considered using the same formulation.
- In the present work FG beams have been investigated only under static loadings. This study can be extended to the analysis of FG beams with various dynamic loadings and buckling analysis along with post buckling analysis.
- The present study is takes into account third order variation of shear deformation (Reddy's theory), however other beam theories may be followed to include other higher order of shear so that precise results for thick stubby beams can be obtained successfully.
- The effect of uniform rotation may be included to extend the studies further to include a number of applications. It is felt that only an extra term of centrifugal force has to be included in the formulation.
- The analysis of pre-twisted beams is a significant research area to study the relevant applications to turbo-machine blade design. The present formulation can be extended to include a pre-twist configuration and their corresponding behavior may be studied.
- The formulation can also be extended to study the behavior of piezo-electric FG beams used in sensors and actuators especially used in aerospace and biomedical areas.

- The analysis of beams under non-rigid support conditions is also an open area that can be explored through small inclusions in the formulations.
- In the present study of unified higher order beam theory has been derived taking into consideration uniform cross-section of been. Varying cross=section along the axis of the beam may be considered.
- The formulation can be extended to explore two dimensional plate analysis as well, that is a separate research area of interest.
- The vibration and dynamic studies pertinent to present formula and extendable to above cases is an interesting research area in the present context.
- The present study is based on computational technique for analysis; it may be validated using experimental procedures.
- The approximation using B-spline collocation can be extended to NURBS-collocation, more sophisticatedly called as isogeometric collocation. The use of Isogeometric formulation in numerical solutions is a trending topic for engineering research community.
- A FEA code has been developed in the present work to analyze FG beams with various holes incorporated. Only two-dimensional geometry of beam can be developed by this code. It can be modified to build three-dimensional FG beams and plates with incorporation of more varieties of holes in addition to circular and elliptical holes.

In addition to the above, a number of application areas specific to the need of engineering may be explored for design with added reliability and safety.

References

[1] Giannakopoulos, A. E., & Suresh, S. (1997). Indentation of solids with gradients in elastic properties: Part I. Point force. International Journal of Solids and Structures, 34(19), 2357-2392.

[2] Giannakopoulos, A. E., & Suresh, S. (1997). Indentation of solids with gradients in elastic properties: Part II. Axisymmetric indentors. International Journal of Solids and Structures, 34(19), 2393-2428.

[3] Suresh, S., & Mortensen, A. (1998). Fundamentals of Functionally Graded Materials (The Institute of Materials, IOM Communications Ltd., London).

[4] Miyamoto, Y., Kaysser, W. A., Rabin, B. H., Kawasaki, A., & Ford, R. G. (Eds.). (2013). Functionally graded materials: design, processing and applications (Vol. 5). Springer Science & Business Media.

[5] Nakamura, T., Wang, T., & Sampath, S. (2000). Determination of properties of graded materials by inverse analysis and instrumented indentation. Acta Materialia, 48(17), 4293-4306.

[6] Kieback, B., Neubrand, A., & Riedel, H. (2003). Processing techniques for functionally graded materials. Materials Science and Engineering: A, 362(1-2), 81-106.

[7] Bhattacharyya, M., Kapuria, S., & Kumar, A. N. (2007). On the stress to strain transfer ratio and elastic deflection behavior for Al/SiC functionally graded material. Mechanics of Advanced Materials and Structures, 14(4), 295-302.

[8] Mahamood, R. M., Akinlabi, E. T., Shukla, M., & Pityana, S. L. (2012). Functionally graded material: an overview.

[9] Hayun, S., Paris, V., Mitrani, R., Kalabukhov, S., Dariel, M. P., Zaretsky, E., & Frage, N. (2012). Microstructure and mechanical properties of silicon carbide processed by Spark Plasma Sintering (SPS). Ceramics International, 38(8), 6335-6340.

[10] Mahamood, R. M., Akinlabi, E. T., Shukla, M., & Pityana, S. L. (2012). Functionally graded material: an overview.

[11] Udupa, G., Rao, S. S., & Gangadharan, K. V. (2014). Functionally graded composite materials: an overview. Procedia Materials Science, 5, 1291-1299.

[12] Birman, V. (2014). Functionally graded materials and structures. Encyclopedia of thermal stresses, 1858-1865.

[13] Reddy, J. (2000). Analysis of functionally graded plates. International Journal for numerical methods in engineering, 47(1-3), 663-684.

[14] Wang, C. M., Reddy, J. N., & Lee, K. H. (Eds.). (2000). Shear deformable beams and plates: Relationships with classical solutions. Elsevier.

[15] Sankar, B. V. (2001). An elasticity solution for functionally graded beams. Composites Science and Technology, 61(5), 689-696.

[16] Lee, B. K., Lee, J. K., Lee, T. E., & Kim, S. G. (2002). Free vibrations of tapered beams with general boundary condition. KSCE Journal of Civil Engineering, 6, 283-288.

[17] Chakraborty, A., Gopalakrishnan, S., & Reddy, J. (2003). A new beam finite element for the analysis of functionally graded materials. International journal of mechanical sciences, 45(3), 519-539.

[18] Zhu, H., & Sankar, B. V. (2004). A combined Fourier series–Galerkin method for the analysis of functionally graded beams. J. Appl. Mech., 71(3), 421-424.

[19] Tahani, M., Torabizadeh, M.A. and Fereidoon, A., 2006. Nonlinear analysis of functionally graded beams. Journal of Achievements in Materials and Manufacturing Engineering, 18(1-2), pp.315-318.

[20] Tahani, M., & Mirzababaee, S. M. (2007, July). ANALYTICAL SOLUTION FOR NONLINEAR BENDING OF FG PLATES BY A LAYERWISE THEORY. In 16th International Conference on Composite Materials (ICCM16).

[21] Aydogdu, M., & Taskin, V. (2007). Free vibration analysis of functionally graded beams with simply supported edges. Materials & design, 28(5), 1651-1656.

[22] Zhong, Z., & Yu, T. (2007). Analytical solution of a cantilever functionally graded beam. Composites Science and Technology, 67(3-4), 481-488.

[23] Banerjee, A., Bhattacharya, B., & Mallik, A. K. (2008). Large deflection of cantilever beams with geometric non-linearity: Analytical and numerical approaches. International Journal of Non-Linear Mechanics, 43(5), 366-376.

[24] Benatta, M. A., Mechab, I., Tounsi, A., & Bedia, E. A. (2008). Static analysis of functionally graded short beams including warping and shear deformation effects. Computational Materials Science, 44(2), 765-773.

[25] Kadoli, R., Akhtar, K., & Ganesan, N. (2008). Static analysis of functionally graded beams using higher order shear deformation theory. Applied mathematical modelling, 32(12), 2509-2525.

[26] Kapuria, S., Bhattacharyya, M., & Kumar, A. N. (2008). Bending and free vibration response of layered functionally graded beams: a theoretical model and its experimental validation. Composite Structures, 82(3), 390-402.

[27] Li, X. F. (2008). A unified approach for analyzing static and dynamic behaviors of functionally graded Timoshenko and Euler–Bernoulli beams. Journal of Sound and vibration, 318(4-5), 1210-1229.

[28] Sina, S. A., Navazi, H. M., & Haddadpour, H. (2009). An analytical method for free vibration analysis of functionally graded beams. Materials & Design, 30(3), 741-747

[29] Hsu, M. H. (2009). Vibration analysis of non-uniform beams resting on elastic foundations using the spline collocation method. Journal of Applied Science and Engineering, 12(2), 113-122.

[30] Hsu, M. H. (2009). Vibration analysis of pre-twisted beams using the spline collocation method. Journal of Marine Science and Technology, 17(2), 4.106-115

[31] Giunta, G., Belouettar, S., & Carrera, E. (2010). Analysis of FGM beams by means of classical and advanced theories. Mechanics of Advanced Materials and Structures, 17(8), 622-635.

[32] Huang, Y., & Li, X. F. (2010). A new approach for free vibration of axially functionally graded beams with non-uniform cross-section. Journal of sound and vibration, 329(11), 2291-2303.

[33] Li, X.F., Wang, B.L. and Han, J.C., 2010. A higher-order theory for static and dynamic analyses of functionally graded beams. Archive of Applied Mechanics, 80, pp.1197-1212

[34] Mahi, A., Bedia, E. A., Tounsi, A., & Mechab, I. (2010). An analytical method for temperature-dependent free vibration analysis of functionally graded beams with general boundary conditions. Composite structures, 92(8), 1877-1887.

[35] Rahimi, G. H., & Davoudinik, A. R. (2010). Large deflection of functionally graded cantilever flexible beam with geometric non-linearity: Analytical and numerical approaches.

[36] Şimşek, M. (2010). Fundamental frequency analysis of functionally graded beams by using different higher-order beam theories. Nuclear Engineering and Design, 240(4), 697-705.

[37] Yaghoobi, H., & Fereidoon, A. (2010). Influence of neutral surface position on deflection of functionally graded beam under uniformly distributed load. World Applied Sciences Journal, 10(3), 337-341.

[38] Akhras, G., & Li, W. (2011). Stability and free vibration analysis of thick piezoelectric composite plates using spline finite strip method. International journal of mechanical sciences, 53(8), 575-584.

[39] Davoodinik, A. R., & Rahimi, G. H. (2011). Large deflection of flexible tapered functionally graded beam. Acta Mechanica Sinica, 27, 767-777.

[40] Hein, H., & Feklistova, L. (2011). Free vibrations of non-uniform and axially functionally graded beams using Haar wavelets. Engineering Structures, 33(12), 3696-3701.

[41] Mahi, A., Bedia, E. A., Tounsi, A., & Mechab, I. (2011). An analytical method for temperature-dependent free vibration analysis of functionally graded beams with general boundary conditions. Composite structures, 92(8), 1877-1887.

[42] Mohanty, S. C., Dash, R. R., & Rout, T. (2011). Parametric instability of a functionally graded Timoshenko beam on Winkler's elastic foundation. Nuclear Engineering and Design, 241(8), 2698-2715.

[43] Mohanty, S. C., Dash, R. R., & Rout, T. (2011). Parametric instability of a functionally graded Timoshenko beam on Winkler's elastic foundation. Nuclear Engineering and Design, 241(8), 2698-2715.

[44] Reddy, J. (2011). Microstructure-dependent couple stress theories of functionally graded beams. Journal of the Mechanics and Physics of Solids, 59(11), 2382-2399.

[45] Reddy, J. (2011). Microstructure-dependent couple stress theories of functionally graded beams. Journal of the Mechanics and Physics of Solids, 59(11), 2382-2399.

[46] Shahba, A., Attarnejad, R., Marvi, M. T., & Hajilar, S. (2011). Free vibration and stability analysis of axially functionally graded tapered Timoshenko beams with classical and non-classical boundary conditions. Composites Part B: Engineering, 42(4), 801-808.

[47] Shahba, A., & Rajasekaran, S. (2012). Free vibration and stability of tapered Euler–Bernoulli beams made of axially functionally graded materials. Applied Mathematical Modelling, 36(7), 3094-3111.

[48] Ma, L. S., & Lee, D. W. (2012). Exact solutions for nonlinear static responses of a shear deformable FGM beam. European Journal of Mechanics - A/Solids 31, 13–20.

[49] Mohanty, S. C., Dash, R. R., & Rout, T. (2012). Static and dynamic stability analysis of a functionally graded Timoshenko beam. International Journal of Structural Stability and Dynamics, 12(04), 1250025.

[50] Loja, M. A. R., Soares, C. M., & Barbosa, J. I. (2013). Analysis of functionally graded sandwich plate structures with piezoelectric skins, using B-spline finite strip method. Composite structures, 96, 606-615.

[51] Nguyen, D. K. (2013). Large displacement response of tapered cantilever beams made of axially functionally graded material. Composites Part B: Engineering, 55, 298-305.

[52] Rajasekaran, S. (2013). Buckling and vibration of axially functionally graded nonuniform beams using differential transformation based dynamic stiffness approach. Meccanica, 48, 1053-1070.

[53] Rajasekaran, S. (2013). Free vibration of centrifugally stiffened axially functionally graded tapered Timoshenko beams using differential transformation and quadrature methods. Applied Mathematical Modelling, 37(6), 4440-4463.

[54] Shahba, A., Attarnejad, R., & Zarrinzadeh, H. (2013). Free vibration analysis of centrifugally stiffened tapered functionally graded beams. Mechanics of Advanced Materials and Structures, 20(5), 331-338.

[55] Wattanasakulpong, N., & Ungbhakorn, V. (2013). Analytical solutions for bending, buckling and vibration responses of carbon nanotube-reinforced composite beams resting on elastic foundation. Computational Materials Science, 71, 201-208.

[56] Yaghoobi, H., & Torabi, M. (2013). An analytical approach to large amplitude vibration and post-buckling of functionally graded beams rest on non-linear elastic foundation. Journal of Theoretical and Applied Mechanics, 51(1), 39-52.

[57] Zhang, D. G. (2013). Nonlinear bending analysis of FGM beams based on physical neutral surface and high order shear deformation theory. Composite Structures, 100, 121-126.

[58] Mitra, A., & Virendra, M. (2014). Axially functionally graded tapered beams under transverse harmonic excitation. In 59th congress of the Indian Society of Theoretical and Applied Mechanics (ISTAM) (pp. 1-7).

[59] Nguyen, D. K. (2014). Large displacement behaviour of tapered cantilever Euler–Bernoulli beams made of functionally graded material. Applied Mathematics and Computation, 237, 340-355.

[60] Nguyen, D. K., & Gan, B. S. (2014). Large deflections of tapered functionally graded beams subjected to end forces. Applied Mathematical Modelling, 38(11-12), 3054-3066.

[61] Nguyen, N. T., Kim, N. I., Cho, I., Phung, Q. T., & Lee, J. (2014). Static analysis of transversely or axially functionally graded tapered beams. Materials Research Innovations, 18(sup2), S2-260.

[62] Çallıoğlu, H., Sayer, M., & Demir, E. (2015). Elastic–plastic stress analysis of rotating functionally graded discs. Thin-Walled Structures, 94, 38-44.

[63] Reali, A., & Gomez, H. (2015). An isogeometric collocation approach for Bernoulli–Euler beams and Kirchhoff plates. Computer Methods in Applied Mechanics and Engineering, 284, 623-636.

[64] Fang, J. S., & Zhou, D. (2016). Free vibration analysis of rotating axially functionally graded tapered Timoshenko beams. International Journal of Structural Stability and Dynamics, 16(05), 1550007.

[65] Lohar, H., Mitra, A., & Sahoo, S. (2016, September). Free vibration analysis of axially functionally graded linearly taper beam on elastic foundation. In IOP Conference Series: Materials Science and Engineering (Vol. 149, No. 1, p. 012130). IOP Publishing.

[66] Nayak, P., & Saha, K. N. (2017). Analysis of statically indeterminate non-uniform bar problem in post elastic domain by an iterative variational method. Applied Mathematical Modelling, 51, 86-108.

[67] Ghayesh, M. H., & Farokhi, H. (2018). Bending and vibration analyses of coupled axially functionally graded tapered beams. Nonlinear Dynamics, 91, 17-28.

[68] Lakshman, S., Subhashis, S., Kashinath, S., & Shubhankar, B. (2018). Limit elastic speeds of functionally graded annular disks. FME Transactions, 46(4), 603-611.

[69] Lieu, Q. X., Lee, S., Kang, J., & Lee, J. (2018). Bending and free vibration analyses of in-plane bi-directional functionally graded plates with variable thickness using isogeometric analysis. Composite Structures, 192, 434-451.

[70] Mahapatra, D., Sanyal, S. and Bhowmick, S., 2019. An approximate solution of functionally Graded Timoshenko beam using B-spline collocation method. Journal of Solid Mechanics, 11(2), pp.297-310.

[71] Lieu, Q. X., & Lee, J. (2019). A reliability-based optimization approach for material and thickness composition of multidirectional functionally graded plates. Composites Part B: Engineering, 164, 599-611.

[72] Lieu, Q. X., & Lee, J. (2019). An isogeometric multimesh design approach for size and shape optimization of multidirectional functionally graded plates. Computer Methods in Applied Mechanics and Engineering, 343, 407-437.

[73] Nam, V. H., Vinh, P. V., Chinh, N. V., Thom, D. V., & Hong, T. T. (2019). A new beam model for simulation of the mechanical behaviour of variable

thickness functionally graded material beams based on modified first order shear deformation theory. Materials, 12(3), 404.

[74] Chaabani, H., Mesmoudi, S., Boutahar, L., & Bikri, K. E. (2022). Buckling of porous FG sandwich plates subjected to various non-uniform compressions and resting on Winkler–Pasternak elastic foundation using a finite element model based on the high-order shear deformation theory. Acta Mechanica, 233(12), 5359-5376.

[75] Chaabani, H., Mesmoudi, S., Boutahar, L., & El Bikri, K. (2022). A high-order continuation for bifurcation analysis of functionally graded material sandwich plates. Acta Mechanica, 233(6), 2125-2147.

[76] Mesmoudi, S., Askour, O., Rammane, M., Bourihane, O., Tri, A., & Braikat, B. (2022). Spectral Chebyshev method coupled with a high order continuation for nonlinear bending and buckling analysis of functionally graded sandwich beams. International Journal for Numerical Methods in Engineering, 123(24), 6111-6126.

[77] Nouri, Z., Sarrami-Foroushani, S., Azhari, F., & Azhari, M. (2022). Application of Carrera unified formulation in conjunction with finite strip method in static and stability analysis of functionally graded plates. Mechanics of Advanced Materials and Structures, 29(2), 250-266.

[78] Zahari, K., Hilali, Y., Mesmoudi, S., & Bourihane, O. (2022, December). Review and comparison of thin and thick FGM plate theories using a unified buckling formulation. In Structures (Vol. 46, pp. 1545-1560). Elsevier.

[79] Chaabani, H., Mesmoudi, S., Boutahar, L., & El Bikri, K. (2023). A high-order finite element continuation for buckling analysis of porous FGM plates. Engineering Structures, 279, 115597.

[80] Katunin, A., Wachla, D., Santos, P., & Reis, P. N. (2023). Fatigue life assessment of hybrid bio-composites based on self-heating temperature. Composite Structures, 304, 116456.

[81] Mesmoudi, S., Hilali, Y., Rammane, M., Askour, O., & Bourihane, O. (2023). Highly efficient mesh-free approach to simulate the non-linear bending analysis of fg porous beams and sandwich beams with fg face sheets. Thin-Walled Structures, 185, 110614.

[82] Praveen, G. N., & Reddy, J. N. (1998). Nonlinear transient thermoelastic analysis of functionally graded ceramic-metal plates. International journal of solids and structures, 35(33), 4457-4476.

[83] Reddy, J. N., & Chin, C. D. (1998). Thermomechanical analysis of functionally graded cylinders and plates. Journal of thermal Stresses, 21(6), 593-626.

[84] Sankar, B. V., & Tzeng, J. T. (2002). Thermal stresses in functionally graded beams. AIAA journal, 40(6), 1228-1232.

[85] Shen, H. S. (2002). Nonlinear bending response of functionally graded plates subjected to transverse loads and in thermal environments. International Journal of Mechanical Sciences, 44(3), 561-584.

[86] Sundararajan, N., Prakash, T., & Ganapathi, M. (2005). Nonlinear free flexural vibrations of functionally graded rectangular and skew plates under thermal environments. Finite Elements in Analysis and Design, 42(2), 152-168.

[87] Li, S. R., Zhang, J. H., & Zhao, Y. G. (2006). Thermal post-buckling of functionally graded material Timoshenko beams. Applied Mathematics and Mechanics, 27(6), 803-810.

[88] Tahani, M., & Mirzababaee, S. M. (2009). Non-linear analysis of functionally graded plates in cylindrical bending under thermomechanical loadings based on a layerwise theory. European Journal of Mechanics-A/Solids, 28(2), 248-256.

[89] Kiani, Y., & Eslami, M. R. (2010). Thermal buckling analysis of functionally graded material beams. International Journal of Mechanics and Materials in Design, 6, 229-238.

[90] Ma, L. S., & Lee, D. W. (2011). A further discussion of nonlinear mechanical behavior for FGM beams under in-plane thermal loading. Composite Structures, 93(2), 831-842.

[91] Fallah, A., & Aghdam, M. M. (2012). Thermo-mechanical buckling and nonlinear free vibration analysis of functionally graded beams on nonlinear elastic foundation. Composites Part B: Engineering, 43(3), 1523-1530.

[92] Fu, Y., Wang, J., & Mao, Y. (2012). Nonlinear analysis of buckling, free vibration and dynamic stability for the piezoelectric functionally graded beams in thermal environment. Applied Mathematical Modelling, 36(9), 4324-4340.

[93] Zhang, D. G., & Zhou, H. M. (2014). Nonlinear bending and thermal post-buckling analysis of FGM beams resting on nonlinear elastic foundations. CMES, Tech Science, 100(3), 201-222.

[94] Kiani, Y. A. S. S. E. R., & Eslami, M. R. (2014). Thermomechanical buckling of temperature-dependent FGM beams. Latin American Journal of Solids and Structures, 10, 223-246.

[95] Niknam, H., Fallah, A., & Aghdam, M. M. (2014). Nonlinear bending of functionally graded tapered beams subjected to thermal and mechanical loading. International journal of Non-linear Mechanics, 65, 141-147.

[96] Paul, A., & Das, D. (2016). Non-linear thermal post-buckling analysis of FGM Timoshenko beam under non-uniform temperature rise across thickness. Engineering science and technology, an international journal, 19(3), 1608-1625.

[97] Sun, Y., Li, S. R., & Batra, R. C. (2016). Thermal buckling and post-buckling of FGM Timoshenko beams on nonlinear elastic foundation. Journal of thermal stresses, 39(1), 11-26.

[98] Nayak, P., & Saha, K. (2016). Elastic limit angular speed of solid and annular disks under thermomechanical loading. International Journal of Engineering, Science and Technology, 8(2), 30-45.

[99] Paul, A., & Das, D. (2017). A study on non-linear post-buckling behavior of tapered Timoshenko beam made of functionally graded material under in-plane thermal loadings. The Journal of Strain Analysis for Engineering Design, 52(1), 45-56.

[100] Nasirzadeh, R., Behjat, B., Kharazi, M., & Khabazaghdam, A. (2017). Investigation of boundary condition effects on the stability of FGP beams in thermal environment. Journal of Theoretical and Applied Mechanics, 55.

[101] Nguyen, D. K., & Bui, V. T. (2017). Dynamic analysis of functionally graded Timoshenko beams in thermal environment using a higher-order hierarchical beam element. Mathematical Problems in Engineering, 2017.

[102] Majumdar, A., & Das, D. (2018). A study on thermal buckling load of clamped functionally graded beams under linear and nonlinear thermal gradient across thickness. Proceedings of the Institution of Mechanical Engineers, Part L: Journal of Materials: Design and Applications, 232(9), 769-784.

[103] Paul, A., & Das, D. (2019). Free vibration behavior of tapered functionally graded material beam in thermal environment considering geometric non-linearity, shear deformability and temperature-dependent thermal conductivity. Proceedings of the Institution of Mechanical Engineers, Part L: Journal of Materials: Design and Applications, 233(7), 1429-1448.

[104] Nayak, P., Bhowmick, S., & Saha, K. N. (2020). Elasto-plastic analysis of thermo-mechanically loaded functionally graded disks by an iterative variational method. Engineering Science and Technology, an International Journal, 23(1), 42-64.

[105] Mahapatra, D., Sanyal, S., & Bhowmick, S. (2020). An Investigation of Stress and Deformation Behavior of Functionally Graded Timoshenko Beams subjected to Thermo-Mechanical Load. Mechanics Of Advanced Composite Structures, 7(1), 157-176.

[106]Nayak, P., & Saha, K. (2020, October). Dynamic Analysis of Thermo-Mechanically Loaded Functionally Graded Disks by an Iterative Variational Method. In Proceedings of the 6th National Symposium on Rotor Dynamics: NSRD 2019 (pp. 569-577). Singapore: Springer Singapore.

[107]Javaheri, R., & Eslami, M. R. (2020). Thermal buckling of functionally graded plates based on higher order theory. Journal of thermal stresses, 25(7), 603-625.

[108]Javaheri, R., & Eslami, M. (2020). Thermal buckling of functionally graded plates. AIAA journal, 40(1), 162-169.

[109]Chawla, T. C., Leaf, G., & Chen, W. (1975). A collocation method using B-splines for one-dimensional heat or mass-transfer-controlled moving boundary problems. Nuclear Engineering and Design, 35(2), 163-180.

[110]Chawla, T. C., & Chan, S. H. (1979). Solution of radiation-conduction problems with collocation method using B-splines as approximating functions. International Journal of Heat and Mass Transfer, 22(12), 1657-1667.

[111]G. Fairweather, D. Meade, A survey of spline collocation methods for the numerical solution of differential equations. Mathematics for large scale computing, New York, 1989, pp. 297–341.

[112]Patlashenko, I., & Weller, T. (1993). Cubic B-spline collocation method for nonlinear static analysis of panels under mechanical and thermal loadings. Computers & structures, 49(1), 89-96.

[113]Patlashenko, I., & Weller, T. (1995). Two-dimensional spline collocation method for nonlinear analysis of laminated panels. Computers & structures, 57(1), 131-139.

[114]Mizusawa, T., & Kito, H. (1995). Vibration of cross-ply laminated cylindrical panels by the spline strip method. Computers & structures, 57(2), 253-265.

[115]Abrate, S. (1995). Vibration of non-uniform rods and beams. Journal of sound and vibration, 185(4), 703-716.

[116]Bert, C. W., & Sheu, Y. (1996). Static analyses of beams and plates by spline collocation method. Journal of engineering mechanics, 122(4), 375-378.

[117]Mizusawa, T. (1996). Vibration of thick laminated cylindrical panels by the spline strip method. Computers & structures, 61(3), 441-457.

[118]Sun, W. (2001). B-spline collocation methods for elasticity problems. Scientific Computing and Applications, 2001, 133-141.

[119]Lehmann, T. M., Gonner, C., & Spitzer, K. (2001). Addendum: B-spline interpolation in medical image processing. IEEE transactions on medical imaging, 20(7), 660-665.

[120]Botella, O. (2002). On a collocation B-spline method for the solution of the Navier–Stokes equations. Computers & fluids, 31(4-7), 397-420.

[121]Guo, W. (2004). Functional data analysis in longitudinal settings using smoothing splines. Statistical methods in medical research, 13(1), 49-62.

[122]Unser, M., & Blu, T. (2005). Generalized smoothing splines and the optimal discretization of the Wiener filter. IEEE Transactions on Signal Processing, 53(6), 2146-2159.

[123]Johnson, R. W. (2005). Higher order B-spline collocation at the Greville abscissae. Applied Numerical Mathematics, 52(1), 63-75.

[124]Wu, L. Y., Chung, L. L., & Huang, H. H. (2008). Radial spline collocation method for static analysis of beams. Applied mathematics and computation, 201(1-2), 184-199.

[125]Kadalbajoo, M. K., & Yadaw, A. S. (2008). B-Spline collocation method for a two-parameter singularly perturbed convection–diffusion boundary value problems. Applied Mathematics and Computation, 201(1-2), 504-513.

[126]Hsu, M. H. (2009). Vibration analysis of non-uniform beams resting on elastic foundations using the spline collocation method. Journal of Applied Science and Engineering, 12(2), 113-122.

[127]Hsu, M. H. (2009). Vibration analysis of pre-twisted beams using the spline collocation method. Journal of Marine Science and Technology, 17(2), 4.

[128]Auricchio, F., Da Veiga, L. B., Hughes, T. J. R., Reali, A., & Sangalli, G. (2010). Isogeometric collocation methods. Mathematical Models and Methods in Applied Sciences, 20(11), 2075-2107.

[129]Valenzuela, O., & Pasadas, M. (2011). Fuzzy data approximation using smoothing cubic splines: Similarity and error analysis. Applied mathematical modelling, 35(5), 2122-2144.

[130]Kadalbajoo, M. K., & Yadaw, A. S. (2011). Finite difference, finite element and b-spline collocation methods applied to two parameter singularly perturbed boundary value problems1. Jnaiam, 5, 163-180.

[131]Rashidinia, J., & Sharifi, S. (2012). Retraction Note: Survey of B-spline functions to approximate the solution of mathematical problems. Mathematical Sciences, 6, 1-8.

[132]Aguilera, A. M., & Aguilera-Morillo, M. C. (2013). Penalized PCA approaches for B-spline expansions of smooth functional data. Applied Mathematics and Computation, 219(14), 7805-7819.

[133]Aguilera, A. M., & Aguilera-Morillo, M. C. (2013). Comparative study of different B-spline approaches for functional data. Mathematical and Computer Modelling, 58(7-8), 1568-1579.

[134]Zakaria, R., Wahab, A., & Gobithaasan, R. U. (2014). Fuzzy B-Spline surface modeling. Journal of Applied Mathematics, 2014. pp 1-8

[135]Provatidis, C. (2014). Finite element analysis of structures using-continuous cubic B-splines or equivalent Hermite elements. Journal of Structures, 2014.

[136]Sun, L., Pan, Y., & Gu, W. (2014). Data mining using regularized adaptive B-splines regression with penalization for multi-regime traffic stream models. Journal of Advanced Transportation, 48(7), 876-890.

[137]Provatidis, C. (2017). B-splines collocation for plate bending eigenanalysis. Journal of Mechanics of Materials and Structures, 12(4), 353-371.

[138]Mahapatra D., Sanyal S., Bhowmick, S., 2019. B-spline collocation-based approximations for structural problems of fourth order. UPB Scientific Bulletin, Series-D; 81(4), pp.213-228

[139]Bhandari, M., & Purohit, K. (2014). Static response of functionally graded material plate under transverse load for varying aspect ratio. International Journal of Metals, 2014.

[140]Liu, W., & Cheng, X. (2018). A systematic approach based on voxel modelling and APDL analysis for Functional-Graded-Material objects. Procedia CIRP, 78, 138-143.

[141]Hassan, A. H. A., & Kurgan, N. (2022). Modeling Functionally Graded Materials in ANSYS APDL. NATURAL AND ENGINEERING SCIENCES, 107.

[142]Shehab, M. B., Taima, M. S., Sayed, H., & El-Sayed, T. A. (2023). An Investigation into the Free Vibration of Intact and Cracked FGM Plates. Journal of Failure Analysis and Prevention, 23(5), 2142-2168.

[143]Cottrell, J. A., Hughes, T. J., & Bazilevs, Y. (2009). Isogeometric analysis: toward integration of CAD and FEA. John Wiley & Sons.

[144]Suresh S., Mortensen A., 1998. Fundamentals of functionally graded materials. London: IOM Communications Ltd.

[145]Miyamoto, Y. (Ed.), 1999. Functionally graded materials: design, processing, and applications, Materials technology series. Kluwer Academic Publishers, Boston.

[146]Cottrell, J.A., Hughes, T.J.R., Bazilevs, Y., 2009. Isogeometric analysis: toward integration of CAD and FEA. Wiley, Chichester.

[147]J. M. Gere, B. J. Goodno, Mechanics of materials, 7th ed., Cengage Learning, Newyork, 2009.

[148]De Boor C. , A practical guide to splines, Springer-Verlag, Newyork USA 1978

[149]Richard Budynas, Keith Nisbett, Shigley's Mechanical Engineering Design, McGraw-Hill Education; 10th edition (16 February 2014)

[150]Rogers D. F., An introduction to NURBS with historical perspective, Morgan Kauffman publisher, San Fransisco, USA, 2001

[151]Wallerstein, D.V., A Variational Approach to Structural Analysis. John Wiley & Sons; 2002

[152]Dym, C.L., Shames, I.H., Solid mechanics: a variational approach, Augmented edition. ed. Springer Science Business Media, New York.2013

[153]Carrera, E., Giunta, G. and Petrolo, M., 2011. Beam structures: classical and advanced theories. John Wiley & Sons.

[154]Shen, Hui-Shen. “Functionally graded materials: nonlinear analysis of plates and shells” CRC Press 2009

[155]Andreas Öchsner. “Classical Beam Theories of Structural Mechanics” Springer 2021

Mechanics of Advanced Composite Structures 11 (2024) 159 - 176

Semnan University

Mechanics of Advanced Composite Structures

Journal homepage: http://MACS.Journals.semnan.ac.ir

Higher Order Approximations for Bending of FG Beams Using B-Spline Collocation Technique

A. Biswas [a], D. Mahapatra [b*], S. C. Mondal [c], S. Sarkar [c]

[a] *Department of Mechanical Engineering, Heritage Institute of Technology, Kolkata, 700107, India*
[b] *College of Food Technology, IGKV, Raipur, 492012, India*
[c] *Department of Mechanical Engineering, Jadavpur University, Kolkata, 700032, India*

KEYWORDS

Functionally graded material;
Hamilton principle;
B-spline collocation;
Power law;
Axial stress;
Shear stress

ABSTRACT

In the present study, a functionally graded cantilever beam has been analyzed to observe its deformation behavior and stress variations. While the material properties (modulus of elasticity, modulus of rigidity, and density) have been varied along the height of the beam, Poisson's ratio has been considered a constant. The governing equations have been derived using Hamilton's Principle in the framework of higher-order beam theory. The derived equations are then simplified to a single equation, which is similar to that of isotropic beams. However, the work is extended to include a few higher-order terms and to study the effect of the incorporation of these terms on the resulting FG beam behavior. The development of a single governing equation for studying the statics and dynamics of an FG beam with the incorporation of higher-order terms is a unique part of the report. The solution of the governing equation is approached using approximate methods; in this work, the B-spline collocation technique is used to arrive at the results. A sixth-order B-spline basis function is used as an approximating polynomial, and the Greville abscissa has been used to generate collocation points. The obtained results have been verified against standard literature to find a satisfactory match. The results include comparative plots for normalized bending and transverse shear stresses, with and without the inclusion of higher-order terms. The results are then extended to study the effect of material index on the deformation and stress behavior of FG beams. The effect of aspect ratio on results is also studied for comparison of various beam theories.

1. Introduction

Since the mid-1980s, with the advent of Functionally Graded Materials (FGMs), we have been witnessing a new era in the field of material technology. FGMs belong to a class of advanced materials that have continuous variation in properties along a desired direction and in a desired fashion. Compositions (volume of constituents) and hence the properties gradually change over the volume of such materials, resulting in a corresponding change in the properties of the material that is different from either of the parent materials. Functionally graded materials eliminate the sharp interfaces existing in composite materials and structures, where failure is usually initiated. Due to their customized behavior, FGMs may have very wide applications. If their manufacturing cost is reduced by improving the processes, then it may revolutionize the design process as a whole. A thorough overview of FGMs, their manufacturing techniques, modeling and design, and applications can be found in [1–5]. In [6], an exhaustive review of the modeling and analysis of functionally graded materials and their applications has been reported.

Although considerable research on functionally graded materials has been reported since their conceptualization, most of the work in the area of functionally graded structures (beams and plates) has been done only in the last two decades.

The literature search has been categorized into Euler-Bernoulli (Classical beam theory, CBT), Timoshenko (First order shear deformation theory, FSDT), and Reddy-Bickford (Higher order shear deformation theory, HSDT)

* Corresponding author. Tel.: +91-79871-07830
E-mail address: medeepakmahapatra@gmail.com

DOI: 10.22075/macs.2023.29936.1480
Received 2023-02-15 ; Received in revised form 2023-07-23 ; Accepted 2023-09-08.

RESEARCH ARTICLE | JANUARY 05 2024

Unified higher order beam theory for behavioral study of FG beams

Amalendu Biswas; Samar Chandra Mandal; Susenjit Sarkar; Deepak Mahapatra; Shubhankar Bhowmick

AIP Conf. Proc. 2960, 020006 (2024)
https://doi.org/10.1063/5.0183238

Amalendu Biswas 14.03.2024
03.06.2025

Unified Higher Order Beam Theory for Behavioral Study of FG beams

Amalendu Biswas[1 a)], Samar Chandra Mandal[2 b)], Susenjit Sarkar[2 c)], Deepak Mahapatra[3 d)], Shubhankar Bhowmick[4 e)]

[1]*Heritage Institute of Technology, Kolkata, India*
[2]*Jadavpur University, Kolkata, India*
[3]*College of Food Technology, IGKV, Raipur, India*
[4]*NIT Raipur, India*

[a)] *Corresponding author: amalendu.biswas@heritageit.edu*
[b)] *scmondal@mech.jdvu.ac.in*
[c)] *ssarkar@mech.jdvu.ac.in*
[d)] *medeepakmahapatra@gmail.com*
[e)] *sbhowmick@nitrr.ac.in*

Abstract. The study of behavior of functionally graded structural members is a significant area of research these days. The behavior of such structures is studied in the framework of beam theories proposed for isotropic beams. Usually, three governing equations are derived and solved to arrive at solutions for such beams. However, in literature there is a unique method to unify the three equations to a single governing equation for Timoshenko beams. The theory has been also extended to include correction in shear stresses through Reddy-Bickford (Higher order) beam theory. However, in reported literature, few higher order terms have been ignored for brevity.

The authors in this work have formulated a fourth order differential equation following the Higher Order Beam theory and considering more higher order terms unifying all the separate equations representing axial deflection, transverse deflection and rotation with help of a parameter. This formulation has been derived on the basis of Hamilton's principle to obtain a unique equation to study static as well as dynamic behavior of FG beams with various supporting boundary conditions. A comparative study on the effect of higher order term in the formulation for the behavioral study of FGM beams has been reported in this paper. Subsequently comparative studies for deflection and stress behavior of the FG cantilever beams for different cases of aspect ratio and material gradation subjected to uniform loading conditions has been reported.

1. INTRODUCTION

Functionally Graded Materials (FGMs) were first introduced in the middle of the 1980s and with its introduction the area of material technology has entered a new age. FGMs are a subset of advanced materials that continuously vary their properties in the desired direction and in the desired way. In such materials, the structure and, consequently, the composition (volume of constituents) vary gradually over the volume, changing the material's properties in a way that makes it distinct from either of the parent materials. Therefore, functionally graded materials eliminate any sharp interfaces that may be present in composite materials or structures, which are frequently the source of failure. FGMs may have a very broad range of uses because of their individualized activity. If their production costs can be decreased by streamlining the procedures, it might completely alter how designs are created. References [1-5] reports comprehensive description of FGMs, their manufacturing processes, modelling and design, and applications.

Recent Advances in Mechanical Infrastructure
AIP Conf. Proc. 2960, 020006-1–020006-10; https://doi.org/10.1063/5.0183238
Published by AIP Publishing. 978-0-7354-4780-6/$30.00

Amalendu Biswas 19-03-2024 03.06.2024